TO LIM GIM HOON

SOME INTERFACE PHENOMENA ASSOCIATED WITH THE JOHNSEN - RÅHBEK EFFECT

Geoffrey John Levermore

A thesis submitted for the degree of Doctor of Philosophy of the University of London

June 1975

Department of Electrical Engineering,
Imperial College of Science and Technology,
London, S. W. 7.

ABSTRACT

When a highly resistive semiconductor is placed in contact with a metal and a potential of a few hundred volts is applied between them a considerable attractive force is established. This is known as the Johnsen-Rahbek effect, and it has applications in high speed clutches and electro-mechanical devices. These however have been somewhat unpredictable in their behaviour.

Whilst most evidence shows the force to be an electrostatic attraction across the interfacial gap an accurate, quantitative prediction of the forces that should be obtained has not been possible due to the complex nature of the physical, chemical and mechanical phenomena present at the interface. This thesis is an account of further investigation into these phenomena and their influence on the forces obtained.

In order to overcome some of the difficulties which have been encountered in defining the gap between nominally flat surfaces, the work has centred upon the situation of a metal ball of large diameter in contact with a flat semiconductor. Studies have been made using both the semi-pyrolised cellulose carbon as reported by Dudding and Losty as well as electronic conducting glass. Investigations have been conducted in a vacuum of 10^{-5} torr and in atmospheric ambient conditions.

Six dominant factors affecting the forces obtained have been found:

(1) Current flow across the interfacial gap, limited by the semiconductors' resistance which restricts the maximum electric field in the gap to about 8×10^{8} V/m.

(2) The presence of absorbed water in the carbon material.

(3) The temperature of the contact.

(4) The roughnesses of the surfaces.

(5) The area of true mechanical contact and surface deformation.

(6) Etching of the surfaces due to ionisation of the gas in the interfacial gap.

These findings are discussed in the light of previous workers' theories and results and their relevance to a working device assessed.

ACKNOWLEDGEMENTS

I wish to thank Mr. R. W. Dudding for supervising this project, and the Science Research Council for supporting the work as well as giving me a Research Studentship.

I am grateful to the G. E. C. Hirst Research Centre for being able to use specimens of semi-pyrolised cellulose carbon made there and also to Mr. J. E. Still at the Centre for determining the water content of one of the specimens.

Thanks are due to Dr. R. C. Leveson for many useful discussions concerning the project, to Mr. D. G. Morris for advice in constructing the experimental apparatus and to Mr. L. Boroff for the glass work.

I am very grateful to my parents for their encouragement during the project especially during the writing of this thesis. I would also like to thank Miss G. Lim for her assistance.

Credit is due to Miss V. Collins for the neat typing.

TABLE OF CONTENTS

		PAGE
ABSTRACT		2
ACKNOWLEDGEMENTS		3
TABLE OF CONTENTS		4
CHAPTER 1	INTRODUCTION	10
	1.1 A simple explanation of the Johnsen-Rahbek effect	10
	1.2 The development of devices using the effect	12
	1.3 A review of previous investigations of the effect	14
	1.4 The purpose of the present work	17
	Figures 1.1 to 1.2	
CHAPTER 2	THE MATERIALS USED AND THEIR PREPARATION	20
	2.1 Structure	20
	2.1.1 Carbon	20
	2.1.2 Conducting glass	21
	2.2 Electrical contacts to the materials	21
	2.3 Electrical resistivity	22
	2.3.1 Carbon	22
	2.3.2 Glass	25
	2.4 Activation Energy	25
	2.4.1 Carbon	25
	2.4.2 Glass	25

PAGE

2.5 Surface preparation of the specimens 26

2.5.1 Glass and Carbon 26

2.5.2 Metal 26

2.6 Conclusion 27

Figures 2.1 to 2.9 28

CHAPTER 3 PRELIMINARY INVESTIGATIONS 37

3.1 A study of the interfacial gap with a Fizeau interferometer 37

3.1.1 Apparatus 37

3.1.2 Experimental method 38

3.1.3 Results 39

3.1.4 Discussion 40

3.2 Force measurement 41

3.2.1 Apparatus 41

3.2.2 Experimental method 42

3.2.3 Results 42

3.2.4 Discussion 42

3.3 Conclusion 44

Figures 3.1 to 3.13 45

CHAPTER 4 MEASUREMENT OF THE JOHNSEN-RAHBEK FORCE 52

4.1 Force between a metal ball and semiconductor flat 52

4.2 Apparatus 54

4.3 Experimental method 55

4.4 Results 58

4.4.1 Carbon results 58

4.4.2 Glass results 59

4.5 Conclusion 60

PAGE

Tables 4.1 to 4.7 61

Figures 4.1 to 4.8 67

CHAPTER 5 DEFORMATION OF THE CONTACTS 72

5.1 The force/deformation relationship 72

5.2 Observation of the deformation 74

5.3 Discussion of the observations 75

5.4 Discussion of force measurements 76

5.5 Effect of deformation on the current 77

5.5.1 Experimental method 79

5.5.2 Results 79

5.5.3 Discussion 79

5.6 Conclusion 80

Table 5.1 81

Figures 5.1 to 5.9 82

CHAPTER 6 THE EFFECT OF SURFACE ROUGHNESS ON THE FORCE 91

6.1 Previous work 91

6.2 Surface Roughness 92

6.3 Analysis of the roughness of a polished carbon surface 93

6.4 Theory 94

6.4.1 Norminally flat surfaces 95

6.4.2 Curved surfaces 97

6.4.3 Validity of the theories 100

6.5 Force measurements with roughened carbon 100

6.5.1 Experimental method 100

6.6 Results and discussion 101

6.6.1 Comparison of the force measurements with the curved surfaces theory 101

PAGE

6.6.2 Comparison of the force measurements with the theory of nominally flat surfaces 102

6.6.3 Comparison of the current measurements with the theory of curved surfaces 103

6.6.4 Comparison of the current measurements with the theory of nominally flat surfaces 103

6.7 Previous workers' results 104

6.7.1 Stuckes' results 104

6.7.2 Leveson's results 105

6.8 Conclusion 105

Tables 6.1 to 6.3 106

Figures 6.1 to 6.18 109

CHAPTER 7 THE EFFECT OF THE POLARITY OF THE APPLIED VOLTAGE 126

7.1 Current flow across the interfacial gap 126

7.2 The effect of the work function of a surface 129

7.2.1 Experimental method 130

7.2.2 Results and discussion 131

7.3 The environment at the interface 132

7.3.1 Surface contamination 133

7.3.2 Ambient gas pressure 133

7.4 Discussion 133

7.5 Conclusion 135

Tables 7.1 to 7.3 137

Figures 7.1 to 7.2 139

PAGE

CHAPTER 8 THE EFFECT OF HEAT 141

8.1 Desorption 141

8.1.1 Experimental method 142

8.1.2 Results 143

8.1.3 Discussion of results 143

8.2 The effect of heating the contact 145

8.2.1 Theory 145

8.2.2 Experimental method 148

8.2.3 Results 148

8.2.4 Discussion of the results 148

8.3 Conclusion 149

Tables 8.1 to 8.3 151

Figures 8.1 to 8.7 154

CHAPTER 9 SURFACE DEGRADATION AND ETCHING 159

9.1 Preliminary discussion 159

9.2 Measurements under vacuum conditions 161

9.2.1 Experimental method 161

9.2.2 Results of initial experiments 162

9.2.3 Experimental procedure with undesorbed carbon 162

9.2.4 Results obtained with undesorbed carbon 163

9.2.5 Discussion 164

9.3 Measurements under atmospheric conditions 166

9.3.1 Experimental method 167

9.3.2 Results 167

9.3.3 Discussion 168

9.4 Investigation with the Fizeau interferometer 169

9.4.1 Experimental method 169

PAGE

9.4.2 Results 170

9.4.3 Discussion 171

9.5 Conclusion 174

Tables 9.1 to 9.8 176

Figures 9.1 to 9.15 182

CHAPTER 10 SUMMARY AND CONCLUSION 191

10.1 Summary of previous work 191

10.2 Factors affecting a working device 193

10.3 Guidelines for a better device 197

10.3.1 Properties of an ideal semiconductor for a device 197

10.3.2 Properties of an ideal metal for a device 199

10.3.3 The design and construction of a device 199

10.4 Possibly suitable materials for a device 200

10.5 Future work 201

Figures 10.1 to 10.3 203

APPENDIX 1 CIRCUIT MODEL 206

A1.1 The saturation electric field 207

A1.2 The variation of resistivity 207

A1.3 The variation of work function 208

A1.4 The effect of contamination 208

A1.5 The effect of heating the contact 208

Tables A1.1 to A1.3 209

Figures A1.1 to A1.4 212

APPENDIX 2 SURFACE ROUGHNESS 215

APPENDIX 3 THE FRICTIONAL BEHAVIOUR OF GRAPHITE 218

APPENDIX 4 THE SWITCH ON/OFF TIME 221

REFERENCES 223

CHAPTER 1

INTRODUCTION

In their paper of 1923 Johnsen and Rahbek described an experiment in which a slab of lithographic stone was placed in contact with a brass disc. The contacting surfaces were plane and smooth, and when a potential difference of 440 volts was applied between the slab and disc a force of more than 10 N. was required to separate them.

This effect, which came to be known as the Johnsen-Rahbek effect, showed considerable promise for application to practical devices such as relays and clutches since large mechanical forces could be developed very quickly with the application of a small amount of electrical power.

1. 1 A SIMPLE EXPLANATION OF THE JOHNSEN-RAHBEK EFFECT

The Johnsen-Rahbek Effect is basically the electrostatic attraction between two charged surfaces and the magnitude of this force is given by :

$$\text{Force} = \frac{\epsilon_o \, A V^2}{2 \Delta^2} \quad \text{(N)} \qquad (1.1.1)$$

where V, (volts), is the potential difference across the gap, of distance Δ, (m), between two parallel surfaces of area A, (m^2). ϵ_o is the permittivity of free space, (8.854×10^{-12} C^2 N^{-1} m^{-2}).

The force can be increased by simply moving the surfaces together, i.e. reducing Δ. It does not become infinite when the surfaces touch, however, as Δ is limited to a finite value by the roughness of the surfaces. Even highly polished surfaces are rough on a microscopic scale and two such surfaces placed in contact only make contact at a few spots, (Bowden and Tabor). The area of these spots is a minute fraction of the nominal area of contact and when a potential difference is applied between the contact members the current is constrained to flow through these spots. This constraint of the current constitutes a constriction resistance termed R_c, (52). For a contact of radius, d (m), each contact member forms a constriction resistance given

by, (Holm);

$$R_c = \frac{\rho}{4d} \quad (\Omega) \qquad (1.1.2)$$

where ρ (Ω m) is the bulk resistivity of the contact member. This resistance is larger than the bulk resistance of the contact members in most practical cases and so most of the potential difference, Vo, between these members is dropped across the contacts and the interfacial gap. So the approximate force between the members is given by eq. (1.1.1.), replacing V by Vo.

The current flow heats up the contact and if the two contacting members are of the same material, the contact spot can be considered as a sphere of radius d, (the contact radius), of infinite electrical and thermal conductivity embedded in an infinite extent of the contact material of thermal conductivity k ($W\ m^{-1}\ K^{-1}$). The temperature of the sphere, Θ (^{o}C), is, (Carslaw and Jaeger):

$$\Theta = \Theta_o + \frac{IV}{4\pi kd} \qquad (1.1.3)$$

where Θ_o is the ambient temperature of the contact members and I (amps), the current flow. This is a somewhat artificial model of the contact and is used merely to indicate its behaviour. Combining eq. (1.1.3) and eq.(1.1.2) one obtains :

$$\Theta \propto \frac{V^2}{\rho k} \qquad (1.1.4)$$

This shows that materials with a large value of ρk can sustain higher potential differences across their contacts for a given value of Θ. For metals ρk is approximately $10^{-5}\ V^2\ K^{-1}$ which means a few volts across a metal contact would melt it, and the resultant force from this small voltage dropped across the interfacial gap would be small. However, high resistivity semiconductors, with $\rho \sim 10^4\ \Omega$ m have a much higher

value, ρ_k being about $10^4 V^2 K^{-1}$. Insulators have very high values of ρ_k but are of little practical use for a working device, see Appendix 4. As such semiconductors have low thermal conductivities most devices are made with a metal in contact with the semiconductor to lower the contact temperature. This is the combination which has been used by most workers to investigate the effect, but the effect is not solely produced by this combination alone.

1. 2 THE DEVELOPMENT OF DEVICES USING THE EFFECT.

The most common application of the effect was in the form of a clutch, either a band clutch, (fig1.1A), or a disc clutch, (fig.1.1B).

Following their early investigations Johnsen and Rahbek made a number of devices, and one of these, a band clutch, was used to a limited extent commercially for telegraphy. The semiconductor used in the devices was lithographic stone. In common with the semiconductors used by other early workers, lithographic stone was an ionic semiconductor, a porous material whose electrical conductivity depended on its moisture content. Such materials have inconsistent conductivity due to the current flow tending to evaporate the absorbed moisture and electrolysis decomposing the material. This variable property was responsible for interest being lost in devices such as those of Johnsen and Rahbek.

With the development of high resistivity electronic semiconductors which were not so dependent on moisture for their electrical conductivity, interest in the effect was once more aroused.

In 1955, Stuckes constructed a disc clutch consisting of a plate of magnesium orthotitanate, (a hard, polycrystalline, ceramic semiconductor), rubbing against a hard metal plate. Although the clutch had been made of hard materials in the belief that these would reduce wear, this was the main cause of failure for the device. Before wear occurred a typical clutch was capable of a static torque of O.6 N m at 500 volts, (fig.12). Even though Stuckes concluded it would be difficult to produce a reliable clutch, interest was maintained due to the demand for high speed electromechanical devices in

computers.

Fitch, working for I. B. M., realising that ceramic materials were not suitable for clutches, set up six factors to be considered in choosing a good semiconducting material :

(1) Electronic, (not ionic), conduction.

(2) Homogeneous resistivity of the order of 10^4 Ωm.

(3) Reproducibility.

(4) Heat and wear resistance and dimensional stability.

(5) Good frictional characteristics.

(6) Ease of manufacture.

One material satisfying most factors was a rubber based plastic, containing ten ingredients. Using it in a band clutch he overcame the wear problem by feeding a small amount of liquid lubricant onto the cylinder. The static torque produced by various applied voltages is shown in fig.1.2. Its performance was promising, being capable of operating at 2,500 r.p.m., but having to feed an accurate quantity of lubricant onto the cylinder added to the complexity and cost of the device.

Dudding and Losty, working for G. E. C., found a better material; semi-pyrolised cellulose carbon, (Davidson and Losty, 1963; Davidson and Losty, 1960). It was better because it was self lubricating and produced little wear when rubbed against smooth steel. In his paper, Dudding described disc and band clutches developed with this material, and the static torque produced by a typical disc clutch is shown in fig.1.2. These clutches were the best so far developed, and the characteristics of a typical disc clutch compared to those of an equivalent electromagnetic clutch were:

(i) about 100 times faster switching on and off ;

(ii) needed less control power to transmit the same amount of mechanical power than an electromagnetic clutch.

The usefulness of this device was however still limited by unpredictable

performance, the reasons for which were still not fully understood.

1. 3 A REVIEW OF PREVIOUS INVESTIGATIONS OF THE EFFECT

Development of devices utilising the effect has always been more advanced than the understanding of the effect itself. Early workers realised the force was primarily an electrostatic attraction across the interf acial gap but they were hampered in making measurements of it by their unreliable ionic semiconductors. Johnsen and Rahbek found the force varied with applied voltage up to the fifth power indicating that eq. (1.1.1) was far from correct. The force also varied with the electrical conductivity of the semiconductor, the degree of polish that could be given to its surface and the direction of current flow. Maximum force was obtained when the semiconductor was at a negative potential with respect to the metal. Reversing the polarity of the potential produced a force which gradually diminished, becoming negligible after a few minutes. Other early workers, (Antinori 1925, Bergmann 1923, Rottgardt 1922 and Waszik 1924), produced results more dependent on the ionic semiconductor used and its evironment than on the effect itself.

With the advent of electronic semiconductors more reliable results seemed possible. Balakrishnan used discs of magnesium orthotitanate to investigate the effect. To determine whether the force required the presence of moisture in the semiconductor, as early workers had found, he heated some of the discs to about $80^{o}C$, then kept them in a desiccator before measuring the force they produced when a potential difference was established between each disc and a brass plate. After this heat treatment the discs produced a slightly increased force whereas Johnsen and Rahbek found that the force became negligible when their ionic semiconductor was dried. This was because the magnesuim orthotitanate was less dependent on moisture for its conductivity than the ionic semiconductor, the former's resistivity increasing only by 25% to 150% upon drying. Balakrishnan did not estimate how effective his heat treatment was in desorbing all the moisture from his discs and as a temperature of $80^{o}C$ is rather low for desorption one would expect

that desorption of all the moisture would have a greater effect on the force than these results show.

Balakrishnan measured the force with a spring balance recording the force required to lift the brass block from the semiconductor at a given applied voltage. The average of between six and twelve readings was taken for each voltage as a considerable scatter of results was found. This was probably due to the discs peeling apart, as the electrostatic force was unlikely to be symmetrical even if the applied mechanical force was, giving an inaccurate reading. The reading was also altered by the speed of separation of the discs. These readings were regarded as having a rough rather than precise significance and showed the force to vary approximately as the third power of applied voltage. This was attributed to deformation of the contacting surfaces due to the attractive force.

As most investigations had been made with ionic semiconductors of inconsistent resistivity the current also varied considerably. With electronic semiconductors, however, more stable currents could be expected and investigation of them would lead to further insight into the effect. Stuckes measured the current as well as the force at a given voltage applied between a magnesium orthotitanate disc and a steel disc. The current/voltage relationship was non-ohmic, approximately obeying the relationship, worked out by Sillars for current flow through a contact enhanced or dominated by field emission current, (Fowler and Nordheim), flowing across the interfacial gap near the contact. The force, (measured by the same method as Balakrishnan used and presumably subject to the same errors), tended to a limiting value at high voltages because of this current and the high bulk resistance of the semiconductor. An increase in applied voltage would enlarge the area over which field emission occurred until at a high enough voltage, current would flow across the whole interfacial gap. The current would be limited by the high bulk resistance of the semiconductor, limiting the interfacial voltage and also the electric field in the gap to a saturation value termed E_o, (Vm^{-1}).

Stuckes pointed out that field emission would only be important for very flat surfaces, and that other workers had not observed its effects as they had not used discs as flat as hers which had a curvature of about 130m.

The discs used by Stuckes did however have very high bulk resistances so that very little of the applied voltage was dropped across the interfacial gap. This limited E_o to a low value and the forces she obtained do not represent the maximum forces the effect is capable of producing. Using specimens with such high bulk resistances also meant that changes in this resistance would alter the interfacial voltage and hence the force obtained. Balakrishnan had shown that magnesium orthotitanate did change its resistivity when its moisture content was altered and as Stuckes had to apply large voltages to her discs their bulk resistances could well have changed during the experiments. Unfortunately Stuckes did not examine the discs for any change of resistivity. This point is discussed later on when her results are analysed in more detail, and compared with results obtained in the present work.

Although the effect had been extensively investigated an accurate method of force measurement had not been devised. Leveson measured the force by shearing the contact members when under the influence of an applied voltage. Knowing the coefficient of friction the attractive force could be calculated. This method seemed more accurate than pulling the surfaces apart as it avoided the peeling encounted with the latter. It was also a more appropriate method as devices utilise the effect to change the friction force between the surfaces and this method measures this friction force directly.

Semi-pyrolised cellulose carbon was the semiconductor used in the experiments and suspecting that the gas in the interfacial gap could alter the force obtained Leveson maintained his apparatus in a vacuum of 10^{-5} torr. (All previous measurements were done under atmospheric conditions). The contacting surfaces were as flat as those of Stuckes' specimens but no limiting force was found even though the interfacial voltage between the carbon and metal was higher than that between the magnesium orthotitanate and metal.

This was probably because the bulk resistance of the carbon was decidedly less than the constriction resistances of the contacts, unlike the situation for the orthotitanate, and so E_o was not limited to such a low value by the carbon. The forces obtained by Leveson were less than those of Stuckes, taking account of the difference in size of the specimens and comparing them at equal interfacial voltages. Experiments done in the present work elucidate this difference and discussion of the results is left until later.

1. 4 THE PURPOSE OF THE PRESENT WORK

Previous work has shed little light on the factors affecting the Johnsen-Rahbek effect. Much qualitative work has been done but it has yielded little quantitative information. So although Dudding and Losty had developed useful clutches, these were unable to fulfill their initial promise due to unreliability, which suggested that a deeper understanding of the interface effects was still required. This thesis describes the investigation into these effects using a new method of force measurement far more amenable to quantitative analysis than previous methods.

SIMPLE DEVICES

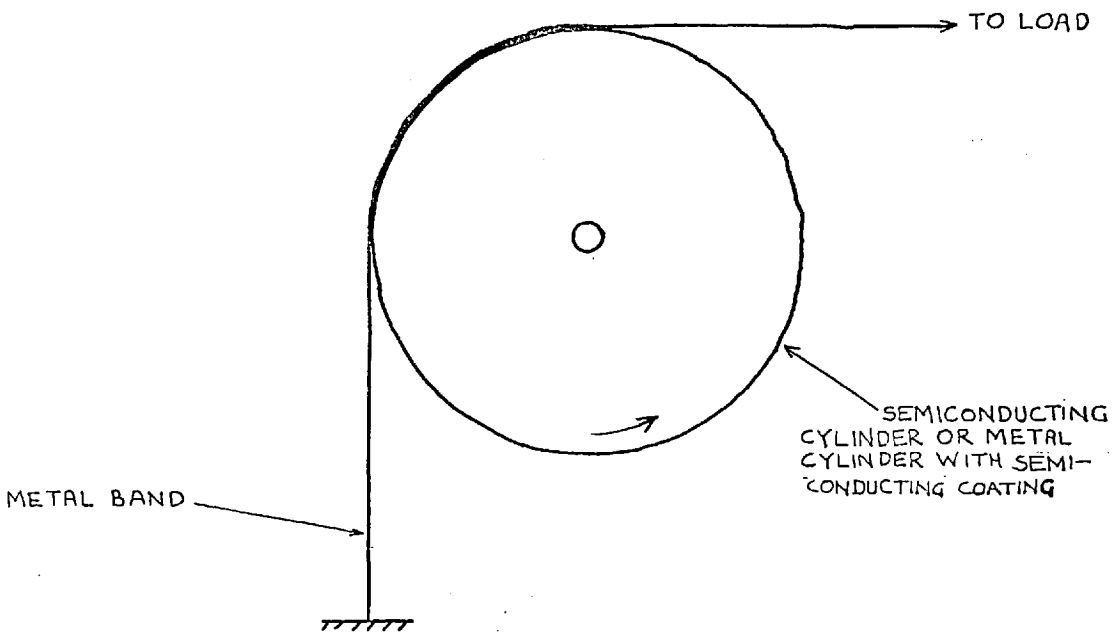

FIG.I.IA

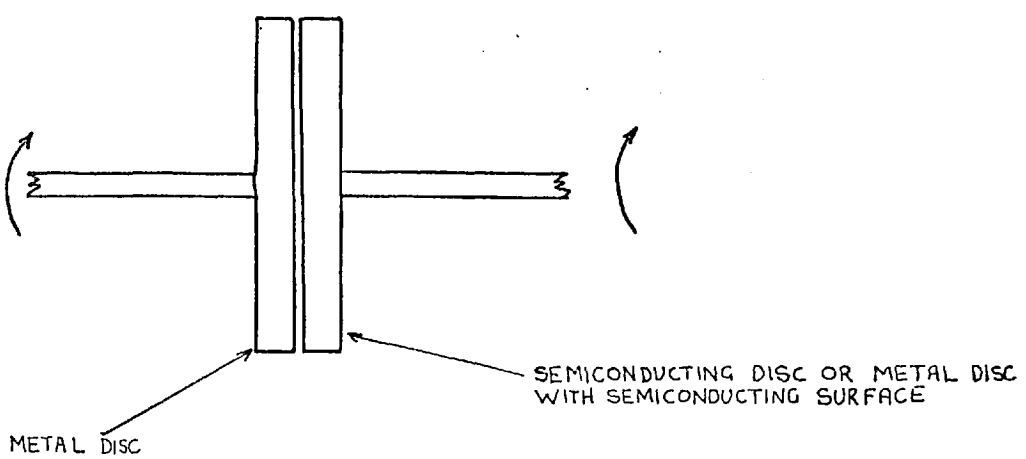

FIG.I.IB

THE PERFORMANCE OF SOME CLUTCHES

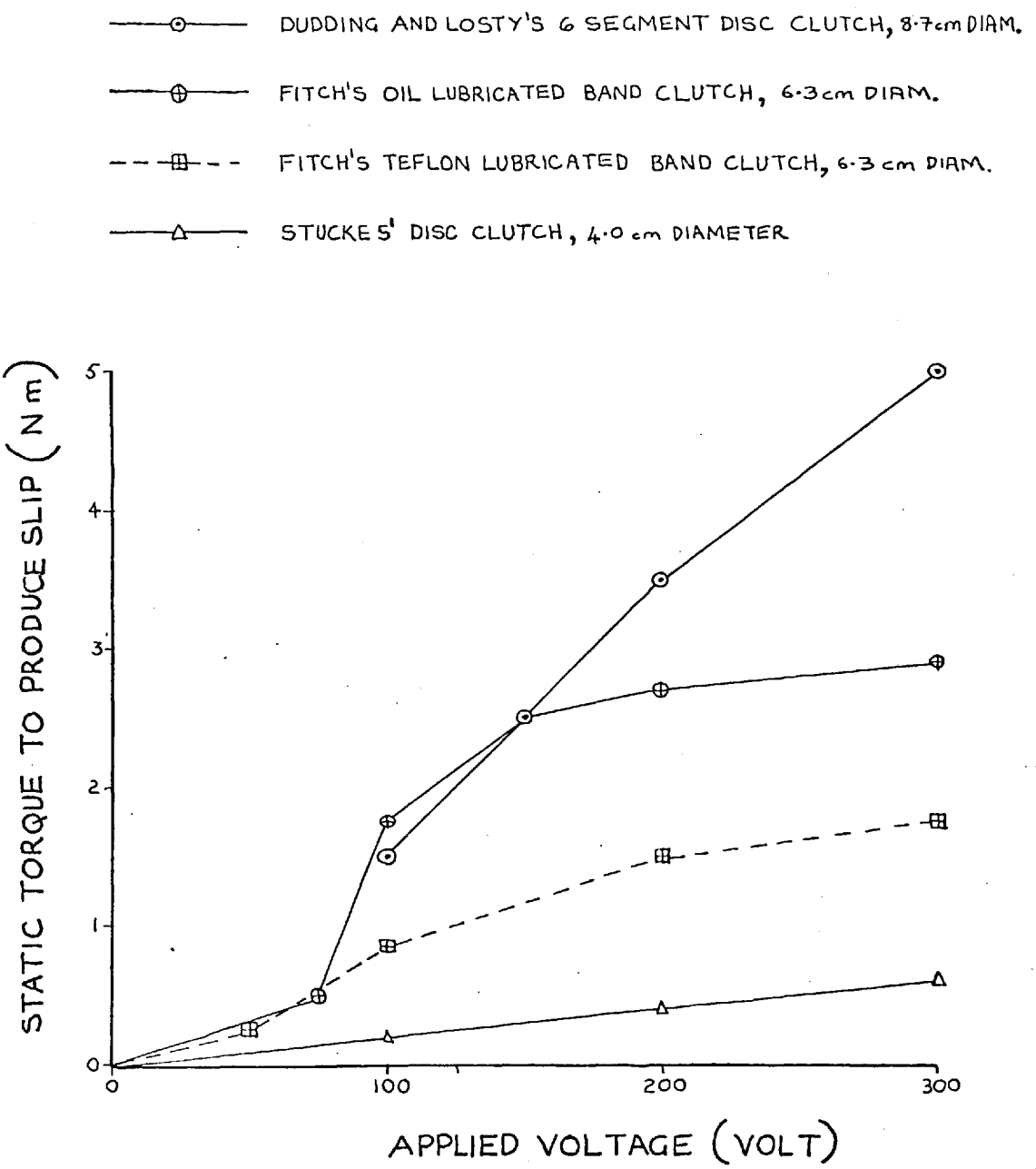

FIG.1.2

CHAPTER II

THE MATERIALS USED AND THEIR PREPARATION

Materials suitable for making devices and sustaining useful forces are those with high values of ρk, as described previously. Many substances satisfy this criterion, but few are satisfactory clutch materials. The most successful semiconductor used in devices utilising the Johnsen-Rahbek effect has been semi-pyrolised cellulose carbon, pioneered by Dudding and Losty. As the present work was concerned with investigating the effect with a view to understanding the phenomena occurring in such a working device, this type of carbon was used. So that the results obtained were not intrinsic to the carbon, measurements were also made with conducting glass.

2. 1 STRUCTURE

2.1.1. CARBON

Davidson and Losty in their paper of 1963 described the preparation and properties of impermeable cellulose carbon, of which semi-pyrolised cellulose carbon is a form, the specimens used in the present work having been heat treated to between 480 ^{o}C and 500 ^{o}C.

The carbon is produced by heating cellulose, which decomposes at an increasing rate above 100 ^{o}C, (Constandinou). The semi-pyrolised cellulose carbon is the amorphous residue of carbon left by the decomposed cellulose. The quantity of cellulose or degraded cellulose matter left in the residue was probably small, the decomposition of the cellulose having been almost complete by about 450 ^{o}C. It was not a pure material though, as examination with an electron microprobe analyser showed scattered areas, $\sim 20 \mu$m large at the most, containing appreciable silicon, with a little caesium and aluminium. Iron was also present in the carbon to a level of 0. 06% . These impurities were not caused by cutting or polishing the carbon as different surface preparations did not significantly alter their levels.

The carbon used was very porous, the graphitization not having commenced, the rate of diffusion of helium through it being 10^{-10} m^{2} sec^{-1} compared with 10^{-16} m^{2} sec^{-1} for the carbon when fully graphitized.

It had a glassy appearance when fractured. The Young's modulus was estimated to be 7×10^{9} N m^{-2}, the flexural strength 8.27×10^{7} Nm^{-2} and the hardness between 100 and 200 Vickers hardness number, this value being approximate as the hardness of a brittle material is very difficult to assess.

2.1.2 CONDUCTING GLASS

The glass specimens were composed of, (mole %); 50% V_2O_5, 10% P_2O_5, 10% MoO_3 and 30% As_2O_3. They are semiconducting oxide glasses which are electron conducting, the electrons hopping between the multivalent ions (e.g. V^{5+} and V^{4+}). Much research has been done on such glasses and Adler's book should be consulted for further numerous references.

Although amorphous this glass contained small crystallites, $\sim 40 \mu m$ in size, which when examined by electron microprobe techniques were shown to be rich in vanadium, phosphorous and arsenic. This would suggest a variation in conductivity from point to point on the surface.

When polished, specimens cut from an ingot of the material produced differences in the surface finish. Approximately one half of the polished surface was smoother than the other half, indicating a gradual variation in the mechanical property of the material across the surface. Force measurements were always carried out on the smoother parts of the surface.

The glass was apparently harder than the carbon since it scratched it quite easily. There is little precise data on the other physical properties of the glass used.

2.2 ELECTRICAL CONTACTS TO THE MATERIALS.

The rectifying contact between a crystalline semiconductor and a metal is well known, as is the fact that much care is needed to form an ohmic contact between such materials. It is therefore surprising that there has been little mention of problems with contacts or special effects associated with surfaces in the papers on electrical transport properties of amorphous semiconductors. This is because these materials are intrinsic semiconductors

and cannot easily be doped, (Mott). Fritzsche made the analogy between an amorphous semiconductor and a crystalline intrinsic semiconductor, with its Fermi level close to the band centre, the potential barrier formed when in contact with a metal being the same for both positive and negative current carriers. So, although amorphous semiconductors cannot be described in terms of the energy band theory, they can be likened to intrinsic crystalline semiconductors as regards contact behaviour.

In the present work contacts were made to the specimens of carbon and glass with silver conducting paint, (Acheson's PAG 915), or with conducting epoxy resin, (CIBA x 83/464 resin).

2. 3 ELECTRICAL RESISTIVITY

2.3.1 CARBON

Although most amorphous semiconductors form ohmic contacts with metals it could not be assumed that the carbon would behave likewise.

Initial measurements were done by bonding fine copper wires onto a disc (1mm thick and 5 cm^2) of carbon with conducting epoxy resin. For the resin to set the disc and electrodes were heated in an oven at 80 ^{o}C for a few hours. When it had been allowed to cool the disc had a resistance which slowly decreased with time. The resistance of the disc was also found to have increased substantially upon being heated. It was suspected that the carbon was chemically changing upon heating.

To avoid heating the specimen electrodes of conducting silver were painted on and allowed to dry under ordinary room conditions and fine copper wires were attached to these electrodes with a further application of the silver coating. The initial measurements of current/voltage characteristics produced non-ohmic plots because the electrodes were too large, passing a high current and heating most of the sample. Electrodes less than 0.5 cm^2 in area produced a more linear plot as the amount of specimen heated was less.

For accurate measurements of the resistance of a low conductivity material

leakage currents across the surface of the specimen can prove deleterious. Employment of a guard ring, (and its connection to the circuit shown in fig. 2. 1), avoids measuring this spurious current. Instead of using a disc of carbon as the specimen, a piece of carbon bonded to a base plate of aluminium was used, a metal stud being bonded onto the base. This enabled the specimen to be handled easily without touching the carbon itself. To ensure the carbon was maintained in a clean environment it was placed in a vacuum chamber with an electrical 'feed-through'. With a guard ring of conducting silver paint around the periphery of the carbon and a small electrode in the middle, the current/voltage characteristic was measured, initially at atmospheric pressure. The current through the whole system, guard ring plus electrode, I_T, and the current flowing through the electrode alone, I_B, were measured. Although the I_T/voltage relationship was slightly non-linear the I_B/voltage relationship was linear. However, when the chamber had been evacuated for five hours to a pressure of 10^{-5} torr, the true bulk resistance had increased by 15% and the total resistance by the same amount. The further change in resistance with time is shown in fig. 2.2.

An attempt to examine the desorption of gases from the carbon was made by placing a disc of carbon with silver electrodes in an ultra-high vacuum system (fig. 2. 3), with a 180^{o} deflection partial pressure gauge. The presence of the carbon did not alter the spectrum of gases obtained, when compared with that obtained with no carbon present in the system. When the ion pump was valved off, and 200 volts was applied to the carbon, the pressure increased at a faster rate than when no voltage was applied. In one experiment upon the application of 400 volts to the carbon a drastic increase in the pressure occurred, and finally the carbon fractured, apparently due to the development of a high hydrostatic pressure within the specimen, (see Chapter 9).

After the system had been baked at 100^{o}C for a day and a pressure of 10^{-7} torr achieved, the resistance of the carbon was typically increased by a factor of ten times. Examination of the spectra of gases in the system with and without the baked carbon showed little difference, and although the pressure increased quicker with a voltage applied to the carbon, when the ion pump was

valved off, the spectrum of gases in the system showed no difference from that produced by the system without the baked carbon present. This is not unexpected since the desorption of both the carbon and the vacuum system took place simultaneously. Desorption by the vacuum system, e.g. of adsorbed water, could not be differentiated from desorption by the carbon, but the results indicate that the adsorbed and absorbed gases of the carbon were similar to normal atmospheric constituents, and not peculiar to the carbon itself. Evidence of atmospheric contamination of the carbon was also provided by the fact that the carbon tended to recover its original resistance upon being left in the atmosphere for a sufficient period of time. This period varied according to the degree of desorption. The period for recovery after desorption in a vacuum of 10^{-5} torr was comparable with the time spent in the vacuum, (fig.2.2), whereas it was much longer after desorption, (including baking), in the better vacuum of 10^{-7} torr. This is shown in fig. 2.4.

Total recovery on exposure to the atmosphere for a time comparable to that for desorption was rarely achieved, the final resistance being at least 10% higher than the initial value. This indicates that a slight change in the composition of the carbon may have occurred.

Further evidence for the nature of the desorbant was obtained by monitoring the capacitance and conductance during desorption. This was acheived using an A.C. bridge and heating the carbon in a vacuum system, (fig. 2.5). The heating produced a quicker desorption of the specimen and the results obtained (fig.2.6) showed the capacitance and conductance increased rapidly upon heating and then decreased upon subsequent desorption. This suggests that the primary desorbant was water vapour, the rapid increase in capacitance being associated with the greater freedom of the molecules to align themselves with the electric field, and the final decrease in capacitance being due to the desorption of the water.

Measurement of the water content of the carbon with apparatus designed

by Still and Cluley, (Still and Cluley, 1965, and 1972), showed an undesorbed specimen to contain 2% by weight of water. The desorption was complete once the slowly increasing temperature of the specimen container had acheived 250°C, (fig. 2.7). Upon leaving this specimen in the atmosphere for 24 hours it reabsorbed 75% of its original water content.

Absorbed water could account for the variable electrical resistivity of the carbon, the water acting as a solvent to produce various ions within the specimen and ionising to an extent itself.

2.3.2 GLASS

The conducting glass did not show absorption to the extent shown by the carbon and as a result its resistance was not variable in vacuum, fig. 2.8. For this reason the glass was used to compare the performance with that of the carbon.

2.4 ACTIVATION ENERGY

2.4.1 CARBON

For this measurement the carbon, with electrodes attached, was placed in an oil bath and its resistance measured as the oil bath was allowed to slowly cool from about 120°C. The oil was kept at a uniform temperature throughout its volume by constant agitation and its temperature measured with a mercury thermometer. Although the carbon desorbed gas rapidly at the higher temperatures, (as witnessed by bubbles streaming from it), it provided a plot of resistance versus temperature consistent with that of a semiconductor with an activation energy of 0.5 eV. This value varied little over the range of applied voltage between 50 and 200 volts, (fig.2.9). This indicated that although the voltage had an effect on the desorption and resistivity of the carbon, it had no effect on this measurement.

2.4.2 GLASS

Previous work has shown the activation energy of vanadium-phosphate glass to be about 0.3 to 0.4 eV, (Linsley et al.; Janakirama-Roa; and Schmid).

2.5 SURFACE PREPARATION OF THE SPECIMENS

Early workers found that the force produced upon application of a voltage to a semiconductor in contact with a metal was dependent on the surface roughness and flatness of the specimens.

To achieve large forces the metal and semiconducting specimens used in the present work were polished to as fine a surface finish as possible.

2.5.1 GLASS AND CARBON

To attain a good surface finish on the specimen it must be rubbed against a softer material holding the polishing material. This avoids the specimen being scratched. The surface on which it is polished must also be flat to the degree required for the specimen. Increased polishing also increases the surface curvature unless the polishing tool is constantly kept true by polishing with a reference tool.

A pitch lap was used for polishing the carbon and glass. It was maintained flat with respect to a piece of 'float' glass, the reference tool, by pressing it against the glass when the pitch had been warmed. Shallow channels were then cut in the pitch to allow for drainage of polishing debris and wear particles.

The polishing material was a fine aluminium oxide grit, (1 μm Linde powder*), a finer final finish being produced with rouge powder.* Although the specimens could be polished to a reproducible surface finish, ($\sim$0.02 μm C.L.A.** for the carbon), the curvature produced was often variable between a radius of 5m and 100m.

The glass produced an inhomogeneous surface finish as mentioned earlier. The roughness of the smoother part of the surface was typically 0.05 μm C.L.A.

2.5.2 METAL

In most of the present work the metal surface was provided by a hard stainless steel ball. This was polished with diamond paste. the size of grit particle being successively reduced from 10 μm, 6 μm and 1 μm to obtain a

* Suspended in water to form a paste.

** This abbreviation is defined in Appendix 2.

finer finish. The paste was applied to a polishing cloth and the ball polished by hand, until a mirror finish was obtained and examination on an optical microscope at a magnification of x 100 showed few flaws. This finish was easily attained, but measurement of it with a surface profilometer was difficult due to the lack of sensitivity in adjusting the instrument to the radius of the ball. The surface finish was superior to that of the semiconducting specimens, (i. e. better than 0. 02 μm C. L. A.).

2. 6 CONCLUSION

The work described in this chapter indicates that the structure and properties of the semiconductors are complex and it is likely that they would affect the Johnsen-Rahbek forces produced.

The most striking feature of the carbon, used extensively in this investigation, is its water content. The effects of this on the forces developed will be examined in the following chapters. By using two different types of specimen i. e. carbon and glass, the influence of the semiconductors' basic properties on the forces developed will also be investigated.

THE GUARD RING CIRCUIT USED IN RESISTANCE MEASUREMENTS

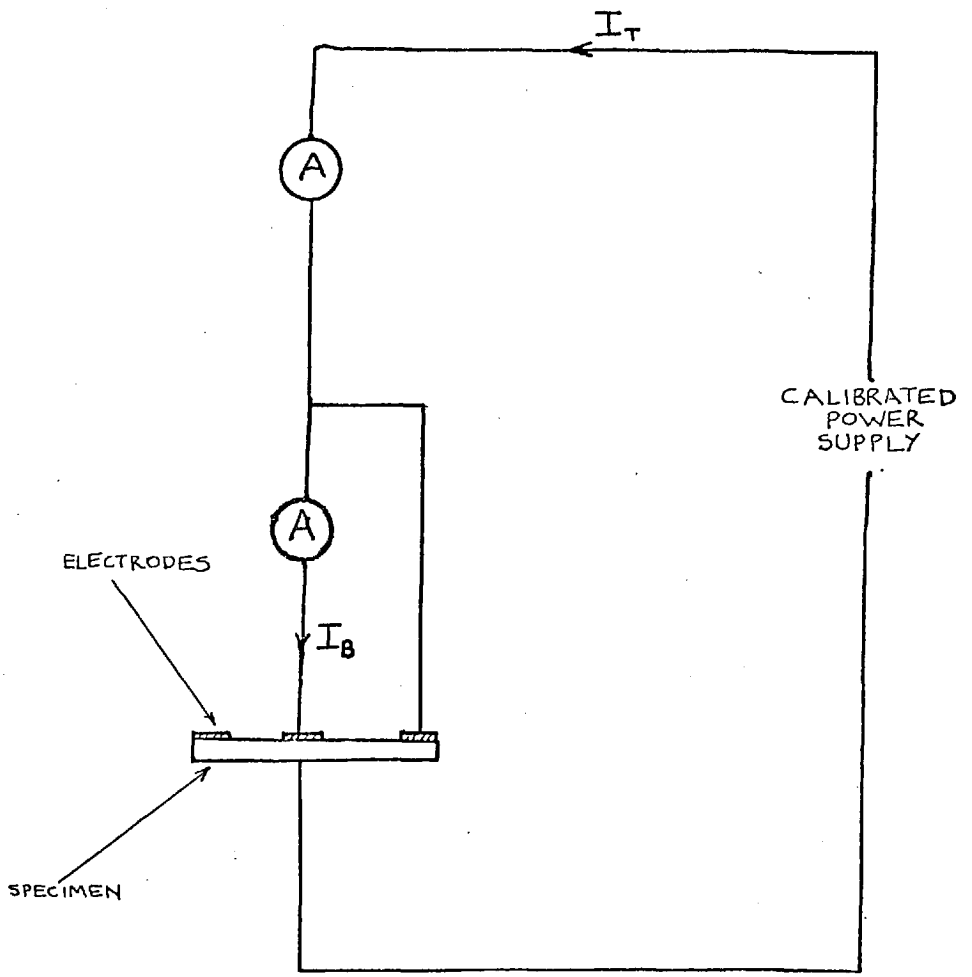

FIG.2.1

A TYPICAL PLOT OF THE RESISTANCE OF A SPECIMEN OF CARBON VERSUS THE TIME IT WAS IN A VACUUM OF 10^{-5} TORR

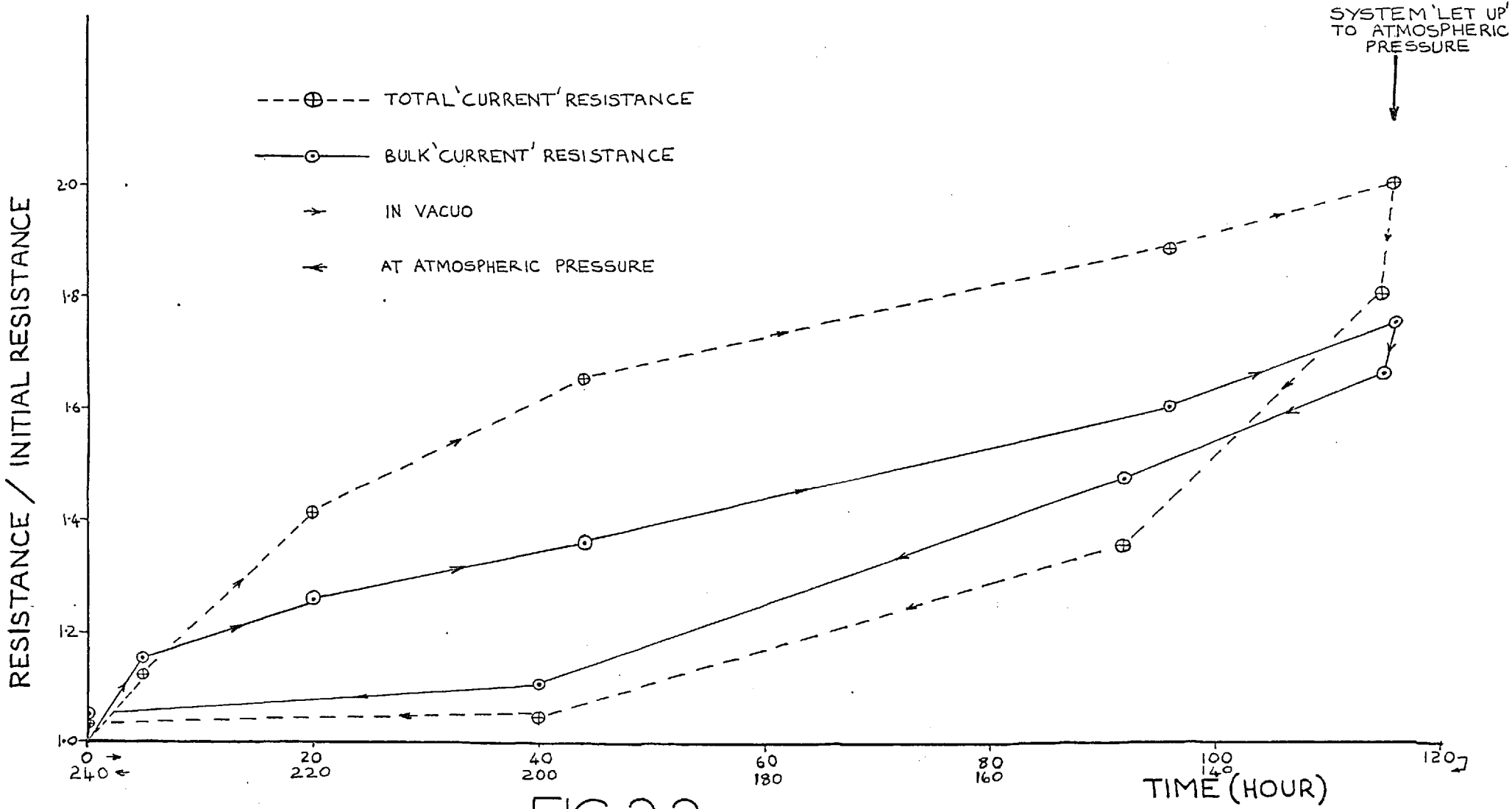

FIG. 2.2

THE ULTRA-HIGH VACUUM SYSTEM

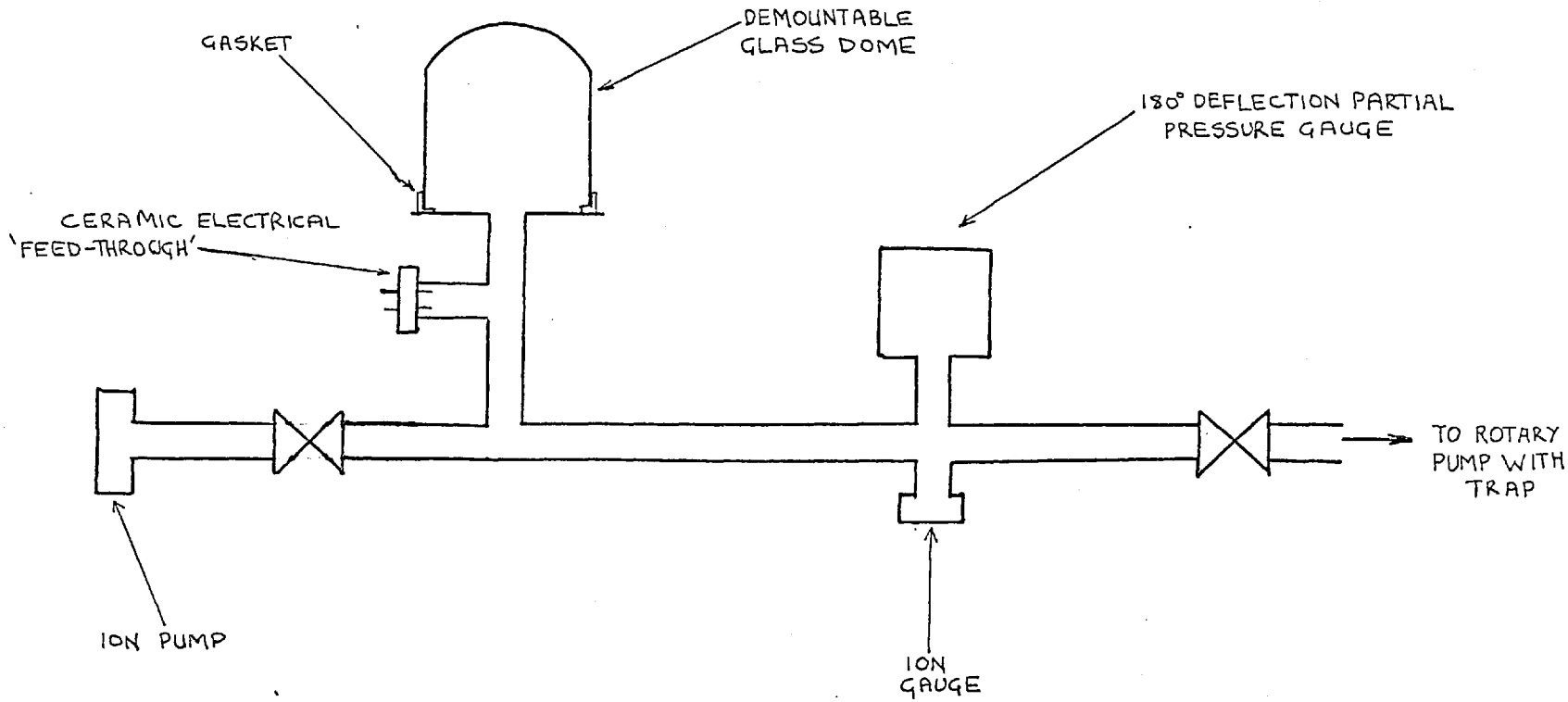

FIG.2.3

A GRAPH OF RESISTANCE OF A CARBON SPECIMEN VERSUS TIME IT IS IN VACUO

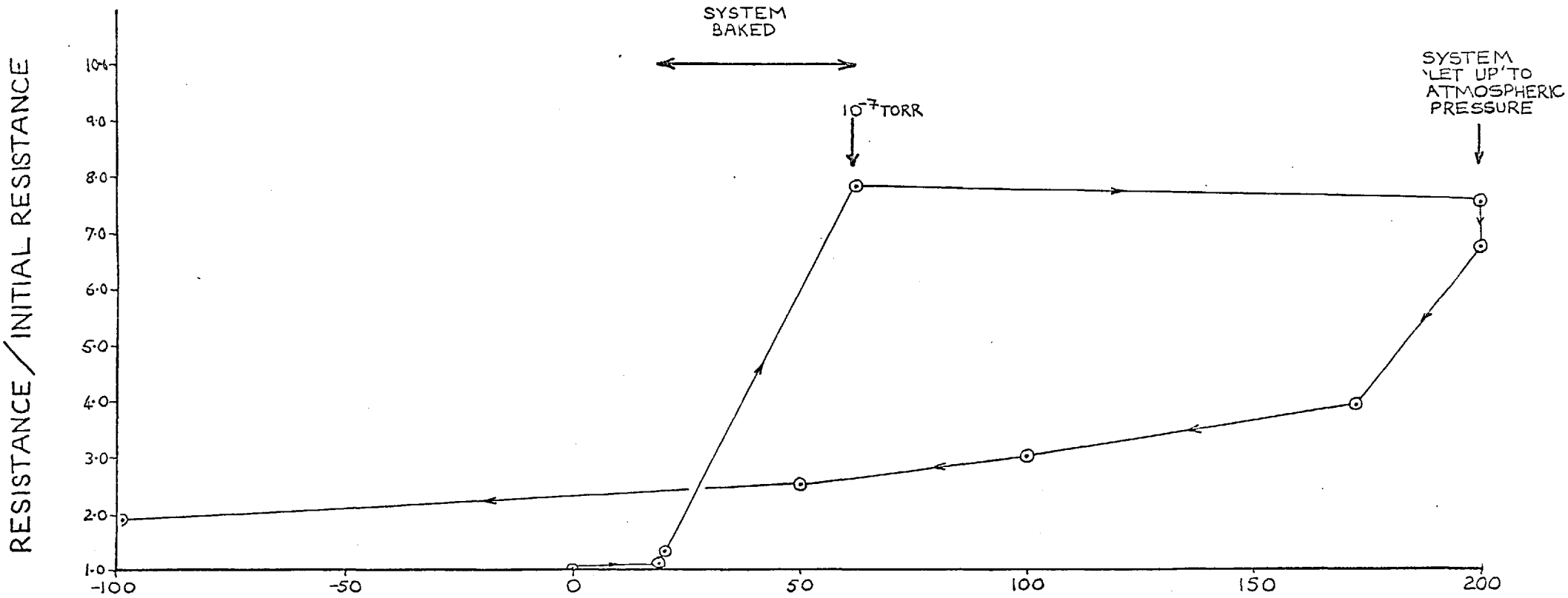

FIG.2.4

THE APPARATUS FOR HEATING A SPECIMEN OF CARBON IN VACUO

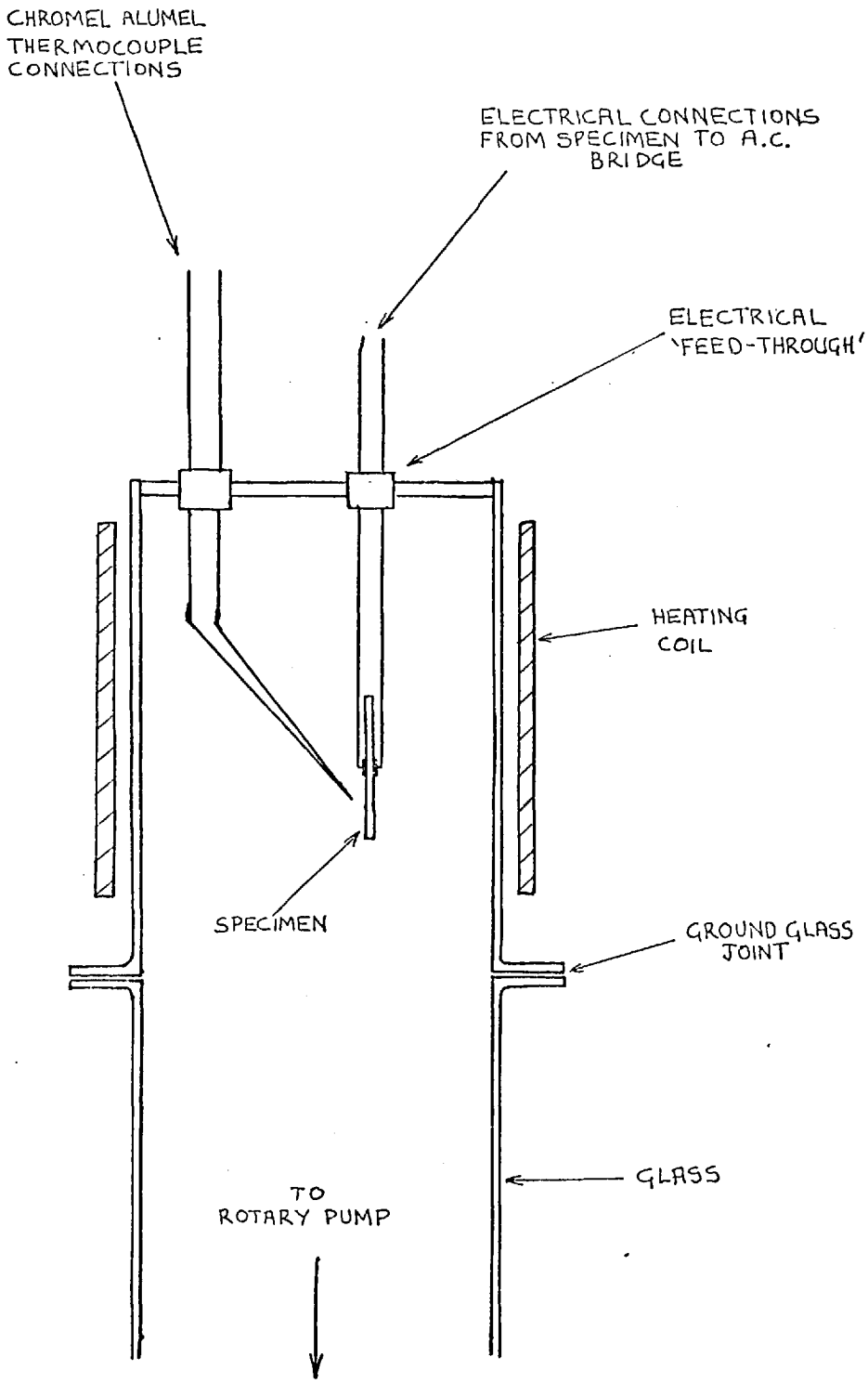

FIG. 2.5

A TYPICAL GRAPH OF THE CONDUCTIVITY AND CAPACITANCE OF A CARBON SPECIMEN VERSUS THE TIME IT WAS HEATED IN VACUO

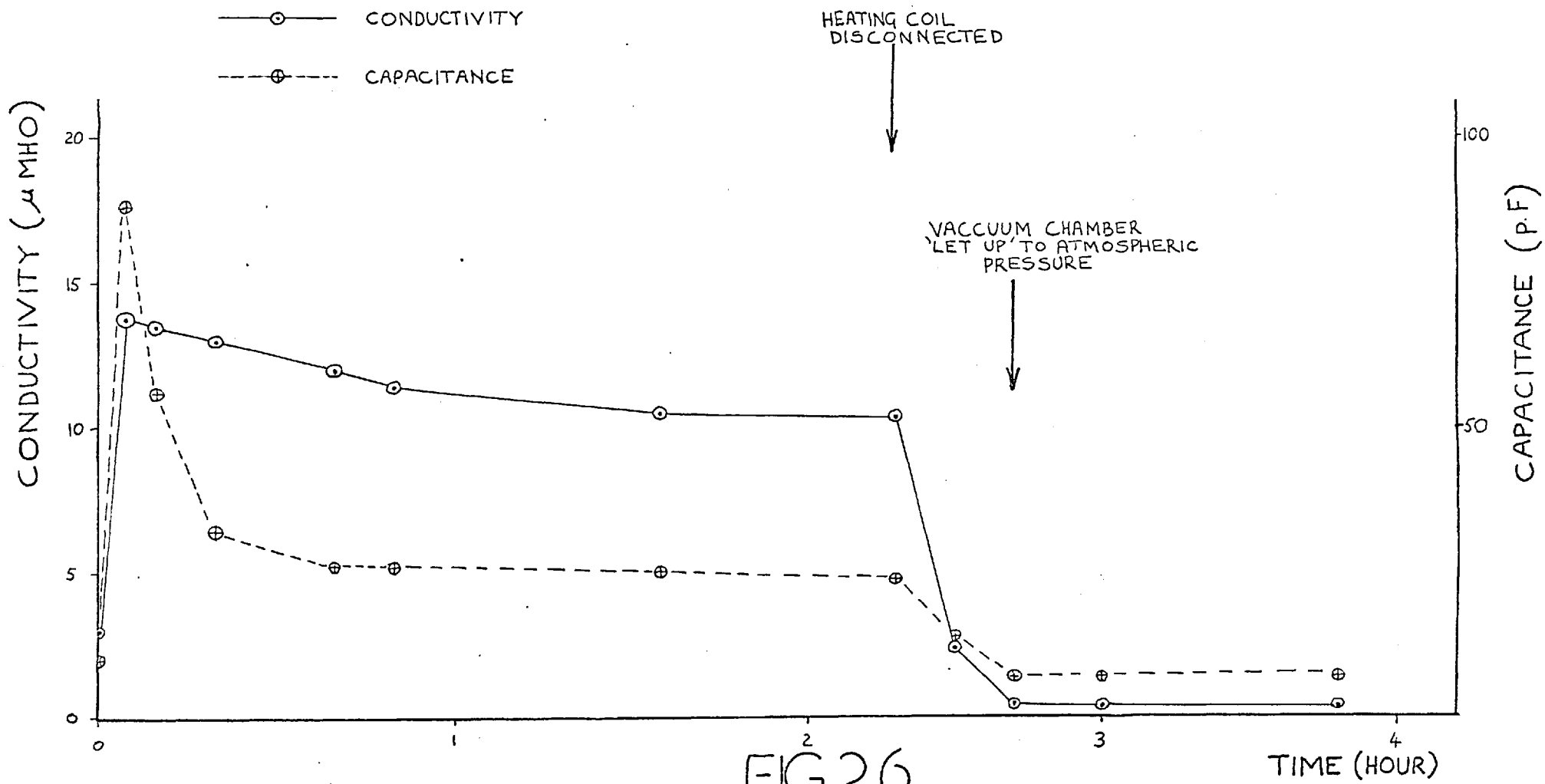

FIG.2.6

A GRAPH OF THE AMOUNT OF WATER DESORBED FROM A CARBON SPECIMEN

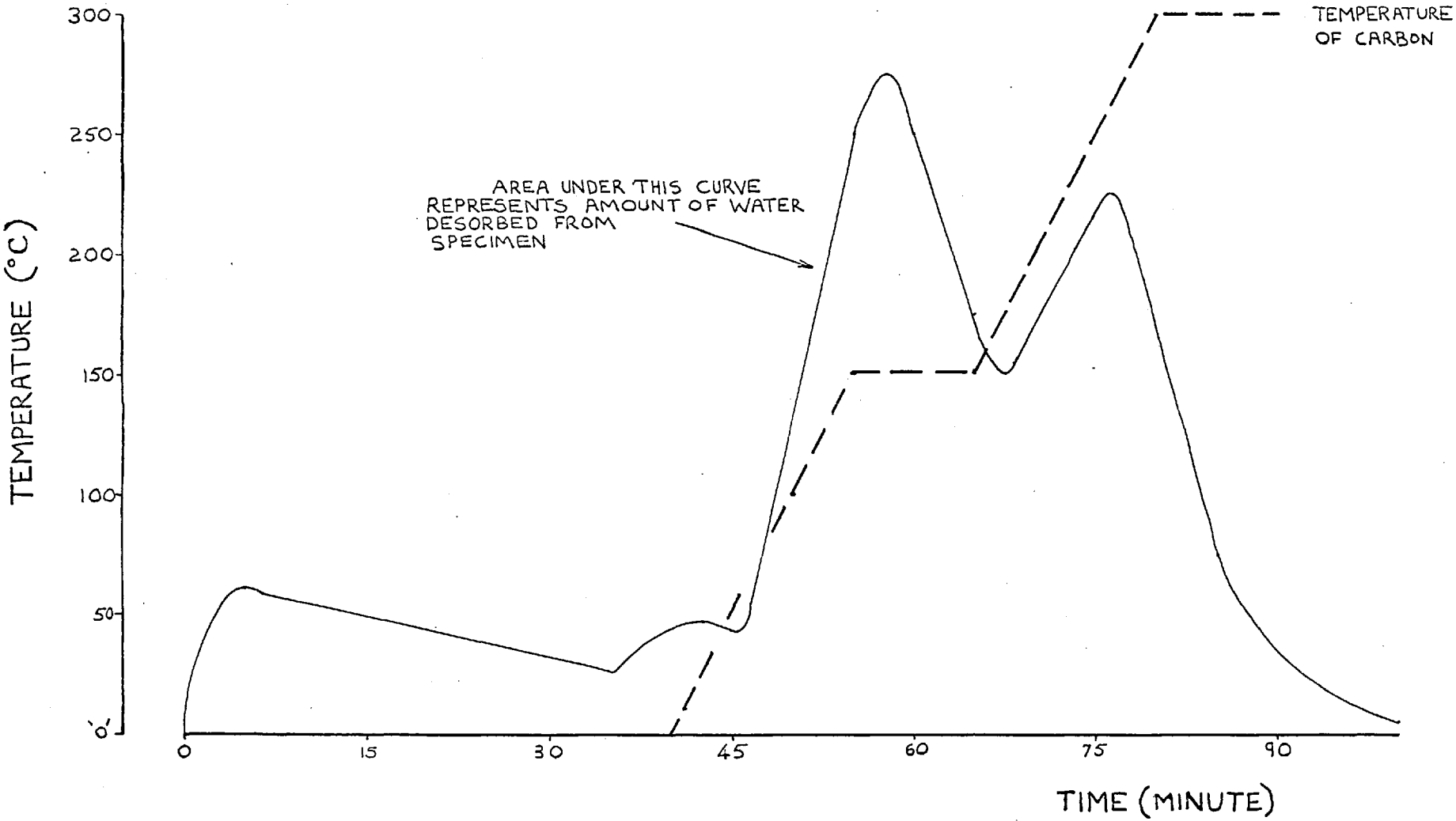

FIG.2.7

A TYPICAL CURRENT/VOLTAGE PLOT FOR A GLASS SPECIMEN

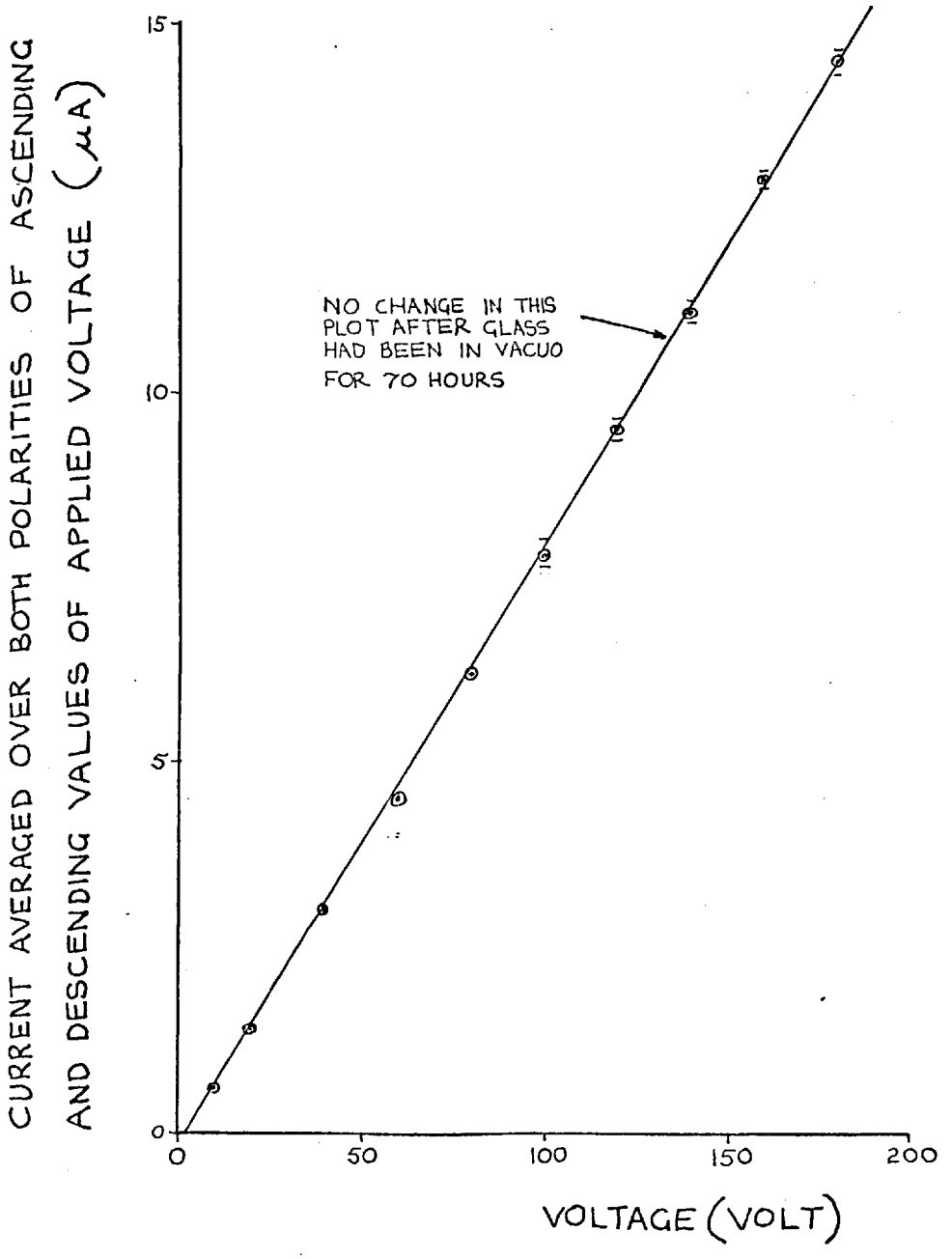

FIG. 2.8

A RESISTANCE/TEMPERATURE PLOT TO DETERMINE THE ACTIVATION ENERGY OF A SPECIMEN OF CARBON

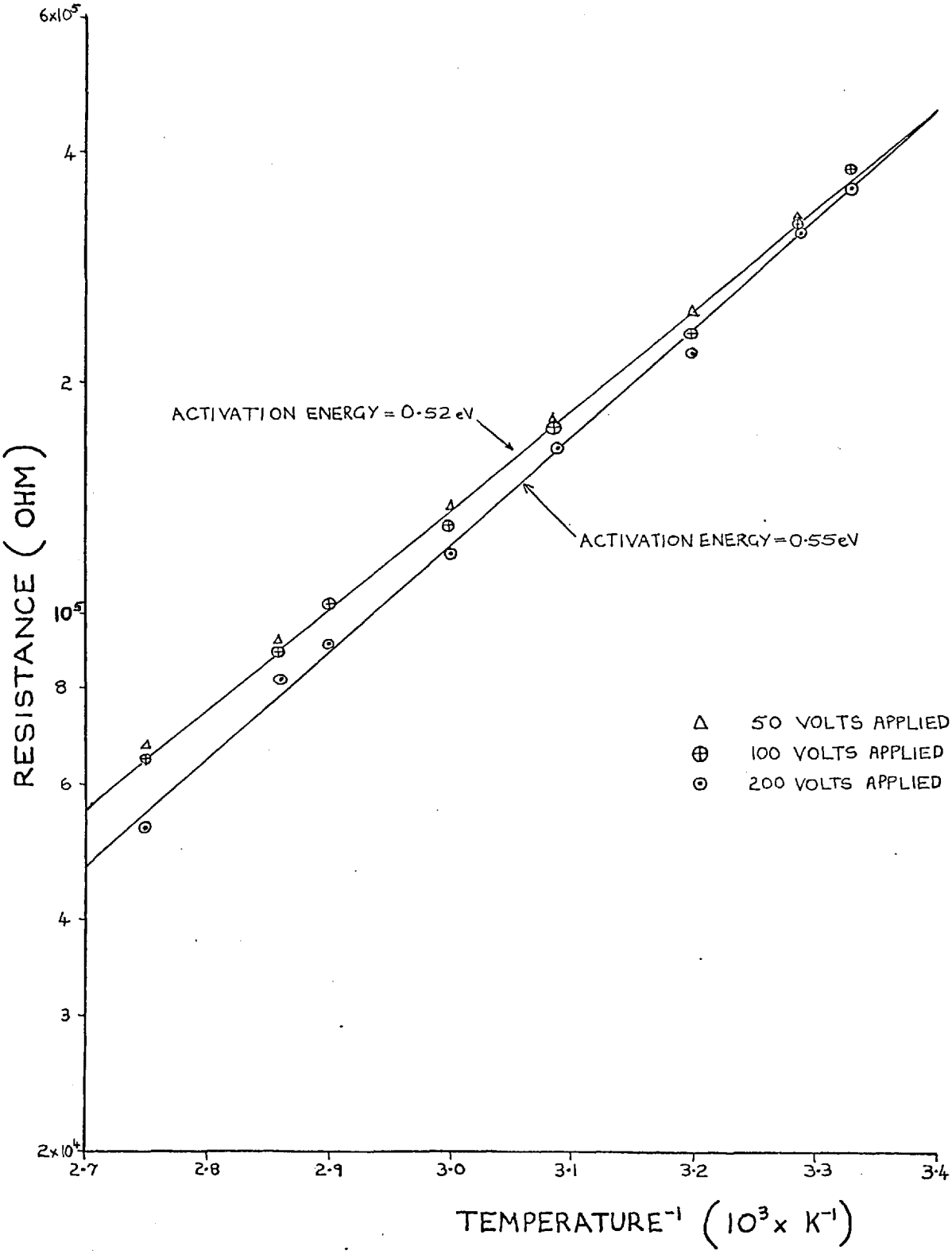

FIG.2.9

CHAPTER III

PRELIMINARY INVESTIGATIONS

The Johnsen-Rahbek effect involves not only the electrostatic attraction between contacting surfaces, but also the deformation of the surfaces due to the force generated and the complex phenomena such as etching, which occur in the interfacial gap. In this chapter the complications that these secondary effects cause in investigating the primary effect are shown and a new method of measuring the force is formulated and discussed.

3. 1 A STUDY OF THE INTERFACIAL GAP WITH A FIZEAU INTERFEROMETER

Accurate force measurements are of little use if the interfacial gap geometry is not known. The curvature and roughness of the specimens can easily be measured, but doubtless when they are placed together and a voltage applied the surfaces are deformed by the force generated between them. Previous workers have considered that significant deformation took place but few measurements were made.

3.1.1 APPARATUS

Deformation between two contacting surfaces can be observed with a Fizeau interferometer arrangement provided one contact member is transparent and its counter surface is optically reflective. This was achieved in the case of a semiconductor and metal in contact by substituting for the metal tin oxide coated glass, a surface conducting transparent material. The electrical conductivity of the surface coating was high and the electrical property of the contact was little altered upon substituting the glass. A potential difference could be applied across the interfacial gap and its subsequent deformation observed.

The apparatus constructed for this observation is shown in fig. 3.1. The deformation of the interface was observed by the collimated monochromatic light reflected from the semiconductor and that reflected from the contacting glass surface interfering and producing fringes. These interference fringes form a contour map of the relative position of the two surfaces. The separation between two fringes represents a change in the interfacial separation of approximately

0.3μm. Deformation of the surfaces is observed as a change in the fringe pattern.

3.1.2 EXPERIMENTAL METHOD

Three specimens of carbon with different surface geometries and different mountings, which provided different mechanical rigidities were used. Specimen 1 had a small radius of curvature while specimen 2 was flatter as can be seen from the fringe patterns they produced shown in fig. 3.3 and fig. 3.6 respectively. Specimen 3 had a complex surface geometry and it was more flexible than the previous specimens due to its being mounted on an epoxy resin backing. The former specimens were bonded with conducting epoxy resin to rigid aluminium bases 2mm thick.

The tin oxide coated glass plate used as the counter surface was 5 cm^2 in area and 2mm thick. A thicker plate than this would have been desireable to increase its rigidity. However, difficulties arose in the tin oxide coating process when thick glass was used as it had to be heated to just below its softening temperature, (about 400^{o}C), and the thicker the specimen the greater the possibility of its cracking, especially specimens greater than 2mm thick. Whether the deformation between the carbon and glass was due to one specimen or both is difficult to determine as calculations of it are very complex. However, the relative deformation can be assessed by comparing the Young's moduli of the specimens as these are the important constants in equations of elastic deformation. The Young's modulus of glass is typically between 4.5×10^{10} and 9×10^{10} Nm^{-2} (Bartenev), compared to $7 \times 10^{9} Nm^{-1}$ for the carbon. From this it would be considered that the carbon would deform more than the glass but it must be remembered that most carbon specimens had aluminium backing plates which increased the rigidity of the specimens and also that the mechanical properties of glass greatly depend on the surface condition of the specimen and its history. The glass specimens used in this experiment were of good surface finish but the effect of heating the specimens during the coating process is unknown. If the deformation was more 'plastic' than elastic then as

the glass is harder than the carbon it would deform less. Thus the carbon would deform more than the glass but to an unknown extent, so the results must be regarded as an approximate guide to the deformation occurring, and they will only be discussed qualitatively.

The glass was regarded as being flat in comparison to the curved specimens of carbon used in the experiment. The electrical circuit connected to the contacts is shown in fig. 3.2.

3.1.3 RESULTS

Specimen 1 showed a large increase in the contact area with applied voltage, fig.3.3. A measure of this contact is taken as the area of the first circular fringe. Fig. 3.5 shows how this deformation rapidly increased with the applied voltage and current flow. Adjusting the glass on the carbon, which moved the contact slightly and changed the interfacial gap geometry, produced a different rate of deformation upon the application of a voltage as shown in fig.3.4. The current flow was twice as high as that for the first position. Fig.3.4 also shows the hysteresis of the deformation, the fringe pattern not returning to its original shape.

Specimen 2, showed the fringe pattern to be changing slightly with time at 200 volts. The specimen was flatter than the previous specimen and the fringe pattern consisted of an area of uniform brightness except for 3 fringes around two 'high' spots. Gradually, over about half a minute the asperities were flattened, all the fringes disappearing except one.

Specimen 3 was very flexible and initially upon the application of about 350 volts it would rapidly deform until the whole surface was within 0.6 μm of the glass surface, only a few high spots separating them. After high voltages had been applied for about 15 minutes the surface was found to have been dulled by etching which could be seen with the naked eye. The surface initially had been of high surface finish with a roughness of 0.03 μm C.L.A. With the further application of voltages up to 500 volts the area of close contact started to diminish

and the fringes began to gradually broaden becoming more diffuse as the surface roughened. Fig.3.7 shows the deformation of this specimen after initial applications of high voltage had dulled it. After 500 volts had been applied for a few minutes the current started to decrease and the surfaces started to peel apart. This was due to the roughening of the carbon surface diminishing the attractive force. Profilometer traces of the carbon showed it to have roughened from 0.03 μm C.L.A., (before any voltage was applied), to 0.29 μm C.L.A. during 30 minutes of use in the interferometer with voltages of up to 500 volts having been applied. The glass was not affected.

As with all the other specimens used, specimen 3 was maintained at a negative potential with respect to the glass, the opposite polarity producing more severe etching. This is discussed further in Chapter 9.

3.1.4. DISCUSSION

Specimen 1 which had a very curved surface showed a lot of deformation. The hysteresis of the deformation, fig.3.4, was considered to be due to a permanent deformation of the carbon or the crushing of surface asperities. Another indication of this permanent change was the decrease in roughness during the investigation, the roughness before being 0.17 μm C.L.A. and that afterwards being 0.14 μm C.L.A. The change in the current flow upon adjusting the glass illustrates the difficulty of obtaining a consistent characteristic current/voltage relationship for such a specimen. Indeed measurement of the characteristic with this specimen against a mild steel plate produced many inconsistent and different relationships. The change in the rate of deformation also indicates that the force generated at a given voltage had changed.

The results obtained with specimen 2 show high spots being crushed. These high spots could have been irregular asperities, polishing powder embedded in the carbon, or just dust particles, although the specimens were thoroughly cleaned before use. The results support the theory that permanent deformation of the carbon surface occurs when the effect is generated, as was considered to be happening with specimen 1. This theory is also supported by the fact that

Leveson attributed the ageing of his specimens, (slipping the carbon about 5 times against the steel plate at high voltages), before consistent measurements could be obtained,to the crushing of these irregularities.

Specimen 3 demonstrated how a flexible specimen could be deformed to a large extent and also how etching in the atmosphere could roughen a surface and reduce the force, shown by the surfaces peeling apart.

These experiments demonstrate that the carbon deforms relative to the glass to an extent depending on its surface geometry and mechanical rigidity. This means that the force generated by the effect depends on the geometry and mechanical properties of the specimen of carbon used. The force is also affected during the application of a voltage by the etching occurring in the gap which must also be taken into account when force measurements are made.

The different geometries and mechanical properties of the specimens used by previous workers probably account for the discrepancies between their results.

3. 2 FORCE MEASUREMENT

As the Johnsen-Rahbek force is a function of the gap width between the contact members any separation of them alters the force. Unfortunately a force cannot easily be measured without displacing its point of action slightly. Hence it is difficult to accurately measure the force. When the surfaces are pulled apart under an applied voltage they tend to peel apart giving an inaccurate measurement. Shearing the contacts, however, avoids this peeling and measures the actual force which is generated in a working device. This was initially considered to be the best method of measuring the force and so an apparatus similar to Leveson's was built.

3.2.1 APPARATUS

The apparatus is shown in fig. 3. 8 It consists of a mild steel plate mounted horizontally, on top of which rests a carbon specimen with an aluminium backing. The lever was capable of applying a tangential force of 4ON to the carbon and strain gauges mounted on the lever monitored this force. When the

mechanical force applied through the lever equalled the frictional force the carbon slipped. Knowing the coefficient of friction the normal electrostatic force could be calculated. The apparatus was maintained in a vacuum system capable of a pressure of 10^{-5} torr to avoid excessive etching. The voltage and current were measured with the circuit shown in fig. 3.9.

3.2.2 EXPERIMENTAL METHOD

Measurements were made with a carbon specimen of roughness 0.38 μm C.L.A. and a curvature of 13m, against a steel plate of 0.17 μm C.L.A. with a curvature of 40m.* The specimens were thoroughly cleaned with acetone and iso-propyl alcohol, the procedure being described in more detail in Chapter 4.

The carbon was initially slipped against the steel six times at 500 volts to age the specimens which Leveson had said was necessary for consistent readings. During the measurements the carbon was maintained at a negative potential with respect to the steel plate to reduce any etching. Force measurements were made with increasing applied voltage and the current flow was measured before and after each force measurement.

The coefficient of friction between the carbon and steel was measured by mechanically loading the carbon and measuring the tangential force to produce slip. From these measurements it was calculated to be 0.3

3.2.3 RESULTS

The force measurements made with these contacts are shown in the graph of fig.3.10 Two sets of force measurements were made, the first set making the upper graph, the second making the lower graph. The corresponding current measurements are shown in fig.3.11, these show the current to have varied during each force measurement.

3.2.4 DISCUSSION

The two sets of force measurements are not very consistent, probably due to changing conditions at the interface and in the carbon. These will be discussed

* Determined from optical flat

in detail later but are mentioned here to indicate that the force measurements are rather inconsistent.

The voltage applied to the two contacts is not the same as the voltage appearing across the interfacial gap. The bulk resistance of the carbon, R_B, where

$$R_B = \frac{\rho l}{A} \qquad (3.2.1)$$

l being the specimen thickness and A its surface area, is of the order of $10^5 \Omega$ and with currents of the order of 1 mA flowing, a significant fraction of the applied voltage is dropped across the bulk. Futhermore, the calculation of the interfacial voltage is subject to the variation of the current at that particular voltage. Even if there was no variation in the current the calculation of the interfacial voltage would only be approximate as the voltage varies across the surface. So the inconsistency of the force measurement is added to the error in calculating the interfacial voltage in determining the relationship between the two.

Further inaccuracy in determining the Johnsen-Rahbek force is introduced by the assumption that the coefficient of friction is constant. The coefficient of friction of carbon varies with the environment and the absorbed gases, (Braithwaite). It is also likely to change as the roughness of the carbon is altered slightly with the force measurements.

Investigation of the effect was also hindered by the deformation of the interfacial gap and the area of mechanical contact not being known. Also, as will be shown later, the force is significantly reduced when the area of mechanical contact is large, as it is when the members are in contact.

When the surfaces were examined after the measurements little damage was found. When similar specimens were used for measurements in the atmosphere they were found to be severely etched, (fig. 3. 12). Voltages up to 500 volts had been applied to them and the polarity altered during the experiment. The surface profiles taken before and after the measurements are shown in fig. 3. 13. These

results demonstrate that the environment in which the measurements are made can easily affect the surfaces and hence alter the force.

3. 3 CONCLUSION

The results of these initial experiments demonstrate the Johnsen-Rahbek effect to be complicated by many interdependent phenomena occurring in the interfacial gap. The interfacial gap has been shown to alter when the effect is generated between the two surfaces and the shearing of the surfaces to measure the force tends to change the force produced.

To investigate the effect a contact is required to produce the force in a simple, well defined situation, reducing the variables complicating the previous results. Such a contact is that between a metal ball in contact with a flat semiconducting disc. The interfacial gap is well defined and symmetrical and the deformation can be assessed.

The force produced can be accurately measured by separating the surfaces as the peeling occurring when flat specimens are separated is reduced by the electrical force being symmetrical. The symmetrical contact between the ball and flat also enables the current/voltage relationship to be analysed more easily. This was not the case with the specimens used in the present experiment where large currents tended to heat the carbon, altering its temperature and desorbing it, producing a variable current for a given voltage.

The difficulty of having to produce specimens with surfaces equally flat so that the measurements made with them would be comparable is avoided with the 'ball-on-flat' method. Provided the curvature of the semiconductor's surface is significantly less than that of the ball, it is of negligible importance, but the surface finish must be reasonably high for experimentally measureable forces to be produced.

Many reasons can be given for using the ball-on-flat method to investigate the effect but the basic reason for its use is that it yields results capable of quantitative rather than qualitative analysis. Most of the subsequent thesis will be devoted to analysing the effect with this method.

THE PRINCIPLE OF THE FIZEAU INTERFEROMETER

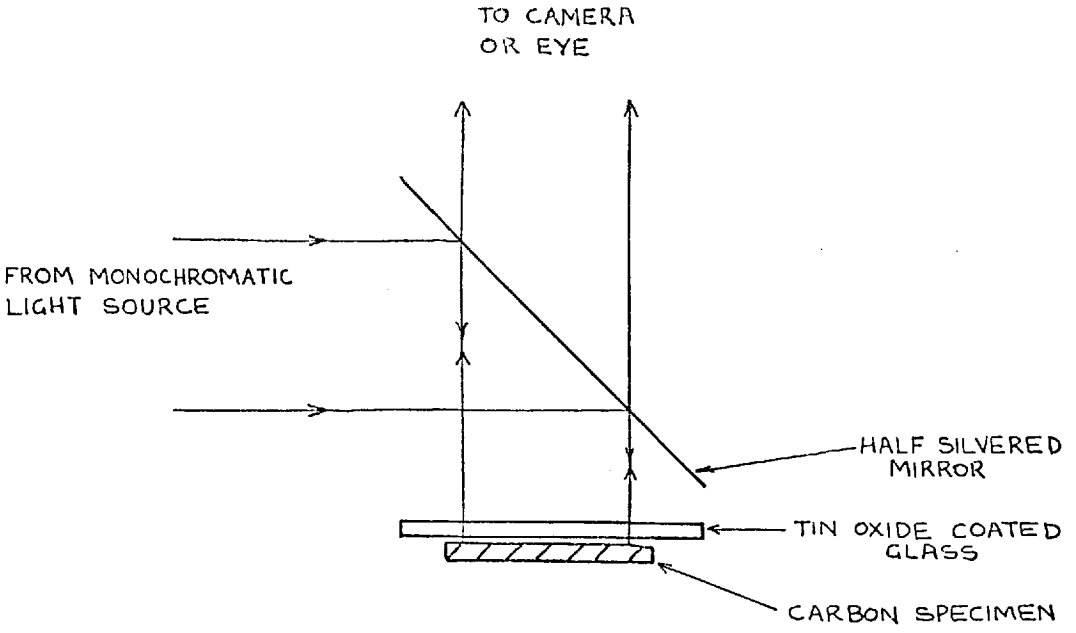

FIG.3.1

THE ELECTRIC CIRCUIT USED IN THE FIZEAU INTERFEROMETER

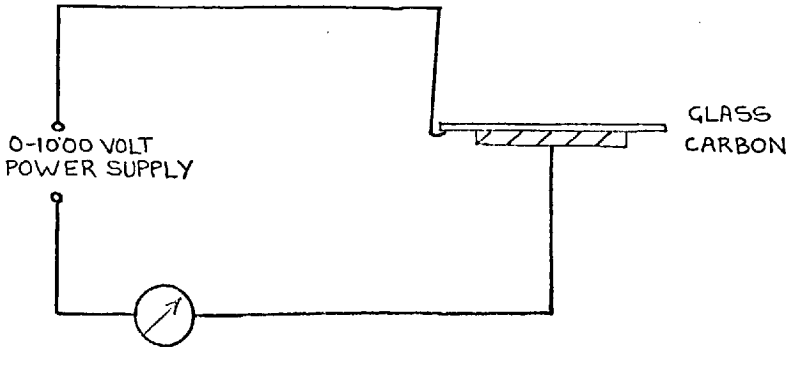

FIG.3.2

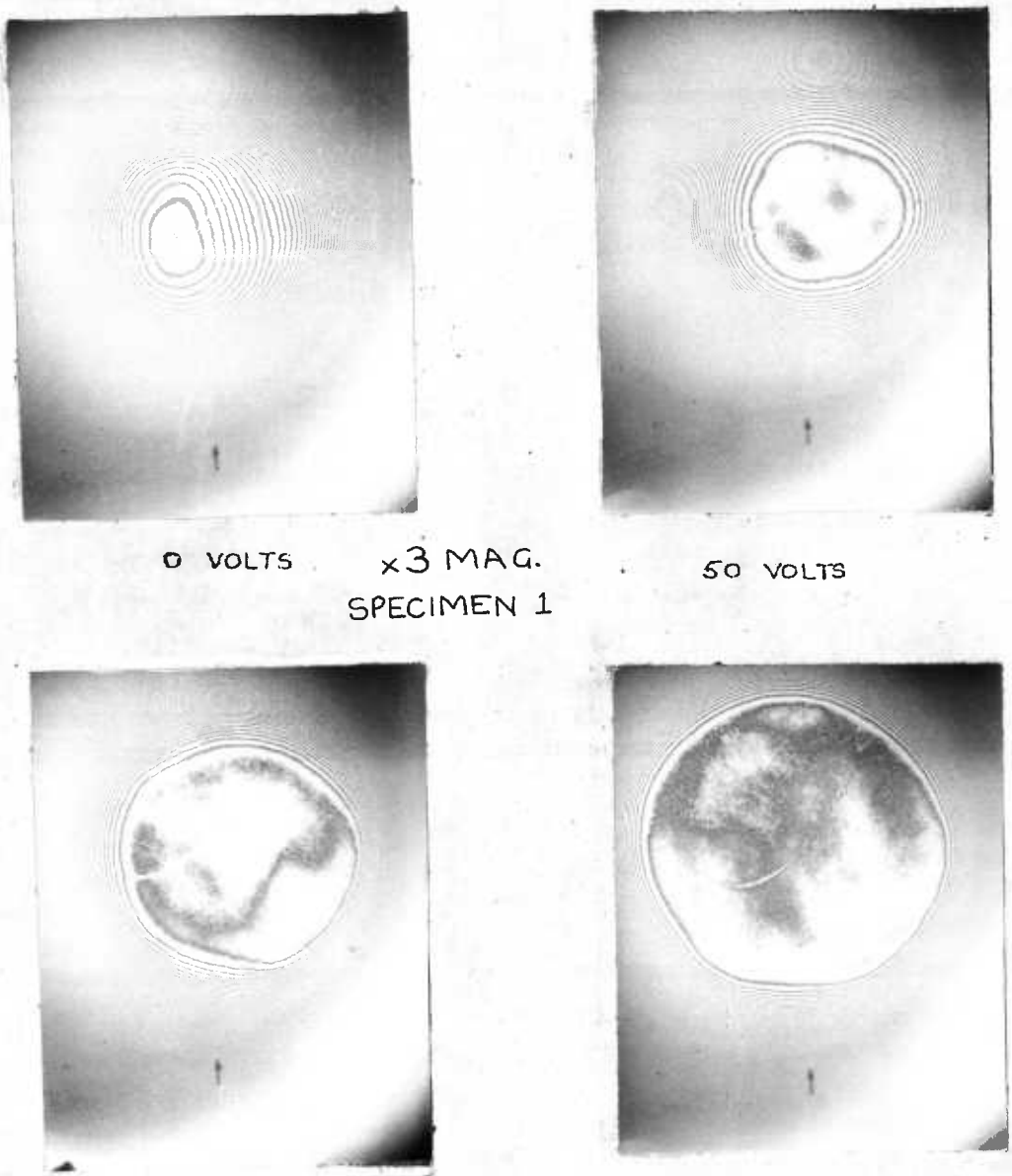
0 VOLTS
x3 MAG.
SPECIMEN 1
50 VOLTS
200 VOLTS
500 VOLTS

FIG.3.3

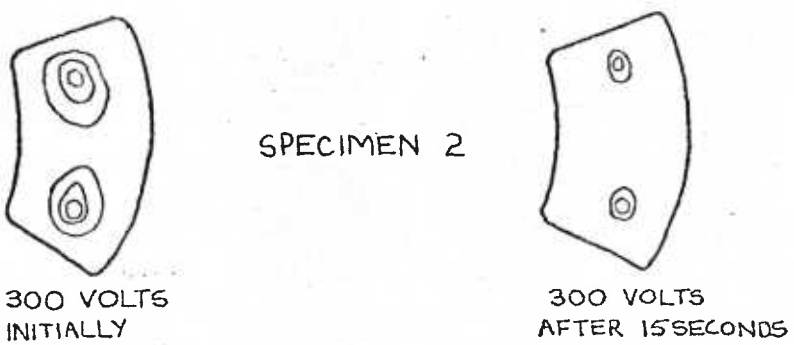
SPECIMEN 2
300 VOLTS
INITIALLY
300 VOLTS
AFTER 15 SECONDS

FIG.3.6

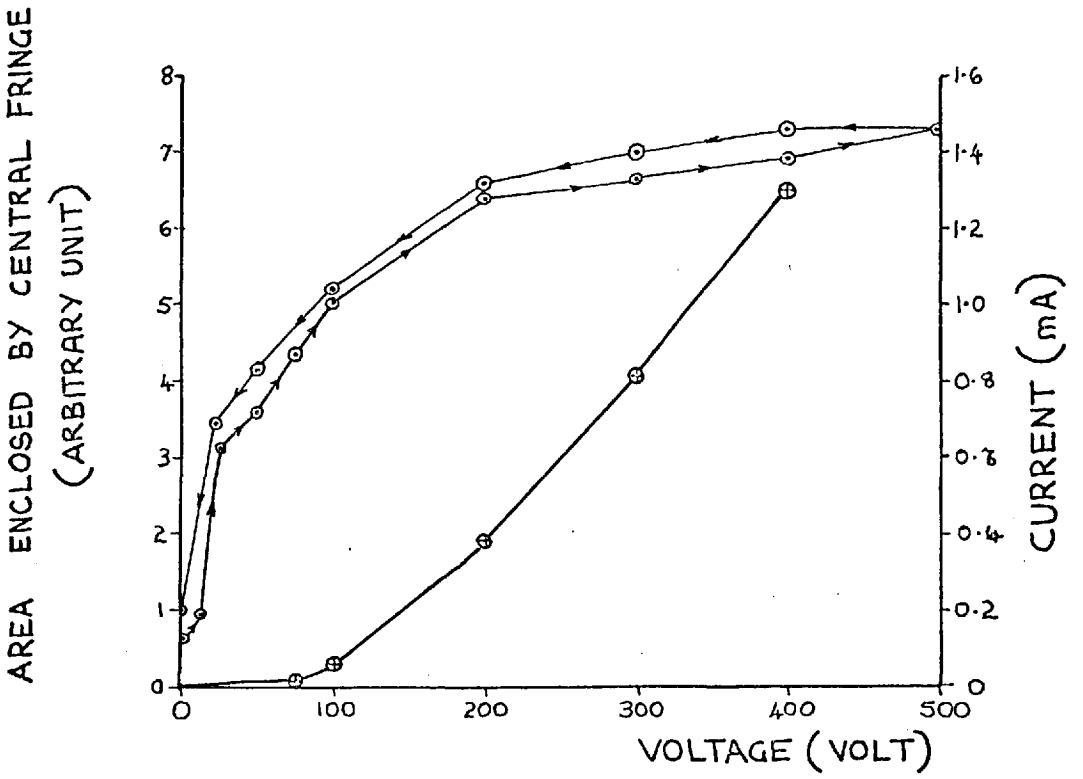

FIG.3.4

—⊙— AREA

—⊕— CURRENT

GRAPHS OF CONTACT AREA AND CURRENT FOR CARBON SPECIMEN I IN DIFFERENT POSITIONS

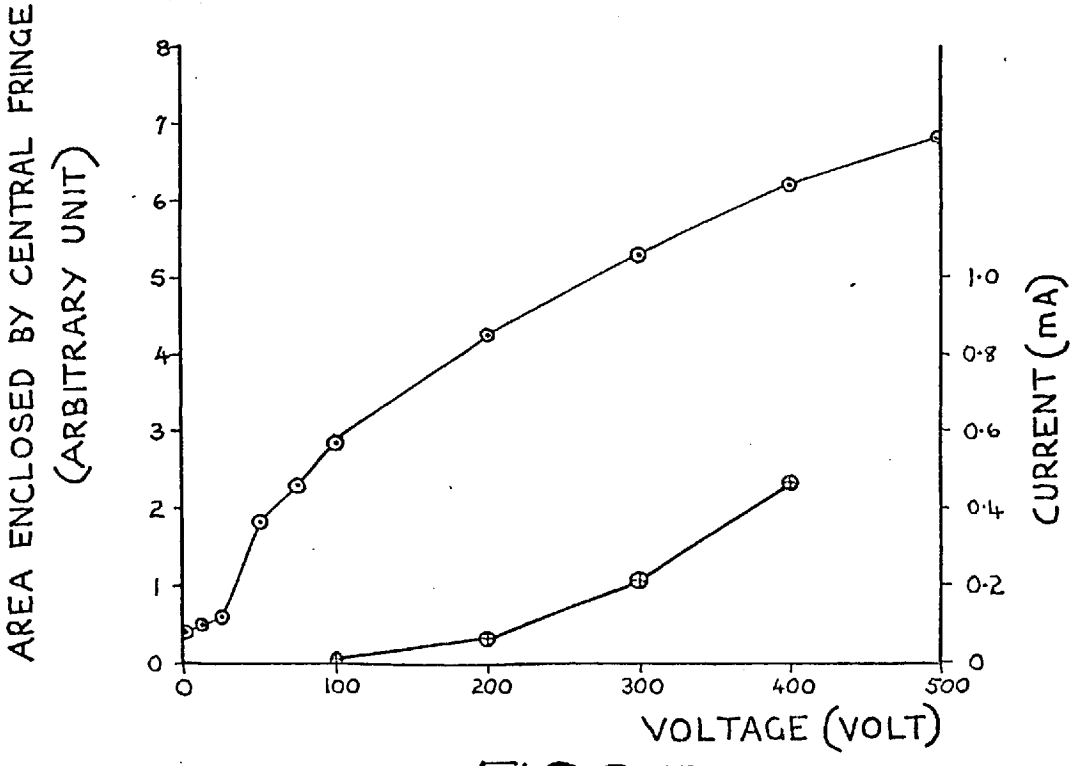

FIG.3.5

100 VOLTS

300 VOLTS

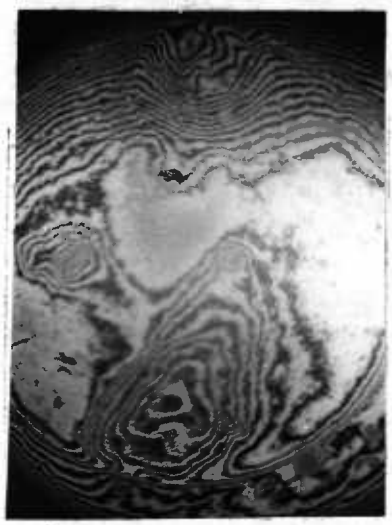

450 VOLTS

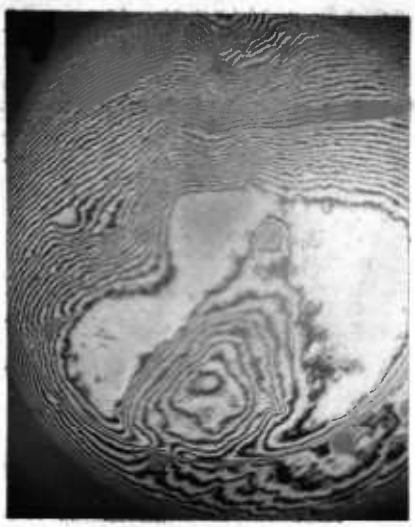

500 VOLTS

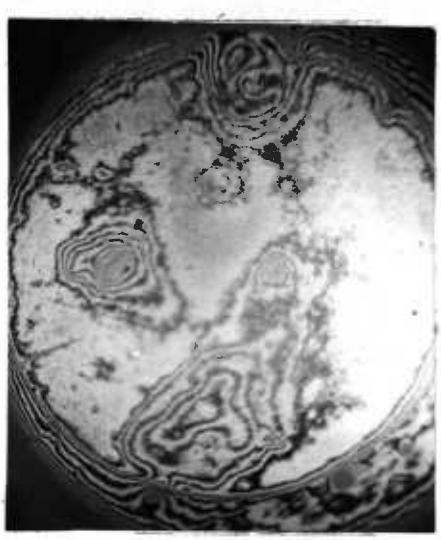

500 VOLTS
PREVIOUS RUN

CARBON SPECIMEN
AFTER EXPERIMENT

×2 MAG.
SPECIMEN 3

FIG.3.7

INITIAL FORCE MEASURING APPARATUS

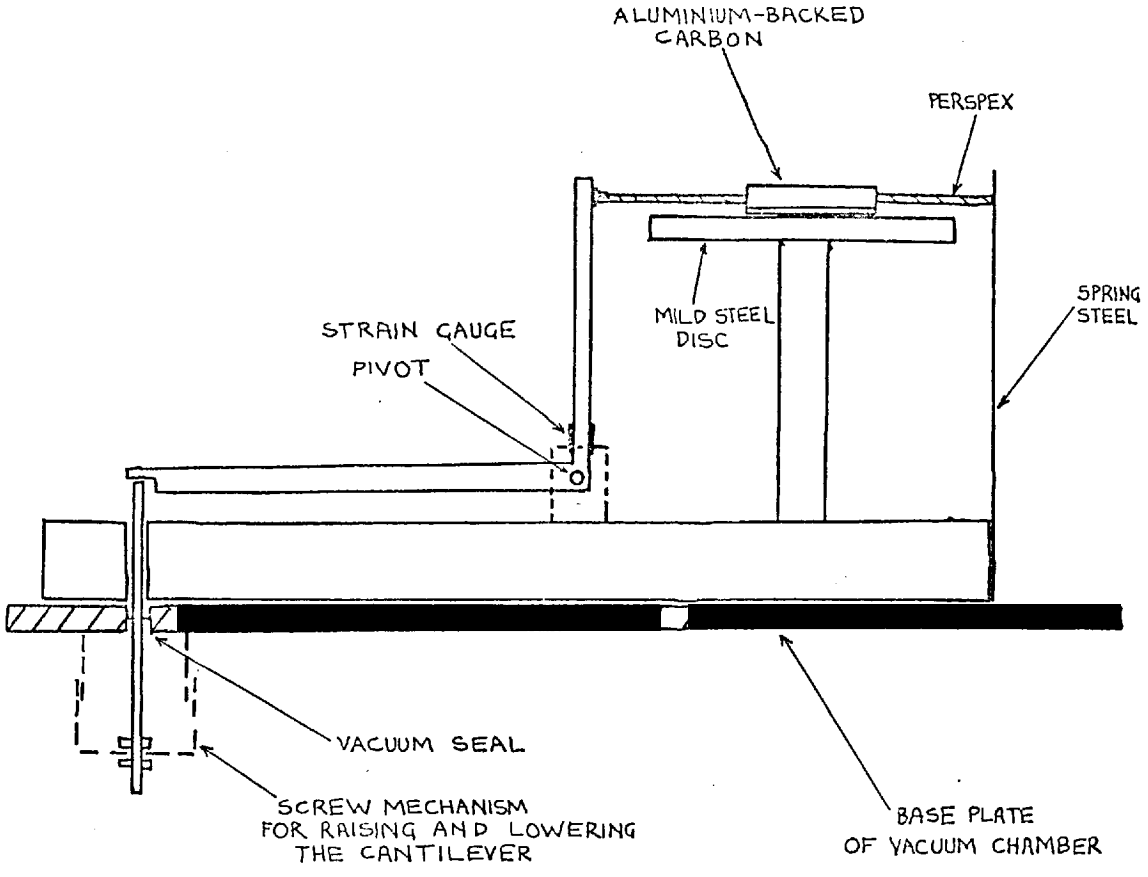

FIG.3.8

ELECTRIC CIRCUIT FOR INITIAL FORCE MEASUREMENTS

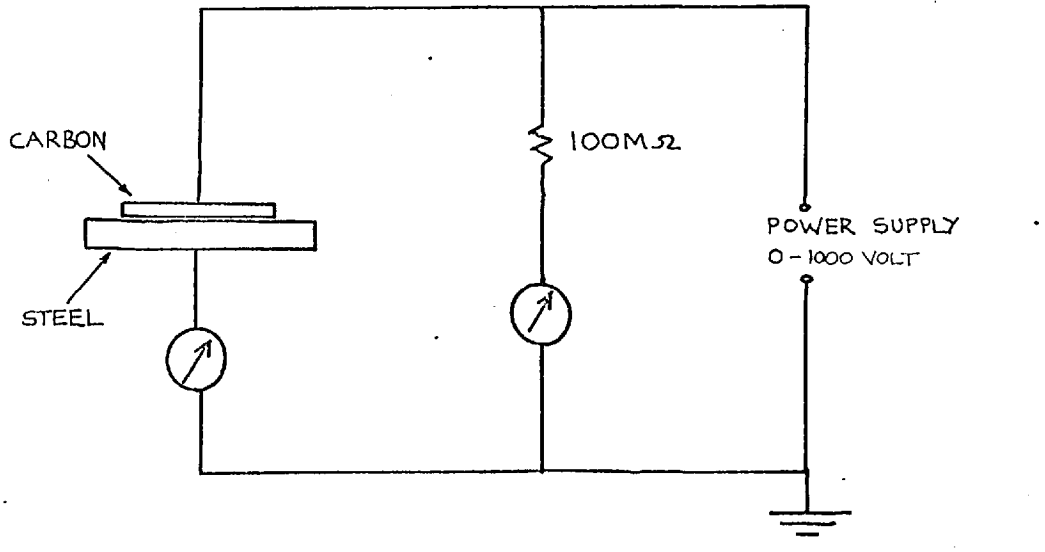

FIG.3.9

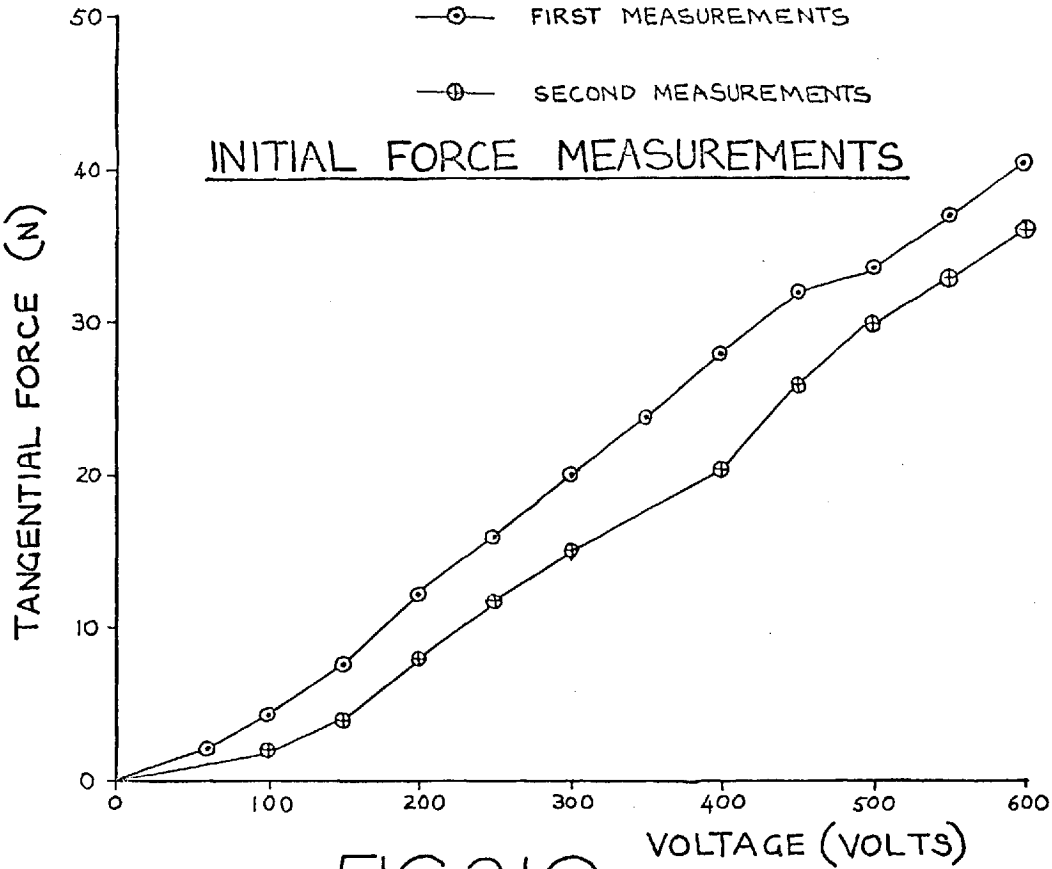

FIG.3.10

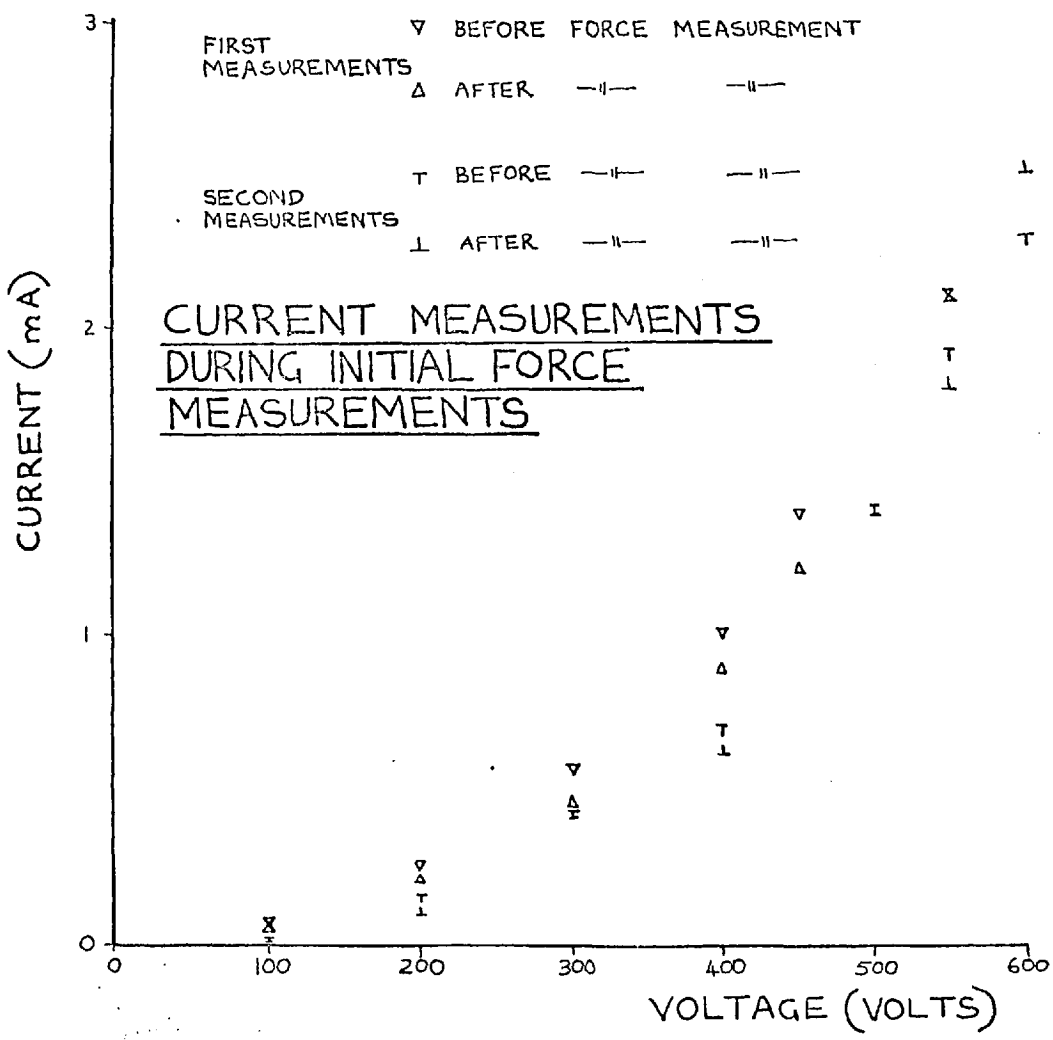

FIG.3.11

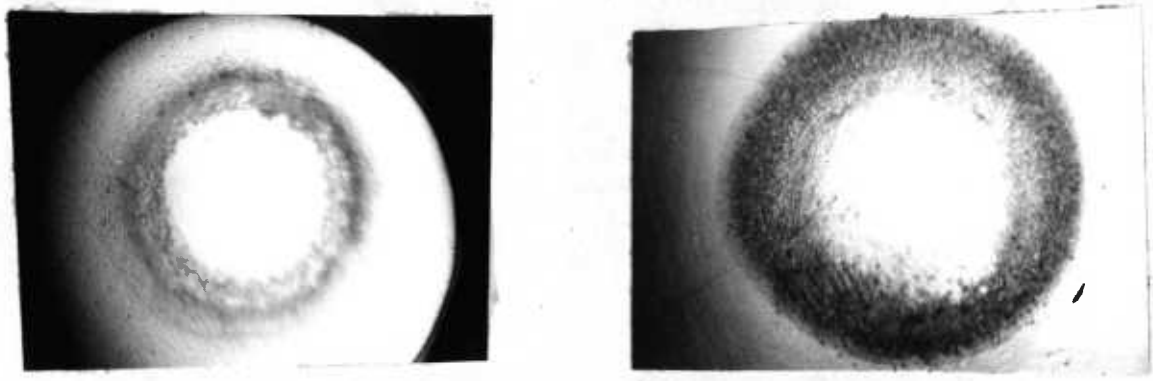

×2 MAG.

FIG.3.12

CARBON MILD STEEL

AFTER

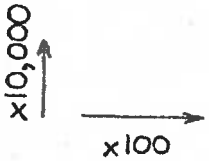

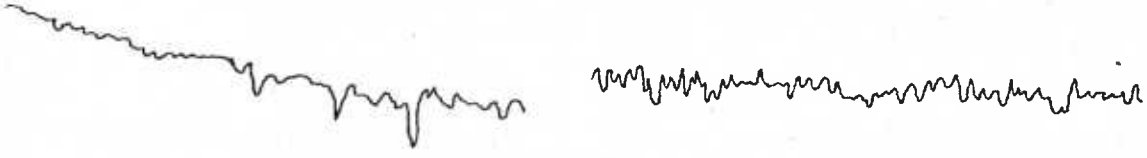

BEFORE

FIG.3.13

CHAPTER IV

MEASUREMENT OF THE JOHNSEN-RAHBEK FORCE

In the previous chapter the difficulties involved in measuring the Johnsen-Rahbek force were discussed and a more accurate method of measurement was proposed. In this chapter the method is developed and taken from theory to practice. An apparatus was built to measure the force and the measurements made with it are discussed.

4. 1 FORCE BETWEEN A METAL BALL AND SEMICONDUCTING FLAT

The theory developed in this section is based on the formulae of Sillars who derived the current/voltage relationship and the electric field in the interfacial gap of a metal ball in contact with a flat semiconductor. He stated that it was most probable that at high fields a current flowed across the gap around the mechanical contact. Over this region of current flow the field is assumed to be constant, at a value E_o, regardless of the applied voltage.
The basis of this assumption, as mentioned in Chapter 1, is that the semiconductor's resistance limits the current flow and hence the interfacial voltage across the region of current flow which sustains the electric field. Appendix 1 shows this assumption to be valid.

Denoting the radius of the mechanical contact (fig.4.1), as d, (m), the radius of the current emitting region c (m),and r (m), denoting a general radius the following assumptions are made in deriving the equation of the force:

(i) the force is developed over a region where $r \ll R$, R,(m) being the ball radius, so that

$$2R\Delta = r^2 \qquad (4.1.1)$$

(ii) $$d \ll c \qquad (4.1.2)$$

(iii) the semiconductor is of infinite extent so that the only resistance to current flow is that of the constriction.

Assumption (ii) is based on the fact that the force is measured by separating the surfaces, and presumeably when these part d is negligible and the approximation is justified. Experimental evidence was found to justify the approximation and it is discussed in more detail later.

Assumption (iii) was deemed valid as the bulk resistance of the specimens

used was negligible compared with the constriction resistance of the contact. The specimens were not of infinite extent, however, but their finite dimensions did not significantly alter the resistance of the constriction as the ratio of the thickness of the specimen to the radius of mechanical contact, h/a, was $\geqslant$ 10, (Foxhall & Lewis).

Solving Laplace's equation for the ball and flat, Sillars obtained;

$$c^2 = \frac{RV_o}{E_o} \qquad (4.1.3)$$

$$I = \frac{8}{3\rho}\left(\frac{R}{E_o}\right)^{\frac{1}{2}} V_o^{3/2} \qquad (4.1.4)$$

where I is the current, (amps), and V_o the total voltage applied to the system. To calculate the force of attraction the interfacial voltage, V_{int} is required. Sillars' equation for this is:

$$V_{int} = \left(\frac{4E_o}{\pi R}\right)\int_d^c a\cos^{-1}\left\{\frac{a}{r}\right\} da, \quad r \geqslant c \qquad (4.1.5)$$

Using assumption (ii) and integrating this becomes :

$$V_{int} = \left(\frac{E_o r^2}{\pi R}\right)\left\{\left(\frac{2c^2 - r^2}{r^2}\right)\cos^{-1}\left(\frac{c}{r}\right) - \frac{\left(r^2 - c^2\right)^{\frac{1}{2}}}{r^2}c + \frac{\pi}{2}\right\} \qquad (4.1.6)$$

This interfacial voltage produces a field, V_{int}/Δ, in the gap where $r \geqslant c$, which from eq. (1.1.1) creates a force :

$$F_{N\,E} = \int_{1.0}^{\infty}\left(\frac{4\epsilon_o E_o^2 c^2 \lambda}{\pi}\right)\left\{\left(\frac{2-\lambda^2}{\lambda^2}\right)\cos^{-1}\left(\frac{1}{\lambda}\right) - \frac{\left(\lambda^2-1\right)^{\frac{1}{2}}}{\lambda^2} + \left(\frac{\pi}{2}\right)\right\}^2 d\lambda \quad (N) \qquad (4.1.7)$$

where $\lambda = r/c$ and F_{NE} denotes the force over that region of the gap, where no current flows. The upper limit of integration taken as $\lambda = 15.0$ beyond which the integral is effectively zero.

The region of current flow across the gap, $0 \leq r \leq c$, produces the force:

$$F_E = \frac{\epsilon_o \pi c^2 E_o^2}{2} \quad (N) \qquad (4.1.8)$$

again using eq. (1.1.1)

Eq.(4.1.7) evaluated by numerical integration this yields :

$$F_{NE} = 0.98 \epsilon_o \pi c^2 E_o^2 \qquad (4.1.9)$$

The total force, F_T is given by :

$$F_T = F_{NE} + F_E = 1.48 \epsilon_o \pi c^2 E_o^2 \qquad (4.1.10)$$

Upon combining with eq. (4.1.3) one obtains :

$$F_T = 1.48 \epsilon_o \pi R V_o E_o \quad (N) \qquad (4.1.11)$$

4.2 APPARATUS

The apparatus to measure the Johnsen-Rahbek force between a ball and flat is shown in fig. (4.2).

There was a certain amount of friction in the pivot due to the lever having a groove in it, into which the razor edge fitted loosely, ensuring that the pivot position on the lever did not alter and that the lever did not twist on the pivot. Riders attached to the underside of the lever prevented the mechanical force, applied through the cantilever, from lifting it off the pivot. The

semiconductor was attached to the lever with conducting silver paint in the case of the glass specimens or bolting it on in the case of the carbon specimens which had studs attached to aluminium base plates. For both the carbon and the glass specimens good electrical contact was ensured as these were connected into the electrical circuit by a wire attached to the razor edge pivot. To ensure that the ball was insulated from the pivot its supporting table was made of perspex.

A mechanical force could be applied to the lever by the cantilever being moved up by a screw mechanism connected through the top plate of the vacuum chamber. The screw mechanism was arranged so as to move the cantilever up and down only, (see fig.4.3), the movement being 1.0 mm per turn.

The cantilever was made of spring steel and two strain gauges attached to either side of it near its clamped end enabled the mechanical force it applied to the lever to be monitored. The strain gauges formed a bridge circuit supplied by a constant voltage supply, the offset voltage of the bridge recorded by a D.V.M. corresponding to the force applied. The D.V.M. was sensitive to 0.01 mV, which corresponded to 0.28 gm.f. applied to the lever.

The whole apparatus was kept in a vacuum system capable of a vacuum of 10^{-5} torr maintained by an oil diffusion pump and a rotary backing pump as shown in fig.4.3. A vacuum was required to reduce the contamination of the contact surfaces due to atmospheric absorption and adsorption which could affect the force obtained and the current flow in the gap, (this is discussed later), and to provide a consistent environment and prevent breakdown between parts of the apparatus at high voltages.

4.3 EXPERIMENTAL METHOD

The balls used in the measurements had been polished to a mirror finish and then stored in an evacuated desiccator. Immediately before insertion into

the apparatus each ball was then polished for a few minutes with 1μm diamond paste on a hand held polishing cloth to remove any tarnish accumulated since it was last polished. It was then cleaned three times with paper tissues soaked in iso-propyl alcohol. This was repeated with tissues soaked in acetone. The proceedure was followed again with lint free tissues and ended by wiping the ball with dry lint free tissues to remove any dust. The ball was then inserted into the apparatus.

The semiconductor specimen was likewise quickly polished with rouge and then cleaned and inserted. Absolute cleanliness was not acheived by this process but it was considered that the specimens were as clean as, or cleaner than, those that would be used in a device.

Upon insertion of the semiconductor the lever often needed slight biasing to get the semiconductor in touching contact with the ball. This was done by adding small wire riders to it. Then the thread from the cantilever was attached to the lever and adjusted until it was vertical. The chamber was then evacuated to a pressure of 10^{-5} torr over a period of about one hour.

To investigate the electrical characteristics of the contact a current/voltage plot was recorded on an XY recorder connected to the circuit shown in fig. 4.4. The applied voltage was decreased by allowing the voltage across a 0.25μF capacitor to decay from about 350 volts. A capacitor was used as it produced a steady decay of voltage obviating the attendant noise produced in reducing the voltage by means of a variable transformer or other potentiometric device. A current/voltage plot was made for both polarities of voltage applied to the semiconductor and the ball. These plots will be referred to as "static IV plots"; "dynamic IV plots" referring to the current/voltage plot when the ball and flat are being separated. The XY recorder traced plots accurate to approximately 5% of voltage and current. More accurate values if required were obtained from the meters in the circuit.

It was found that there was little leakage current across the semi-conductor when a guard ring of conducting silver was painted around the outside of a piece of carbon and the current between it and the ball was measured with and without the guard ring in circuit, (fig. 4.5). The measurements were done under vacuum conditions and on the strength of these measurements guard rings were considered unnecessary for obtaining accurate readings of current in subsequent experiments.

To measure the force between the ball and flat approximately 350 volts was applied between them and a mechanical force was applied to the contact via the cantilever. The power supply was then disconnected from the circuit allowing the capacitor voltage to decay through the contact and the circuit. When the mechanical force equalled the Johnsen-Rahbek attractive force the surfaces separated, displayed on the XY recorder by the current of the dynamic IV plot falling to zero, (fig. 4.6). To ensure accuracy the voltage through the capacitor was allowed to decay twice more with the same mechanical force applied to the contact. The accuracy of the value of the voltage at break, V_{BR} was 6 %* approximately. The corresponding value of current, I_{BR}, was accurate to better than 13%*.

For the same mechanical force three more measurements of break voltage were made with the polarity of the voltage applied to the ball and flat reversed.

About 40 separations were made to form a set of readings for analysing the force/voltage relationship up to 350 volts. and up to about 15gm. f. After a set of readings had been made, which took about 20 minutes, another static IV plot was taken to find if there was any change in the contact during the force measurements.

Fig. 4.6 shows that there was vibration of the contact during the force measurements just before the contacts separated. This was due to the electrostatic force varying with the relative positions of the contacts. The dynamics of the force measurements, i.e. the rate of decay of the voltage

* standard deviation

and the speed of separation of the contacts, affect the measurement and as such the results following are to a degree unique to the measuring system employing a 0.25 μf value capacitor. This is discussed in more detail later.

4.4 RESULTS

Force measurements were made with specimens of conducting glass and semi-pyrolised carbon. The carbon specimen was kidney shaped, 2.5 cm^2 in area, 1mm thick, flat to a curvature of 20m and had a roughness of 0.014 μm C.L.A. The glass specimen of resistivity 7.4×10^3 Ωm, had a surface area of 1.45 cm^2, was 2.7 mm thick, flat to a curvature of 6m and had a roughness of 0.03 μm C.L.A.

4.4.1 CARBON RESULTS

In order to verify the equation,(4.1.11)force measurements were made with three different steel balls of diameters 5.08, 3.18 and 2.54 cm (i.e. 2", $\frac{5"}{4}$ and 1") in contact with the same specimen of carbon. The force/voltage relationship for all measurements was linear. The slopes and intercepts of the straight line graphs were calculated using the least squares method, (Barford). The saturation electric field, E_o, was calculated from the slope of the graph and the values obtained from the measurements are shown in table 4.1. All three balls produced approximately the same value of E_o demonstrating that eq. (4.1.11) was valid. There was, however, a significant difference between the value of E_o when the carbon was at a negative potential with respect to the ball than when it was positive.

More than one set of force measurements was taken for each ball as the static IV plot taken after a set showed the current to have decreased,(table 4.2), and the further sets were taken to see if the value of E_o changed. It was found to be altered slightly as can be seen from table 4.1, measurements subsequent to the initial set showing a lower value of E_o.

Although the determination of E_o from the graphs of force measurements was accurate to a few per cent, E_o did not directly correspond to the force

produced, as the graphs did not go through the origin of the axes. The intercepts were significant and were probably caused by the lever being slightly biased.

The decrease in current after a set of force measurements shown by the static IV plots. did not alter the relationship between current and voltage, the current varying with voltage to approximately the power 1.4 , table 4.3

Considering the accuracy of the plots produced by the XY recorder this value is in good agreement with Sillars' eq.(4.1.4). Below about 30 volts this relationship did not hold; the values were inconsistent due to the nature of the conduction process in the carbon and the degree of contact between the carbon and the ball. No change in the current was found when the polarity of the voltage applied to the ball and flat was reversed, even when accurate measurements were made using the meters rather than monitoring it on the XY recorder. The only change was that which occurred during the force measurements and this is discussed later.

The current at break, I_{BR}, did however show a change when the voltage polarity was reversed. It only occurred at voltages higher than 150 volts when it was larger with the carbon positive with respect to the ball. I_{BR} was difficult to determine from the dynamic IV plot as there was vibration before separation giving a considerable scatter of values for a given voltage and force. I_{BR} varied with the voltage to the power 1.5 (table 4.4), a slightly higher value than that for the static IV readings.

The ball and flat were left in vacuo between each set of measurements for each ball, and the result of making between 100 and 200 separations on the same contact spot was that the carbon and to a lesser extent the ball were damaged, fig.4.7. The damage appeared to be crushed carbon adherring loosely to the ball and flat. It was easily wiped away leaving a few small pits, a few microns wide, in the ball and the carbon. The roughness of the damaged region could not easily be measured with a profilometer as its needle disturbed the débris.

4.4.2 GLASS RESULTS

Force measurements were only made with the 5.08 cm. diameter ball as

it was considered that the carbon results verified that the force was proportional to the ball diameter. Measurements were made with the glass to compare with those made with the carbon.

Three sets of measurements were taken which yielded linear plots of force versus voltage. Table 4.5 shows the values of E_o, calculated from the slopes of the graphs, to be less accurate than those of the carbon.

Unlike the carbon plots the static IV plots did not alter to such an extent after a set of force measurements had been taken. In fact they showed a slight increase in current, table 4.6. The plots still had the same relationship between current and voltage that the carbon plots had, the current varying with the voltage to approximately the power 1.45 Again this is in reasonable agreement with Sillars' equation.

The static IV plots for the glass, as with those of the carbon, showed no variation with the polarity of voltage applied to the ball on flat. The current at break, though, did show a change with the polarity of voltage at voltages greater than about 100 volts. The relationship of I_{BR} to the voltage was similar to that for the carbon, table 4.7.

A change in the saturation field, E_o with the polarity of voltage applied to the ball on flat was found, but the change diminished with the number of force measurements. The glass was found to be damaged over the contact spot when it was examined on an optical microscope afterwards, fig.4.8. Examination of the ball also showed faint etch marks corresponding to those on the glass but their faintness prevented a satisfactory photomicrograph being taken.

4.5 CONCLUSION

These results demonstrate the validity of the theory and also provide the basis for further work. They have not been fully discussed as the following chapters will be concerned with describing further experiments concerned with elucidating some of the effects and anomalies concerning them, e.g. the difference in E_o with the polarity of voltage applied to the ball and flat whereas the static current shows no polarity dependence

TABLE 4.1

DATA OF FORCE/VOLTAGE PLOTS MADE FROM MEASUREMENTS WITH THE CARBON SPECIMEN.

ORDER OF SETS OF MEASUREMENTS	BALL DIAMETER (cm)	SATURATION ELECTRIC FIELD E_o ($10^8 Vm^{-1}$)		INTERCEPT OF PLOT ON VOLTAGE AXIS	
		CARBON AT A NEGATIVE POTENTIAL	POSITIVE POTENTIAL	CARBON AT A NEGATIVE POTENTIAL	POSITIVE POTENTIAL
1st	5	$5.8^{+}_{-}0.2$	$5.1^{+}_{-}0.05$	$13^{+}_{-}5$	$8^{+}_{-}4$
2nd	5	$4.5^{+}_{-}0.2$	$4.3^{+}_{-}0.2$	$-6^{+}_{-}9$	$-11^{+}_{-}7$
3rd	5	$5.2^{+}_{-}0.3$	$4.8^{+}_{-}0.2$	$-11.5^{+}_{-}10$	$-33^{+}_{-}8$
4th	5	$5.5^{+}_{-}0.1$	$4.7^{+}_{-}0.1$	$-6.1^{+}_{-}3$	$-36^{+}_{-}4$
AVERAGE VALUES		5.24	4.71	-3	-18
1st	2.5	$5.4^{+}_{-}2$	$5.0^{+}_{-}0.1$	$6^{+}_{-}5$	$2^{+}_{-}5$
2nd	2.5	$5.5^{+}_{-}0.3$	$4.8^{+}_{-}0.1$	$16^{+}_{-}12$	$-3^{+}_{-}6$
3rd	2.5	$5.1^{+}_{-}0.2$	$4.3^{+}_{-}0.2$	$26^{+}_{-}7$	$10^{+}_{-}7$
AVERAGE VALUES		5.3	4.7	16	3
1st	3.2	$6.25^{+}_{-}0.2$	$5.4^{+}_{-}0.1$	$20^{+}_{-}5$	$7^{+}_{-}2$
2nd	3.2	$5.4^{+}_{-}0.2$	$5.1^{+}_{-}0.1$	$9^{+}_{-}6$	$6^{+}_{-}2$
3rd	3.2	$4.8^{+}_{-}0.2$	$5.6^{+}_{-}0.3$	$1^{+}_{-}9$	$-6^{+}_{-}13$
AVERAGE VALUES		5.5	5.0	10	2

TABLE 4.2

THE CHANGES IN CURRENT DURING FORCE MEASUREMENTS WITH CARBON CALCULATED FROM THE STATIC IV PLOTS AT 200 VOLTS.

ORDER OF SETS OF MEASUREMENTS	BALL DIAMETER (cm)	CHANGE IN CURRENT DURING A SET OF MEASUREMENTS (%)	OVERALL CHANGE IN CURRENT (%)
1st	5.1	- 13	
2nd	5.1	- 14	- 34
3rd	5.1	- 16	
4th	5.1	- 3	
1st	2.5	- 5	
2nd	2.5	- 2	- 8
3rd	2.5	- 8	
1st	3.2	- 15	
2nd	3.2	- 12	- 36
3rd	3.2	- 8	

TABLE 4.3

THE STATIC IV RELATIONSHIP WITH THE CARBON, (i.e THE INDEX, X, in $I \propto V_o^x$), DETERMINED FROM A LOG./LOG. PLOT.

ORDER OF SETS OF MEASUREMENTS	BALL DIAMETER (cm)	INDEX x	FROM IV PLOT BEFORE (B) OR AFTER SET (A)	VALID FOR RANGE OF VOLTAGE, V_o (VOLT)
1st	5.1	1.42 1.42	B A	> 30
2nd	5.1	1.42 1.42	B A	> 17
3rd	5.1	1.44 1.45	B A	> 30
4th	5.1	1.37 1.37	B A	> 50
AVERAGE		1.42		
1st	2.5	1.37 1.50	B A	> 50
2nd	2.5	1.38 1.53	B A	> 50
3rd	2.5	1.50 1.50	B A	> 30
AVERAGE		1.46		
1st	3.2	1.36 1.36	B A	> 50
2nd	3.2	1.36 1.40	B A	> 50
3rd	3.2	1.38 1.38	B A	> 30
AVERAGE		1.37		

TABLE 4.4

THE DYNAMIC IV RELATIONSHIP WITH CARBON, (i.e. THE INDEX, Y, in $I_{BR} \propto V_o^Y$), DETERMINED FROM A LOG./LOG. PLOT.

ORDER OF SETS OF MEASUREMENTS	BALL DIAMETER (cm)	INDEX Y	VALID FOR RANGE OF VOLTAGE, V_o
1st	5.1	1.37	> 17
2nd	5.1	1.1 1.64	<100 >100
3rd	5.1	1.47	>100
4th	5.1	1.34	>100
AVERAGE VALUE		1.38	
1st	2.5	1.0 2.3	<150 >150
2nd	2.5	1.2 1.96	<150 >150
3rd	2.5	1.86	>100
AVERAGE VALUE		1.66	
1st	3.2	1.17 1.71	<150 >150
2nd	3.2	1.03 1.54	<100 >100
3rd	3.2	1.05 2.77	<200 >200
AVERAGE VALUE		1.55	

TABLE 4 5

DATA OF FORCE/VOLTAGE PLOTS WITH GLASS SPECIMEN IN CONTACT WITH 5 cm DIAMETER BALL.

ORDER OF SETS OF MEASUREMENTS	SATURATION ELECTRIC FIELD E_o (10^8 Vm^{-1})		INTERCEPT OF PLOT ON VOLTAGE AXIS GLASS AT A	
	NEGATIVE POTENTIAL	POSITIVE POTENTIAL	NEGATIVE POTENTIAL	POSITIVE POTENTIAL
1st	6.0 ± 0.6	4.1 ± 0.3	21 ± 15	1 ± 17
2nd	2.84 ± 0.04	2.70 ± 0.15	15 ± 3	16 ± 4
3rd	2.80 ± 0.05	2.72 ± 0.05	-7 ± 4	-6 ± 4
AVERAGE VALUES	3.9	3.2	10	5

TABLE 4.6

THE CHANGES IN CURRENT DURING FORCE MEASUREMENTS WITH GLASS, CALCULATED FROM THE STATIC IV PLOTS AT 200 VOLTS.

ORDER OF SETS OF MEASUREMENTS	CHANGE IN CURRENT DURING A SET OF MEASUREMENTS (%)	OVERALL CHANGE IN CURRENT
1st	8	
2nd	1.6	8.2
3rd	-1.3	

TABLE 4.7

THE DYNAMIC IV RELATIONSHIP WITH GLASS, (i.e. THE INDEX, z , in $I_{BR} \propto V_o^{z}$), DETERMINED FROM A LOG./LOG. PLOT

ORDER OF SETS OF MEASUREMENTS	INDEX z	VALID FOR RANGE OF VOLTAGE, V_o
1st	1.52	>17
2nd	1.46	>50
3rd	1.51	>100
AVERAGE VALUE	1.50	

THE CONTACT BETWEEN A BALL AND A FLAT

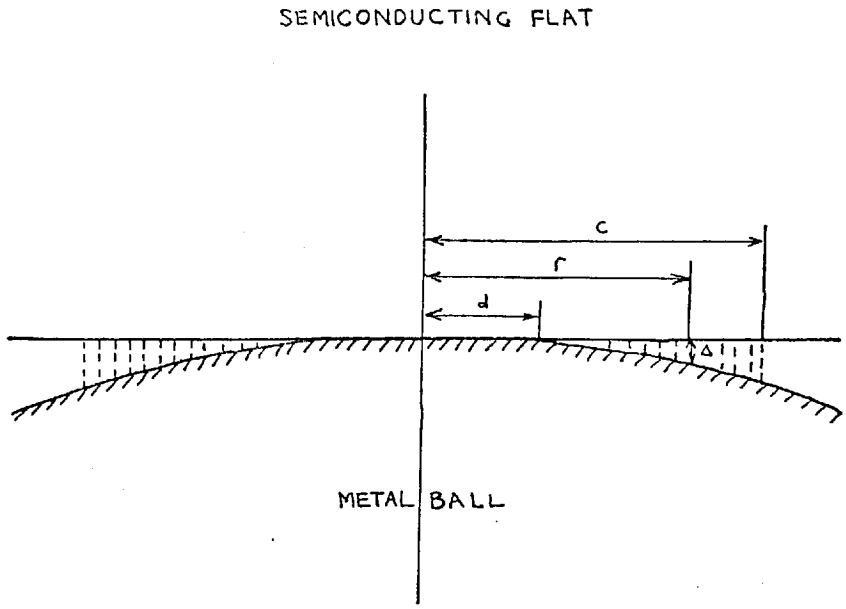

FIG.4.1

THE GUARD RING CIRCUIT FOR BALL-ON-FLAT MEASUREMENTS

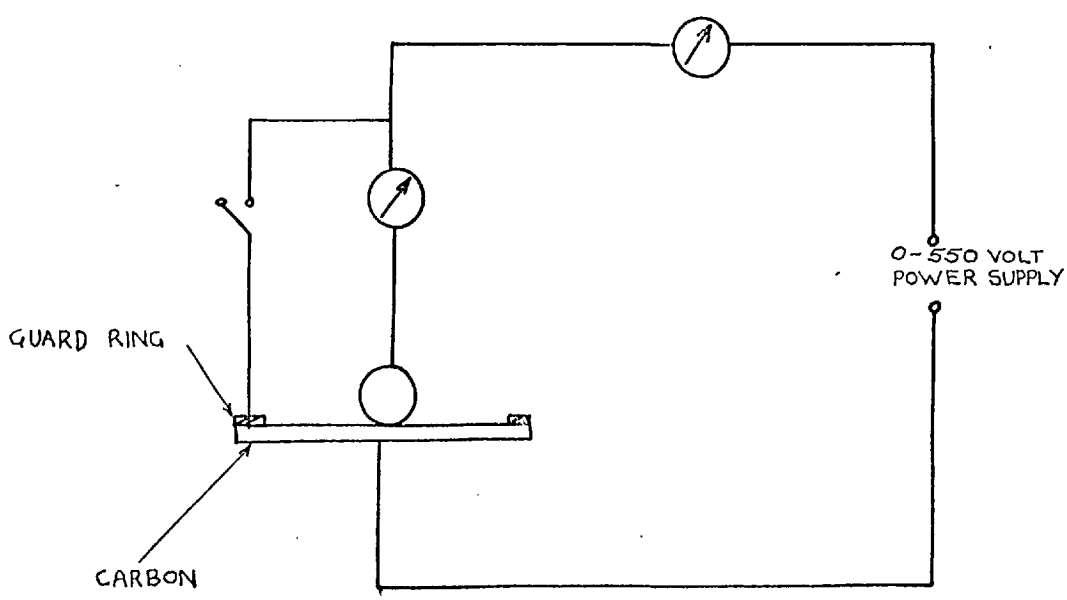

FIG.4.5

THE ELECTRICAL CIRCUIT FOR THE BALL-ON-FLAT APPARATUS

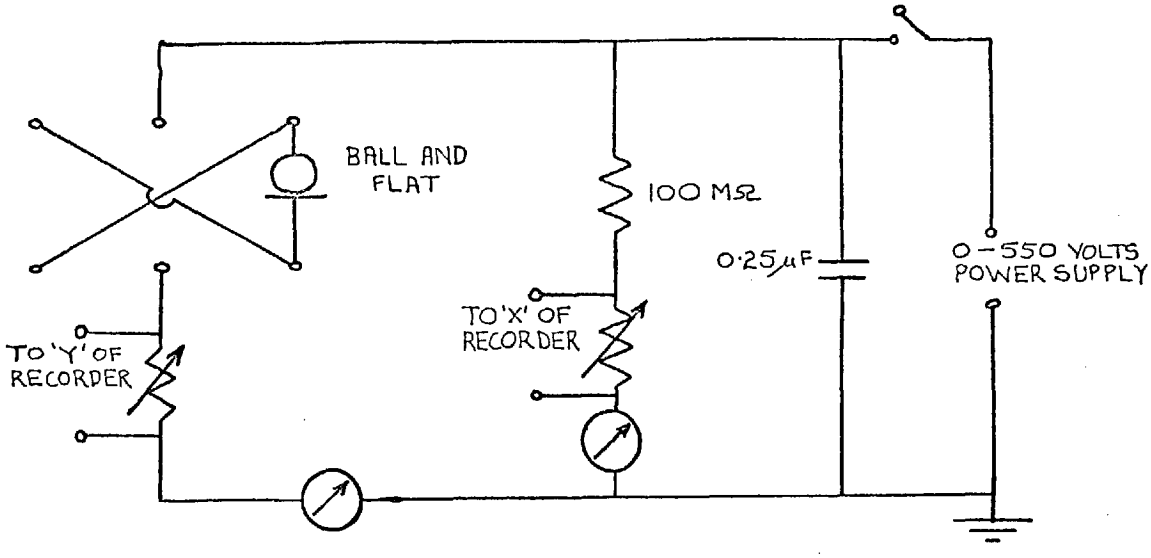

FIG.4.4

THE BALL-ON-FLAT APPARATUS

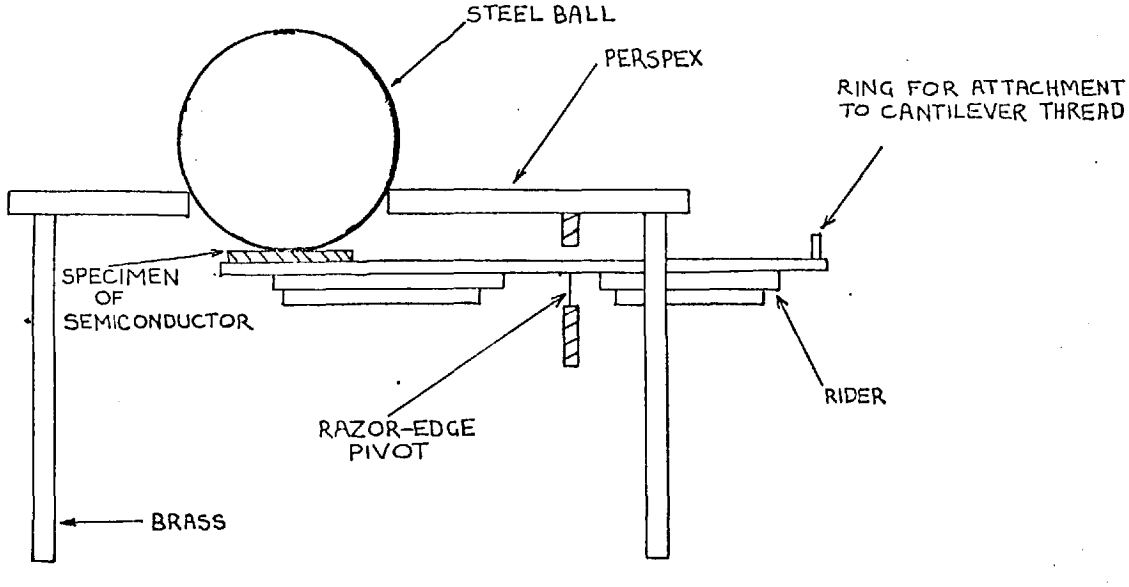

FIG.4.2

THE VACUUM SYSTEM FOR THE BALL-ON-FLAT APPARATUS

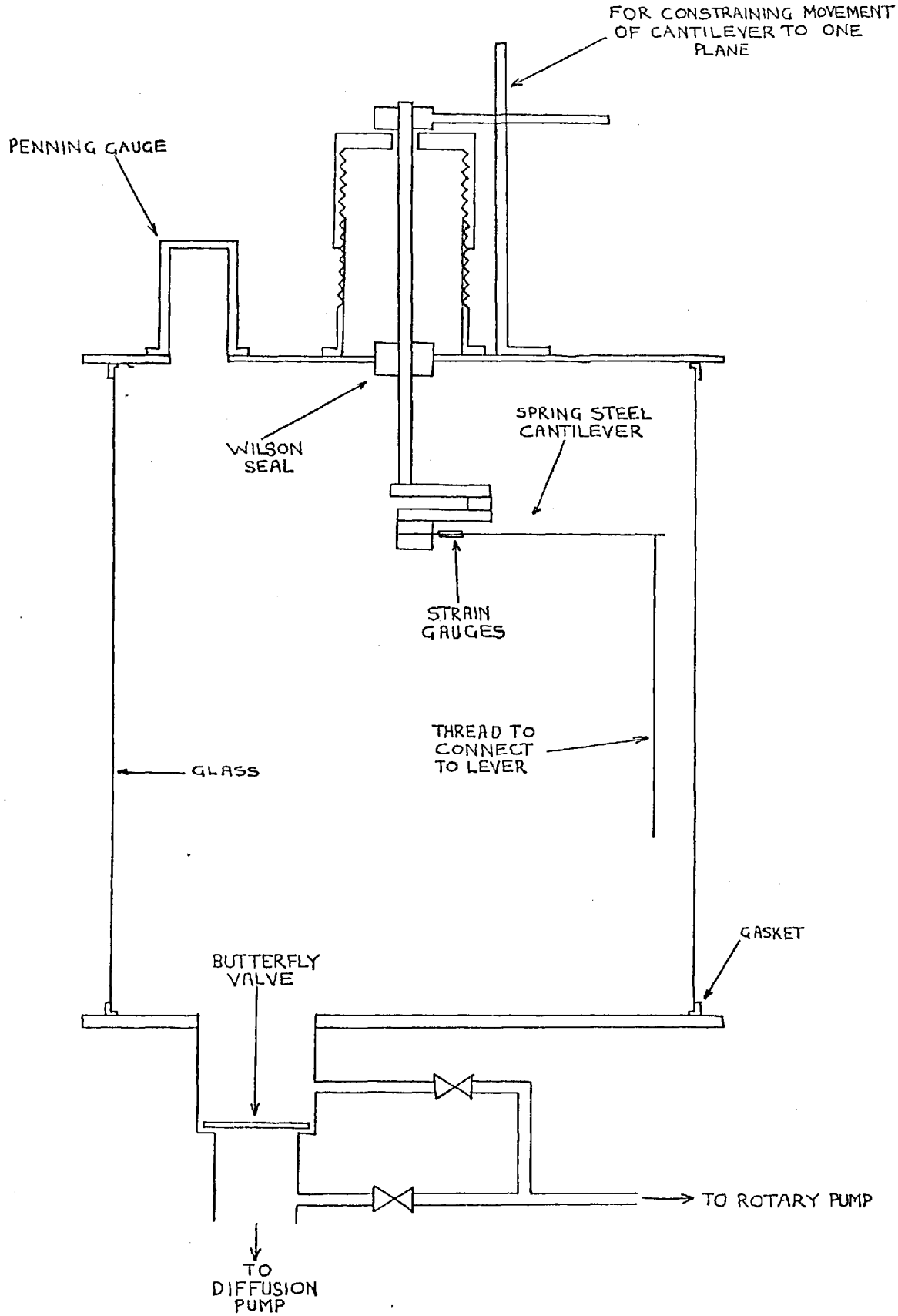

FIG.4.3

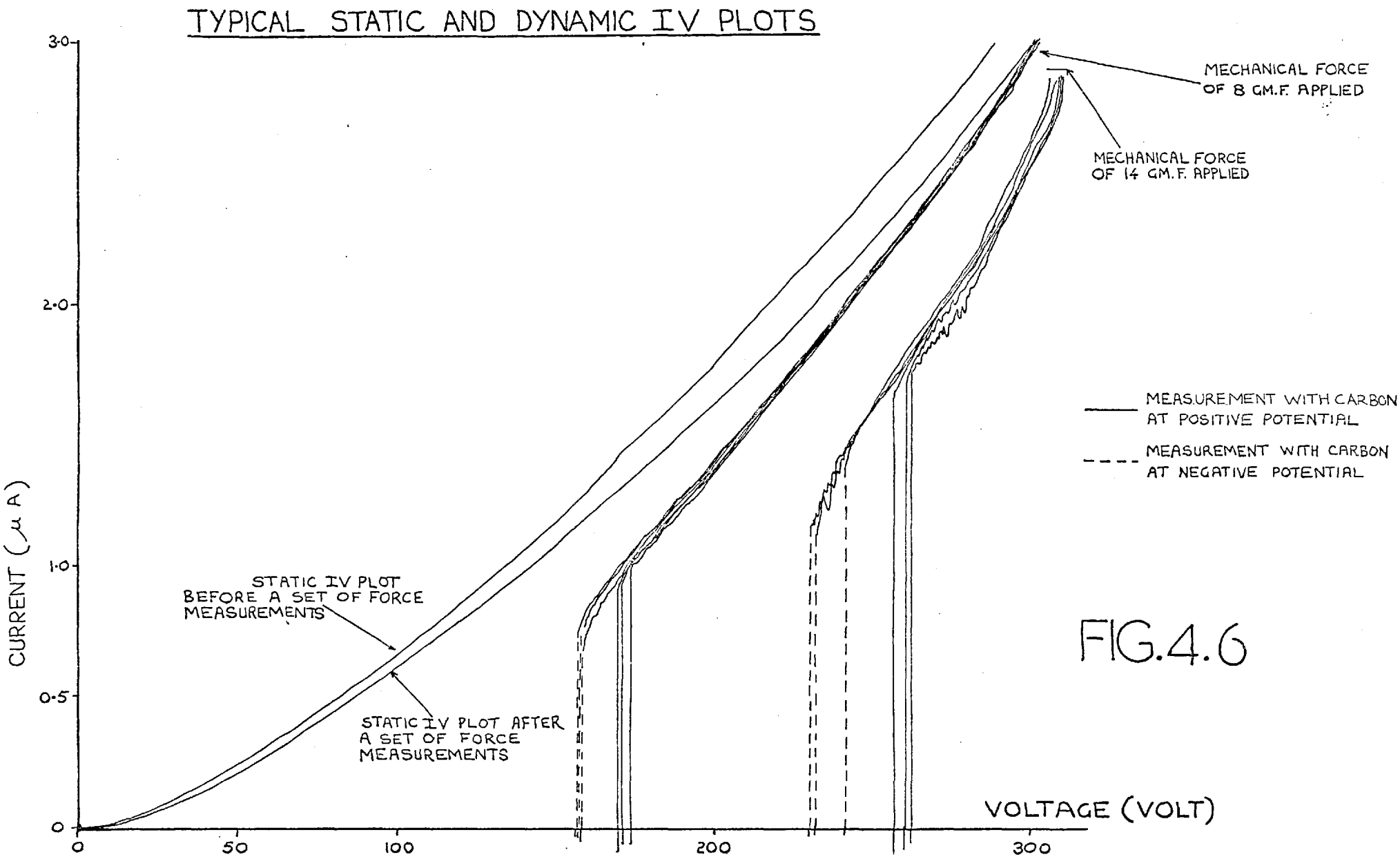
TYPICAL STATIC AND DYNAMIC IV PLOTS
CURRENT (μA)
3·0
2·0
1·0
0·5
0
0
50
100
200
300
VOLTAGE (VOLT)
MECHANICAL FORCE OF 8 GM.F. APPLIED
MECHANICAL FORCE OF 14 GM.F. APPLIED
MEASUREMENT WITH CARBON AT POSITIVE POTENTIAL
MEASUREMENT WITH CARBON AT NEGATIVE POTENTIAL
STATIC IV PLOT BEFORE A SET OF FORCE MEASUREMENTS
STATIC IV PLOT AFTER A SET OF FORCE MEASUREMENTS

FIG.4.6

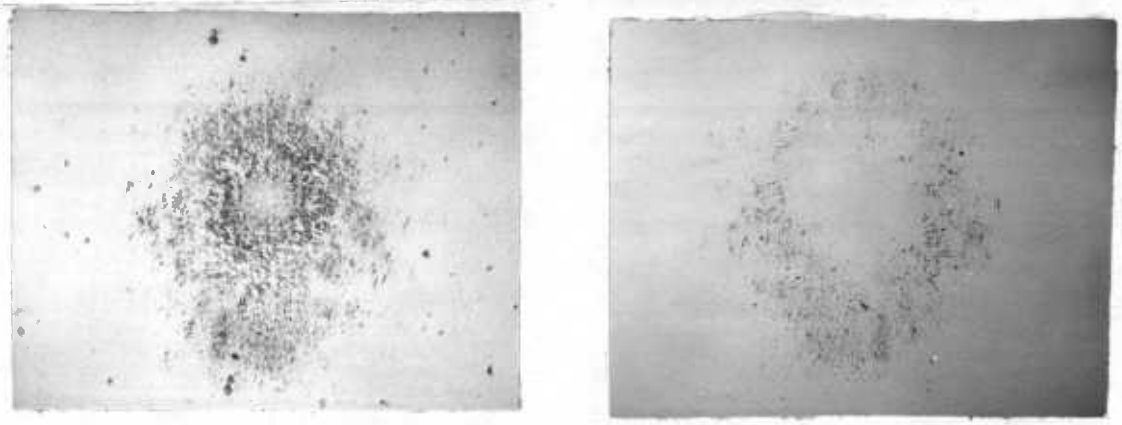

5 cm BALL

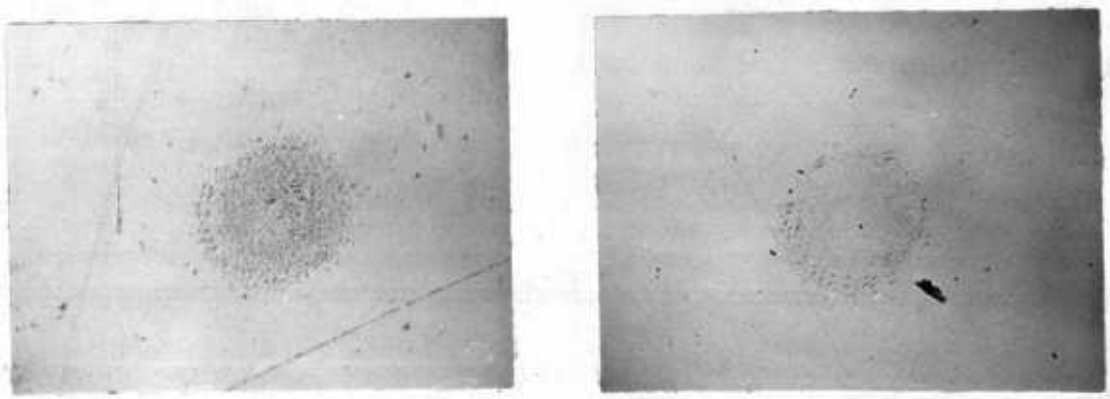

3·2 cm BALL

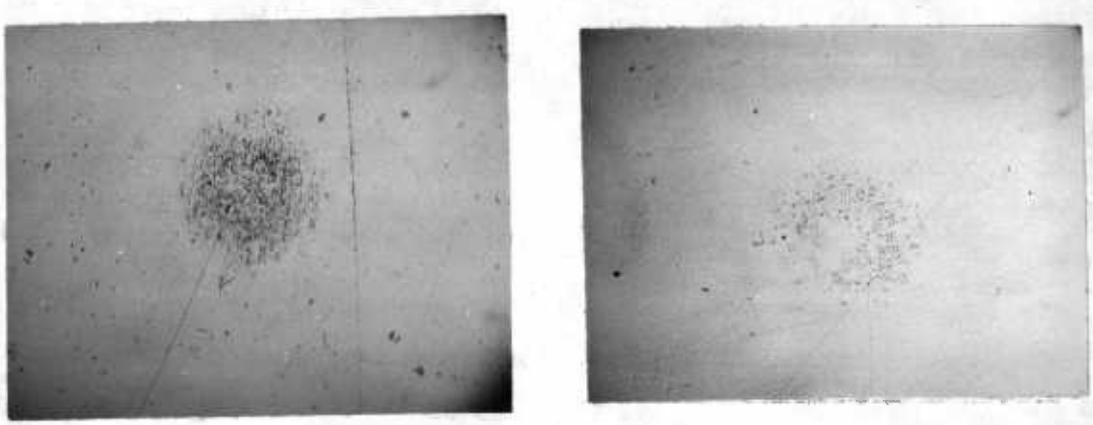

2·5 cm BALL

CARBON x140 MAGNIFICATION STEEL BALL

FIG.4.7

GLASS x140 MAGNIFICATION

FIG.4.8

CHAPTER V

DEFORMATION OF THE CONTACTS

As was stated in Chapter 3 the Johnsen-Rahbek force is a function of the gap width between the contact members, and any separation of them alters the force. However, to measure the force the contacts must be separated; either sheared or pulled apart. Thus the variation of the force with the separation of the members, which is dependent on the deformation occurring at the contact, must be known in order that the force can be determined accurately.

5. 1 THE FORCE/DEFORMATION RELATIONSHIP

In the calculation of the force between the ball and flat in Chapter 4 it was assumed that the radius of the mechanical contact, d, was negligible when the flat separated from the ball. This could be assumed then but not for the case when the ball and flat are in contact and not being separated. Considering d to be non-negligible the geometry of the contact now depends on d as do the interfacial voltage and current flow. Eq. (4.1.3) for the radius of current emission becomes:

$$c^2 - d^2 = \frac{RV_o}{E_o} \qquad (5.1.1)$$

and eq. (4.1.6) for V_{int} becomes:

$$V_{int} = \frac{E_o}{\pi R}\left\{(2c^2-r^2)\cos^{-1}\left(\frac{c}{r}\right) - (r^2-c^2)^{\frac{1}{2}}c - (2d^2-r^2)\cos^{-1}\left(\frac{d}{r}\right) + (r^2-d^2)^{\frac{1}{2}}d\right\} \qquad (5.1.1)$$

from which the force over the non-emitting region of the gap can be derived:

$$F_{NE} = \left(\frac{4\epsilon_o R E_o V_o}{\pi}\right)\int_{1.0}^{\infty} \frac{\lambda^5}{(\lambda^2-K^2)^2\,(1-K^2)}\left\{\frac{V_{int}}{E_o}\right\}^2 d\lambda \qquad (5.1.2)$$

The symbols have the same meanings as those in Chapter 4, except that d has

been expressed in terms of c,

$$K = \frac{d}{c} \qquad (5.1.3)$$

The force over the region of current flow remains the same, as defined by eq. (4.1.8):

$$F_E = \frac{\epsilon_o \pi R V_o E_o}{2} \qquad (5.1.4)$$

The variation of F_T with K, (the applied voltage being constant), is shown in fig. 5.1.

The variation of F_T with the approach of the contacts, Δ_o, can be calculated assuming the simplified deformation shown in fig 5.2. The value of Δ_o is given by

$$\Delta_o = \frac{d^2}{2R} \qquad (5.1.5)$$

which combined with eq. (5.1.1) gives

$$\Delta_o \propto \frac{K^2}{1 - K^2} \qquad (5.1.6)$$

Fig. 5.3 shows the variation of F_T with $K^2 / (1 - K^2)$, i.e. with the approach of the contacts, demonstrating that the maximum force is at the point of negligible contact.

The exact value of the approach depends on the mode of deformation, i.e. either elastic or plastic. Thus the value of K and hence the Johnsen-Rahbek force depend on the mechanical properties of the contacts. If the mode is elastic then Hertz's equation for the deformation of a ball loaded against a flat can be used:

$$d = \left(WR \left[\frac{1 - \nu_1^2}{E_1} - \frac{1 - \nu_2^2}{E_2} \right] \right)^{\frac{1}{3}} \qquad (5.1.7)$$

where W is the mechanical load, ν the Poisson ratio and E the Young's

modulus, the subscript 1 for the ball and subscript 2 for the flat. For a carbon specimen in contact with a 5cm diameter steel ball ,

($E_1 = 20 \times 10^{10}$ Nm^{-2} and $\nu_1 \sim 0.3$);

$$d = 1.98 \times 10^{-4} \; W^{\frac{1}{3}} \qquad (5.1.8)$$

This assumes $\nu_2 \sim 0.3$. E quating, by iteration, the force resisting deformation, given by Hertz's equation, to the Johnsen-Rahbek force, (assuming $E_o = 5 \times 10^8$ Vm^{-1}), shows how the deformation alters the latter, fig.5.4. This shows that the force when the surfaces are in contact at equilibrium and not being separated is less than that when there is negligible mechanical contact, (i. e. K = O). The calculations, however, are not exact as the stress distribution due to the Johnsen-Rahbek force is different from that due to the mechanical load assumed in Hertz's equation.

When the flat separates from the ball however, the force can be calculated assuming the voltage dropped across the shortest part of the gap is :

$$V_o - \beta E_o \qquad (5.1.9)$$

where β is the width of this part of the gap. The calculation is discussed in Chapter 6 in connection with the effect of surface roughness on the force and only the results are quoted here. Fig.5.5 shows that F_T decreases rapidly as β increases, and that the maximum force is at the point of contact.

5. 2 OBSERVATION OF THE DEFORMATION

The previous work has been theoretical, but to find the extent to which deformation affects the force produced the deformation must be measured. In Chapter 3 the deformation of specimens of carbon relative to a glass plate was observed with a Fizeau interferometer. Deformation between the ball and flat is more difficult to measure. However, etch annuli were found to be formed when the carbon was maintained at a positive potential with respect to the ball in the atmosphere, (see Chapter 9). The annuli approximately marked the region of current flow across the gap, the unetched circle in the middle (see fig.9.9).

representing the area of mechanical contact.

5. 3 DISCUSSION OF THE OBSERVATIONS

With the Fizeau interferometer the deformation was observed to be large with certain specimens, (fig. 3.3 &fig.3.7). Consider specimen 1. At 500 volts the area of intimate contact was about 1.5cm in diameter. If current emission occurred over the rest of the specimen's surface, (i.e. to a diameter of 2.5cm) then the value of K would be 0.6 and the force would be about 20% or more lower than the maximumpossible force.

The etch annuli also show a large amount of deformation to occur in the carbon when in contact with the steel ball. Table 5.1 shows the measured values of c and d for various voltages and the calculated values of K. The values of K tend to a value of 0.5 to 0.6 indicating that the forces are between 13% to 18% below the maximum forces obtainable at those voltages. As K varies slowly with the voltage the force can be taken as approximately proportional to $E_o V_o$. Thus a graph of $E_o V_o$ versus d is effectively a graph of force versus d. Fig.5.6 shows a graph of the values from table 5.1 which indicates a relationship of :

$$d \propto \text{Force}^{0.4} \qquad (5.3.1)$$

If the deformation were Hertzian then the relationship would be :

$$d \propto \text{Force}^{\frac{1}{3}} \qquad (5.3.2)$$

and if the deformation were 'plastic' it would be (Bowden and Tabor) :

$$d \propto \text{Force}^{\frac{1}{2}} \qquad (5.3.3)$$

Thus the observations indicate the deformation to be elastic rather than plastic.

Plastic deformation of brittle materials is difficult to define and measure, (Bowden and Tabor), but when plastic deformation occurs the average pressure over the deformed region attains the value of H, the hardness of the deformed material. Dudding and Losty crudely estimated H for the carbon to be between 10^9 Nm^{-2} and 2×10^9 Nm^{-2} (assuming the Vickers hardness number, which was the unit they quoted to be expressed in $Kg.f.mm^{-2}$ as is usual).

This value of H would indicate no plastic deformation of the carbon as the maximum pressure generated by the effect is about 5×10^6 Nm^{-2} when E_o is taken as 10^9 Vm^{-1}. However, the crushed carbon found on the ball and flat after force measurements had been made, (see Chapter 4), indicates that plastic deformation had occurred during the measurements.

5. 4 DISCUSSION OF FORCE MEASUREMENTS

From the previous theory which considers the force generated between two contacts when they are in contact and separated, it can be seen that the maximum force is generated when d is zero. This means that when the force is measured by separating the contact members it initially increases as the members begin to separate, fig. 5. 3, until the mechanical contact is zero and then the surfaces suddenly part when the Johnsen-Rahbek force equals the applied mechanical force. When the surfaces are sheared, however, the normal electrostatic force is not a maximum for the given voltage but depends on the mechanical contact area, which depends on the mechanical properities of the specimen. Thus a measurement of the force by separating the contacts is more a measure of the Johnsen-Rahbek effect than the method of shearing the contacts.

The former method would also yield measurements of the force higher than those of the latter method, as the previous theory shows, fig. 5.4. This is found to be the case when Stuckes' measurements, (done by separation), are compared to Leveson's, (done by shearing). Stuckes measured forces up to 3.ON over a unit area whereas Leveson measured forces only up to 1.5N over a unit area, and the specimens they used were equally flat, although Stuckes' specimens could have been smoother, (their roughness was not quoted).

The previous theory can also be invoked to explain the oscillation that occurred before the surfaces separated during a force measurement, as noted in Chapter 4. As the voltage across the contact decreases the flat moves away from the ball slightly, to a new equilibriun position but the applied mechanical

force would tend to move the flat beyond the equilbrium position whereupon the Johnsen-Rahbek force would increase and resist this motion. Hence an oscillation would be set up. The oscillation would increase as the applied mechanical force and the Johnsen-Rahbek force became equal. From this it can be seen that the measurement of the force depends on the rate of decay of the voltage and the dynamic response of the cantilever applying the mechanical force. So the force measurement is to an extent a function of the force measuring system. In his experimental work Balakrishnan noticed this when he observed that the measurement of the force varied with the speed the contacts were separated. The oscillation of the flat at the break point is also probably responsible for damaging the carbon, fig.4.7, and to a lesser extent the glass fig.4.8.

5.5 EFFECT OF DEFORMATION ON THE CURRENT

So far the effect of the deformation of the contact on the current flow has not been discussed. It is difficult to assess the effect for nominally flat contacts as the current is variable (see Chapter 3). For the ball on flat, however, it is easier. Sillars' equation, eq.(4.1.4) becomes:

$$I = \frac{8}{3\rho} \frac{E_o d^3}{R} \left[\left(1 + \frac{V_o R}{E_o d^2} \right)^{3/2} - 1 \right] \qquad (5.5.1)$$

when the value of d is non-negligible. This can be expanded, if $V_o R/E_o d^2 < 1$ to:

$$I = \frac{4}{\rho} dV_o \left[1 + \frac{1}{4} \left(\frac{V_o R}{E_o d^2} \right) + \ldots \right] \qquad (5.5.2)$$

This shows that the I V_o relationship becomes more ohmic when the second term in brackets is much less than 1.0. The variation of I with V_o depends on how d varies with the force and V_o. For small changes of force, such that d changes little and K varies slowly, it can be assumed that

$$\text{Force} \propto V_o \qquad (5.5.3)$$

assuming E_o is constant. If the deformation is elastic and follows Hertz's equation, then :

$$d \propto \text{force}^{\frac{1}{3}} \qquad (5.5.4)$$

this means :

$$d \propto V_o^{\frac{1}{3}} \qquad (5.5.5)$$

Combining the Hertz equation, eq. (5.1.7) for the carbon specimen with eq. (5.5.1), the current/voltage relationship becomes :

$$I = 3.54 \times 10^{-9} V_o \left[(1 + 0.22 V_o^{\frac{1}{3}})^{3/2} - 1 \right] \qquad (5.5.6)$$

with $R = 2.5\text{cm}$, $E_o = 5 \times 10^8 \text{Vm}^{-1}$, ρ taken as $5 \times 10^4 \Omega\text{m}$ and the values used in eq. (5.1.8). Fig. 5.7 shows this relationship, and it is found that instead of the current varying with the voltage to the power 1.5 it is 1.4. If the lever were biased, so that the carbon was pressed against the ball the index would be further reduced. This can be seen by considering the lever biased with an 18 gm weight (this being the case in the experimental work). The index decreases to 1.2 as fig. 5.7 shows.

If the deformation were plastic then :

$$\text{force} = H \pi d^2 \qquad (5.5.7)$$

Making the same assumptions as for elastic contact and taking H to be 10^9Nm^{-2} then the current/voltage relationship becomes :

$$I \propto V_o^{3/2} \qquad (5.5.8)$$

and the relationship between I and d becomes :

$$I = 8.53 \times 10^{-3} d^3 \qquad (5.5.9)$$

This produces a current/voltage relationship very similar to the relationship where d is negligible, as fig. 5.7 shows.

When the surfaces are being separated the current/voltage relationship is dominated by the value of d again. The situation is analagous to that of

the flat being pressed against the ball except that in this case the bias is negative, reducing the contact rather than increasing it. If a mechanical force of 9 gm.f. , (0.088 N), is applied to separate the flat from the ball then Hertz's equation gives :

$$d = 1.98 \times 10^{-4} \left[5.22 \times 10^{-4} V_o - 0.088 \right]^{\frac{1}{3}} \qquad (5.5.10)$$

using the same values as in eq. (5.5.6). Combining this with eq. (5.5.1) the dynamic IV plot can be constructed, fig.5.8. This shows the current to become zero at 168 volts, and the dynamic IV plot to have little curvature, indicating that the index has tended towards 1.0 from 1.5.

5.5.1 EXPERIMENTAL METHOD

The situation of a ball being pressed against a flat can be realised experimentally by loading the lever of the ball-on-flat apparatus. This was done by placing an 18 gm. weight on the lever below its attachment to the cantilever. For making the measurements a specimen of carbon was used which was cleaned in the usual manner before insertion into the apparatus as was the 5cm ball in contact with it. The measurements were done at 10^{-5} torr for various forces applied between the ball and flat, and the loading was adjusted by the cantilever.

The theory related to the dynamic IV plot can be compared with previous measurements.

5.5.2 RESULTS

The current/voltage characteristics for the carbon loaded and unloaded is shown in fig. 5.9. With the weight on the lever the index was 1.26 and without, 1.42.

The dynamic IV plots used to compare with the theory are those measured with the force measurements in Chapter 4, typical plots being shown in fig. 4.6.

5.5.3 DISCUSSION

The static IV plots with the lever loaded and unloaded agree well with the

theory which assumes the contact deformation to be elastic rather than plastic. It is interesting to note that the index when the system is unloaded is less than 1.5, as was found with the results of Chapter 4. The present theory indicates that this is caused by d being non-negligible. This is supported by the latter results which showed the index of the I_{BR} V_o relationship to be higher than the static index due to d being much reduced if not negligible in the former case.

The theoretical dynamic IV plot also agrees well with the plots in fig. 4.6, indicating that the reduction in current compared with the static IV plot is due to d becoming diminished, tending to become negligible at the break point as was assumed in Chapter 4. This assumption is supported by the previous theory which showed that the force is a maximum when d is zero and indicates that the surfaces would only separate when the applied mechanical force equalled this maximum force.

Measurements made with a specimen of conducting glass supported the above results, but the current was found to be much lower than that with the carbon, (as was consistently found to be the case), although its resistivity was 7×10^3 Ωm as compared to the carbon's 5×10^4 Ωm. This is not fully understood so the results are not quoted.

5. 6 CONCLUSION

The theory and results in this chapter demonstrate that the mechanical properties of a contact can greatly affect the force generated in the interfacial gap. It has also been shown that the maximum force occurs when the mechanical contact area is negligible and this maximum force can be measured by pulling the contacts apart but not by shearing them.

The results also indicate that the deformation of the carbon when in contact with the steel ball is elastic although the oscillation at the break point of a force measurement does cause permanent damage to it.

TABLE 5.1

VALUES OF K, ($= \frac{d}{c}$), CALCULATED FROM THE DIMENSIONS OF ETCH ANNULI.

APPLIED VOLTAGE V_o (VOLT)	RADIUS OF MECHANICAL CONTACT, d (μm)	RADIUS OF CURRENT EMMISSION, c (μm)	$K = \frac{d}{c}$
25	30	40	0.8
50	30.0	62	0.5
75	41	82	0.5
100	50	88	0.6
125	56	106	0.5
150	60	119	0.5
175	68	119	0.6
250	89	149	0.6

THE VARIATION IN THE JOHNSEN-RAHBEK FORCE BETWEEN A BALL AND FLAT WITH THE MECHANICAL CONTACT BETWEEN THEM

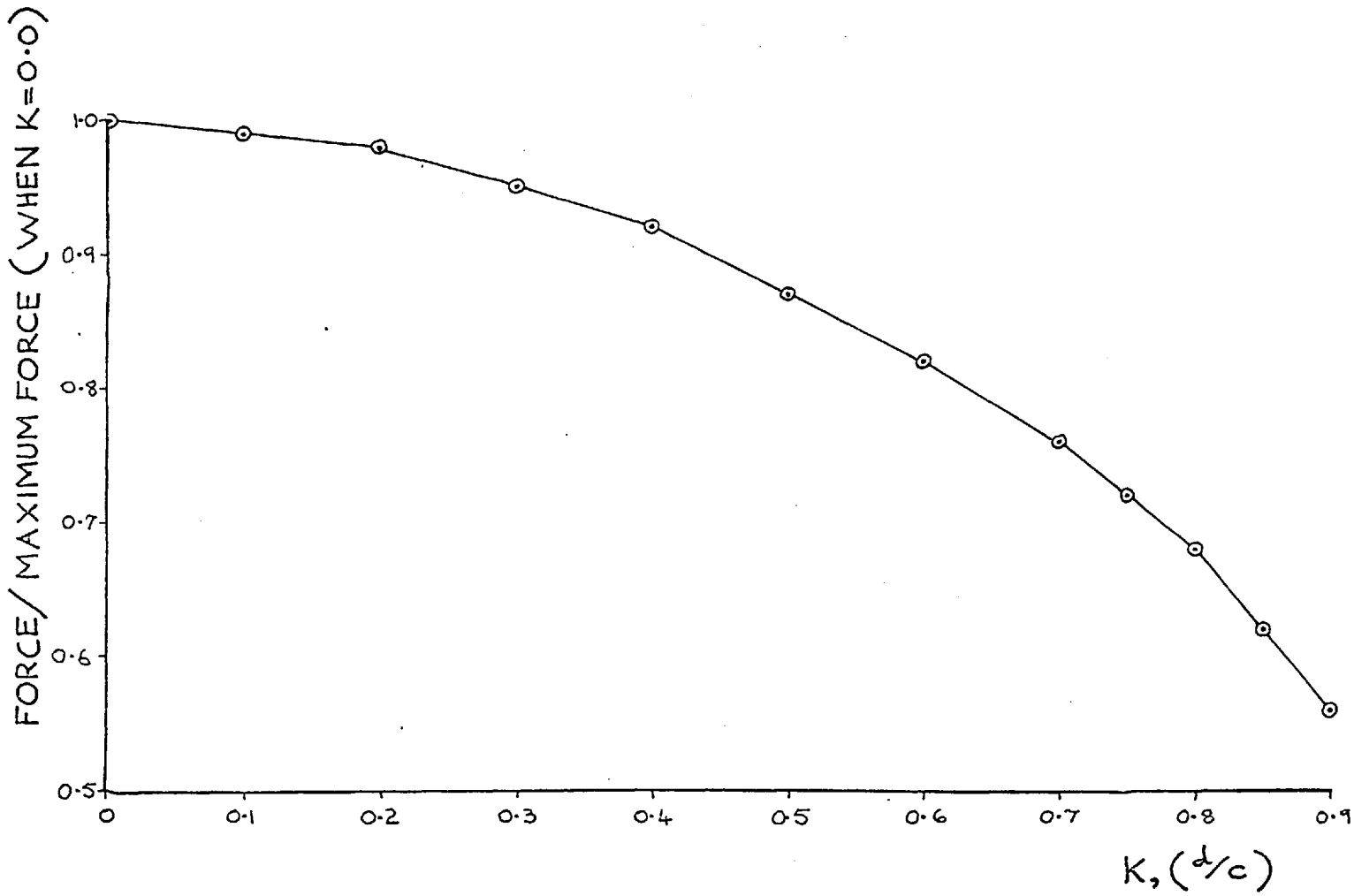

FIG.5.1

A HYPOTHETICAL CONTACT BETWEEN A BALL AND FLAT

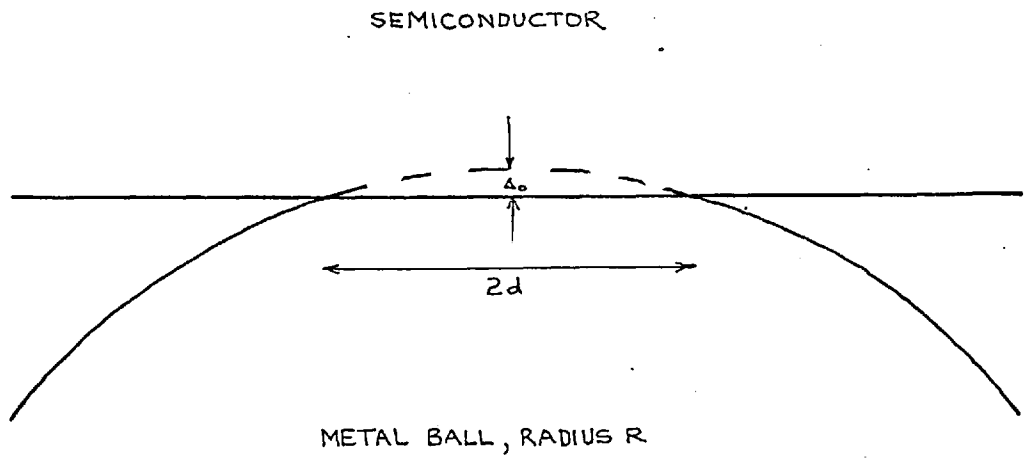

FIG.5.2

THE VARIATION IN THE JOHNSEN-RAHBEK FORCE BETWEEN A BALL AND FLAT WITH THEIR APPROACH

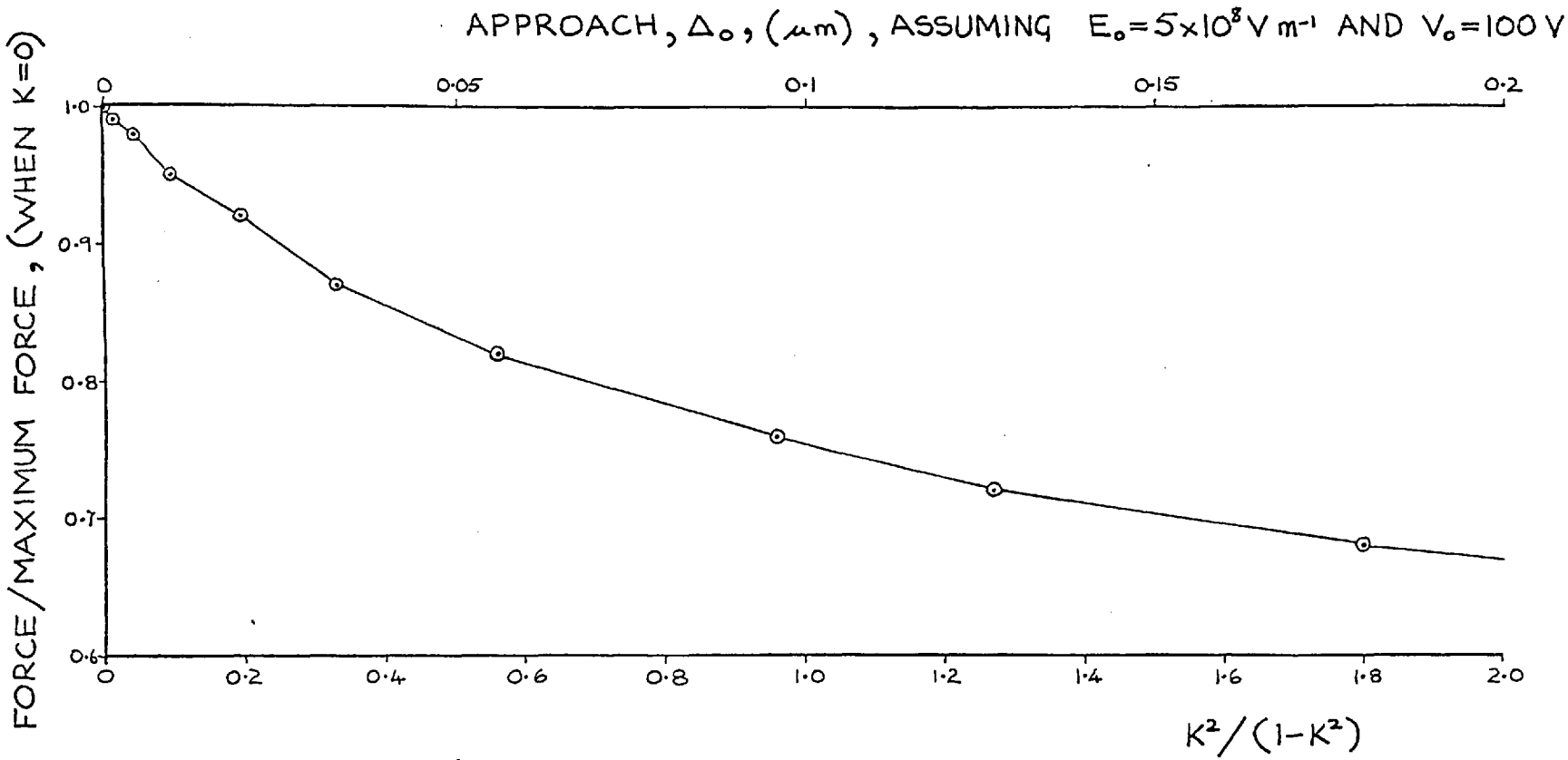

FIG.5.3

THE DECREASE IN THE JOHNSEN-RAHBEK FORCE BETWEEN A BALL AND CARBON FLAT DUE TO ELASTIC DEFORMATION OF THE FLAT

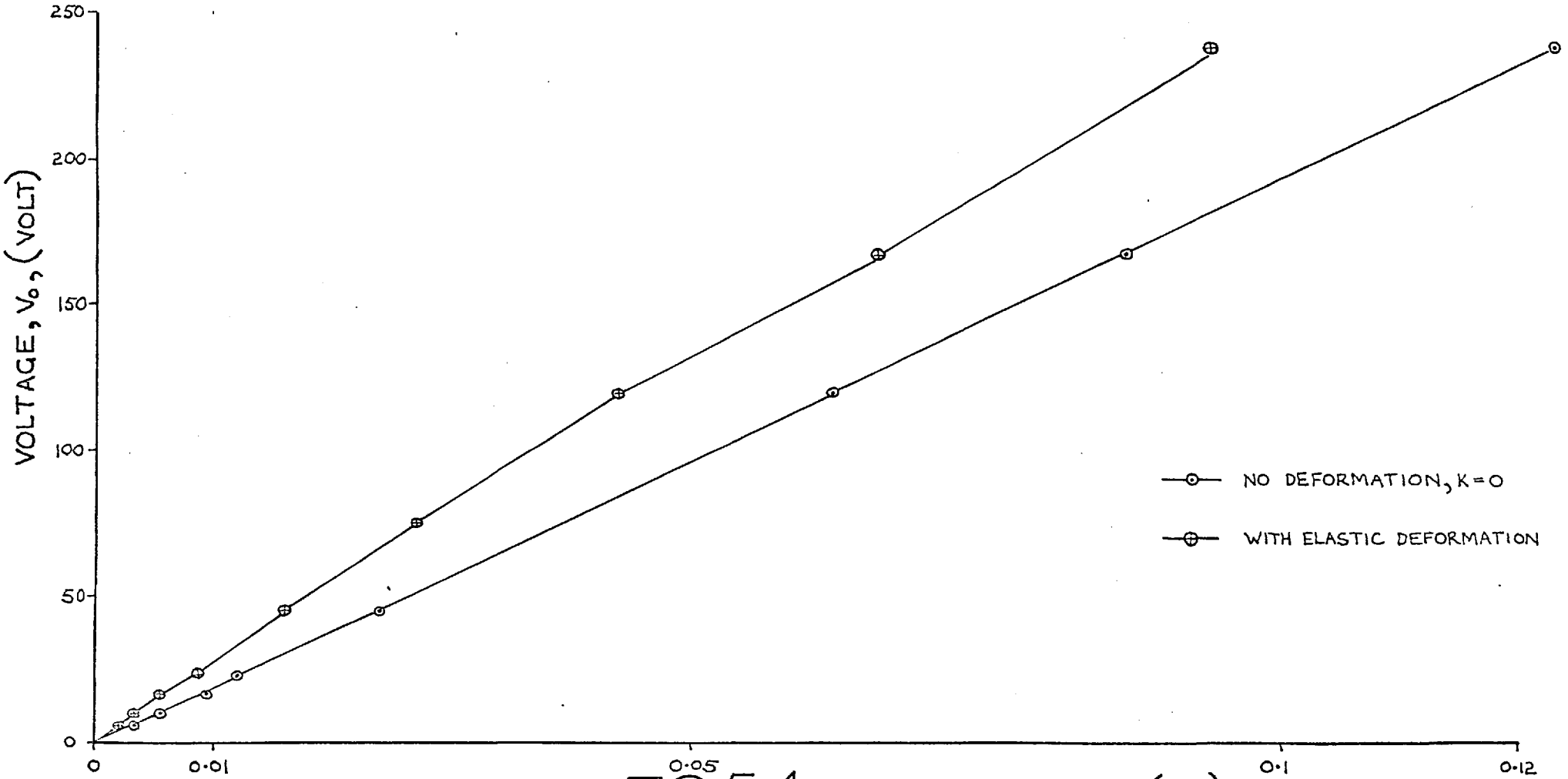

FIG.5.4

THE VARIATION OF THE JOHNSEN-RAHBEK FORCE WITH THE SEPARATION BETWEEN THE BALL AND FLAT

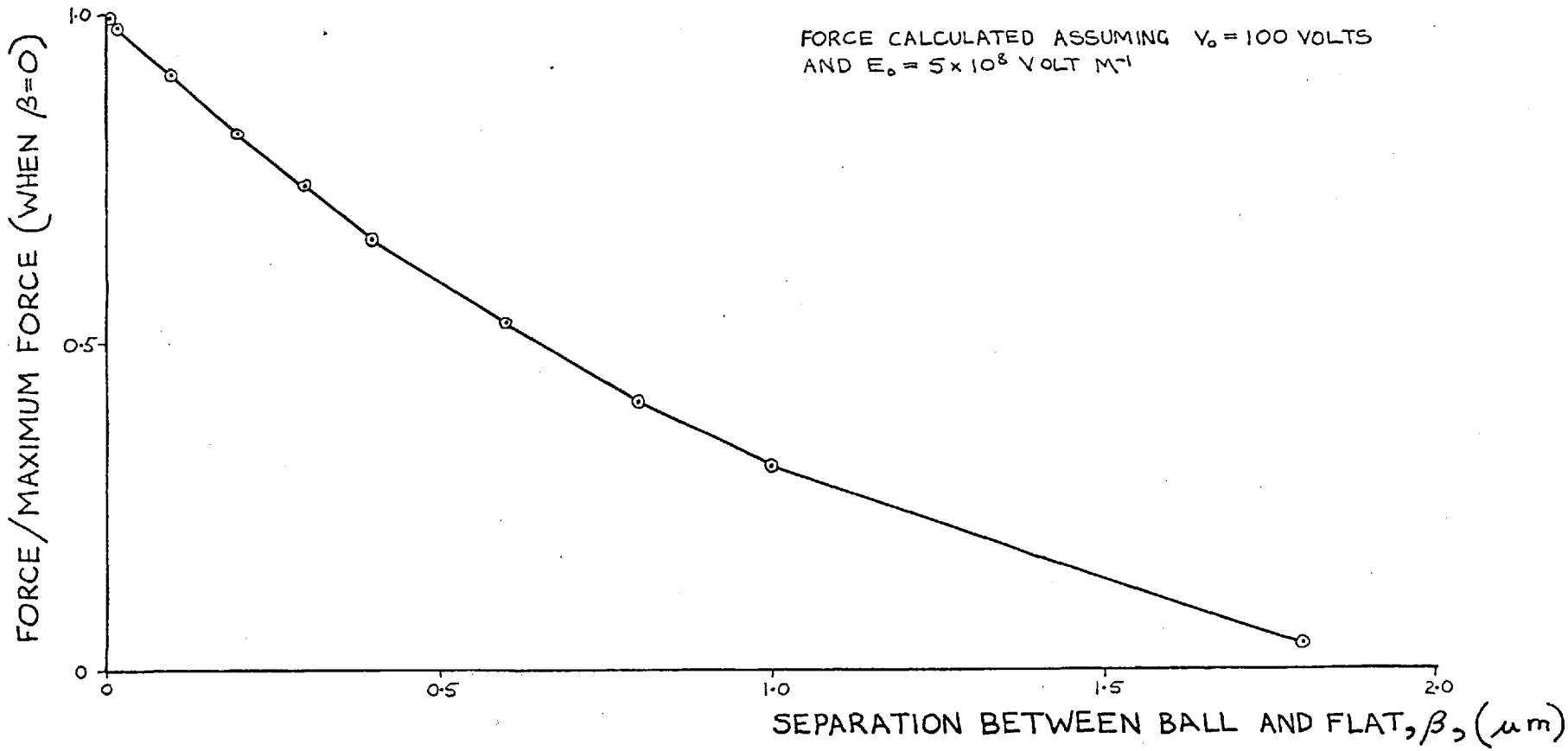

FIG.5.5

THE VARIATION OF THE MECHANICAL CONTACT BETWEEN A BALL AND CARBON FLAT WITH THE FORCE GENERATED BETWEEN THEM. THE CONTACT WAS MEASURED FROM ETCH ANNULI.

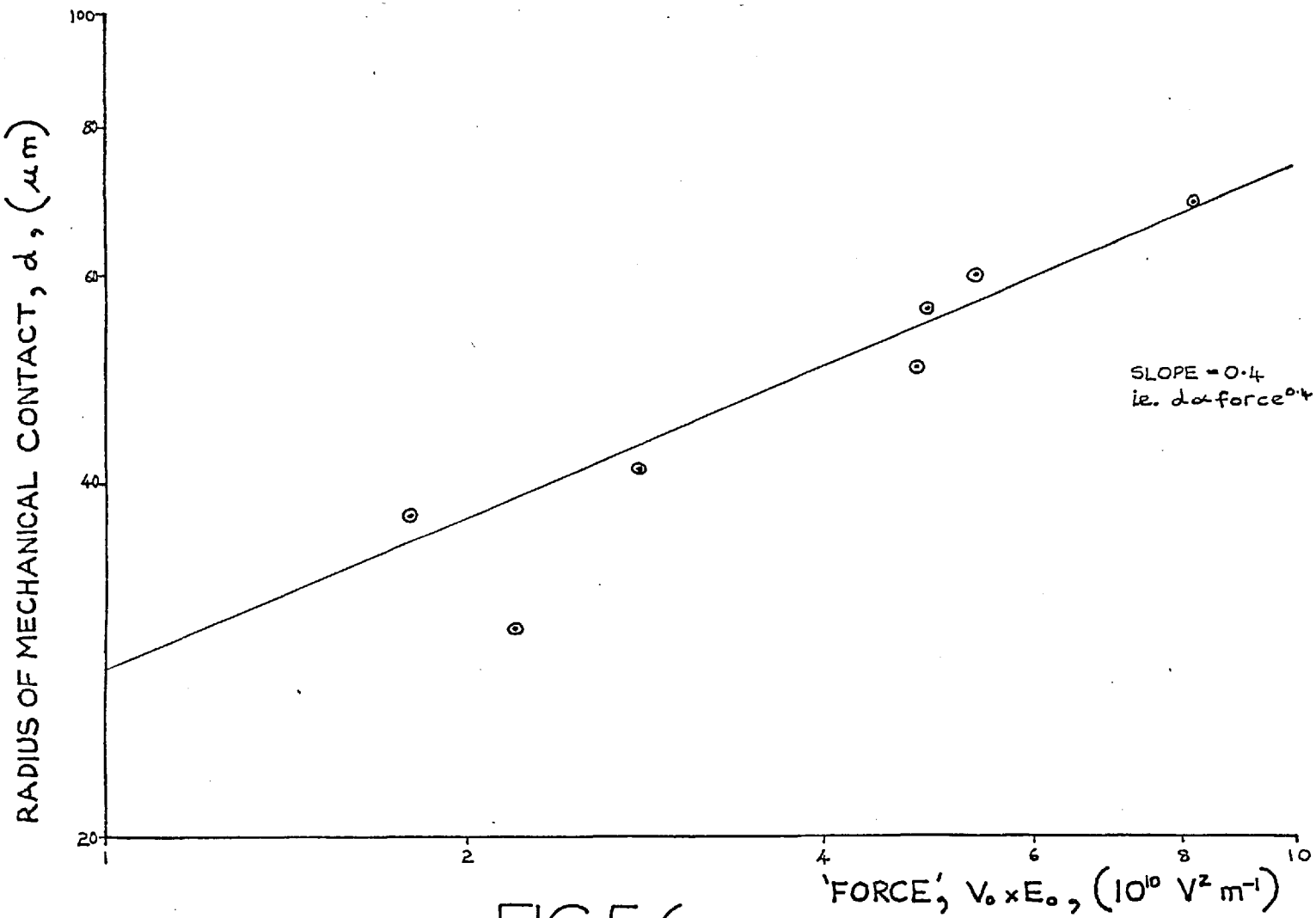

FIG.5.6

THEORETICAL STATIC IV PLOTS FOR VARYING DEGREES OF DEFORMATION BETWEEN THE BALL AND FLAT

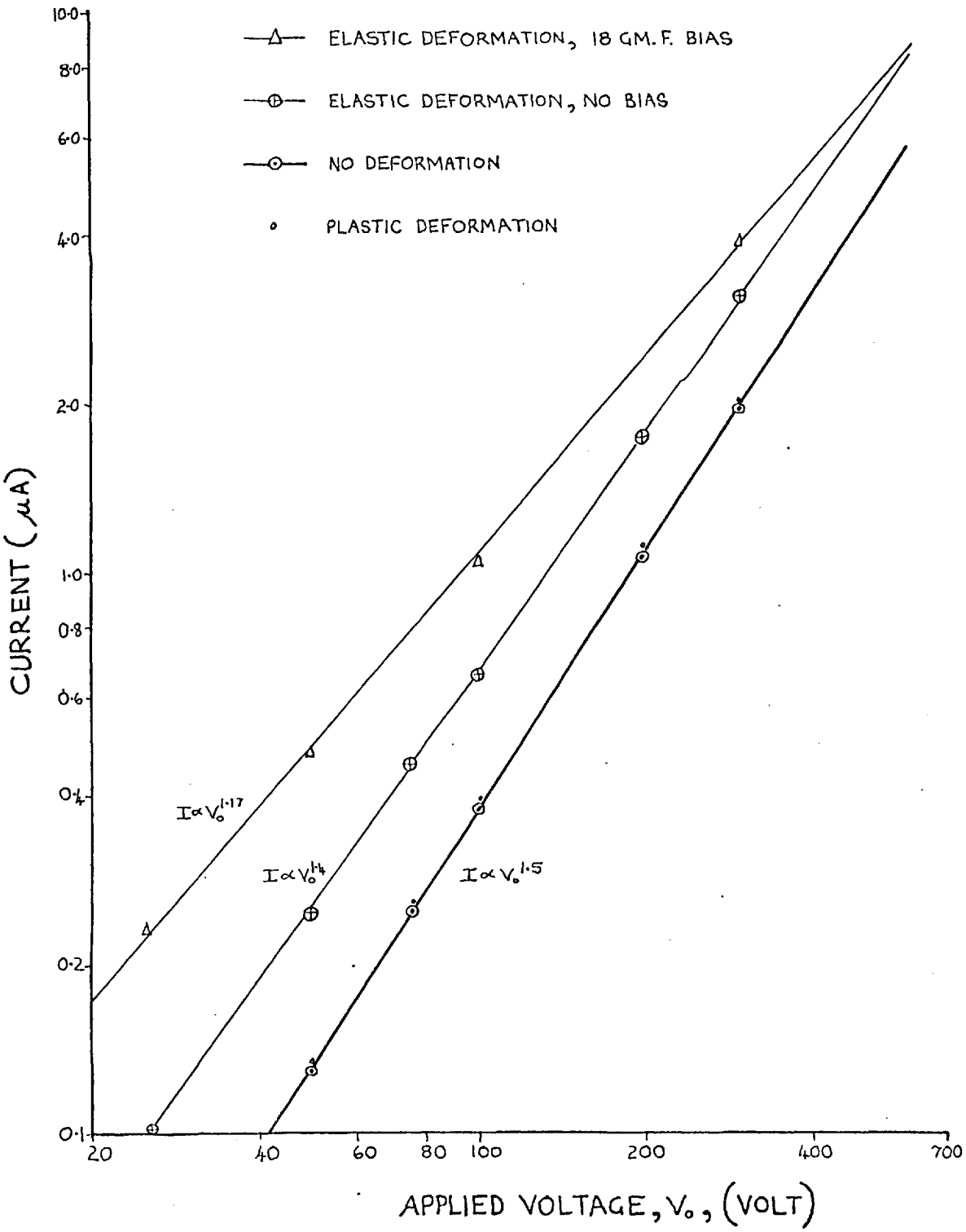

FIG.5.7

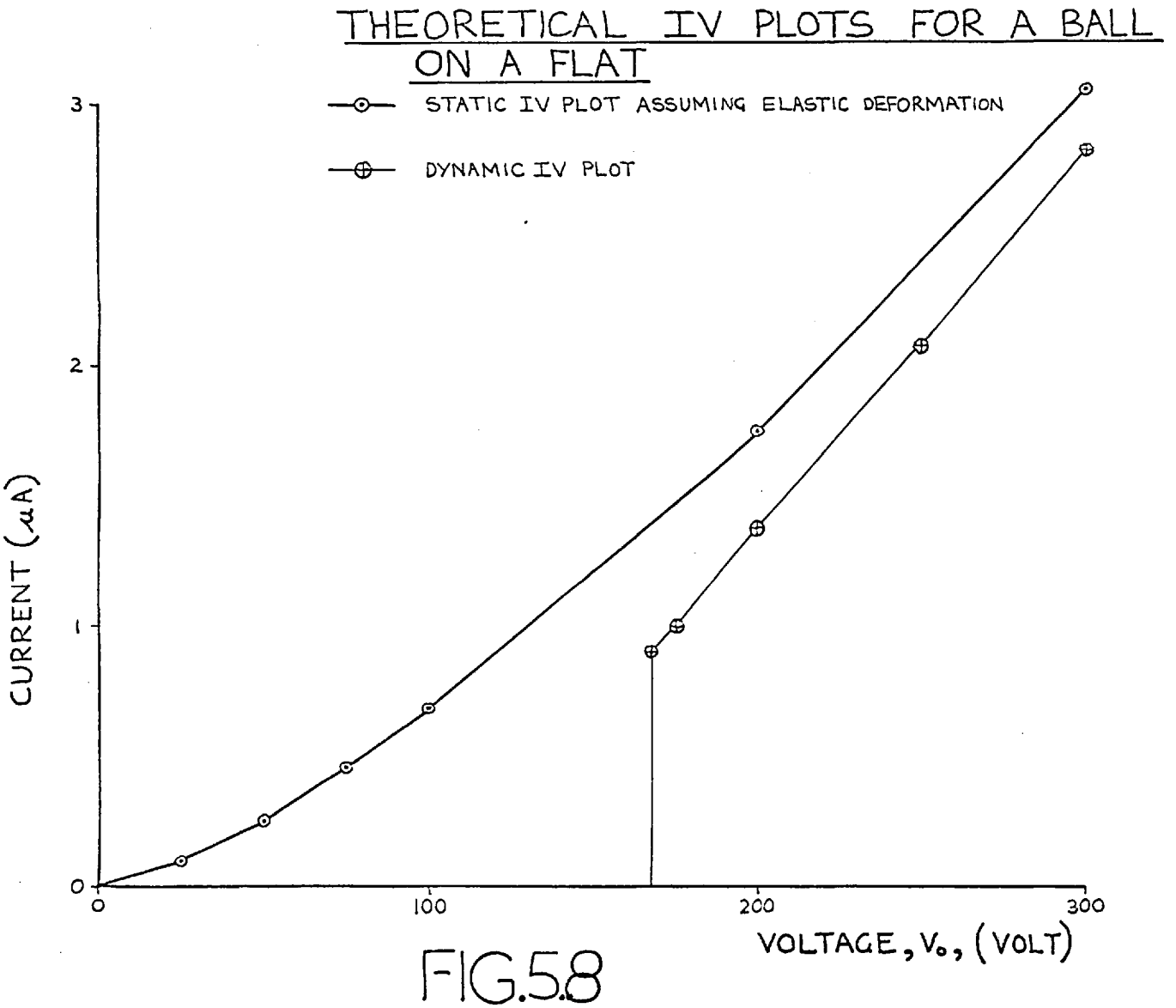
THEORETICAL IV PLOTS FOR A BALL ON A FLAT
STATIC IV PLOT ASSUMING ELASTIC DEFORMATION
DYNAMIC IV PLOT
CURRENT (μA)
VOLTAGE, V₀, (VOLT)
0
1
2
3
0
100
200
300

FIG.5.8

OBSERVED STATIC IV PLOTS FOR VARYING DEGREES OF DEFORMATION BETWEEN THE BALL AND CARBON FLAT

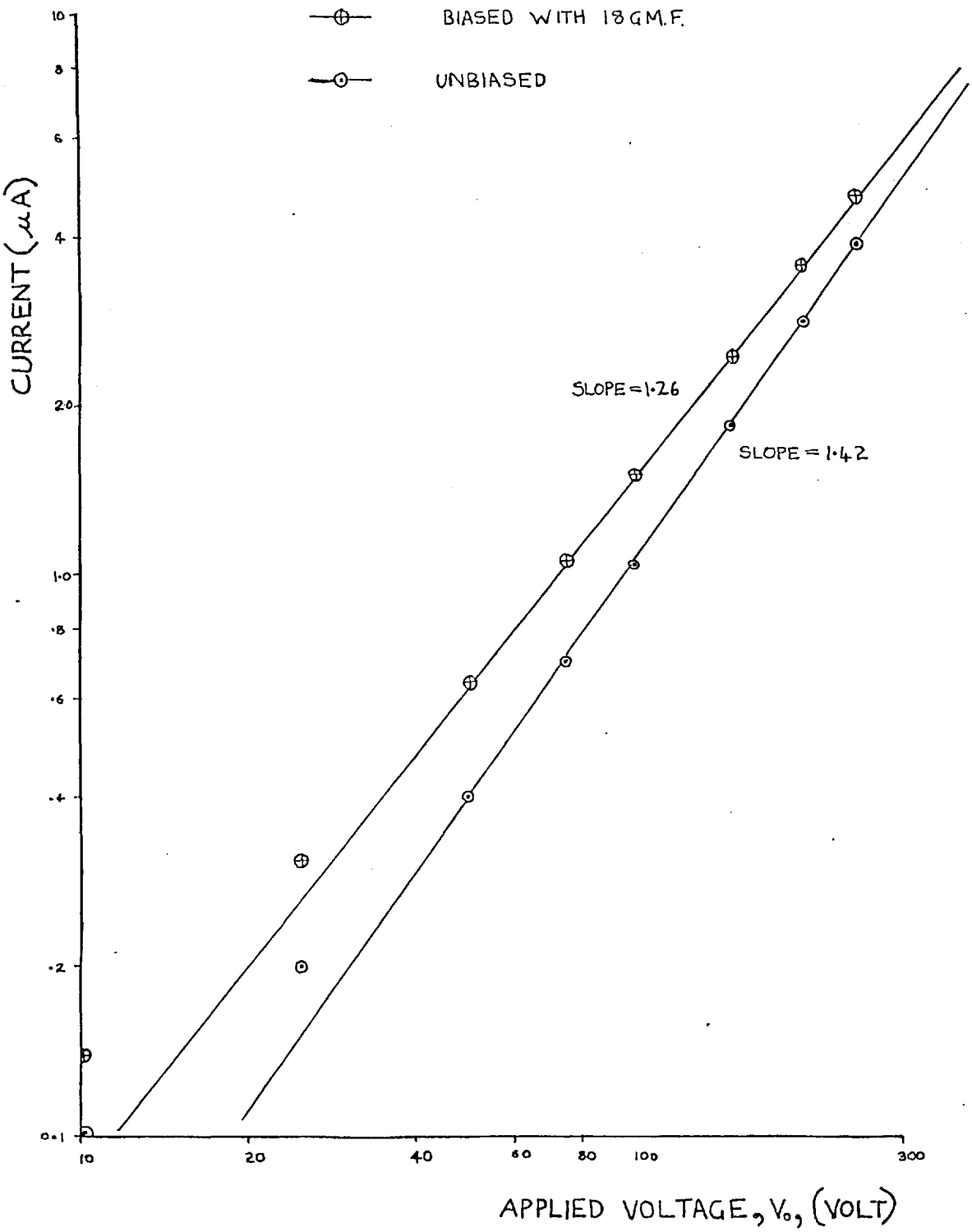

FIG.5.9

CHAPTER VI

THE EFFECT OF SURFACE ROUGHNESS ON THE FORCE.

In the calculation of the Johnsen-Rahbek force between a ball and flat, (Chapter 4), the roughness of the surfaces was not considered; they were regarded as smooth. In fact surfaces are far from smooth on a microscopic scale and table 6.1 shows the roughnesses of typical engineering surfaces. When surfaces touch the interfacial gap separation is determined by their roughnesses. The Johnsen-Rahbek force is very dependent on this separation and hence very dependent on the surface finish. A ground surface would produce a force much less than that produced by a highly polished surface.

A knowledge of the effect of roughness on the force is also relevant to predicting the performance of practical devices, as their surfaces alter with the amount of wear occurring.

6.1 PREVIOUS WORK

Early workers found that surface roughness was a dominant factor in determining the force. Their work, however, was qualitative and yielded little useful data.

Balakrishnan measured the force between a brass plate and some semiconducting discs varying in roughness from 0.25 μm to 0.59μm. The discs varied in curvature from 25 m concave to 50m convex and also varied in resistance from 0.16 MΩ to 2.5 MΩ. Measurements with the discs showed the force to be a varying function of the applied voltage. This, combined with the variation in the surface geometry of the specimens makes it difficult to assess the effect of the roughness.

Leveson also measured the forces that a carbon specimen produced when its surface was roughened from 0.33μm C.L.A. to 0.5μm C.L.A. and finally to 1.9μm C.L.A. His results were difficult to analyse because of the method of force measurement, but they are discussed more fully later.

Atkinson formulated an equation for the results Stuckes obtained. Only the results obtained with the semiconductor at a negative potential with respect to the metal were considered in the calculations. The equation was derived by constructing an average asperity, representative of the surface roughness, and calculating the force such an asperity would produce at a given voltage. Three asperity shapes were tried; a cone, a sphere and a "two-tiered onion shape', fig. 6.1. The latter asperity gave theoretical results closest to the experimental measurements, fig. 6.1. It was constructed on the assumption that the heights of the contacting surfaces formed a Gaussian distribution,(see Appendix 2), and the two-tiered onion shape was constructed by twisting and rotating the Gaussian density function. The calculations made with this asperity were complex and the size of the model was varied until the best fit to Stuckes' data was obtained.

Although Atkinson's equation was relatively accurate it referred only to Stuckes' specimens of unknown roughness, and to particular results obtained with them. It neglected the curvature of the surfaces and surface deformation.

6.2 SURFACE ROUGHNESS

Before the effect of surface roughness can be analysed, the roughness must be examined in more detail besides simply measuring the C. L. A. value. It has been extensively investigated in connection with friction and wear and much work has been done to characterise a surface statistically after various treatments.

The most common instrument for measuring surface roughness is the stylus profilometer which produces a magnified trace of the surface from an electrical signal produced by a fine stylus moving across the surface. This signal can be electronically integrated to give a centre line average, (C. L. A.), reading which is a measure of the roughness. Using the profilometer and analysing the traces it has been found that most surfaces, (Greenwood and Tripp), especially ground or grit blasted surfaces have an almost Gaussian distribution of asperity heights. Greenwood and Williamson took profiles of a surface parallel to each other and made up a three dimensional map of it. For a number of surfaces they found that asperity heights and surface heights measured at equal intervals along the profiles obeyed a Gaussian distribution. This analysis

was done by digitising the output from the profilometer so that it was suitable for computer analysis.

Earlier investigations of surface roughness, however, had been made by manual observations of profilometer traces from which bearing area curves, (see Appendix 2), had been constructed, (Abbot and Firestone). As no apparatus was available for digitising the output from the profilometer used in the present work, this latter technique was employed. Highly polished surfaces such as are used to produce Johnsen-Rahbek forces have not been thoroughly analysed, although Greenwood and Williamson state that polished metal surfaces are most probably Gaussian. It was therefore considered necessary to analyse the roughness of the surfaces used in this investigation.

6. 3 ANALYSIS OF THE ROUGHNESS OF A POLISHED CARBON SURFACE.

In the present investigation of the effect of roughness on the force using the ball-on-flat apparatus, it was easier to analyse the roughness of the flat semiconductor than the ball. Moreover, the ball was far smoother than the flat. Carbon as opposed to conducting glass was used for this work as it had a homogeneous surface texture which the glass did not have. As the carbon specimens varied in their electrical resistance slightly, (depending on the amount of absorbed water vapour), and often had different surface curvatures, measurements were made on two specimens designated C5 and C6. A surface profile trace was made of each specimen before force measurements described later, were made. After each set of force measurements had been made the carbon specimen was roughened with an increasing size of 'polishing' powder, and then another profile trace was taken. Some of the profile traces are shown in fig. 6.2.

From each profile a bearing area curve was constructed by drawing between five and ten parallel section lines, depending on the roughness, at four separate sections of the profile to get an average curve of the whole profile. Each section represented 1mm of the specimen's surface and the four sections were taken from different parts of the profile. The four sections were matched up as the

surfaces were not truely flat and the sections were often at slight angles to each other. Typical bearing area curves obtained from the sections are shown in fig. 6. 3.

Although these curves are not as accurate as those produced by digitized output from a profilometer, they are a good guide to the surface shape. To check whether the distribution of heights was Gaussian the curves were drawn on probability graph paper on which a Gaussian distribution function would be a straight line. Typical results are shown in fig. 6. 4. The results for all the surfaces analysed are summarised in table 6. 2. The surfaces were found to have slightly skewed distributions of heights. (Sharman obtained similar results with ground surfaces). The degree to which the distributions were skewed varied between the specimens which was probably due to their differences in surface curvature. Specimen C5 had a radius of curvature of 12m and C6 a radius of curvature of 60m.

The standard deviations, σ, of the surfaces were in good agreement with the measured C. L. A. values. The C. L. A. value characterising a surface was the mean of seven values each taken with a traversal of the profilometer stylus across a different section of the same surface. Although the surfaces did not have an exact Gaussian distribution of heights, about 80% of a surface could be regarded as Gaussian. The other 20% represented the peaks and valleys of the surface. In the following theory the surfaces generating the Johnsen-Rahbek effect will be regarded as Gaussian.

6. 4 THEORY

Having examined the roughness of the carbon's surface, its effect on the force can be calculated. The calculation is very complex, however, and simplifying assumptions have to be made. One simplification is to consider nominally flat, parallel rough surfaces to be generating the effect. Any calculations, however, would have to be compared with results obtained from the ball-on-flat method of measuring the force, which employs a very curved surface in the form of the ball. Consequently two theories are developed; one considering norminally flat surfaces and the other curved surfaces where the surface curvature is the dominant factor rather than the roughness.

In both theories the situation assumed is that of a rough semiconductor surface in contact with a smooth metal surface. This is effectively the practical situation with a smooth ball in contact with a rougher semiconductor.

6.4.1 NOMINALLY FLAT SURFACES

The roughness of the semiconductor is assumed to be described by a Gaussian distribution of the surface heights. An average asperity of this distribution is the Gaussian distribution function, F (x), (see Appendix 2), rotated about the x-axis, through an angle of 2π, fig. 6.5. This is a more accurate and less complicated asperity than Atkinson's two-tiered onion shape, the latter asperity having zero normal surface area at the mean surface height, μ. It is assumed in the present work, and as Atkinson assumed in his calculations, that the semiconductor surface is an equipotential surface outside the region of current emission. This is a great simplification but it does not alter the form of the force/voltage relationship, it only introduces a numerical error. This is as in the calculation of the force between a ball and flat. If the above assumption had been made there eq. (4.1.11) would have become :

$$F_T = 2.5 \pi R \epsilon_o E_o V_o \qquad (5.4.1)$$

producing no error of form but simply a numerical error.

The calculations made with the Gaussian asperity are similar to Atkinson's but simpler. Fig. 6.5 defines the notation used in the calculations, where z_o is the depth of the current emitting region at a given voltage and z is the standardised variable of the distribution, where

$$z = (x - \mu) / \sigma \qquad (6.4.2)$$

with $\mu = 0$ and $\sigma = 1$. The radius of the current emitting region is $F(z_o)$, so the force over this region is

$$F_E = \frac{\epsilon_o \pi F^2(z_o) E_o^2}{2} \quad (N) \qquad (6.4.3)$$

E_o being the saturation electric field in this region. The force developed over

the non emitting region is

$$F_{NE} = \int_{o}^{\infty} \frac{\epsilon_o \pi F(z) f(z) E_o^2 (M - z_o)^2}{(M - z)^2} d \qquad (6.4.4)$$

where $V_o = E_o (z_o - M) \sigma$ (6.4.5)

The voltage across the interface is the total applied voltage, V_o, as the bulk resistances of the semiconductors used in the present work are negligible in comparison to the constriction resistances.

The value of M is critical in determining the force developed. Atkinson did not state the value he used. Greenwood and Williamson theoretically derived a value between -4σ and -3σ for metal surfaces in contact, and Williamson derived a value nearer to -2σ for aluminium surfaces 1.15 μm C. L. A. rough. Examination of the profilometer traces indicates a value nearer to -2σ. The value of M, moreover, would be changed by the force between the surfaces which would cause deformation of the contact. So calculations were made with three values of M; -1σ, -2σ and -4σ. Evaluating eq. (6.4.4) by numerical integration, where the upper limit is taken as $+4.0\sigma$ yields the force/voltage relationships shown in fig. 6.6 .

It is interesting to note the relative contributions of the emitting and non-emitting regions to the total force, as the larger the emitting region the higher the current flow with its attendant heating and etching, (discussed later). Thus in the design of a device the criterion of maximum permitted current flow could be the dominant consideration rather than the maximum force acheived.

These calculations have been made in terms of z_o, the depth of penetration of the emission region over the asperity. The variation of the force with the measured roughness is required, however and z_o can be related to the measured roughness, (the C. L. A. value), by the following relationship :

$$z_o = M + \frac{V_o}{E_o \times 1.2 \times (C.L.A)} \qquad (6.4.6)$$

This is eq. (6.4.5) with σ replaced by the C. L. A., (Appendix 2).

As z_o is a function of the applied voltage and the roughness of the surface, the effect of the roughness on the force can only be considered in conjunction with the voltage applied. With an applied voltage of 100 volts, maximum forces can be obtained with a surface of roughness $0.03\,\mu m$ C. L. A. whereas for a surface of roughness $1\,\mu m$, C. L. A. nearer 3,000 volts is required for an equivalent force

Fig. 6.7 shows a graph of the force for various reasonable values of V_o/E_o, and indicates that the relationship is approximately exponential, the force rapidly decreasing with increasing roughness,

$$\text{Force} \propto \exp(-\text{C. L. A.}) \qquad (6.4.7)$$

This model cannot easily be used to show the effect of surface roughness on the current flow. The effect can, however, be discussed qualitatively by considering an average asperity of the surface. As the roughness of a surface increases the area of the contacting surfaces in intimate contact decreases. This increases the constriction resistance and hence the ohmic current decreases. However, current emission can occur in the gaps between the asperities enhancing the current. Also the electric field at the tip of an asperity in the interfacial gap will be enhanced locally, producing more current flow from the asperity. Although the enhancement due to an asperity is complex to calculate and involves many factors, (Lewis), it can be taken as approximately inversely proportional to the radius of curvature of the asperity tip. Due to this enhancement of the field, a rougher surface would probably pass more current than a smoother surface at low voltages. When the voltage increases however, the smoother surface has a larger area for current emission and so passes more current than the rougher surface.

6.4.2 CURVED SURFACES

In the last section the force developed across an average asperity was calculated. In this section a theory is developed considering the surfaces to be smooth, but separated from each other by a distance, β, proportional to the

roughness. This is effectively regarding the rougher semiconducting surface as having its most significant surface area near to the average height of the asperities, μ, and the surface to be separated from the ball by approximately M. This is truer for smoother surfaces than for rougher surfaces with higher values of σ, but the approximation is still applied. The idea essentially, is that as the rough carbon surface becomes rougher, then β increases, effectively separating the surfaces further. Thus the effect of the roughness and curvature of the surface upon the force can be calculated. The same assumptions are made as those that were made in the derivation of the force between a ball and flat, Chapter 4.

The separation of the surfaces reduces the region of current emission, c , in the interfacial gap from that produced by smooth surfaces to

$$c^2 = \frac{RV_o}{E_o} - R\beta \qquad (6.4.8)$$

Effectively, the separated surfaces can be regarded as being in contact except that a voltage $V_o - \beta E_o$ rather than V_o is applied between them. This concept depends on the fact that the equipotential lines in the gap are parallel to the metal surface and that the interfacial gap distance in the region over which the force is developed changes slowly with the distance from the contact.

Putting

$$\phi = \frac{\beta E_o}{V_o} \qquad (6.4.9)$$

the equations for the non-emitting and emitting forces becomes :

$$F_E = \frac{\epsilon_o \pi R V_o E_o}{2} (1 - \phi) \qquad (6.4.10)$$

and

$$F_{NE} = \frac{4 \epsilon_o R E_o (1-\phi) V_o}{\pi} \int_{1.0}^{\infty} \left\{ \frac{(1-\phi)^2}{\left[1 - \phi\left(\frac{\lambda^2 - 2}{2}\right)\right]^2} V^2_{int} \right\} d\lambda \qquad (6.4.11)$$

where V_{int} is given by eq. (4.1.6).

Evaluating the integral numerically yields

$$F_T = 1.48\,\pi R\,\epsilon_o E_o\,(1.0 - 0.68\,\phi)\,V_o\,(1 - \phi) \qquad (4.4.12)$$

The term $(1 - 0.68\,\phi)$ was determined from a graph of F_T versus $1.48\,\pi R\,\epsilon_o E_o V_o (1 - \phi)$, shown in fig. 6.8

Comparing this equation with eq. (4.1.11) derived for smooth surfaces, $(\phi = 0.0)$, it can be seen that no force can be generated unless a voltage satisfying

$$V_o > \beta E_o \qquad (6.4.13)$$

is applied. Also, eq. (6.4.12) shows that the force/voltage relationship is non-linear as can be seen by combining equations (6.4.9) and (6.4.12)

$$F_T = 1.48\pi R\,\epsilon_o E_o V_o \left[1 - \frac{1.68\beta E_o}{V_o} + \frac{0.68\beta^2 E_o^2}{V_o^2} \right] \qquad (6.4.14)$$

With β equated to twice and four times the C.L.A. (c.f. the value of M in the previous section), eq. (6.4.14) versus C.L.A. is shown in fig. 6.9. The effect of surface roughness on the current flow can be calculated by replacing V_o by $V_o - \beta E_o$ in eq. (4.1.4), giving :

$$I = \frac{8}{3\rho} \left(\frac{R}{E_o} \right)^{\frac{1}{2}} V_o^{3/2} \left(1 - \frac{\beta E_o}{V_o} \right)^{3/2} \qquad (6.4.15)$$

At low voltages the current is very dependent on the surface roughness but at higher voltages the current/voltage relationship tends to that of smooth surfaces, although the current varies with voltage to an index slightly above

that of 1.5 for smooth surfaces, see fig. 6.15. The value of this index depends on the surface roughness and the applied voltage. This also applies to eq. (5.5.1) where d is non negligible. Upon substituting $V_o - E_o\beta$ in place of V_o it becomes :

$$I = \frac{8}{3\rho} \frac{E_o d^3}{R} \left[\left(1 + \frac{(V_o - \beta E_o) R}{E_o d^2} \right)^{3/2} - 1 \right] \qquad (6.4.16)$$

If

$$\frac{(V_o - E_o\beta) R}{E_o d^2} < 1 \qquad (6.4.17)$$

then the equation can be expanded to :

$$I = \frac{4d}{\rho} (V_o - E_o\beta) + 4 \frac{(V_o - E_o\beta)^2 R}{\rho E_o d} \qquad (6.4.18)$$

showing that the current which flows is significantly reduced by the roughness at low voltages and only when the voltage becomes higher does current emission occur significantly.

6.4.3 VALIDITY OF THE THEORIES

Both of the previous models are rather crude and simple but they give an indication of how the surface roughness affects the force. They do not provide analytical solutions but approximate calculations. Neither model accurately describes the ball-on-flat situation but the theories do overlap slightly. Although the theory of nominally flat surfaces does not apply directly to the situation it does apply to small sections of the interfacial gap near the contact where the effect of surface curvature is not so marked. The second theory, although it applies to the ball-on-flat situation does not deal adequately with the region close to the contact where surface roughness dominates over curvature. The theories are complementary.

6.5 FORCE MEASUREMENTS WITH ROUGHENED CARBON

6.5.1 EXPERIMENTAL METHOD

The forces generated between two specimens of carbon, C5 and C6 each in

contact with a 2.54 cm diameter steel ball were measured for varying roughness of the carbon specimens. The surface roughness was measured before each set of force measurements was made as was described earlier. The force measurements were taken under the same conditions as those discussed in Chapter 4, and the procedure was the same. Approximately 12 force measurements were made for each polarity of voltage applied to the ball-on-flat for each roughness of the surface. Mechanical forces greater than 7 gm. f. were not applied to the contact as it was considered that the damage to the carbon caused by large forces might alter the surface roughness. The carbon was not kept for longer than two hours inside the vacuum chamber so that it would not desorb and alter its resistance excessively. After the carbon had been roughened and a new surface texture obtained it was cleaned in the usual manner, as was the ball, before insertion into the force measuring apparatus.

It was found that when the C5 specimen was roughened to 1.3μm C.L.A. very small forces were generated upon the application of voltages in the region of 400 volts and the force measurements were very inaccurate. So the ball-on-flat method is limited to measuring forces on specimens with surfaces smoother than 1.3μm C.L.A.

The current measurements made in the present experiment were taken from the meter rather than the XY recorder so that accurate comparisons between the currents produced by the various surface textures could be made.

6.6 RESULTS AND DISCUSSION

The force/voltage graphs obtained from these force measurements were straight lines and the data obtained from them, summarised in table 6.3, was calculated using the method of least squares. The calculation of β is discussed later. The current/voltage plots are displayed on log-log graphs to show the relationships of the variables.

6.6.1 COMPARISON OF THE FORCE MEASUREMENTS WITH THE CURVED SURFACES THEORY

The C6 results show that the voltage intercept of the force/voltage plot increases with increasing surface roughness as the theory indicates. The theory

shows that the value of β can be calculated assuming E_o is constant at a value that would be obtained with smooth surfaces. Using the highest value of E_o obtained with the C6 specimen, 9.2×10^8 V.m^{-1}, very small values of β are obtained. Such values, much less than the C. L. A. for the surface, indicate that gross deformation of the surface would have taken place, but no such deformation was observed on the specimen after the measurements. The value of E_o decreased with surface roughness, however, and if the measured value is used to calculate β, values approximately 1.0 times the C. L. A. are obtained.

The C5 results, although taken over a smaller range of surface roughness, give values of β about 1.3 times the C. L. A. even though the intercepts with this specimen are much smaller and less accurate than those of the C6 specimen.

The total force, however, is not represented by E_o, but has to include the intercept voltage. Deriving ϕ for each value of surface roughness at 100 volts, the total force can be calculated from eq. 6.4.14. The calculated force agrees well with the theoretical curve for the C6 results, fig.6.11, but not very well for the C5 results.

Results obtained from the second model agree reasonably well with the experimental results of the C6 specimen, but less well with the C5 specimen. Moreover, this model assumed that E_o remained constant, only altering due to the curvature of the force/voltage plot. There is little evidence for any curvature of the force/voltage plots in the results obtained, except for the C5 results shown in fig.6.12. The rougher surfaces show little curvature, less than the theory predicts and certainly not enough for the value of E_o to be calculated as low as the values obtained from the C6 results, fig.6.12.

6.6.2 COMPARISON OF THE FORCE MEASUREMENTS WITH THE THEORY OF NOMINALLY FLAT SURFACES

The saturation electric field, E_o, is found to decrease with increasing roughness. Analysis of the variation of E_o with surface roughness shows that the relationship is approximately exponential, (figs. 6.13 and 6.14). The theory

predicts the force to decrease approximately exponentially with roughness and if the force/voltage line goes through the origin of the axes then E_o is proportional to the force. Even when this is not the case, E_o can approximately be regarded as the force, especially over the region near the contact. The results show a more gradual decrease in E_o than the theory predicts. This is considered to be due to the fact that eq. (6.4.6) is not accurate for curved surfaces, where the value of M has to be averaged over the whole region of the contact, making z_o less dependent on the C. L. A. value depending on the curvature of the surface.

The more rapid decrease of E_o with roughness for C5 compared with the C6 results is probably due to its higher surface curvature. The C. L. A. value does not take into account the slight curvature of the surface, but the force generated in the gap is very sensitive to variations in gap width. It is difficult to quantify this with the results of only two specimens, but empirically the relationships seem to be related by dividing the C. L. A. value by the square root of the surface curvature of the specimen.

6.6.3 COMPARISON OF THE CURRENT MEASUREMENTS WITH THE THEORY OF CURVED SURFACES

The C6 results, fig 6.16, show that the current decreased with surface roughness approximately as the theory indicated. At low voltages the theory is not in good agreement with the results, (see fig. 6.15 & fig. 6.16), but at higher voltages the agreement is better. The theory also shows better agreement with the C5 results, (fig. 6.17), at higher voltages.

6.6.4 COMPARISON OF THE CURRENT MEASUREMENTS WITH THE THEORY OF NOMINALLY FLAT SURFACES

The C5 results, fig. 6.17, show that when the carbon surface in initially roughened slightly the current flow is enhanced at low voltages and the rougher surface passes slightly more current than the smoother surface. This only occurred for small changes in surface roughness and is attributed to the increasing

curvature of the asperities as discussed in the theory of nominally flat surfaces. The C6 results do not show this enhancement of current as there was a greater difference in the roughness of each surface and although the asperities were of greater curvature the area for current emission had greatly diminished.

6. 7 PREVIOUS WORKERS' RESULTS

The results show that the value of E_o varies as the negative exponential of the surface roughness and when these values of E_o are inserted into the equation for the force derived from the theory of curved surfaces, eq.(6.4 .14), reasonably accurate calculations of the force can be made. So an empirical formula for the force is :

$$F_T = 1.48\,\pi R\,\epsilon_o\,E_{om}\,\exp\left(\frac{-C.L.A.}{0.04\sqrt{r}}\right)(1-\phi)(1-0.68\phi) \qquad (6.7.1)$$

where E_{om} is the value of E_o for smooth surfaces, R the radius of the ball and r the radius of curvature of the semiconductor. The other symbols have their usual meanings. This only applies to the ball-on-flat situation but the equation and the theories previously discussed can be checked with previous workers' results:

6.7.1 STUCKES' RESULTS

Using the theory of nominally flat parallel surfaces with $M = -1\sigma$ the calculations are found to agree well with the results, fig.6.10 , better than Atkinson's calculations. The surfaces of the specimens were only slightly curved, (the radius of curvature was about 10^2m), so the whole region could be regarded as equivalent to the region of the ball and flat near the contact for which the theory of nominally flat surfaces applies.

This demonstrates that the theory can apply to slightly curved surfaces provided an average value of M for the whole surface, which includes the effect of surface curvature, is used. The present results also show that the theory is most accurate for a value of M of about -1σ .

6.7.2 LEVESON'S RESULTS

These results, fig 6.18, are difficult to analyse as the contact geometry is not known and the force/voltage plots are non-linear for reasons previously stated. However, significant forces were found for surfaces as rough as 1.9μm C.L.A. The present work would indicate the value of E_o to be about $10^6 Vm^{-1}$ for such a rough surface, using the eq.(6.7.1), and a small force to be generated, much less than the force actually measured. This is because very little current emission would occur across the surface and the force would be mainly the electrostatic attraction across the non-emitting regions. In terms of the present theories, ϕ and M would be very small and the theories are very inaccurate for these values. The force can be calculated by assuming no current emission across the interfacial gap to occur. The present empirical relationship can be modified by adding this term but it is not an important term as surfaces as rough as Leveson used are not practicable for generating the effect.

6.8 CONCLUSION

It has been shown that the roughness of a surface is a major factor in determining the force developed by that surface. The results show that the force decreases significantly for small increases in surface roughness and the theory developed accounts for this. Although the results and theory only apply to a ball-on-flat situation with surfaces smoother than about 1.3μm; they indicate the behaviour of the force in other systems, e.g. flat-on-flat.

The results indicate that the curvature of the flat surface is also important in determining the value of E_o and the force. The ratio C.L.A./$\sqrt{F}$ was the determining parameter of this value and it is proposed that the quality of a surface, with respect to the force it can generate, can be quantized by this ratio, the value of E_o being proportional to the negative exponential of it.

TABLE 6.1

THE ROUGHNESSES OF TYPICAL ENGINEERING SURFACES (AFTER HALLING AND EL-REFAIE)

SURFACE PREPARATION	ROUGHNESS OF SURFACE AFTER THIS PREPARATION (μm C.L.A.)
SUPER FINISHING	0.15
GRINDING	0.75
FINE TURNING	1.0
MILLING	2.25
FINE SHAPING	7.5
SHAPING	12.5

TABLE 6 2

ANALYSIS OF THE DISTRIBUTION OF SURFACE HEIGHTS FROM BEARING AREA CURVES OF VARIOUS SURFACE TEXTURES OF CARBON SPECIMENS.

SPECIMEN	MEASURED ROUGHNESS OF SURFACE (μm C.L.A.)	C.L.A. x 1.2	DATA FROM PROBABILITY PLOTS				NUMBER OF LINES FOR CONSTRUCTION OF THE BEARING AREA CURVE	DISTANCE BETWEEN CONSTRUCTION LINES (μm)
			STANDARD DEVIATION (σ) FOR UPPER PART OF CURVE	RANGE OF UPPER PART OF CURVE (%)	STANDARD DEVIATION (σ) FOR LOWER PART OF CURVE	RANGE OF LOWER PART OF CURVE (%)		
C6	0.026 ± 0.002	0.03	0.05	67-100	0.021	0-67	7	0.02
C6	0.18 ± 0.01	0.21	0.33	60-100	0.14	0-60	8	0.01
C6	0.37 ± 0.01	0.44	0.51	54-100	0.26	0-54	10	0.2
C5	0.014 ± 0.002	0.017	0.025	80-100	0.015	0-80	5	0.02
C5	0.016 ± 0.001	0.019	0.016	45-100	0.012	0-45	7	0.01
C5	0.026 ± 0.002	0.03	0.02	15-100	0.05	0-15	7	0.02
C5	0.036 ± 0.002	0.043	0.08	84-100	0.03	0-84	5	0.04
C5	0.048 ± 0.004	0.06	0.052	18-100	0.12	0-18	8	0.04

TABLE 6.3

DATA ON FORCE/VOLTAGE PLOTS CONSTRUCTED FROM FORCE MEASUREMENTS MADE ON TWO SPECIMENS OF CARBON WITH VARIOUS SURFACE TEXTURES.

SPECIMEN	MEASURED SURFACE ROUGHNESS (μm C. L. A)	POLARITY OF POTENTIAL OF CARBON (POS/NEG)	SATURATION ELECTRIC FIELD, E_o ($10^8 Vm^{-1}$)	VOLTAGE INTERCEPT OF PLOT V_{o1} (VOLT)	CALCULATE SEPARATION OF SURFACE $= E_o/V_{o1}$ (μm)
C6	0.026 ± 0.002	POS	7.0 ± 0.2	15 ± 5	0.022
		NEG	9.2 ± 0.3	40 ± 3	0.043
C6	0.18 ± 0.01	POS	4.5 ± 0.4	47 ± 15	0.103
		NEG	4.7 ± 0.2	47 ± 5	0.1
C6	0.37 ± 0.01	POS	2.2 ± 0.1	92 ± 10	0.42
		NEG	2.2 ± 0.1	82 ± 8	0.38
C5	0.014 ± 0.002	POS	7.5 ± 0.6	19 ± 10	0.025
		NEG	8.5 ± 0.5	28 ± 6	0.033
C5	0.016 ± 0.001	POS	7.4 ± 0.4	28 ± 17	0.038
		NEG	8.7 ± 0.8	30 ± 10	0.036
C5	0.026 ± 0.002	POS	6.2 ± 0.2	4 ± 4	0.007
		NEG	6.8 ± 0.3	9 ± 5	0.013
C5	0.036 ± 0.002	POS	6.4 ± 0.5	27 ± 11	0.043
		NEG	6.0 ± 0.3	16 ± 8	0.027
C5	0.048 ± 0.004	POS	5.1 ± 0.2	10 ± 6	0.02
		NEG	6.3 ± 0.4	26 ± 9	0.04

ATKINSON'S ASPERITY AND RESULTS

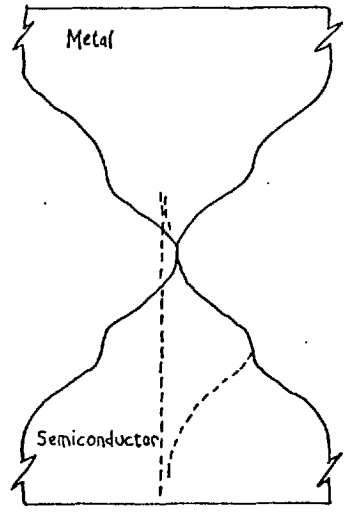

(AFTER ATKINSON)

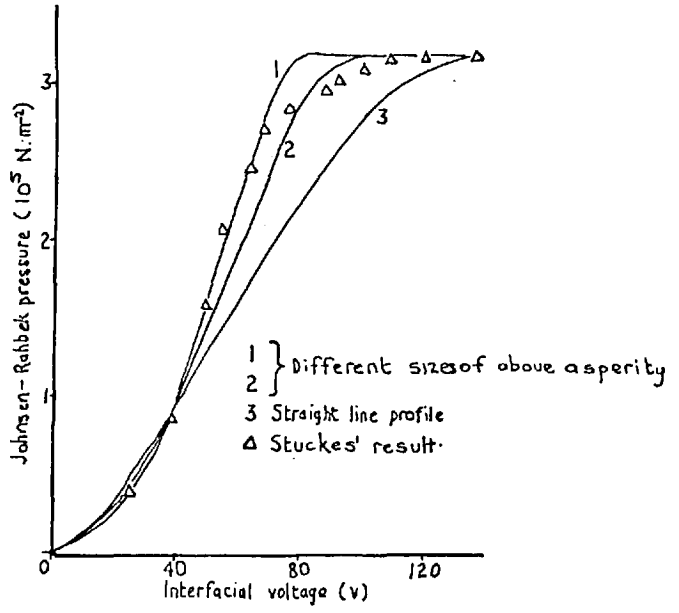

(AFTER ATKINSON)

FIG. 6.1

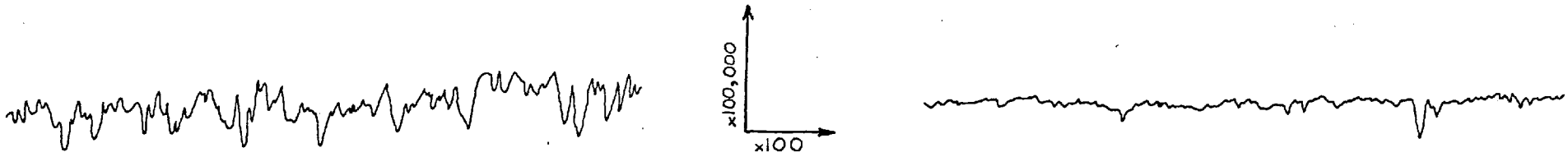

PROFILES OF DIFFERENT CARBON SURFACES

FIG.6.2

BEARING AREA CURVES OF ABOVE PROFILES

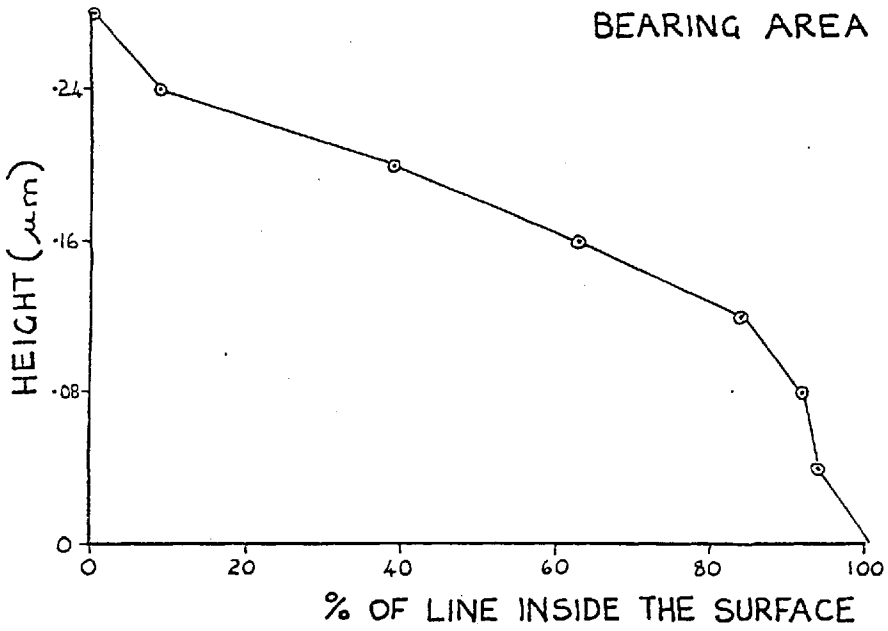

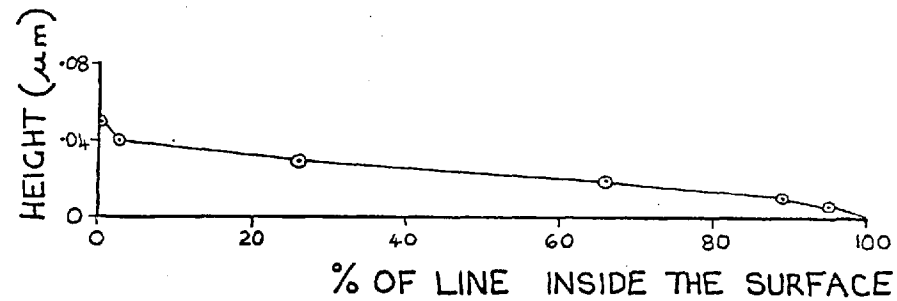

FIG.6.3

A TYPICAL BEARING AREA CURVE DRAWN ON PROBABILITY PAPER

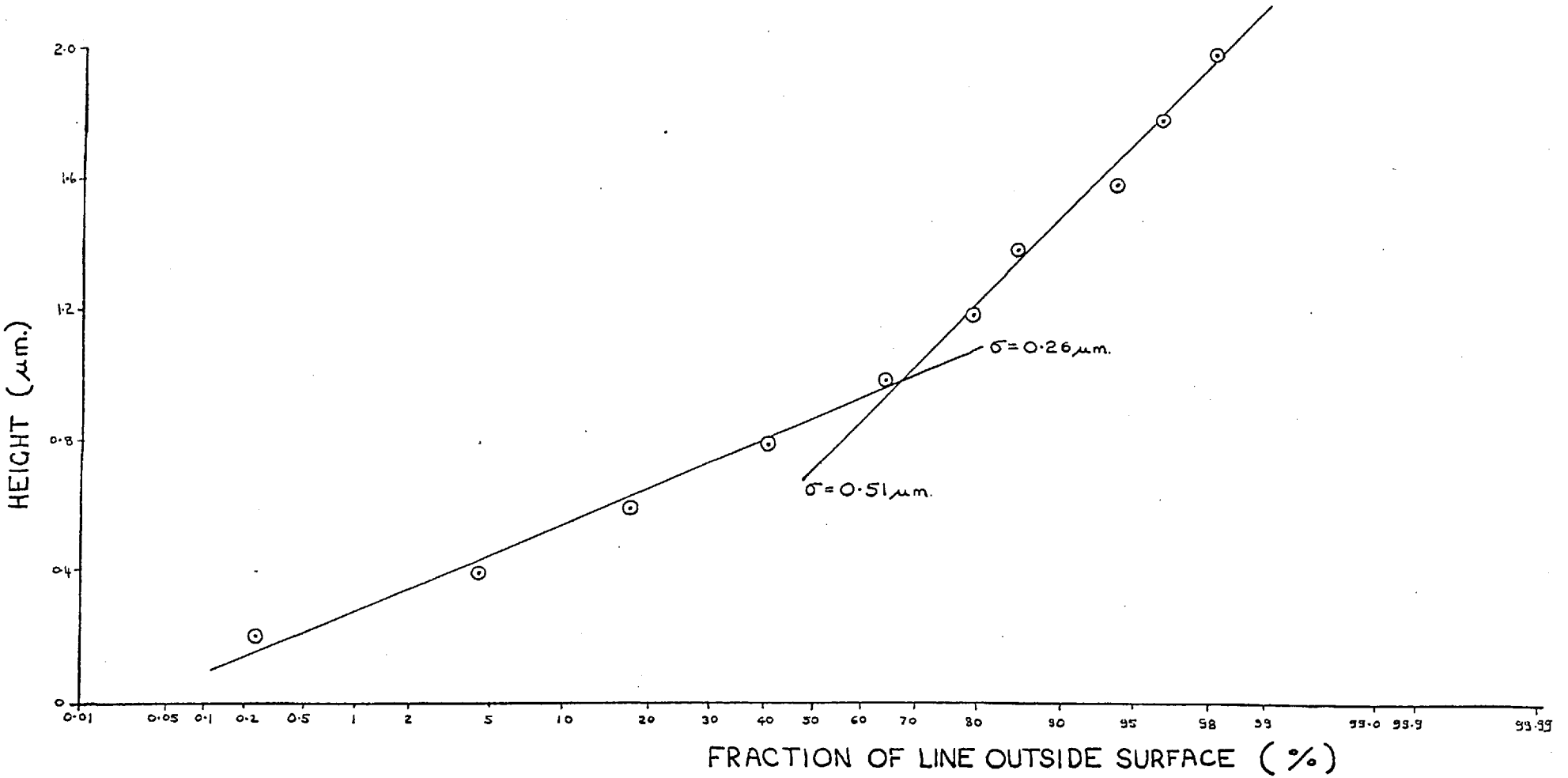

FIG.6.4

AN AVERAGE ASPERITY OF A ROUGH SEMICONDUCTOR'S SURFACE IN CONTACT WITH A SMOOTH METAL'S SURFACE

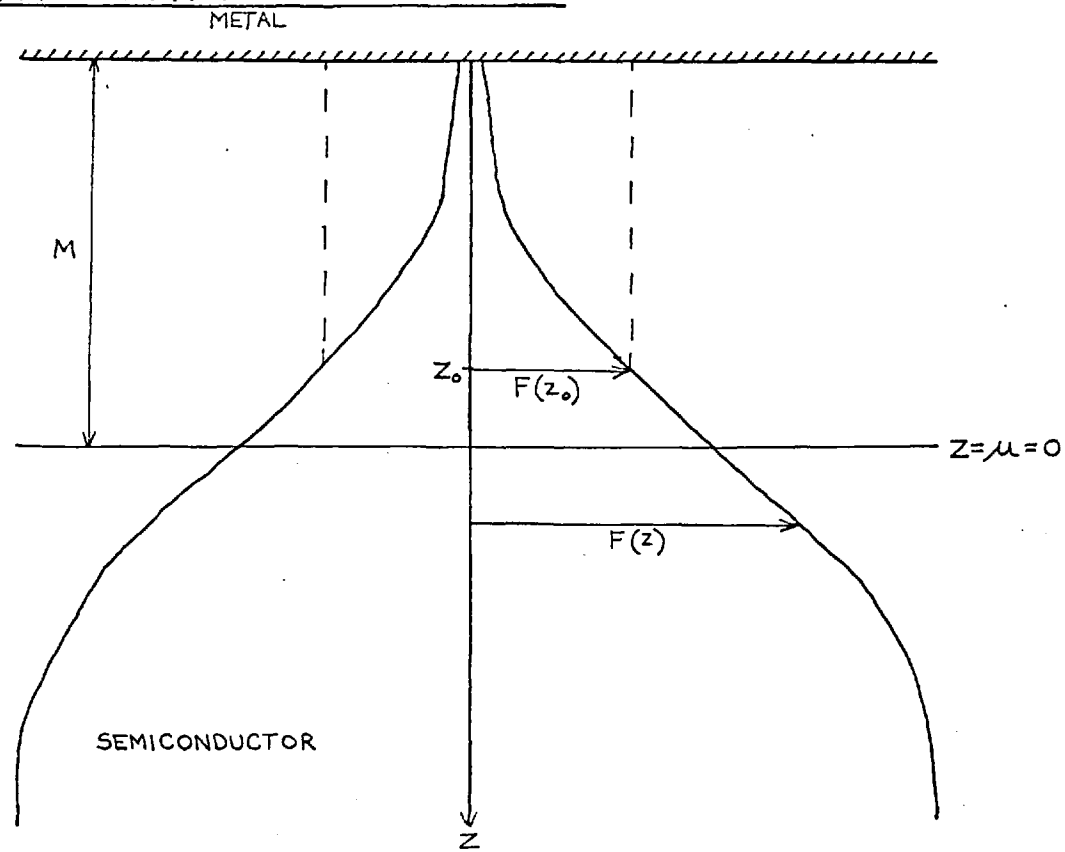

FIG.6.5

THE VARIATION IN THE JOHNSEN-RAHBEK EFFECT WITH VARIOUS SEPARATIONS BETWEEN FLAT SURFACES

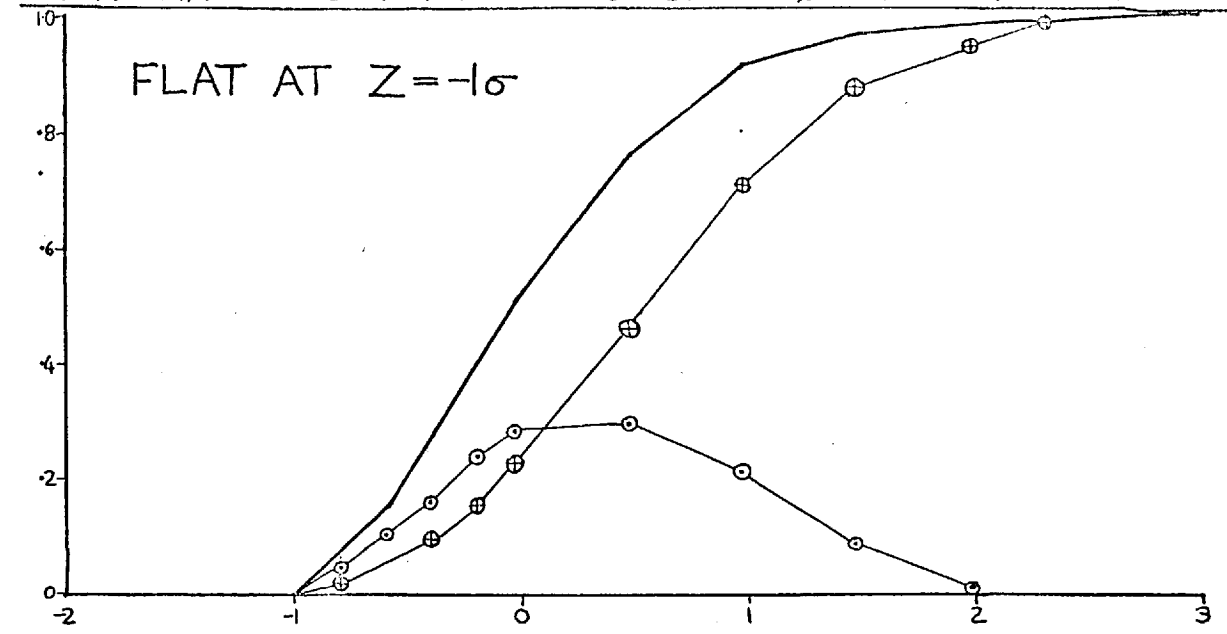

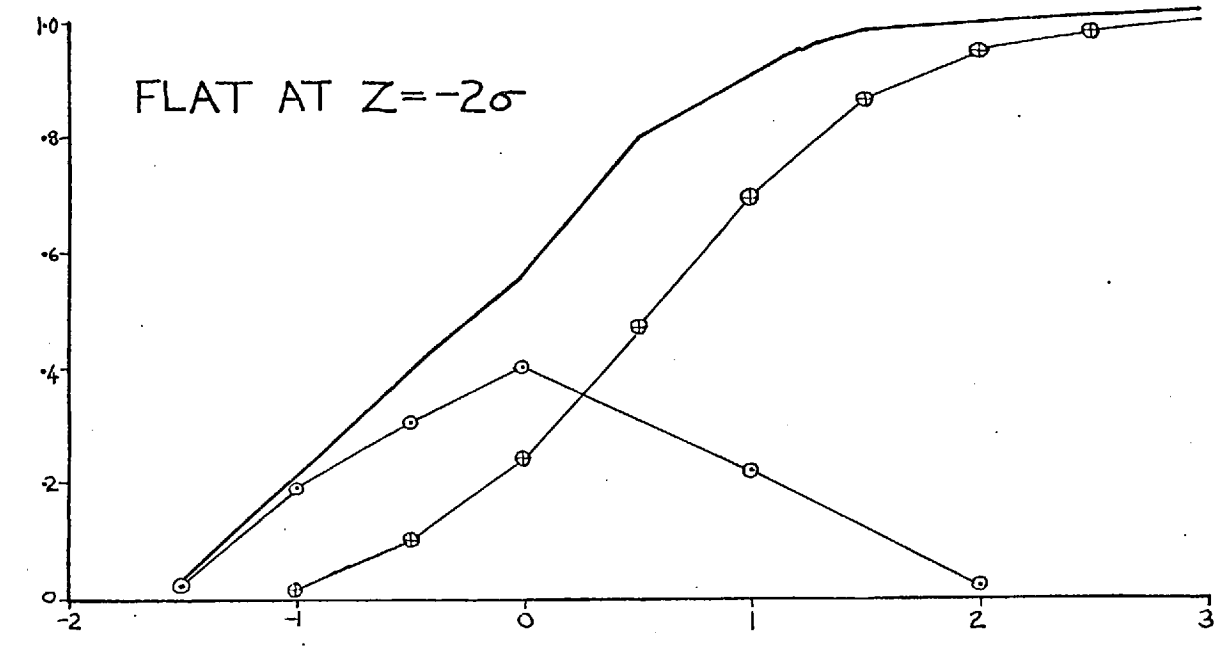

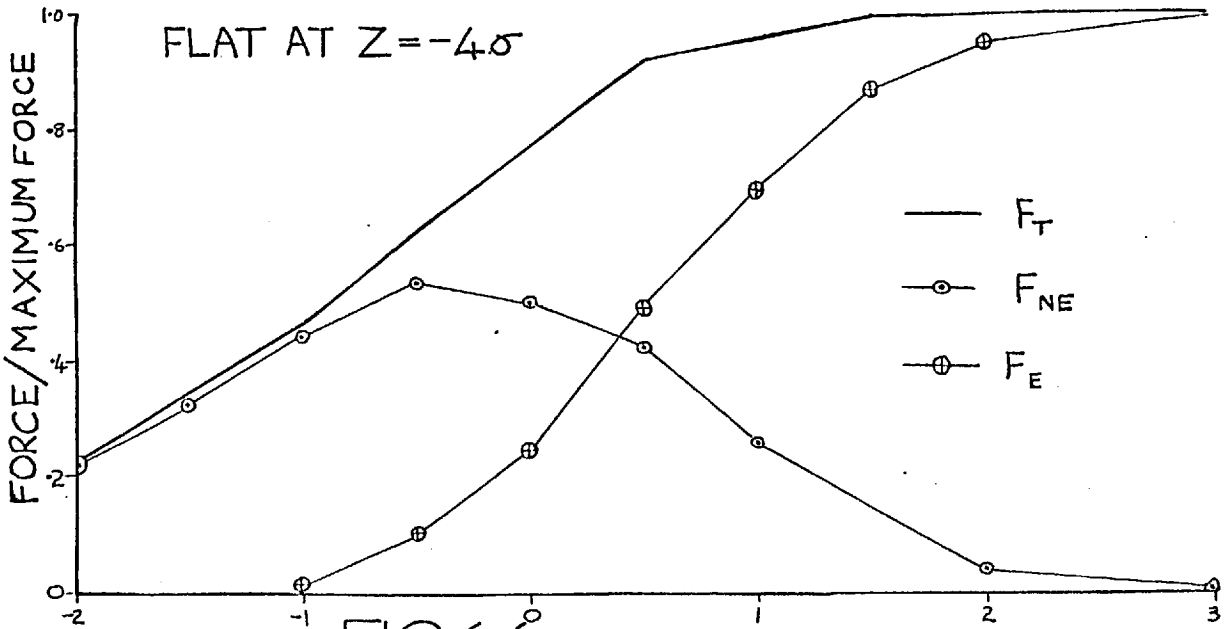

FIG.6.6

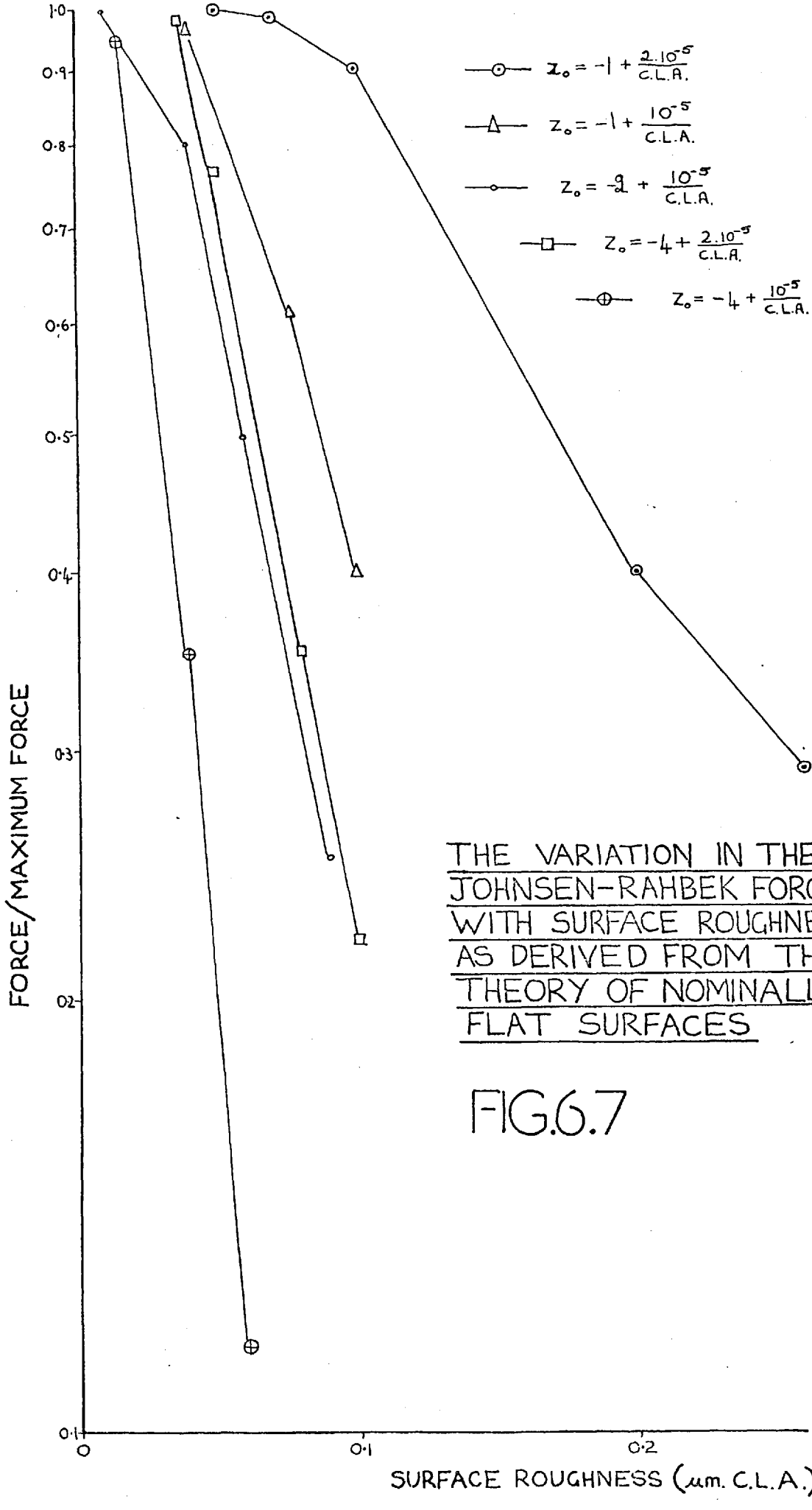

THE VARIATION IN THE JOHNSEN-RAHBEK FORCE WITH SURFACE ROUGHNESS AS DERIVED FROM THE THEORY OF NOMINALLY FLAT SURFACES

FIG.6.7

A GRAPH TO DETERMINE A CONSTANT IN THE FORCE FORMULA DERIVED FROM THE THEORY OF CURVED SURFACES

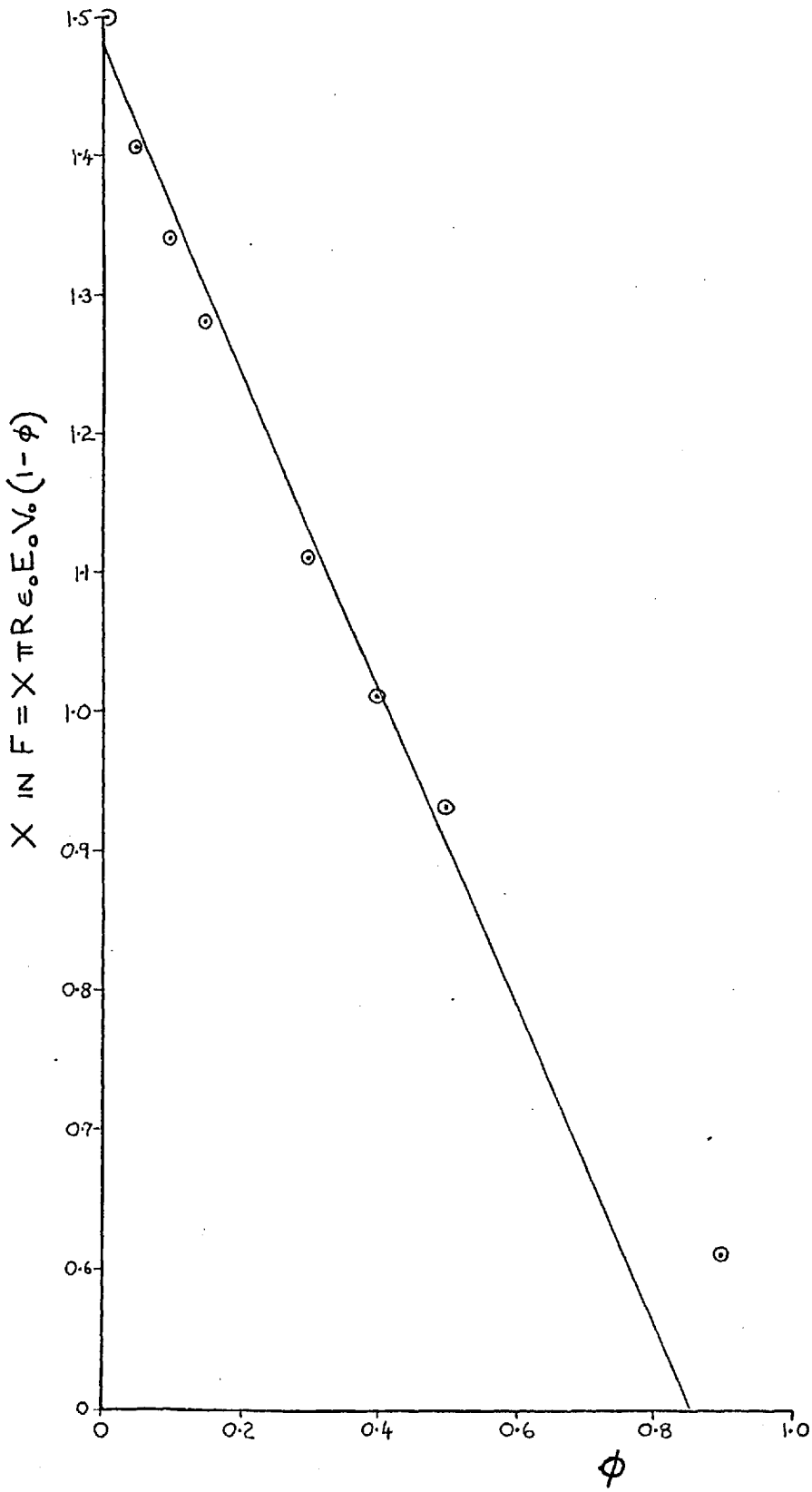

FIG.6.8

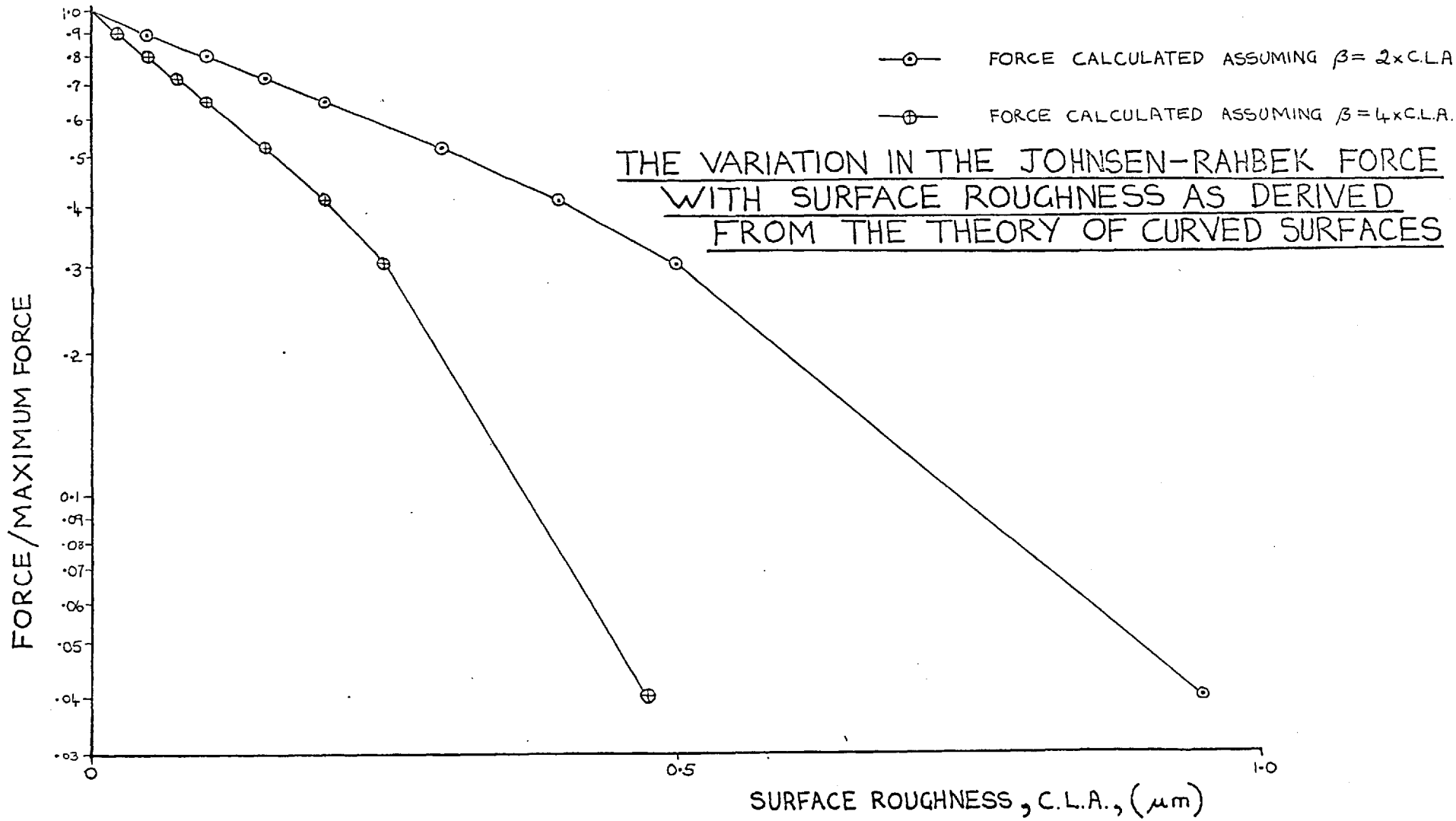
FORCE CALCULATED ASSUMING β = 2 × C.L.A
FORCE CALCULATED ASSUMING β = 4 × C.L.A.
THE VARIATION IN THE JOHNSEN-RAHBEK FORCE WITH SURFACE ROUGHNESS AS DERIVED FROM THE THEORY OF CURVED SURFACES
FORCE/MAXIMUM FORCE
1·0
·9
·8
·7
·6
·5
·4
·3
·2
0·1
·09
·08
·07
·06
·05
·04
·03
0
0·5
1·0
SURFACE ROUGHNESS, C.L.A., (μm)

FIG.6.9

A COMPARISON BETWEEN CALCULATIONS FROM THE THEORY OF NOMINALLY FLAT SURFACES AND STUCKES' RESULTS

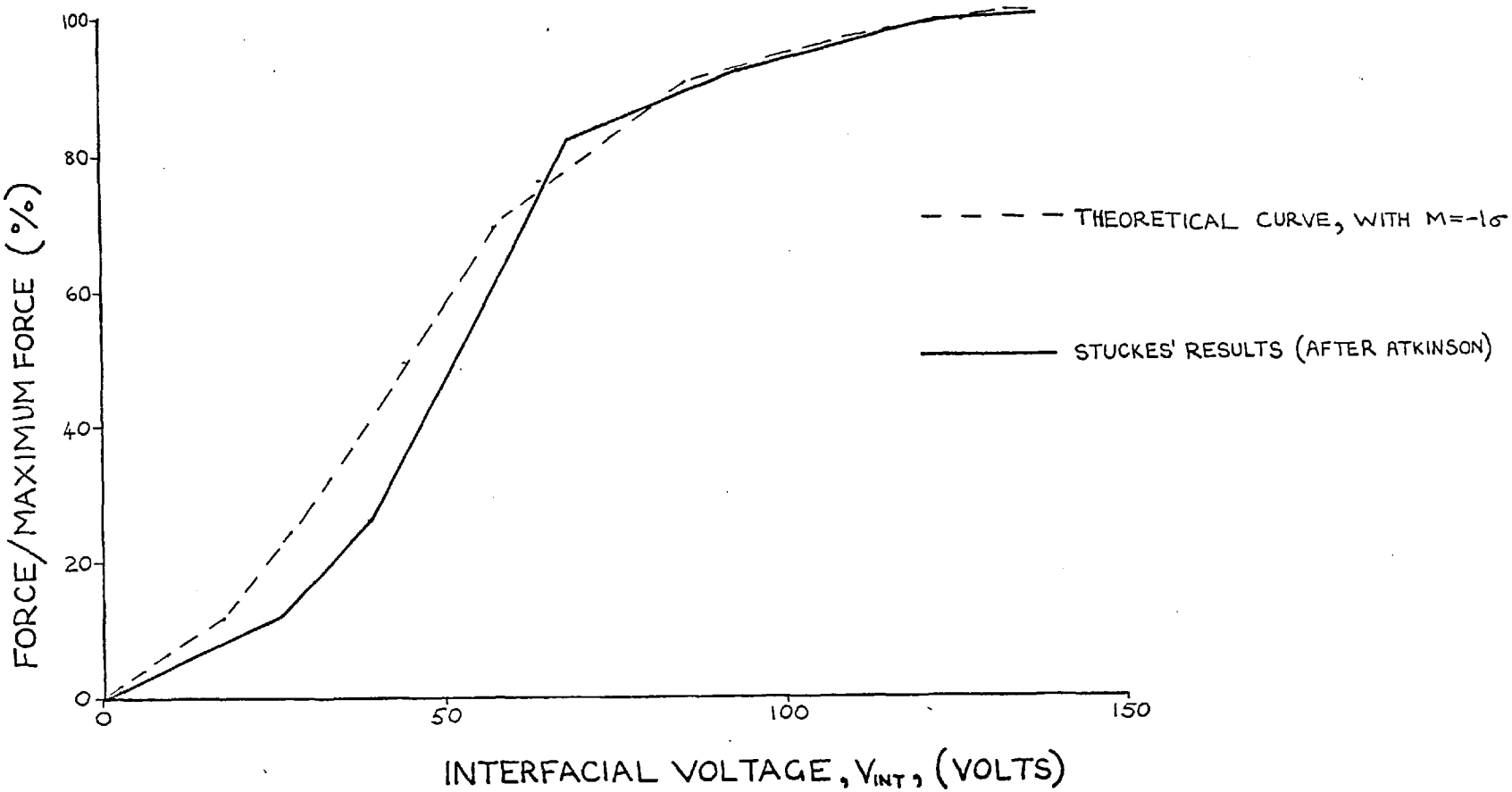

FIG.6.10

A COMPARISON OF EXPERIMENTAL RESULTS WITH CALCULATIONS BASED ON THE THEORY OF CURVED SURFACES

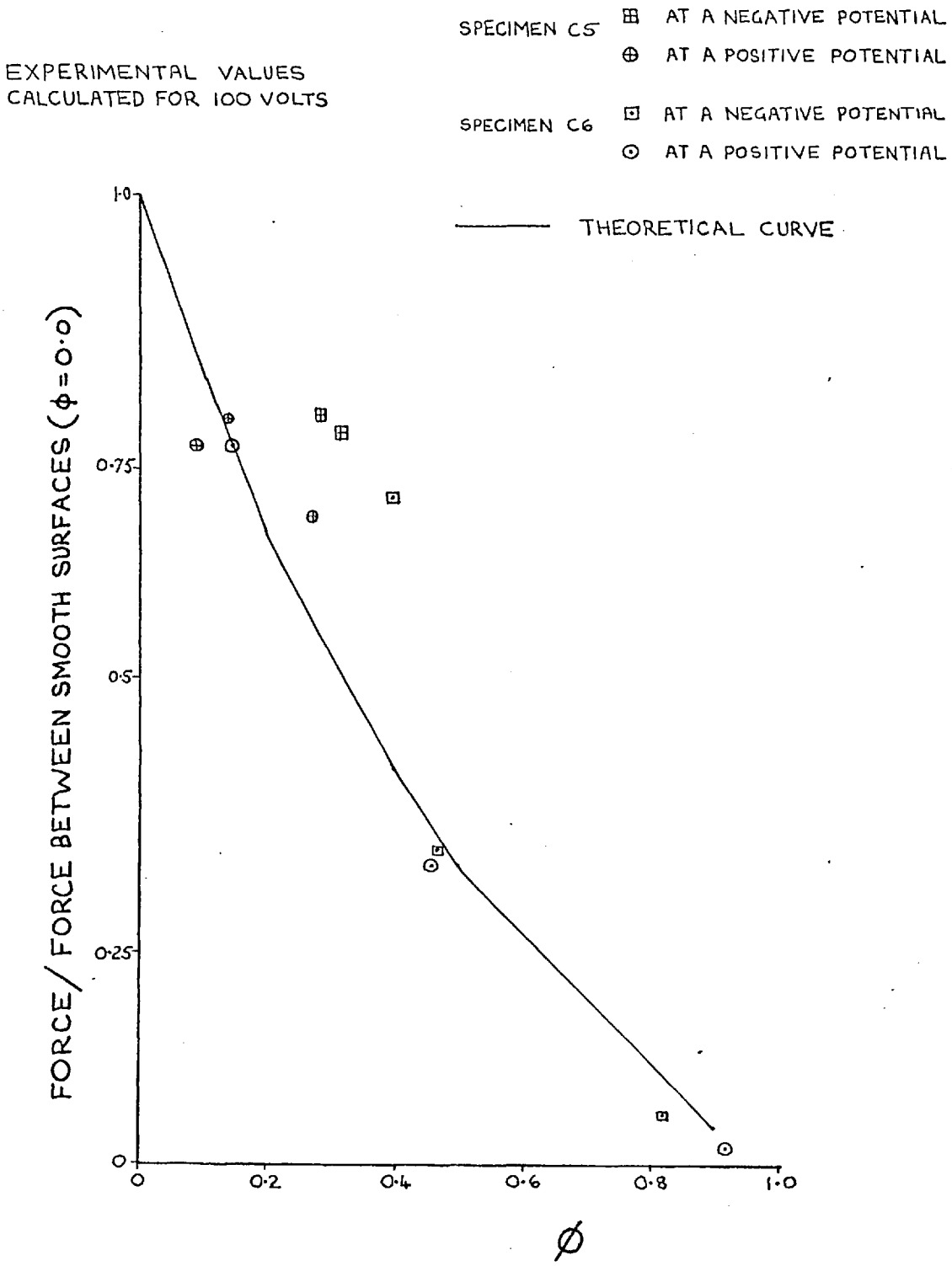

FIG.6.11

FORCE / VOLTAGE PLOTS SHOWING LITTLE CURVATURE

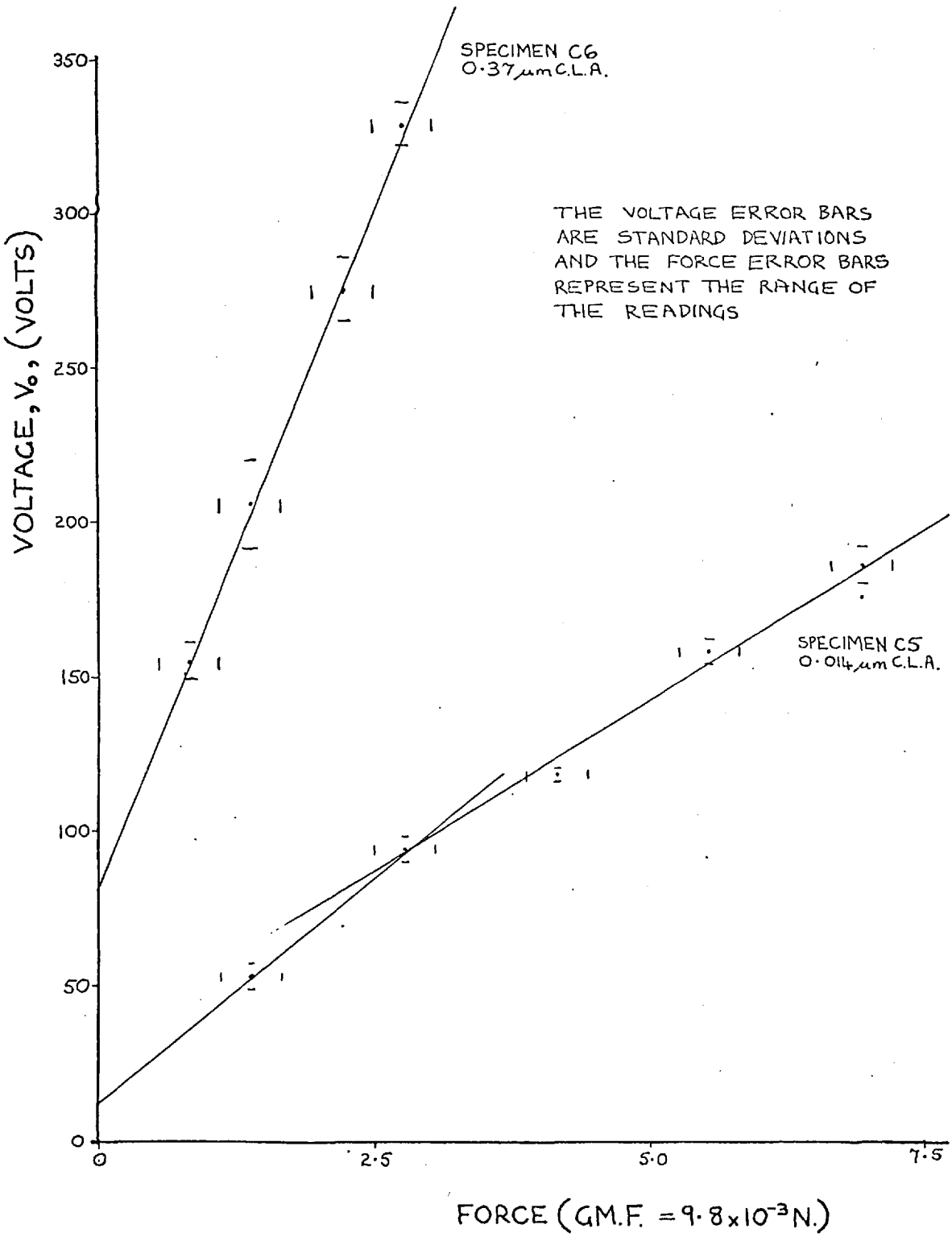

FIG.6.12

THE OBSERVED DECREASE IN THE SATURATION ELECTRIC FIELD WITH INCREASING SURFACE ROUGHNESS OF CARBON SPECIMEN 5

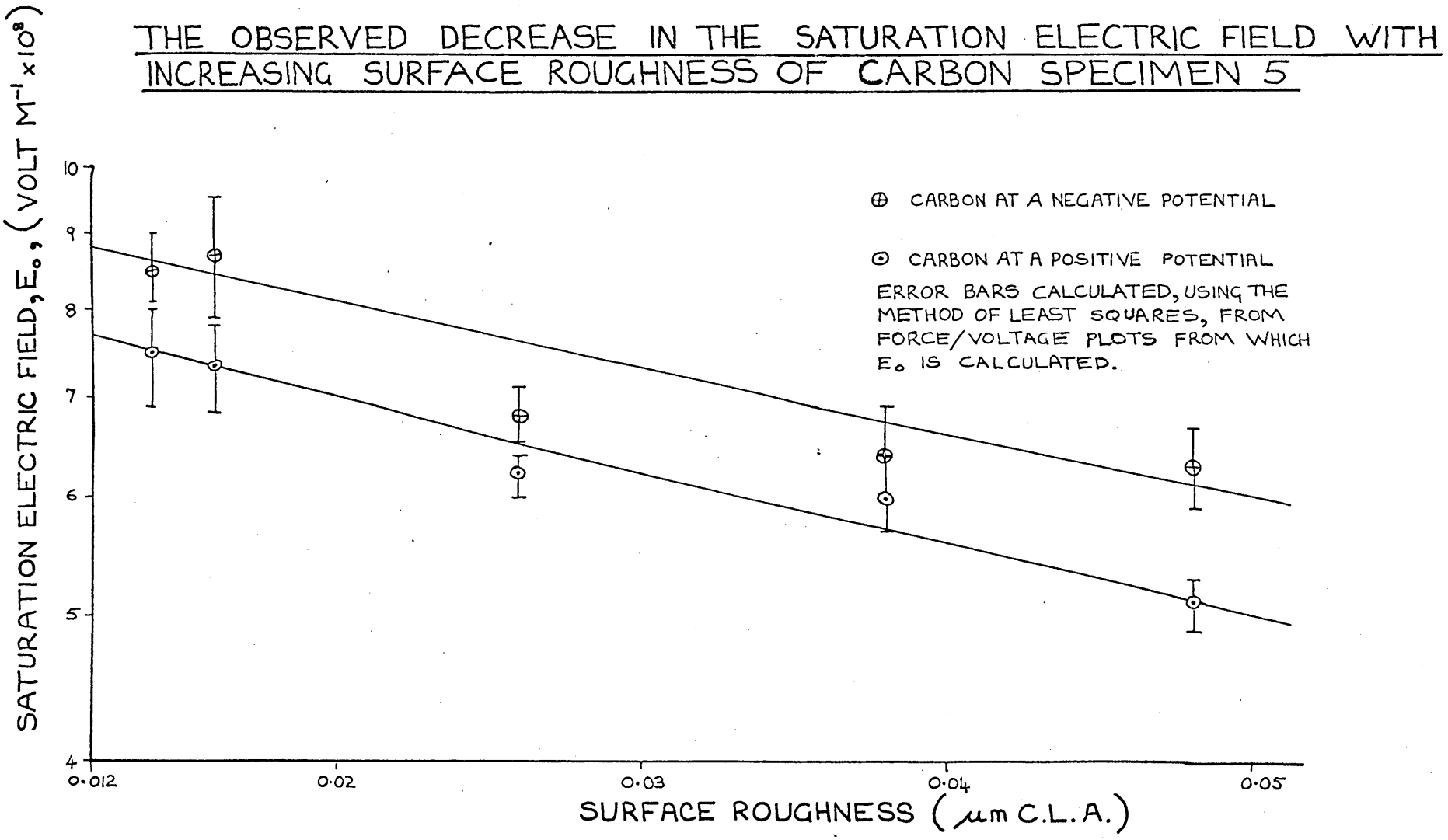

FIG.6.13

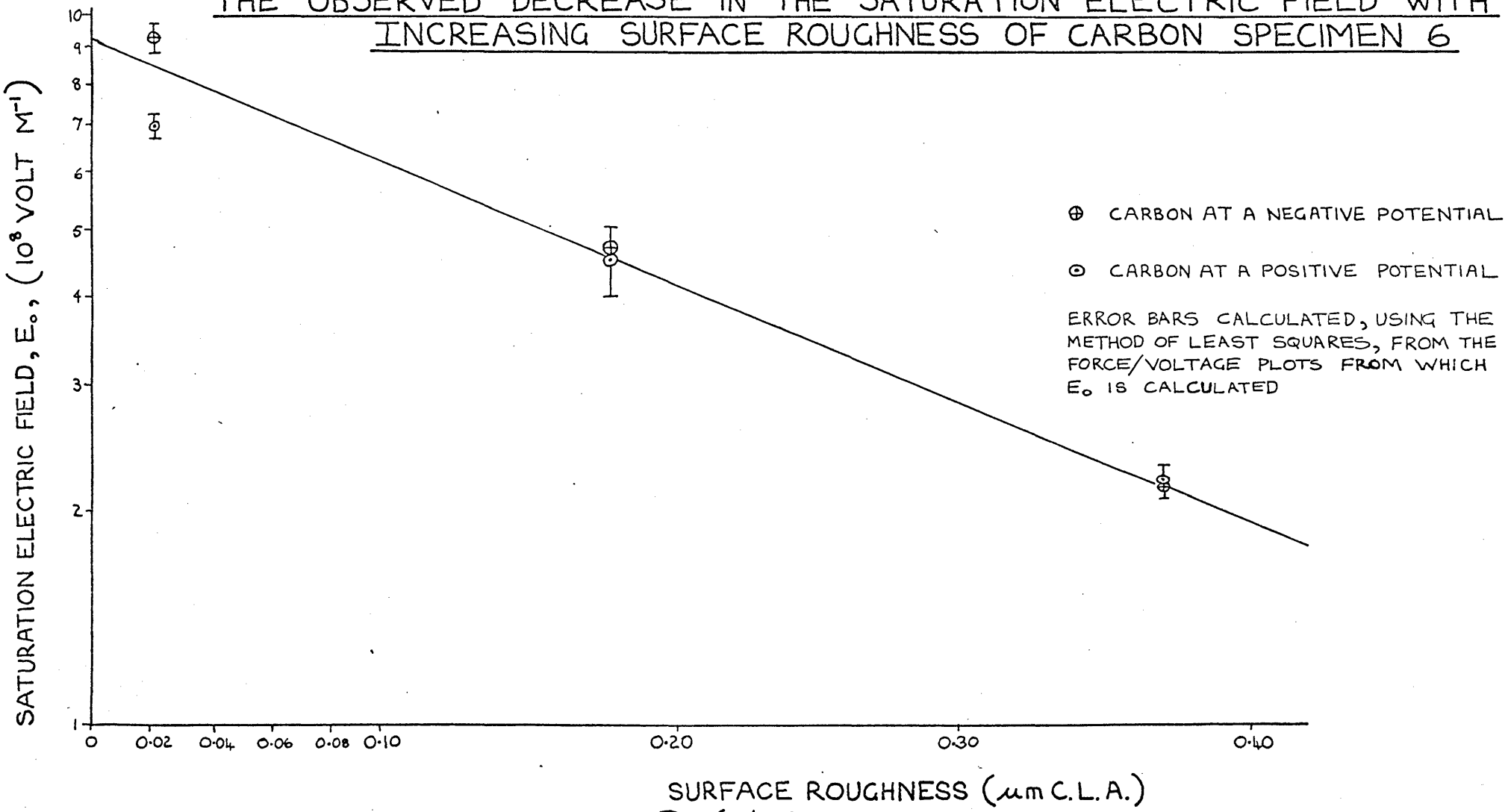
THE OBSERVED DECREASE IN THE SATURATION ELECTRIC FIELD WITH INCREASING SURFACE ROUGHNESS OF CARBON SPECIMEN 6
SATURATION ELECTRIC FIELD, E_o, (10^8 VOLT M^{-1})
10
9
8
7
6
5
4
3
2
1
0
0·02
0·04
0·06
0·08
0·10
0·20
0·30
0·40
SURFACE ROUGHNESS (μm C.L.A.)
⊕ CARBON AT A NEGATIVE POTENTIAL
⊙ CARBON AT A POSITIVE POTENTIAL
ERROR BARS CALCULATED, USING THE METHOD OF LEAST SQUARES, FROM THE FORCE/VOLTAGE PLOTS FROM WHICH E_o IS CALCULATED

FIG. 6.14

THEORETICAL STATIC IV PLOTS FOR A BALL ON FLATS OF VARYING ROUGHNESSES

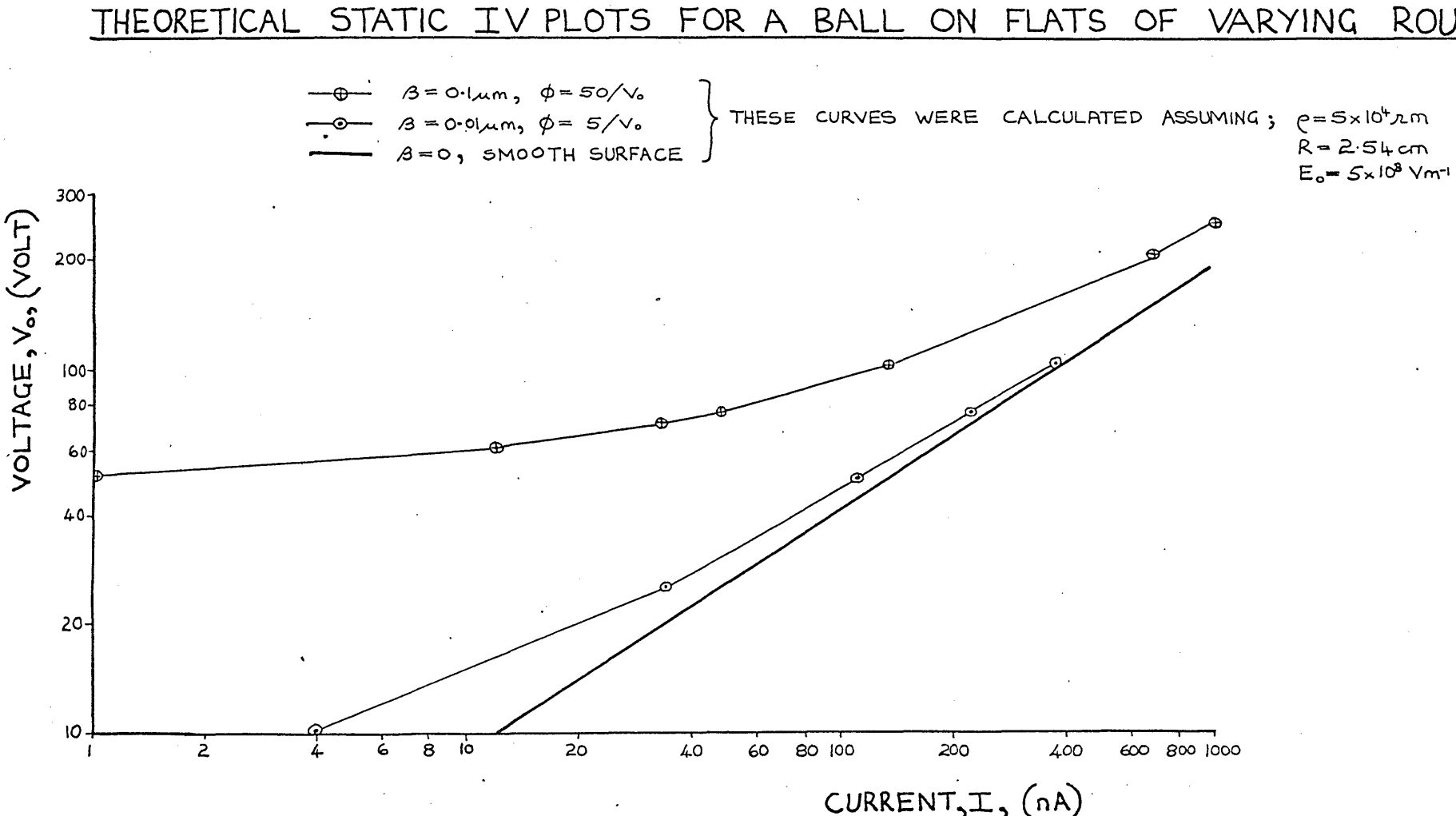

FIG.6.15

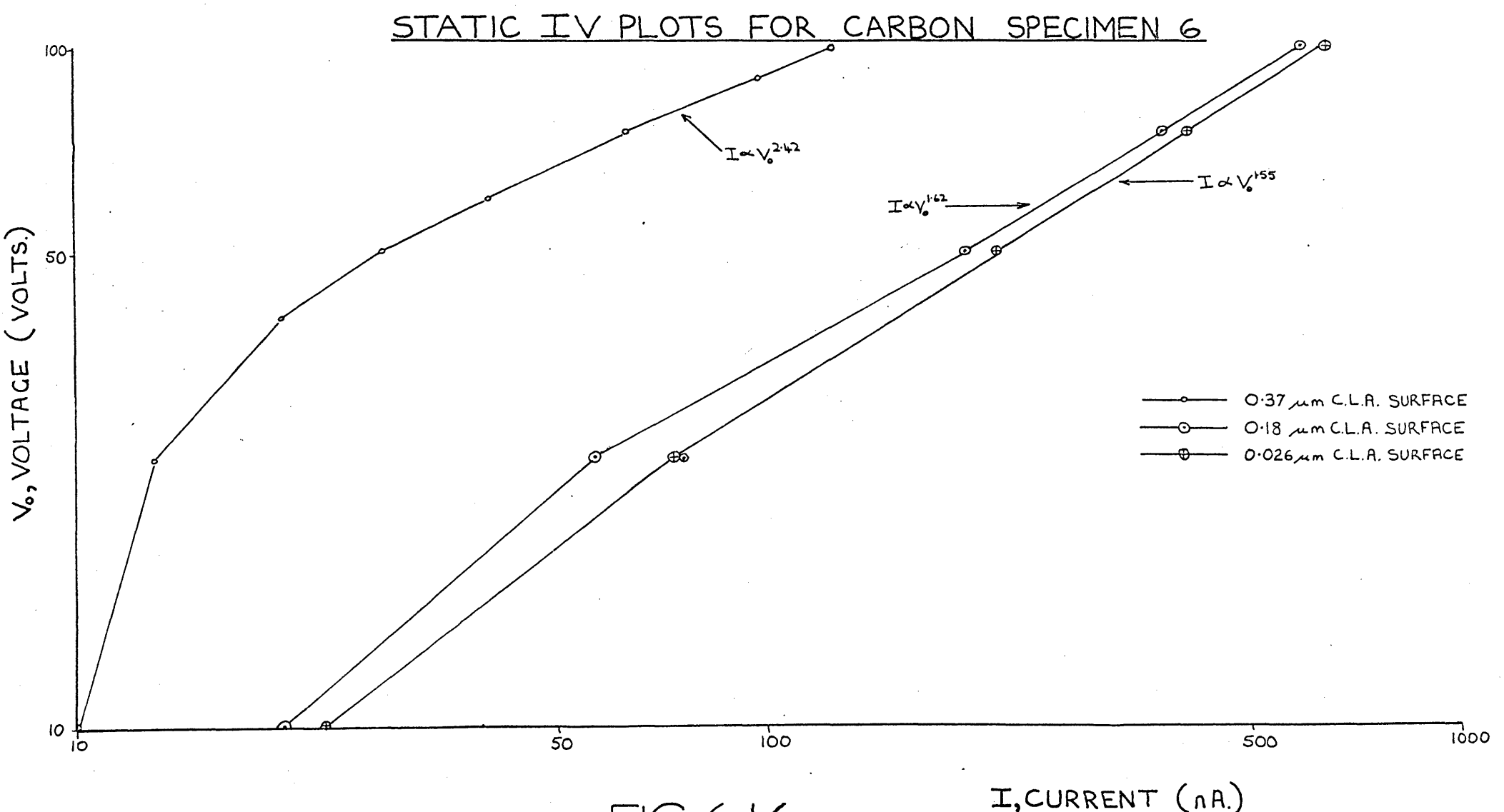
STATIC IV PLOTS FOR CARBON SPECIMEN 6
100
50
10
10
50
100
500
1000
V₀, VOLTAGE (VOLTS.)
I, CURRENT (nA.)
I∝V₀^2·42
I∝V₀^1·62
I∝V₀^1·55
0·37 μm C.L.A. SURFACE
0·18 μm C.L.A. SURFACE
0·026 μm C.L.A. SURFACE

FIG.6.16

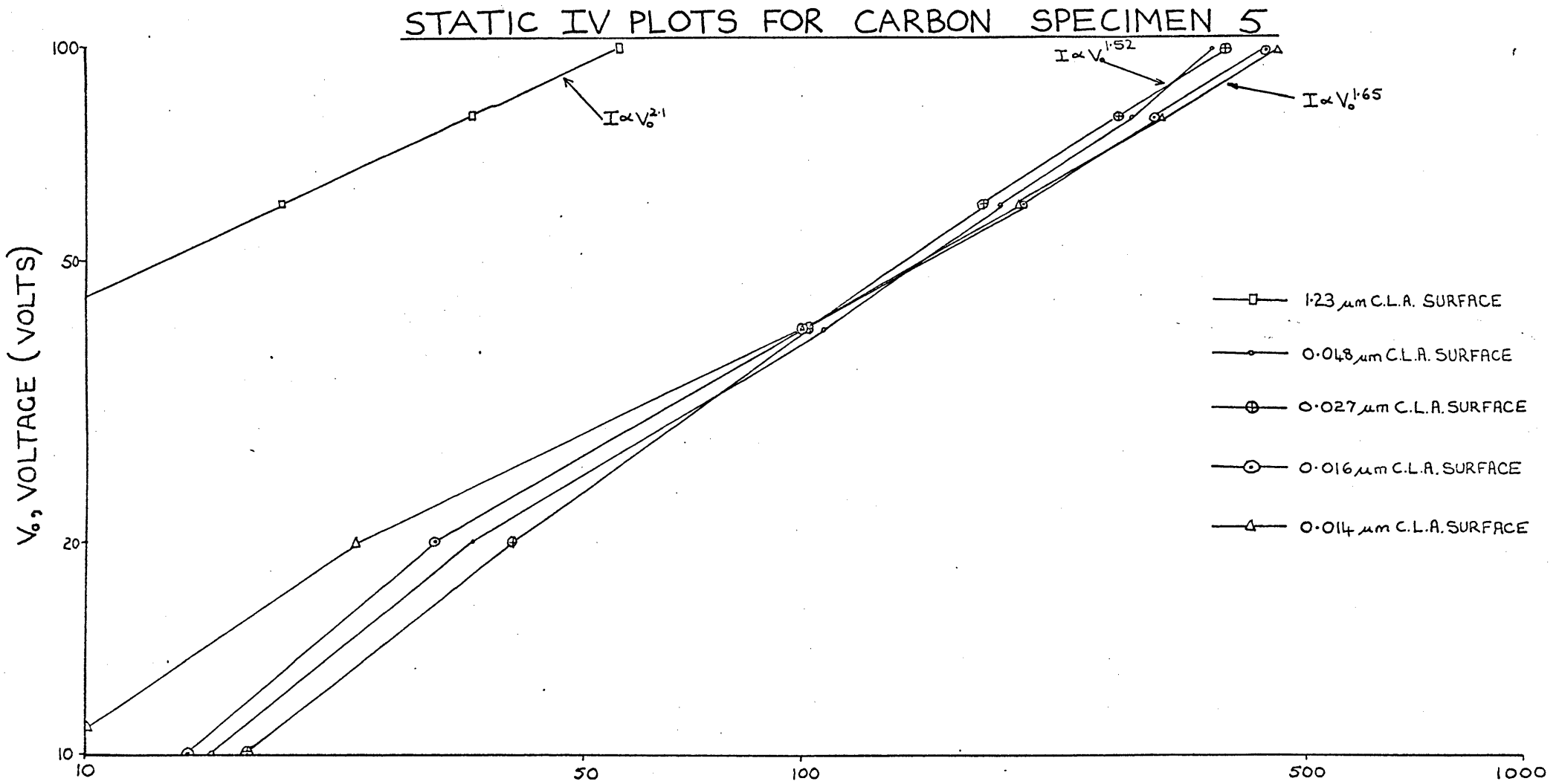
STATIC IV PLOTS FOR CARBON SPECIMEN 5
$I \propto V_o^{2.1}$
$I \propto V_o^{1.52}$
$I \propto V_o^{1.65}$
1·23 μm C.L.A. SURFACE
0·048 μm C.L.A. SURFACE
0·027 μm C.L.A. SURFACE
0·016 μm C.L.A. SURFACE
0·014 μm C.L.A. SURFACE
V_o, VOLTAGE (VOLTS)
100
50
20
10
10
50
100
500
1000
I, CURRENT (nA)

FIG.6.17

LEVESON'S RESULTS

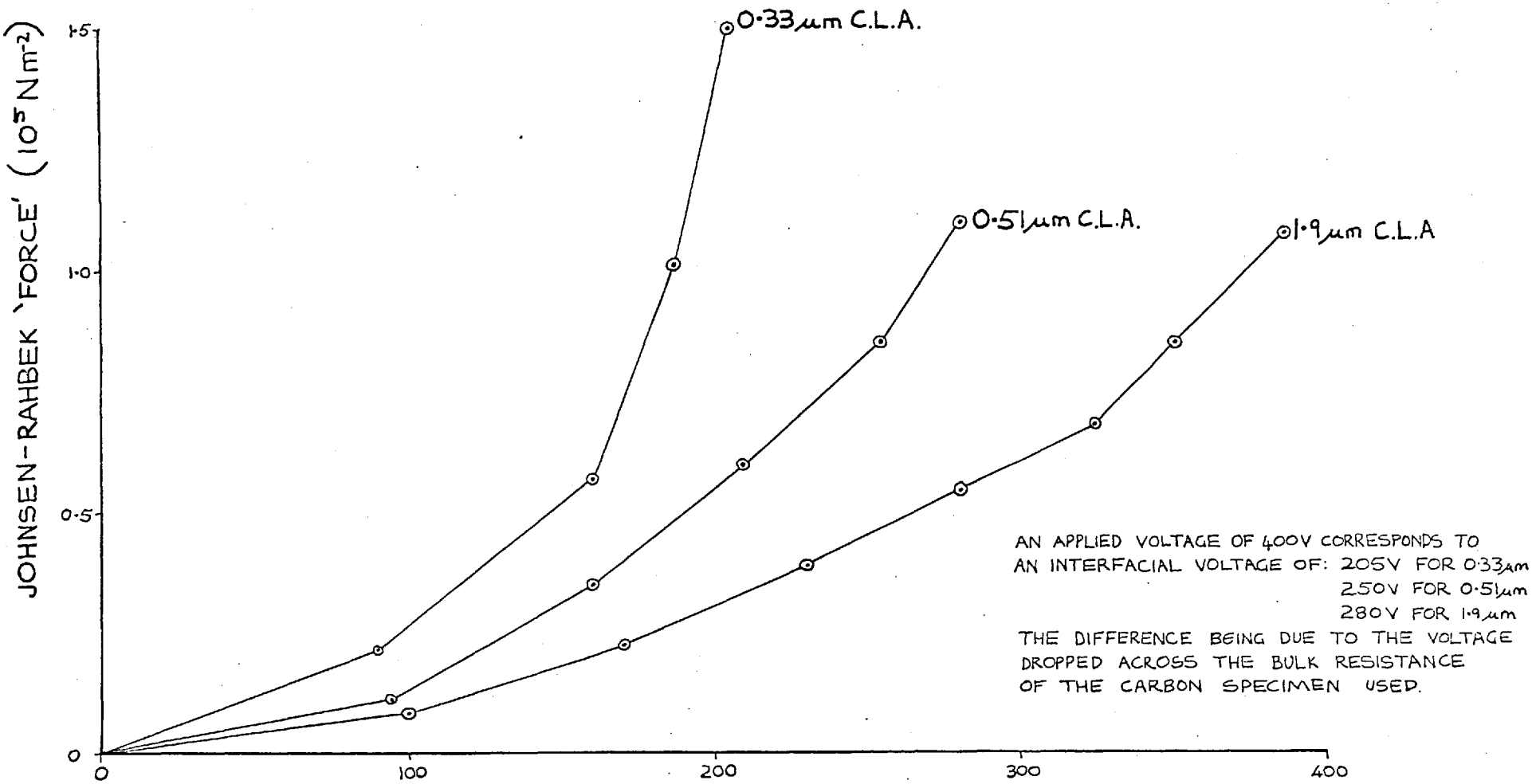

FIG.6.18

CHAPTER VII

THE EFFECT OF THE POLARITY OF THE APPLIED VOLTAGE.

Johnsen and Rahbek found that when a voltage was applied between an ionic semiconductor and a metal, with the semiconductor at a positive potential with respect to the metal, the force developed soon diminished. With the opposite polarity the force remained constant. This was attributed to electroosmosis occurring in the semiconductor, and was simply due to the nature of the ionic semiconductor. Stuckes, using an electronic semiconductor, still found that the polarity of the applied voltage influenced the force developed. The results were not similar to Johnsen and Rahbek's, they just showed that when the semiconductor was at a positive potential with respect to the metal the force was higher. Leveson, however, found no change in the force upon reversing the polarity of the applied voltage, although the current did alter slightly.

In the present work, (see Chapter 4), the force was found to alter when the potential of the semiconductor was reversed. The value of the saturation electric field, E_o, was higher when the semiconductor was negative and the voltage intercept of the force/voltage plot was higher.

Although these findings differ, the effect of the polarity of the applied voltage on the force developed seems basic to the Johnsen-Rahbek effect and is important in the operation of a working device.

7. 1 CURRENT FLOW ACROSS THE INTERFACIAL GAP.

A change in the polarity of the applied voltage most probably alters the current flow, so the effect of the polarity on the force is essentially the effect of the current flow on the force. For a reliable semiconductor, (e.g. electronic as opposed to ionic conducting), the polarity of the applied voltage only effects the current by altering the surface potential barrier at the contacts and across the interfacial gap. In the case of an amorphous semiconductor the potential barrier at the contact is independent of the voltage polarity, (see Chapter 2). This means that the current flow across the gap is solely responsible for the polarity effect.

Current flow across the gap has been assumed to occur, as almost infinite fields would be developed near the contact if no current flowed. Even a high vacuum between metal electrodes breaks down at fields of the order of 10^7 Vm^{-1}, (Hawley). This breakdown from an insulating to a conducting state is caused by initial electrons causing an avalanche of current at high fields, (Townsend), and although a semiconductor of high resistivity would quench it, a current would still flow.

The evidence for this current flow is the limitation of the forces that Stuckes measured and the agreement of the current measurements with Sillars' theory assuming interfacial current to flow. The present work also upholds Sillars' theory and etching of the surfaces, (see Chapters 3 and 9), is attributed to this current.

This current is basically due to field emission and Fowler and Nordheim's theory shows that it is the tunnelling of electrons through the surface barrier of a cathode when a high field, of about $10^9 Vm^{-1}$, is developed at its surface. The current also depends on the work function, (Gundry and Tompkins) of the surface. Most of the work that has been done on field emission has been concerned with emission from metals, but other factors have to be considered for crystalline semiconductors, (Margulis, Stratton and Gomer). In this discussion, however, the word semiconductor is used merely in the sense of a conductor of considerably higher resistance than that of a metal. The effect of the semiconducting properties on the field emission current are not of direct relevance in this discussion.

Field emission currents can readily be detected between very clean, smooth electrodes in a high vacuum, (10^{-10} torr) when electric fields of the order of 10^7 Vm^{-1} are applied. These fields are lower than the Fowler-Nordheim theory indicates due to small asperities on the cathode surface enhancing the field locally by a factor of between 10 and 100. These asperities are due to the surface finish of the cathode, but even on highly polished metal surfaces it has been shown that they are created after the application of a high field, (Little and Smith). The origin of these protrusions is not completely understood, (Davies).

As the pressure increases to above 10^{-5} torr these asperities are blunted by ion bombardment in the residual gas, (Alpert et al.) Also the increasing rate of molecules impinging on the surfaces increases the possibility of adsorption on the electrode surfaces. At a pressure of 10^{-10} torr approximately 10^{12} molecules per second impinge on unit area. If 0.1 of these stick, a monolayer is formed in 3 hours. For a pressure of 10^{-5} torr approximately 10^{17} molecules per second impinge on unit area and a monolayer is formed in 0.1 seconds. This monolayer can drastically alter the work function of the surface, (Jenkins and Trodden), thus altering the field emission current.

Apart from these considerations even for thoroughly degassed electrodes, at pressures of 10^{-5} torr an instantaneous pressure rise can occur in the gap due to desorption of adsorbed residual gas layers from the electrode surfaces by electron and ionic bombardment, (Llewellyn-Jones and Owen), which alters the current flow.

If the pressure between the electrodes becomes atmospheric the emission process is more complex depending on the gas. Air can produce progressive changes in a metal cathode surface due to the formation of oxides and other tarnish layers which profoundly affect the emissive properties, (Llewellyn-Jones and de la Perelle 1953; Llewellyn-Jones and Morgan 1953). The emission process is a cold emission process like field emission, and the results obey an equation analytically the same as the Fowler-Nordheim equation, but evaluation of the constants with a field enhancement factor of 10 gives a work function of 0.5 eV, (the measured value is $\sim$ 4e V), and an emitting area of 10^{-18} m^{-2} for a nickel cathode, (Llewellyn-Jones). It was assumed that the electrons were emitted from sites of low work function such as negative ions of oxygen or water vapour on the cathode surface.

This discussion has been limited to separations between the electrodes of less than the mean free path for ionising collisions between electrons and neutral atoms. Even so, as the pressure increases the probability of an electron ionising a molecule in collision increases depending on the gas between the

electrodes, (von Engel). This means that the current becomes more dependent on the gas in the gap and current generation becomes more of an ionisation process.

Although the results discussed above are related to metal electrodes, they show how complex the phenomena of current flow across an interfacial gap is and how complex the current flow across a gap between a semiconductor and a metal is likely to be.

7. 2 THE EFFECT OF THE WORK FUNCTION OF A SURFACE.

A practical device utilizing the Johnsen-Rahbek effect operates at atmospheric pressure which is far from a clean ultra-high vacuum. The vacuum system in the present work was not an ultra-high vacuum system, and the ball and flat were not degassed before use. This meant that the contacting surfaces were coated with chemisorbed and physisorbed gases from the atmosphere and probably cleansing solvent.

To estimate whether this affected the force and current developed and whether true Fowler-Nordheim field emission was occurring, the force and current were measured with balls of different work functions, as the carbon and steel used in previous measurements have similar work functions, (table 7.1). The Fowler-Nordheim equation shows

$$\ln J \propto - \frac{\phi^{3/2}}{E} \qquad (7.2.1)$$

where J is the current density; (Am^{-2}), ϕ the work function, (eV) of the cathode and E (Vm^{-1}), the electric field . This shows that changing the work function of the cathode greatly alters the electric field for a given current density. This equation is dealt with in more detail in Appendix 1 where the effect of altering the work function is calculated from the simple circuit model of the contact. This calculation, considering an annular section of the interfacial gap 1 μm wide near the contact, shows that the value of E_o increases by about 40% when the work function is increased from 4 eV to 5 eV,

(table A1.2), and that the total current flow decreases slightly. For a section further from the contact, however, R_B would be less and the change in current would be greater which suggests that the current flow for the whole interfacial gap could decrease to a greater extent.

7.2.1 EXPERIMENTAL METHOD

To estimate the effect of the work function on the force and current developed, measurements were made with platinum coated steel balls and uncoated steel balls, 1" in diameter, as the work function of platinum is higher than that of steel and carbon, (table 7.1).

The platinum coated balls were R.F. sputtered with platinum to a thickness greater than $1\mu m$. The adhesion of a sputtered film to a substrate is little understood, (Chapman), but estimates show it to be approximately equal to the force of physisorption, in terms of pressure about 10^7 Nm^{-2}, (Harrach and Chapman). As the maximum pressure that the Johnsen-Rahbek effect exerts, (given by $\epsilon_0 E_0^2/2$ Nm^{-2}), is about 5×10^6 N m^{-2} when E_0 equals 10^9 Vm^{-1}, the semiconductor specimens were examined after the force measurements to see if any platinum had been pulled off the balls onto the semiconductor. The specimens were examined with an electron microprobe analyser which showed no platinum on either the carbon or glass specimen. Thus the results obtained with the sputtered balls apply to a genuine platinum surface.

Force measurements and static IV plots were taken for glass and carbon specimens in contact with the balls. Forces less than 7 gm. f. were measured so as not to damage the semiconductor or the sputtered film to a large extent. The ball and semiconductor specimens were cleaned in the usual manner immediately before measurements were made. The carbon specimens were only left in the vacuum system for a short time before measurements were made so that the effect of desorption would not be great. Measurements were made with two specimens of carbon to avoid any erroneous measurements due to desorption, and also with different platinum coated balls and different steel balls as they varied slightly in surface roughness.

Meter readings were made of the current to observe any small changes when the polarity of the applied voltage was reversed.

7.2.2. RESULTS AND DISCUSSION

All the force measurements formed straight line plots of force versus voltage from which the slope was calculated using the least squares method. The values of E_o calculated from the plots are shown in tables 7.2 and 7.3.

From the previous calculations with the circuit model and knowing the work function of platinum to be higher than that of the carbon it would be expected that the value of E_o would be higher when the platinum coated ball was the cathode, i.e. the carbon was positive. The carbon results, (table 7.2), do not show this. In fact they show E_o to be larger when the carbon is the cathode. The results obtained with the glass specimen also show this, (table 7.3). Although the work function of the glass is unknown, if the previous theory was correct it would be calculated to be much higher than that of the platinum, which appears to be rather improbable.

The saturation electric field when the platinum ball was the cathode was not very different from that generated with the steel ball as cathode when both were in contact with carbon. The glass results do not show this to the same extent, but they are rather inaccurate due to the contact spot being unavoidably changed when the ball was changed.

This change of contact spot also produced a change in current. The current between the steel ball and glass was almost three times that between the glass and the platinum coated ball. The carbon measurements, however, showed less difference between the static and dynamic IV plots for the various balls.

No change in current was observed upon reversing the polarity of the applied voltage but only a small change would be expected if the theory was correct.

The results give no evidence that the work function of a surface alters the force generated by the effect or that true Fowler-Nordheim field emission is

occurring. It must therefore be considered that the contamination of the surface and the residual gas in the interfacial gap are the factors governing the current flow across the gap.

7. 3 THE ENVIRONMENT AT THE INTERFACE.

The previous discussion has been confined to the electrode surfaces and their work functions, but equally important is the environment at the interface, i. e. the gas in the interfacial gap. Depending on the gap width, the electric field, the gas between the electrodes and its pressure, the gas can amplify the current flow by ionisation. If these parameters obey Paschen's law then the gas breaks down and becomes conducting.

These parameters do not obey Paschen's law in the case of the ball on flat, however. Indeed, the mean free path for collisions between electrons and oxygen molecules for instance, is about 250μm at a pressure of 1 torr. Although the possibility of an electron colliding with a molecule and forming an ion is small, the gas in the gap can be augmented by gas desorbed from the surfaces of the undesorbed electrodes by heating and bombardment of electrons, and to a lesser extent ions, forming the current flow. This increases the possibility of ion formation, as also does the bombardment of adsorbed layers on the electrode surfaces by ions (Mansfield) and field desorption of adsorbed polar molecules (Tarasova) similar to desorption in a field ion microscope, (Müller). (To a rough approximation physisorbed 'forces' are around 10^{7}Nm^{-2} so that the electrostatic 'force' in the gap between a ball and flat, which is about 5×10^{6}Nm^{-2}, can desorb weakly bound physisorbed molecules.)

The high resistivity of the semiconductor would,however,limit any large increase in current, but the ionisation process would render the gap more conducting, tending to short-circuit the contact constriction resistance. Space charge could also build up affecting the current flow.

It is difficult to calculate the effect on the force and current of the environment at the interface, but it can be qualitatively assessed from the experiments discussed briefly below.

7.3.1 SURFACE CONTAMINATION.

Desorption of contamination from the electrode surfaces into the interfacial gap increases the gas pressure and also the possibility of ion formation. This contamination can be adsorbed atmospheric gas, oil vapour back-diffusing from the difusion pump, polishing debris and cleaning solvent.

The effect of contamination from the polishing process on the current flow can be demonstrated by spraying a fine film of polishing lubricant onto a specimen of carbon. This lubricant is a viscous liquid lubricant and small traces of it are probably inadvertently left on most 'cleaned' specimens anyway.

Fig. 7.1 shows the static IV plots of the carbon specimen in a vacuum of 10^{-5} torr, with and without the lubricant. The lubricant greatly increased the current either due to its electrical conductivity or most likely its breakdown into ions in the gap.

7.3.2 AMBIENT GAS PRESSURE

Increasing the ambient gas pressure also affects the current. A piece of carbon was cleaned and put into the vacuum chamber which was then evacuated to a pressure of 10^{-5} torr. It was left in this vacuum for eight hours to desorb as much surface contamination as possible. After eight hours a static IV plot was taken. The chamber was then brought back to atmospheric pressure and another static IV plot taken.

When the carbon was at a negative potential with respect to the ball, the current increased, fig.7.2, probably due to ionisation . With the voltage reversed the current decreased, however, due to the current etching the carbon. This is discussed more fully later, but these results show that the interface environment is important.

7.4 DISCUSSION

The previous results show that the work function of a pure electrode does alter the Johnsen-Rahbek effect but that surface contamination and the residual gas in the interfacial gap are the factors affecting the force and current flow.

However, the saturation electric field is always found to be greater and the break current less when the semiconductor is at a negative potential with respect to the ball. It seems probable that this could be due to the method of measuring the force which necessitates separating the surfaces whilst a current flows, generating conditions similar to those between metal contacts, at break, where discharges occur. At the moment of separation of the semiconductor from the ball the mechanical contact, d, is considerably reduced from that when no mechanical force is applied, and more current flows across the interfacial gap. Assuming this current to consist of electrons, these electrons lose their kinetic energy in colliding with the anode and heating it. The temperature rise of the anode is given approximately by

$$\Theta = \Theta_o + \frac{IV}{\pi kr} \qquad (7.4.1)$$

(Carslaw and Jaeger), where V is the voltage across the gap and I, (A), the current bombarding the region of the anode of radius r. The semiconductor has a higher thermal conductivity, k, than the metal (about 10^{-1} Wm^{-1} K^{-1} and 20 Wm^{-1} K^{-1} respectively) so it has a greater temperature rise, Θ, when it is the anode. As the force decreases when Θ increases, (as will be discussed in Chapter 8), then the force decreases more when the semiconductor is the anode. Replacing r in eq. (7.4.1) by c, the radius of current emission and using eq. (4.1.4), this becomes :

$$\Theta = \Theta_o + \frac{8V\ V_o}{3\varrho\pi k} \qquad (7.4.2)$$

which assumes that d is negligible, and that the contact is at the ambient temperature Θ_o before the members are parted. The voltage across the gap, V, does not equal the total applied voltage V_o, but determining its exact value is difficult as it varies with the gap width from zero to $V_o/2$. The value is taken as $V_o/2$ to give an order of magnitude estimate.

Putting $k = 10^{-1} Wm^{-1} K^{-1}$, an approximate value for the carbon, (Davidson and Losty), the temperature rise is about $40^{o}C$ at 300 volts and

about $5^{o}C$ at 100 volts. For the glass, a typical value of k is about $2 \times 10^{-1} Wm^{-1} K^{-1}$ (Adler), which means a temperature rise of $20^{o}C$ at 300 volts and about $3^{o}C$ at 100 volts.

These results show that the temperature rise, and therefore the decrease in force, increases rapidly with increasing voltage. This agrees well with all the force measurements which show that the differences in E_o and break current for the different polarities of the applied voltage are greater at the higher voltages. Typical dynamic IV plots demonstrating this are shown in fig. 4.6.

Although the increase in the temperature of the semiconductor is only moderate, other secondary effects could enhance it. The semiconductor could desorb gas due to the heating,especially the carbon, which would enhance the current and increase the temperature. Also the contact members oscillate at about 1.5 k.Hz. just before the break point damaging the semiconductor and forming debris in the gap which could be ionised and would again increase the current and the temperature. These effects would mainly contribute to increasing the temperature of the semiconductor when it was the anode as its thermal conductivity is much less than that of the ball. Although these secondary effects probably do not alter the temperature of the semiconductor to a great extent, the processes occurring in the gap can cause discharges to occur (see Chapter 9), which means that the electrodes can acheive high temperatures locally over very small regions.

7.5 CONCLUSION

Although Fowler-Nordheim field emission is the basic process for current flow across the interfacial gap, the results show that the condition of the electrodes and the gas in the gap are equally important parameters in determining this current flow. This does not mean that the previous theory, such as that of Chapter 4 , which assumed field emission to occur in the gap is wrong as the relationship of the applied voltage to the current, as derived by Sillars, does not depend on the Fowler-Nordheim equation being obeyed. This is because the resistivity of the semiconductor and the geometry of the gap are the dominant parameters in determining the current flow.

The variation in the value of E_o with the polarity of the applied voltage found in the present work was considered to be due to the method of force measurement. The polarity effects found by previous workers were probably due to the condition of the semiconductor used and the environment in which the measurements were made. For instance, Joule heating might have desorbed water vapour from Stuckes' semiconductor between the force measurements at different polarities of applied voltage, altering the resistivity and the forces as can occur with the carbon used in the present work, (see Chapter 8).

TABLE 7.1

WORK FUNCTIONS OF MATERIALS USED FOR FORCE MEASUREMENTS

MATERIAL	WORK FUNCTION (e V)
PLATINUM	5.5
CARBON	4.2
STEEL	4.3

TABLE 7.2

SATURATION ELECTRIC FIELDS CALCULATED FROM FORCE MEASUREMENTS WITH CARBON SPECIMENS IN CONTACT WITH DIFFERENT BALLS.

CARBON SPECIMEN	BALL SPECIMEN	SATURATION ELECTRIC FIELD E_o (10^8 Vm^{-1})	
		CARBON AT A POSITIVE POTENTIAL	CARBON AT A NEGATIVE POTENTIAL
3	PLATINUM SPUTTERED 1	6.6 ± 0.1	6.9 ± 0.1
1	PLATINUM SPUTTERD 2	6.5 ± 0.2	6.95 ± 0.25
AVERAGE VALUES		6.55	6.93
3	NON-SPUTTERED 1	6.1 ± 0.1	6.4 ± 0.1
1	NON-SPUTTERED 1	6.6 ± 0.3	6.55 ± 0.2
1	NON-SPUTTERED 2	7.0 ± 0.4	7.7 ± 0.4
AVERAGE VALUES		6.6	6.9

TABLE 7.3

SATURATION ELECTRIC FIELDS CALCULATED FROM FORCE MEASUREMENTS WITH GLASS SPECIMENS IN CONTACT WITH DIFFERENT BALLS.

GLASS SPECIMEN	BALL SPECIMEN	SATURATION ELECTRIC FIELD E_o ($10^8 Vm^{-1}$)	
		GLASS AT A POSITIVE POTENTIAL	GLASS AT A NEGATIVE POTENTIAL
1	PLATINUM SPUTTERED 3	4.2 ± 0.2	6.7 ± 0.4
1	NON-SPUTTERED 2	4.95 ± 0.3	7.1 ± 0.4

STATIC IV PLOTS DEMONSTRATING THE EFFECT OF CONTAMINATION ON THE CARBON SURFACE

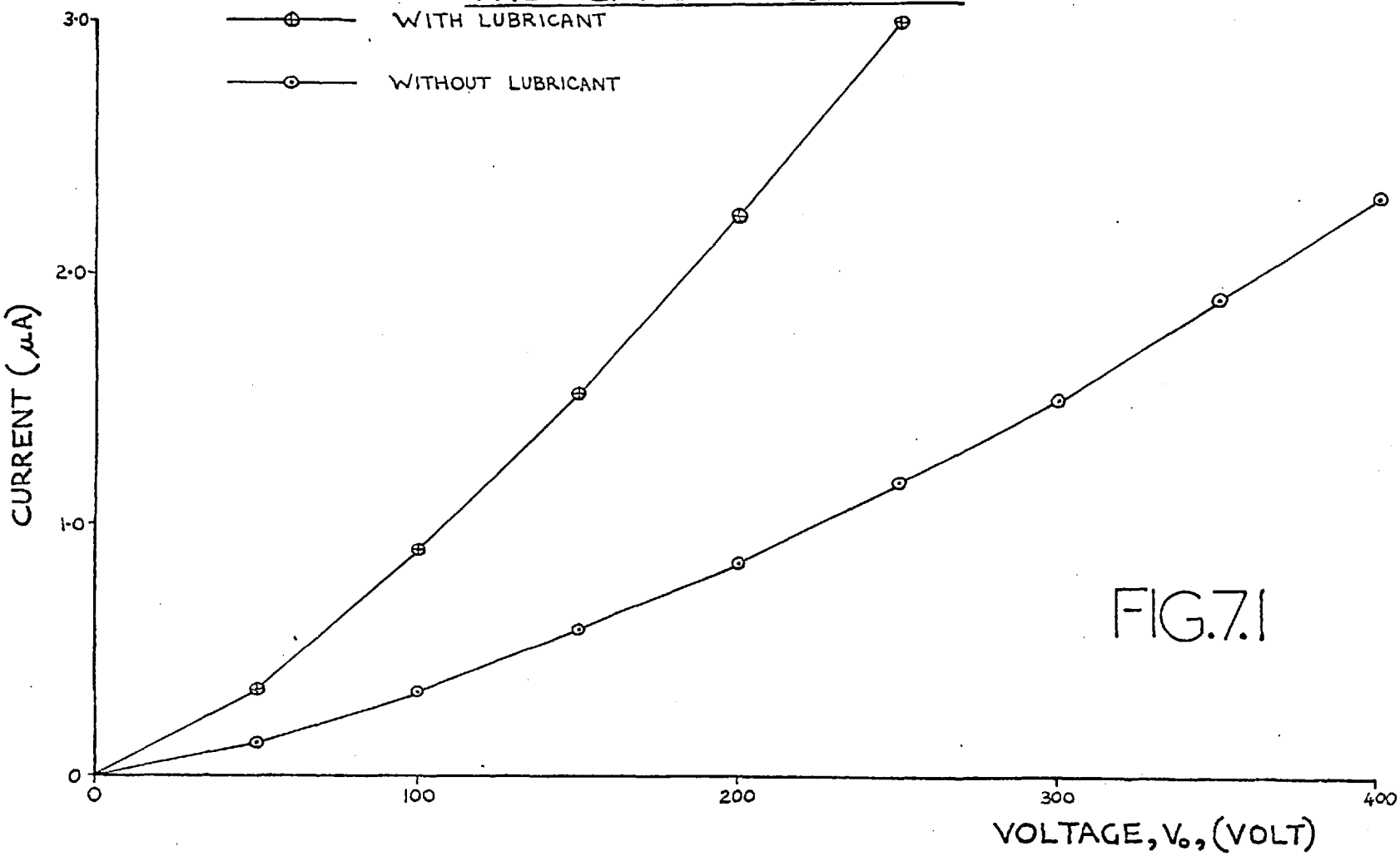

FIG.7.1

STATIC IV PLOTS TAKEN IN ATMOSPHERIC CONDITIONS AND IN VACUO

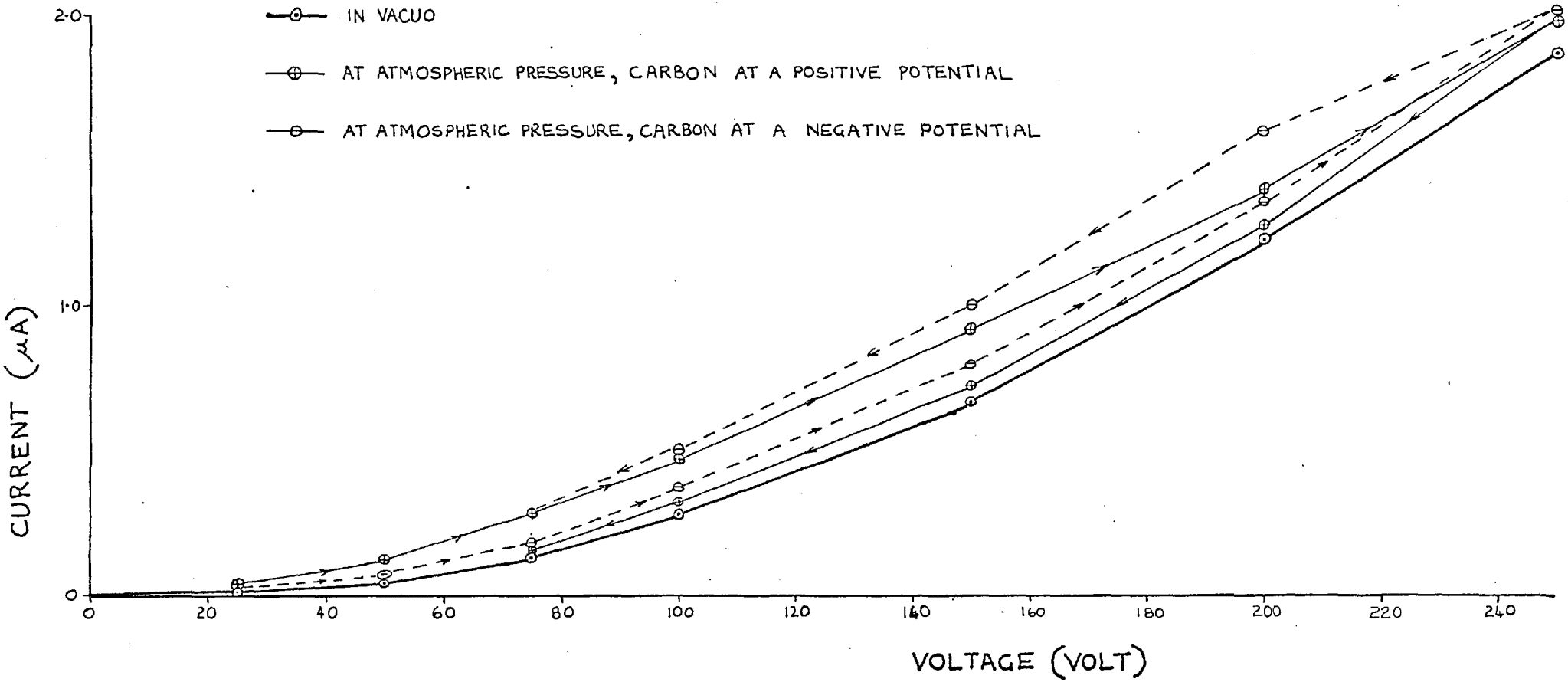

FIG.7.2

CHAPTER VIII

THE EFFECT OF HEAT

The Johnsen-Rahbek effect depends on one of the contact members generating it being a semiconductor with a high value of ρk. A semiconductor, however, has a low thermal conductivity, k, which means that it can achieve high temperatures when it is heated. An increase in temperature would drastically change the electrical resistance around the heated region because the resistivity, ρ, of a semiconductor obeys the relationship:

$$\rho = \rho_{\infty} \exp\left(\frac{\Delta E}{2k'\theta}\right) \qquad (8.0.1)$$

where ΔE is the activation energy, ρ_{∞} is a constant, θ the absolute temperature and k' is the Boltzman constant. The change in resistivity would alter the equipotentials and hence the interfacial voltage and thus the force. With semi-pyrolised cellulose carbon as the semiconductor any temperature rise would also desorb water vapour from the carbon altering its resistivity and the force.

The dependence of the force on the temperature is important as a working device utilizing the effect may operate at a mean temperature of around $80^{o}C$, (Dudding), due to frictional heating. and the temperatures of contacting asperities will be substantially higher than $80^{o}C$, (Heighway; Fury).

In the second part of this chapter this effect is discussed, the first part, however, considers the effect on the force of the desorption of absorbed gases due to the heating of a semiconductor such as carbon.

8. 1 DESORPTION

Semi-pyrolised cellulose carbon contains a maximum of about 2% by weight of water, and the variation in this water content alters the carbon's resistivity, (see Chapter 2). Desorption of this water was probably the cause of the current decreasing and also E_o decreasing with the increasing number of force measurements as discussed in Chapter 4. During all the measurements

with each ball the current on average decreased by 30%, (see table 4.2), whilst E_o tended to diminish, the value obtained from the initial set of measurements for each ball being approximately 10% higher than the average value, (see table 4.1).

The results obtained with the glass specimen, however, showed a slight increase in current after the force measurements, (table 4.6), indicating that the decrease in current, and possibly in E_o, with the carbon specimen was due to desorption of water from the carbon. This was investigated in the following experiment.

8.1.1 EXPERIMENTAL METHOD

To assess the effect of desorption on the force and current the carbon was initially heated in an oven at atmospheric pressure for half an hour at 80^{o} C. The carbon was cleaned in the usual manner and attached to the lever before the heat treatment so that it was not handled during the treatment and so that it could be inserted into the apparatus quickly when taken from the oven minimising reabsorption of water vapour. After the heat treatment the carbon was wiped with a lint free tissue to remove any dust before it was placed in the force measuring apparatus and the containing vacuum chamber evacuated to 10^{-5} torr. When the pressure of the vacuum chamber was stable at 10^{-5} torr after approximately an hour, during which time the carbon cooled to room temperature, a static IV plot was taken and then force measurements were made. The static IV plot was then repeated. The mechanical forces applied did not exceed 7 gm.f. in order not to damage the carbon surface to a great extent. This proceedure was repeated after the carbon specimen had been further desorbed in the oven at temperatures up to 120^{o} C.

The results were obtained with a specimen of carbon of curvature ~ 0.7 m and of 0.15 μm C.L.A. roughness. They were compared with results obtained with a different specimen of carbon, flat to a curvature of 7 m and of 0.11 μm C.L.A. roughness, which was desorbed for 4 hours in an oven at 250^{o} C and at atmospheric pressure. This temperature was chosen as being suitable for

desorbing most of the water from the carbon, (see fig. 2.7).

8.1.2 RESULTS

Fig. 8.1 shows the effect that desorbing water from the carbon had on the current. Comparing the initial current with that of the specimen desorbed at 250^{o}C shows that the water content of the carbon can change the current flow by a factor of 10. The relationship between current and voltage was not significantly altered during the desorption as fig. 8.2 shows.

The water content did not, however, alter the saturation electric field, E_o, to such an extent as it altered the current as table 8.1 shows. The change was significant though, as E_o decreased by 30% of its initial value of $6 \times 10^{8} Vm^{-1}$. The intercepts of the force/voltage plots did not alter significantly with desorption, so that the force decreased to the same extent as E_o.

The current was found to have decreased after force measurements were made as an examination of the static IV plots before and after the measurements showed, (see table 8.2).

8.1.3 DISCUSSION OF THE RESULTS

The results show that when the carbon is desorbed the current and the force decrease to an extent dependent on the degree of desorption. The value of E_o obtained with the specimen desorbed at 250^{o}C was not lower than that obtained with the specimen desorbed at 120^{o}C probably because the latter had an inferior surface quality.

The indices of the static IV plots did not significantly alter during the experiment, (see fig.8.2), and examination of the I/V relationship, (eq. (4.1.4) or eq. (5.5.1)), indicates that an increase in the electrical resistivity, ρ, was responsible for the current and force decreasing. Desorption of water vapour from the carbon into the gap during the force measurements, indicated by the current decreasing during the force measurements, (table 8.2), could have altered the force slightly, as discussed in Chapter 7, but examination of the IV relationship shows ρ to be the dominant factor. The experimental observations

can be compared with estimates of the change in E_o when ρ is altered, calculated from the simple equivalent circuit model of the contact in Appendix 1. These calculations show that for a decrease in the current by a factor of 10, (i.e. ρ increasing by a factor of 10), the value of E_o decreases by approximately 20%. This compares reasonably well with the observed decrease of 30%.

The present observations also elucidate the problem of desorption of the carbon during force measurements, as noted in Chapter 4. The force measurements were done under vacuum conditions but the vacuum alone does not seem capable of desorbing the carbon to the extent that is found after force measurements have been made. Fig. 8.1 shows that when the carbon was not heat treated and simply left in the vacuum chamber for 75 minutes the current decreased by 14%. This is approximately the change in current after a set of force measurements has been made on an undesorbed specimen, but it only takes 20 minutes to take such a set of measurements. The results of the measurements made with a carbon specimen discussed in Chapter 4 showed a decrease in current of about 30% after a number of sets of measurements had been made. In that experiment the carbon was left in a vacuum for less than 24 hours whilst the measurements were made. The vacuum alone would have probably desorbed the carbon, causing a decrease in current of about 20%,(see fig. 2.2), which is much less than that observed. The increased desorption was most likely due to the heating of the contact during the force measurement, (discussed in Chapter 7), or electroosmosis, (discussed in Chapter 9).

These results also have implications for other workers' results. They indicate that Balakrishnan's desorption of his specimens at 80°C was probably not effective in removing all the absorbed water. Also, if Stuckes' specimens had contained moisture it could have influenced her results as the high voltages used, up to 1300 volts, could have desorbed the water by Joule heating or electroosmosis affecting the force as the present results show.

Relating these results to a working device utilizing an absorbant semiconductor such as carbon would indicate that the performance of such a device

would change with time. The Johnsen-Rahbek force could be greatly reduced once the device started running, the friction heating it up to its running temperature of about $80^{o}C$ and consequently desorbing the semiconductor. This is probably the cause of the current flow through a device decreasing with time, (Dudding[6]).

8. 2 THE EFFECT OF HEATING THE CONTACT

Stuckes discounted Joule heating affecting the Johnsen-Rahbek force at low voltages. Eq. (1.1.3) would support this by indicating a small temperature rise for a typical carbon contact with the ball which has a value of d of about $50\,\mu m$.

However, in a working device frictional heating does raise the temperature of the semiconductor and the metal especially at the contact spots. It is at these contact spots that the Johnsen-Rahbek force is greatest and therefore at these same spots that the effect of heat would most affect the force. This effect of heating the contact will be investigated in this section, the primary concern being to estimate how frictional heating, as opposed to Joule heating, affects the force.

8.2.1 THEORY

Consideration of the equivalent circuit of the contact in Appendix 1 shows that if the whole semiconductor is heated, then its resistivity decreases, and the current increases as does E_o. In this simple model an order of magnitude decrease in the resistivity increases the field by approximately 10% to 20%. For a semiconductor such as carbon with an activation energy of 0.5 eV a temperature rise of $70^{o}C$ would be required for such a change. This situation is similar to that described in the last section where ρ increased with desorption and altered the force, except here ρ decreases instead of increasing.

What is of more interest here, however, is the case where the region around the contact is at a higher temperature than the bulk of the material, as in the frictional heating of a contact. In this instance the force decreases, contrary to the case where the whole material is heated. This decrease in

force can be explained, using the equivalent circuit model of the contact in Appendix 1, in terms of R_c decreasing whereas R_B remains constant. A larger proportion of the applied voltage is dropped across R_B and less across R_c and the gap. Hence the force decreases. For the circuit values chosen in Appendix 1 the model predicts only a small decrease in E_o and hence the force. This decrease is larger for circuits where the ratio of R_c to R_B is larger, i.e. further from the contact spot.

A different model is required to examine how the equipotentials change and how the field in the gap alters due to the contact heating. Such a model is shown in fig. 8. 3. This is a very simple model but to solve the problem accurately Laplace's equation needs to be solved with the correct boundary conditions. This is very complex and does not yield an explicit solution. Hence this simple model was used, and the calculations based on a solution of a similar problem by Collins. It gives only an approximate answer to the problem but indicates in a general way the behaviour of the contact.

The sphere of infinite thermal and electrical conductivity replaces the contact spot. The sphere is at a temperature θ_m, greater than the temperature of the bulk of the carbon, θ_o. No heat flows into the ball, as is the case in the experimental situation described later where the ball is at a higher temperature than the carbon , or into the interfacial gap. This arises as the gap is smaller than the mean free path of the gas at 10^{-5} torr, the pressure in the experimental situation. At this pressure the thermal conductivity of the gas is proportional to the mean free path, so it is very small. Assuming thermal equilibrium has been reached and that the isothermal surfaces in the carbon are hemispherical then the temperature of an isotherm r from the centre of the ball is given by :

$$\theta(r) = \theta_o + \frac{Q}{4\pi kr} \qquad (8.2.1)$$

where Q is the power of the heat source, (the sphere of radius d). At the surface of this sphere the temperature is θ_m so :

$$\theta_m = \theta_o + \frac{Q}{4\pi kd} \qquad (8.2.2).$$

Combining eq. (8.2.1) and eq. (8.2.2) gives :

$$\theta(r) = \theta_o + (\theta_m - \theta_o)\ \frac{d}{r} \qquad (8.2.3)$$

The term Q does not include the Joule heating of the contact which is regarded as negligible, as was stated earlier. The increase in temperature results in a decrease in the electrical resistivity, ρ , and a change in position of the equipotentials. If a voltage of V_o is applied to the contact then at a distance r from the sphere the voltage is :

$$V(r,\theta) = V_o \left\{ 1 - \left(\frac{\int_d^r \left(\frac{\rho_\infty \exp \frac{\Delta E}{2k}}{r^2} \right) dr}{\int_d^\infty \left(\frac{\rho_\infty \exp \frac{\Delta E}{2k}}{r^2} \right) dr} \right) \right\} \qquad (8.2.4)$$

This can be evaluated numerically and the interfacial voltage calculated from :

$$V_{int} = V_o - V(r) \qquad (8.2.5)$$

Fig. 8.4 shows the variation of V_{int} with r for a specimen of carbon with the appropriate constants in the previous equations. V_{int} can be seen to decrease with increasing temperature which indicates that the force would similarly decrease, although the complex calculation of this is not done with this simple model.

The decrease of V_{int} with temperature also indicates that c similary decreases. As a consequence of this the current/voltage relationship would become more ohmic i.e. the index would change from 1.5 towards 1.0.

Although this model is crude it does indicate the behaviour of a contact as its temperature increases. This is experimentally investigated in the following sections.

8.2.2 EXPERIMENTAL METHOD

To investigate the behaviour of the Johnsen-Rahbek force when the temperature of the contact is raised above that of the bulk of the semiconductor, a clean specimen of carbon was inserted into the force measuring apparatus with a 5cm diameter steel ball. The ball had been previously heated to about $150^{o}C$, (measured by a chromel-alumel thermocouple attached to the ball), by an infra-red lamp. The perspex table and surrounds were covered with small alumina slabs and aluminium foil to avoid excess heating which would cause outgassing in the vacuum chamber and impede the achievement of a low pressure.

When a pressure of approximately 10^{-4} torr was achieved, by which time the ball had cooled to about $90^{o}C$, measurements of force and current were commenced. Prior to this the carbon had not been in contact with the ball in order that the bulk of the carbon remained at room temperature, but the carbon was placed in contact with the ball for up to a minute for the contact to reach thermal equilibrium before each set of force measurements was made. The temperature of the carbon was not measured as it was found that a thermocouple attached to the carbon hindered the movement of the lever and adversely affected force measurements. Only eight force measurements were made at a given temperature to confine the temperature drop during them to $3^{o}C$ at the most.

8.2.3 RESULTS

Fig. 8.5 shows a typical plot of current versus voltage for various temperatures of the ball. Fig. 8.6 shows these plots on logarithmic paper to indicate the power to which the current increased with voltage. A typical variation of E_o with temperature is shown in fig.8.7 and table 8.3 shows that the intercept of the force/voltage plot varied slightly with the temperature.

8.2.4 DISCUSSION OF THE RESULTS

A plot of the resistivity of the semiconductor, ρ , calculated from the current flow, versus Θ_m does not obey eq. 8.0.1. This indicates

that the carbon was not at a uniform temperature of Θ_m, but that the contact was heated to a temperature above that of the bulk of the semiconductor, Θ_o, required of the experiment.

Fig. 8.6 shows the I/V plot to become more ohmic as the temperature increased, in agreement with the previous theory.

The value of E_o decreased significantly as the temperature increased, fig. 8.7, in agreement with the theory, and the force decreased slightly more due to the intercept increasing with the increased temperature, table 8.3. The variability in the points in fig. 8.7 was probably due to the bulk of the carbon having been heated which would counteract the tendency for the force to decrease with increasing temperature. The force measurements must only be regarded as approximate, indicating that the force can be substantially reduced as the contact temperature, Θ_m, becomes raised above the bulk semiconductor temperature, Θ_o. This means that the performance of a working device will vary as Θ_o and Θ_m alter, especially when the device is started and Θ_o increases from room temperature to 80^oC. The results also indicate that if Joule heating is substantial due to large voltages and high currents then it could reduce the force as Θ_m increased.

In Chapter 7 it was postulated that the heating of the anode as the contacts were separated could account for the difference between force measurements for each polarity of applied voltage. The present results show E_o to be very temperature dependent and confirm the hypothesis that any slight temperature increase of the semiconductor contact would decrease E_o and cause a slight reduction in the attraction force produced.

8. 3 CONCLUSION

The results discussed in this chapter show that the Johnsen-Rahbek force is very dependent on the semiconductor's temperature, both from the point of view of the desorption of the semiconductor, if it is like the carbon, and from the point of view of the difference in temperature between the contact and the bulk. The exact dependency of the force on these factors is complex but the simple

experiments performed indicate that the performance of a working device utilizing an absorbant semiconductor such as carbon would be very variable due to these factors. It is probably this variable performance which has limited the use of devices using the Johnsen-Rahbek effect.

TABLE 8.1

THE DECREASE IN THE SATURATION ELECTRIC FIELD, E_o, AS MORE WATER VAPOUR IS DESORBED FROM A CARBON SPECIMEN. THE FORCE MEASUREMENTS WERE MADE AFTER THE CARBON HAD BEEN IN VACUO IN THE FORCE MEASURING APPARATUS FOR 75 MINUTES.

AVERAGE VALUE OF E_o FOR BOTH POLARITIES OF APPLIED VOLTAGE ($10^8 V_m^{-1}$)	TREATMENT OF THE CARBON SPECIMEN PRIOR TO FORCE MEASUREMENTS
6.0	NO PREVIOUS HEAT TREATMENT
4.9	30 MINUTES IN OVEN AT 80^oC
4.6	FURTHER 30 MINUTES IN OVEN AT 80^oC
4.2	FURTHER 30 MINUTES IN OVEN AT 120^oC
4.5	DIFFERENT SPECIMEN FROM ABOVE. 4 HOURS IN OVEN AT 250^oC

TABLE 8.2

THE DECREASE IN CURRENT AFTER EACH SET OF FORCE MEASUREMENTS.

CURRENT (AT 200 VOLTS)		
BEFORE A SET OF FORCE MEASUREMENTS (μA)	AFTER A SET OF FORCE MEASUREMENTS (μA)	TREATMENT OF THE CARBON PRIOR TO FORCE MEASUREMENTS
1.74	1.68	NO PREVIOUS HEAT TREATMENT
1.18	1.08	30 MINUTES IN OVEN AT 80^{o}C
0. 7	0.64	FURTHER 30 MINUTES IN OVEN AT 120^{o}C
0.20	0.22	DIFFERENT SPECIMEN FROM ABOVE 4 HOURS IN OVEN AT 250^{o}C

TABLE 8.3

THE VARIATION IN THE VOLTAGE INTERCEPTS OF THE FORCE/VOLTAGE PLOTS WITH THE BALL TEMPERATURE.

INTERCEPT (VOLT)	TEMPERATURE OF THE BALL, Θ_m (^{o}C)
12.7 ± 6.2	80
10.3 ± 1.7	70
5.9 ± 3.5	60
5.6 ± 1.4	50
12.4 ± 0.9	20

STATIC IV PLOTS SHOWING THE CHANGE IN CURRENT DUE TO DESORPTION FROM THE CARBON

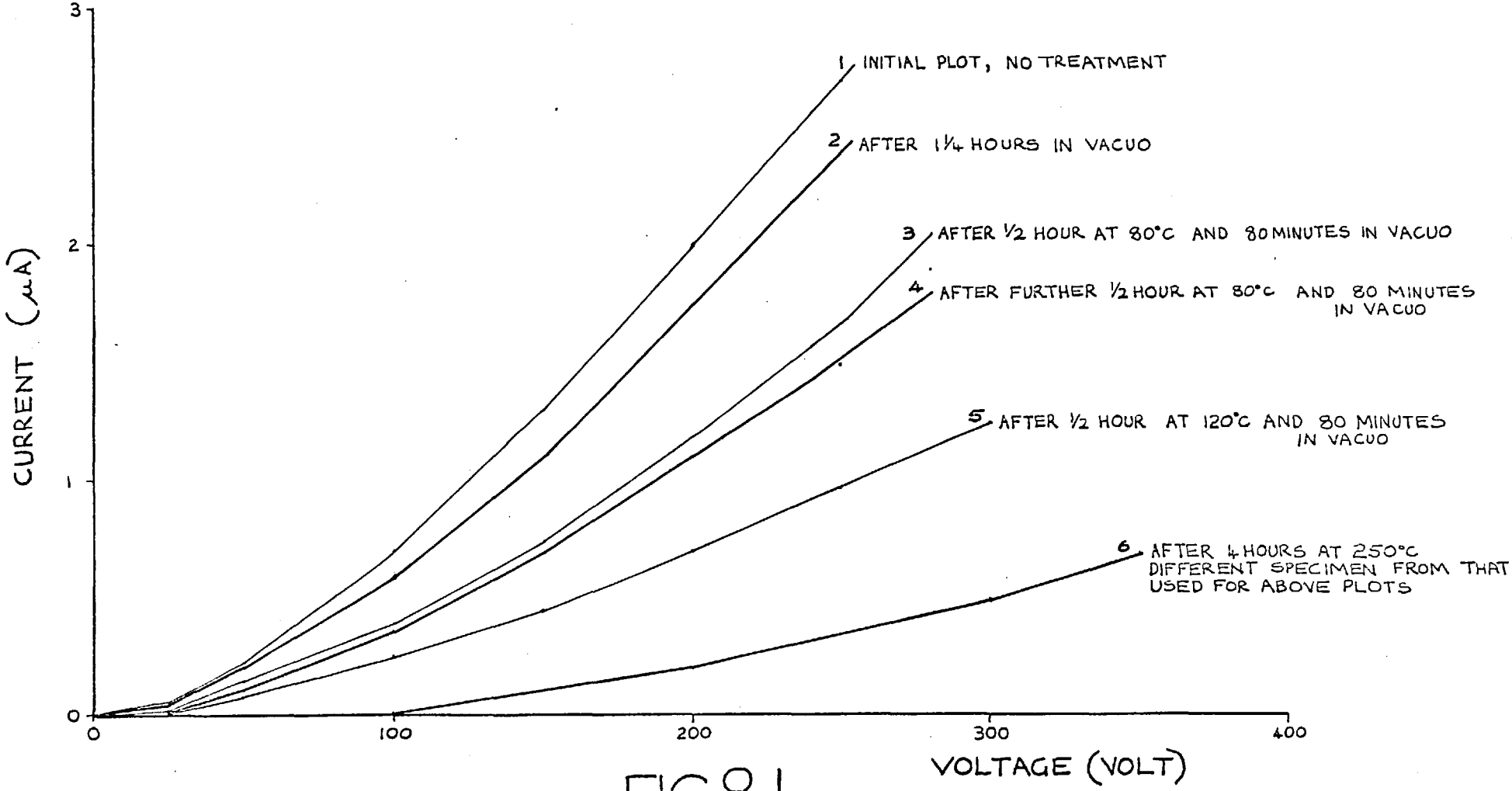

FIG.8.1

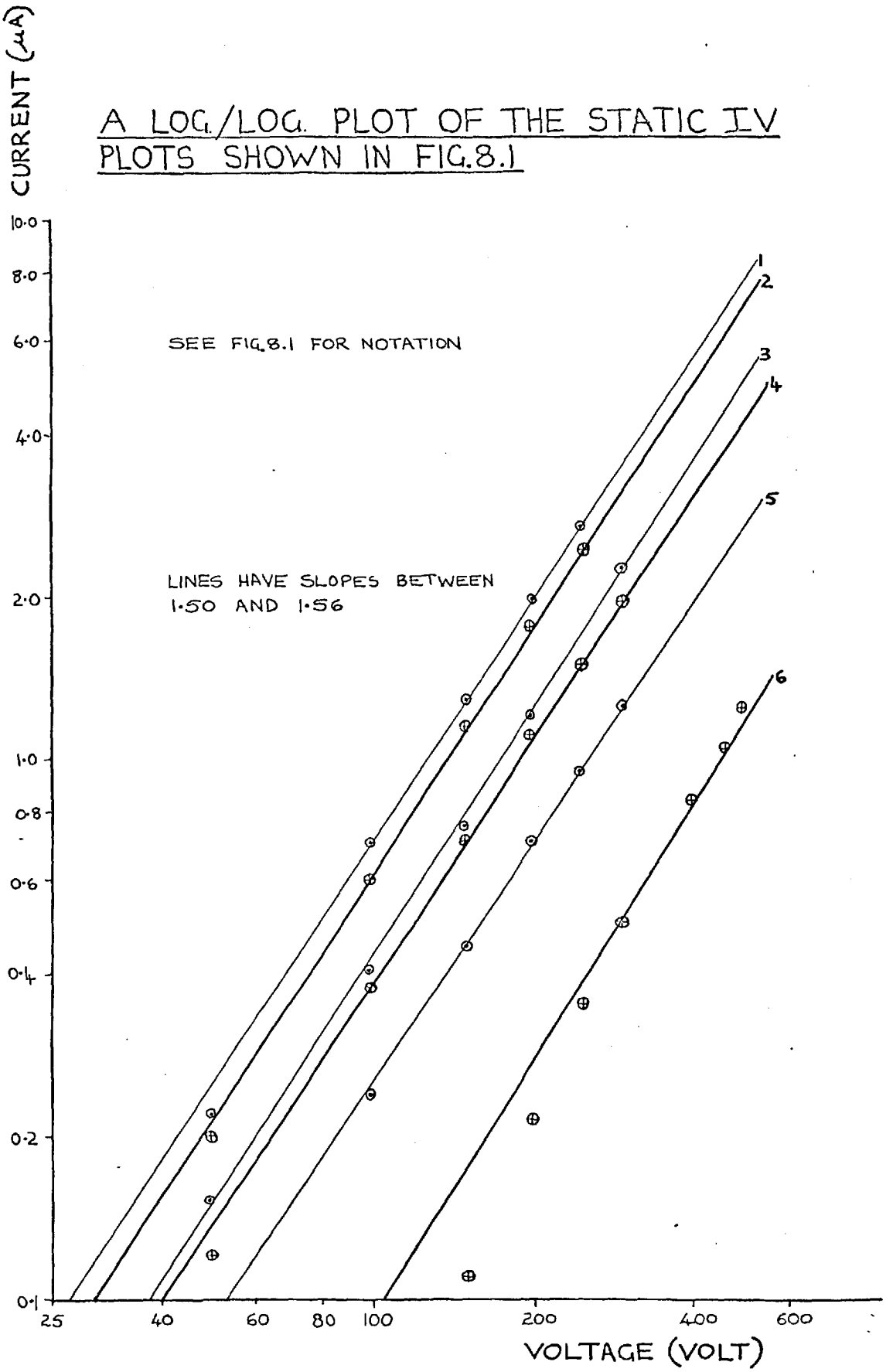
A LOG./LOG. PLOT OF THE STATIC IV PLOTS SHOWN IN FIG.8.1
CURRENT (μA)
10·0
8·0
6·0
4·0
2·0
1·0
0·8
0·6
0·4
0·2
0·1
SEE FIG.8.1 FOR NOTATION
LINES HAVE SLOPES BETWEEN 1·50 AND 1·56
1
2
3
4
5
6
25
40
60
80
100
200
400
600
VOLTAGE (VOLT)

FIG.8.2

A MODEL OF THE CONTACT BETWEEN THE BALL AND FLAT

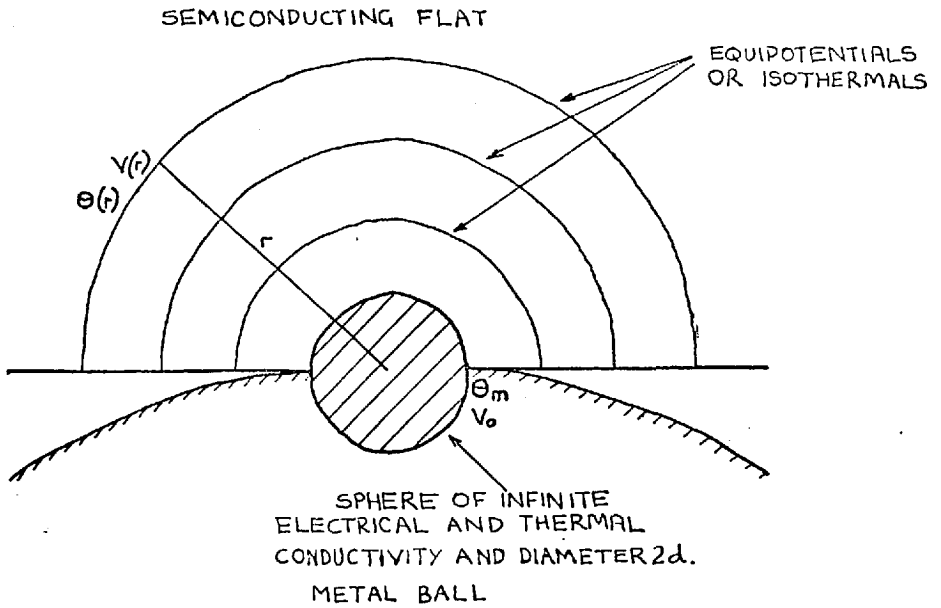

FIG.8.3

THE VARIATION OF THE INTERFACIAL VOLTAGE BETWEEN A BALL AND FLAT WITH TEMPERATURE

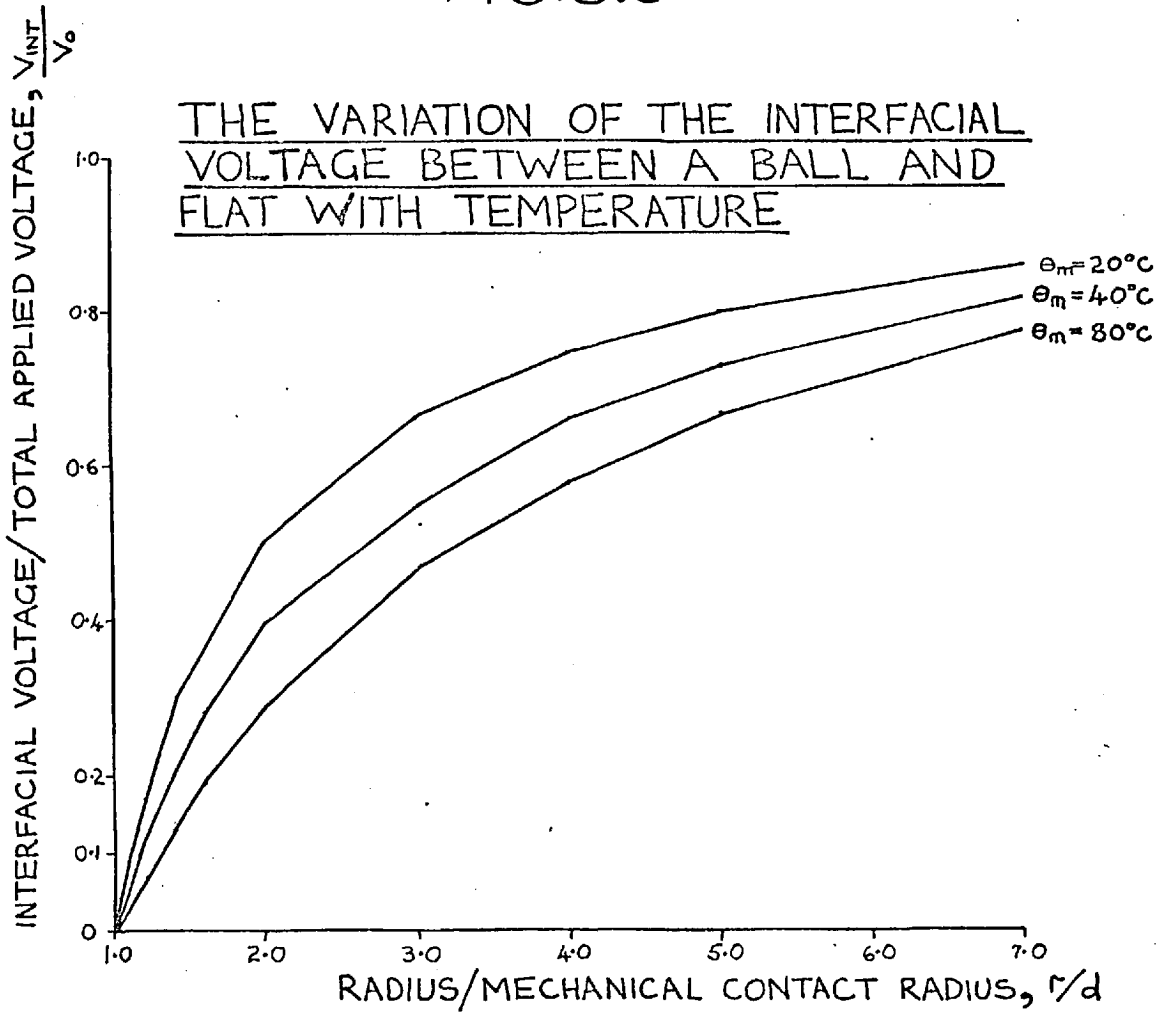

FIG.8.4

STATIC IV PLOTS AT VARIOUS TEMPERATURES

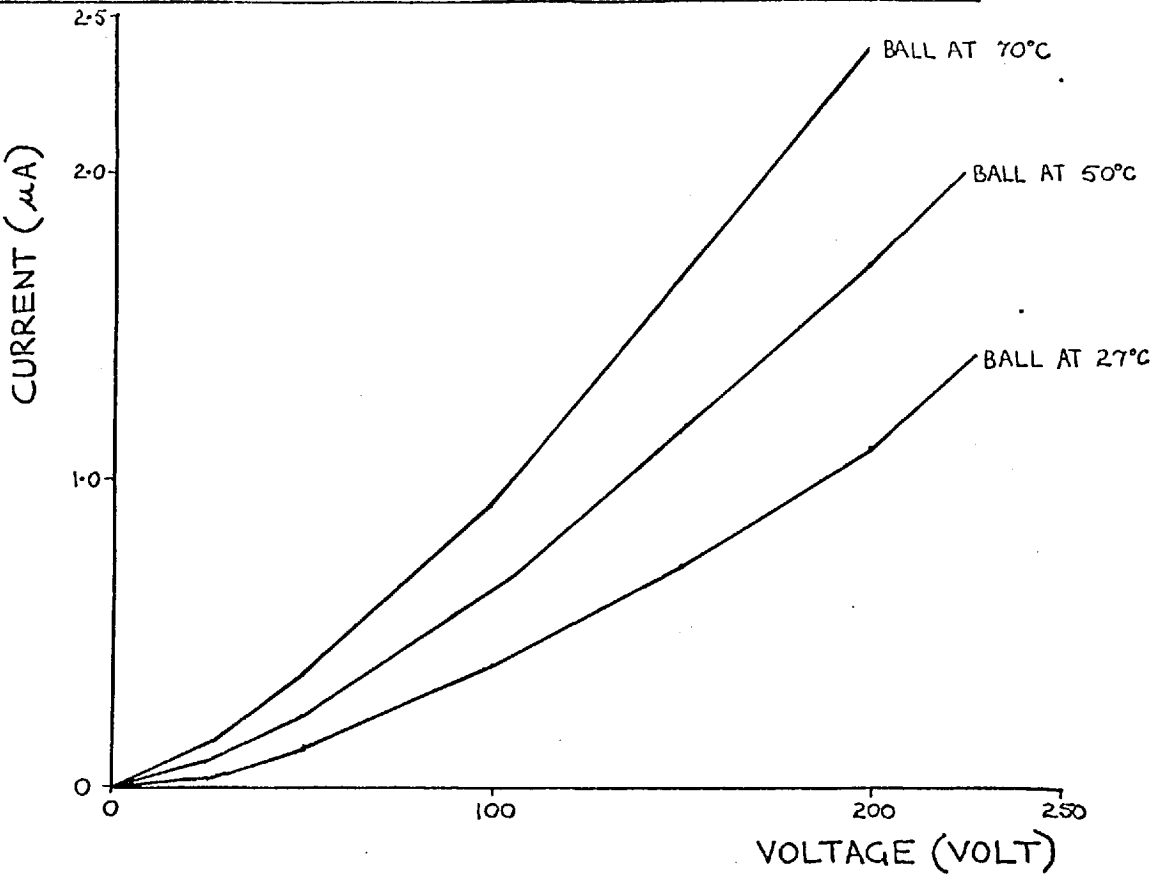

FIG.8.5

A LOG./LOG. PLOT OF ABOVE PLOTS

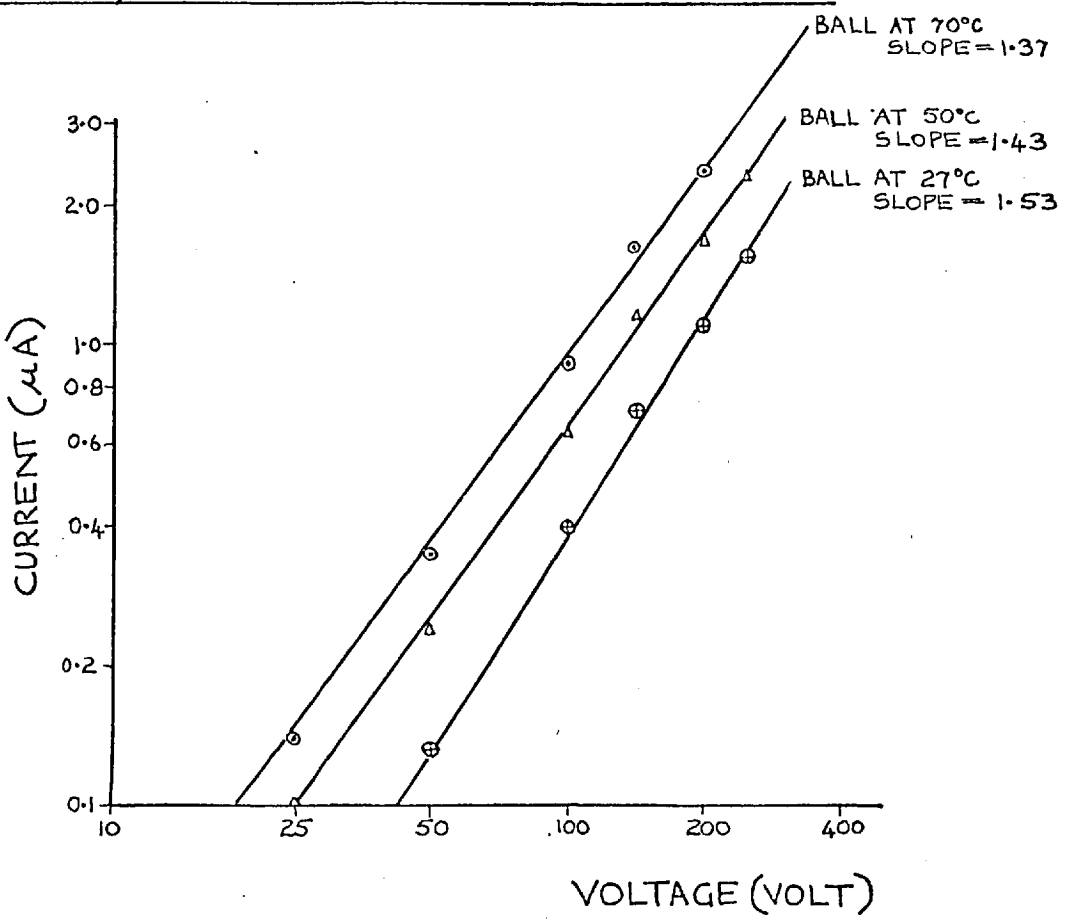

FIG.8.6

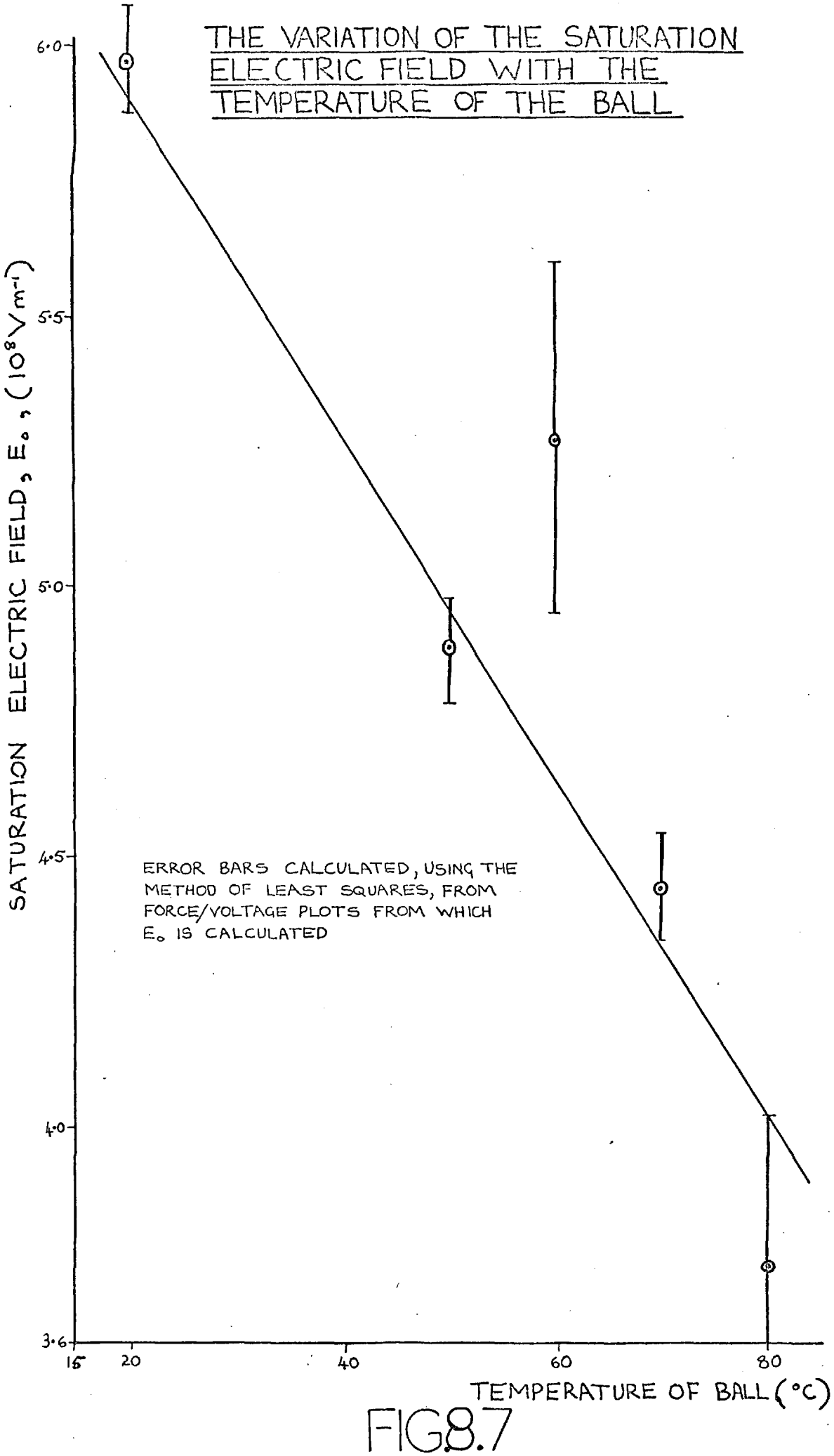
THE VARIATION OF THE SATURATION ELECTRIC FIELD WITH THE TEMPERATURE OF THE BALL
SATURATION ELECTRIC FIELD, E_0, ($10^8 V m^{-1}$)
6·0
5·5
5·0
4·5
4·0
3·6
ERROR BARS CALCULATED, USING THE METHOD OF LEAST SQUARES, FROM FORCE/VOLTAGE PLOTS FROM WHICH E_0 IS CALCULATED
15
20
40
60
80
TEMPERATURE OF BALL (°C)

FIG8.7

CHAPTER IX

SURFACE DEGRADATION AND ETCHING

Johnsen and Rahbek found that discharges occurred between the metal and semiconductor of their devices, which roughened the surfaces and diminished the force. Stuckes also found that the application of a voltage to the devices gradually etched the surfaces. After they had been run for a number of hours at about 500 volts the positive electrode was found to be dulled and etched. The mild steel rusted and the semiconductor became dulled when each was at a positive potential. This was attributed to the moisture in the gap and its interaction with the electronic current since it was found that when the devices were operated in a desiccator the etching was greatly reduced.

Dudding and Losty attributed the greater reliability of their devices, compared to previous ones, to the fact that the polishing of the carbon, due to its sliding against the steel, was counteracted by the etching which tended to keep the surface of the carbon at a constant equilibrium roughness.

In the present work, (Chapter 3), etching was found to severely roughen the carbon and to cause a counter surface of mild steel to rust when each was the anode. As the etching was considered to be due partly to the environment in which the members were situated, force measurements were made in a vacuum of 10^{-5} torr. However, after a number of measurements in vacuo the surfaces of the carbon and the ball were found to be degraded. This showed that even in a vacuum environment similar etching processes were still active.

These results demonstrate that etching of the contacting surfaces can easily roughen them and thus reduce the force between them. This could radically alter the performance of a device and so it was considered essential that the phenomenon be investigated. Experiments were therefore conducted under vacuum and atmospheric conditions as etching occurred to varying extents under both.

9. 1 PRELIMINARY DISCUSSION

Johnsen and Rahbek noted that the etching was due to discharges between the surfaces of their devices. Discharges occur between electrodes when the

current flow avalanches by ionisation of the gas in the gap. This only happens when a certain minimum voltage, V_s, is applied across the gap and Paschen found that there was an empirical relationship between the minimum voltage and the pressure of the gas and the width of the gap, Δ. The relationship varied with the gas between the electrodes, but it was still of the form of that between electrodes in air, shown in fig.9.1. This shows a minimum at 330 volts and $p\Delta \simeq 5 \times 10^{-3}$ torr cm. With $p\Delta$ decreasing below this value, V_s increases again. The curve here however is not made up from experimental results at atmospheric pressure because of experimental difficulties. More recent work, (Germer et al., (1)-(4)), has shown that at atmospheric pressure and small gap widths the rising part of the curve to the left of the minimum was often missing. Breakdown at voltages as low as 50 volts occurred. Fig.9.2 shows the relationship for small gap widths and the failure of Paschen's law.

The reasons for the failure of the law are not completely understood. The theoretical explanation of the law itself was given by Townsend who stated that the ionisation of the gas in the gap produced more current and the process avalanched to breakdown. For short gaps, however, the mean free path for ionising collisions between neutral molecules and electrons is greater than the gap width of the electrodes so that Townsend's explanation does not apply. Some other process must be operative. This may depend on generation of gas from the electrodes, see Chapter 7, or the enhancement of the field emission current from the tarnish layer or negative ions on the cathode surface, which separately or together produce the conditions for Paschen breakdown.

Hence for the generation of the Johnsen-Rahbek effect which requires a small gap between the electrodes and high voltages ($\gtrsim$ 100 volts) breakdown in the gap is possible. Even if breakdown did not occur the ions formed could intereact with the electrodes e.g. they could sputter the cathode when they bombarded it. This, however, would only occur at high voltages as sputtering yields are only significant for ion energies greater than about 60eV depending on the mass of the ion, (Maissel).

9. 2 MEASUREMENTS UNDER VACUUM CONDITIONS

When previous measurements were made under vacuum conditions the electrodes were found to be damaged. This could have been due either to the oscillation during the force measurement, as discussed in Chapter 5, or due to the electrostatic force plucking pieces of carbon from its surface or due to both. To determine to what extent the electrical force alone was responsible a voltage was applied for a few hours to the ball and flat and they were then examined for any signs of damage.

9.2.1 EXPERIMENTAL METHOD

The same vacuum system and force measuring apparatus were used as previously described in Chapter 4. The specimens were prepared and cleaned in the same way before insertion and the vacuum system was allowed to achieve a pressure of 10^{-5} torr before measurements were commenced. A static IV plot was taken and then a given voltage was applied for a number of hours to the ball-on -flat. The current during the application of the voltage was monitored on the meter in the circuit and on a chart recorder to show how the current varied with time. When the experimental run was complete another static IV plot was taken on the XY recorder. The ball and flat were then taken out of the system and examined on an optical microscope for any signs of damage around the contact areas. Although marked etching could be seen with the microscope it was not easy to take photomicrographs of it as the carbon's surface was dark and the ball was curved.

A profile of the etching on the carbon was taken with a profilometer. As the etched region was typically 300μm in diameter it was difficult to position the track of the stylus so that it passed over the etching. To discover whether the stylus had actually gone over the region a small circle of ink was marked around it and after a traversal of the stylus the specimen was examined on the microscope and the path of the stylus determined from the clear track it left in the ink.

A few of the carbon specimens were examined by electron microprobe analysis to find if any material had been transferred from the ball as evidence of any discharges occurring in the gap. High magnification micrographs of the etching were also obtained from the analyser.

This above proceedure was carried out for about 20 experimental runs with different specimens of carbon for different voltages of different polarities and different durations of current flow.

9.2.2 RESULTS OF INITIAL EXPERIMENTS

Applying voltages of both polarites up to 300 volts for durations of between 2 and 5 hours to various specimens of carbon and conducting glass in contact with a 5 cm diameter ball produced a negligible amount of etching. In the case of carbon the static IV plots did, however, show a decrease in current of between 20% and 13% during the application of the voltages.

For undesorbed specimens of carbon, (i.e. specimens which had not been previously heat treated), the etching became marked at 400 volts and severe at 550 volts, (the maximum voltage of the particular power supply used). These results are discussed more fully in the next section.

Under the same conditions no etching was observed on a specimen of glass or on a specimen of carbon which had been desorbed, (by heating at 250^{o}C for 5 hours, as mentioned previously). With both specimens the current initially increased due to Joule heating but in the case of the carbon the static IV plots showed the current to have decreased by approximately 5% during each 3 hour run.

The ball was found to be unetched during these experimental runs except at high voltages when it was in contact with the undesorbed carbon specimens. This is discussed more fully later.

9.2.3 EXPERIMENTAL PROCEEDURE WITH UNDESORBED CARBON

The previous results show that under vacuum conditions etching only occurs with undesorbed carbon. To investigate this further 550 volts was applied between such specimens and the ball for 3 hours. The voltage and duration of current

flow were fixed at these values to standardize the experimental runs. The high voltage was used to maximise the etching and the duration of 3 hours was found to be sufficient for the rate of etching to diminish to an insignificant level. As the specimens varied slightly in resistivity and surface geometry, and as their resistivity increased significantly during a run, probably due to desorption, 4 specimens were used. The same ball was used for all the experimental runs except for two which were made with a 2.5 cm. diameter platinum coated ball for investigating material transfer from the ball to the carbon.

9.2.4 RESULTS OBTAINED WITH UNDESORBED CARBON

The etching created an annulus around the contact spot on the carbon, its appearance depending on the polarity of the applied voltage, as photomicrographs of typical etch annuli show, fig. 9.5. The ball was not greatly affected by the application of the voltage except for a few small etch pits around the contact and sometimes, when the carbon was at a negative potential, a faint browny film could be seen on the ball around the contact region. It was too faint to get good micrographs. When the carbon was at a negative potential the annulus appeared to be a depression with dark etch pits around it. Fig. 9.4, taken with a phase contrast attachment on the microscope, shows this better. When the carbon was at a positive potential there appeared to be two regions comprising the annulus; one being an almost continuous dark inner region of fine pits and the other an outer diffuse ring of larger etch pits.

The dimensions of the annuli were measured, table 9.1, and it was found that they were of approximately the same size. The depths of some of these annuli, as measured from profile traces, are shown in table 9.2. Fig. 9.5 shows typical profile traces and the corresponding etch annuli. These indicate the annuli to be depressions approximately corresponding to the etch marks. It is noticeable that when the carbon was at a positive potential the depth of the annulus was greater.

Examination of the etch marks in an electron microprobe analyser showed no significant traces of iron, (the main element in the ball), above the rather high background count due to traces of iron throughout the carbon, (see Chapter 2).

When a specimen which had been in contact with the 2.5cm diameter platinum coated ball was examined, the large etch pits which constitute the outer region of most 'positive' annuli were found to contain a layer of platinum about 12 Å deep. This was near the limit of resolution of the instrument and it only detected the platinum because the background count was low. There was no trace of platinum outside the pits. Micrographs taken with this instrument show the pits to be 1 μm to 2 μm in diameter, fig.9.6.

The traces of the current taken on the chart recorder, of which fig.9.7 shows typical traces, show that the current, when the carbon was positive, was very noisy initially, consisting of very closely spaced spikes which represented up to 5% of the total current flow. As time passed the noise became less and the trace became almost a straight line. When the carbon was at a negative potential, however, the current trace was completely different. It consisted of sudden 'step-function' decreases which were about 5% of the total current, and showed little noise. The trace, as with the positive carbon trace, eventually became a smooth straight line.

Throughout these traces the current gradually decreased as fig.9.8 shows. The decrease appeared to be independent of the polarity of the applied voltage but dependent on the quantity of absorbed gases in the specimen. Table 9.3 shows the decrease for a number of specimens after 3 hours, the decrease being calculated in the usual way as the ratio of the currents at 200 volts on the two static IV plots. Some specimens were used more than once and provided the subsequent run was made soon after the previous run it was found that the subsequent current initially was never more than the current at the end of the previous run although a different spot on the carbon was used to make contact with the ball. Table 9.4 shows this for one previously unused specimen with which four runs were made over a period of four days.

9.2.5 DISCUSSION

The etching observed in these experiments was different from the degradation of the carbon surface after force measurements had been made. The former

consisted of an annular depression and etch pits, the latter of a layer of crushed carbon and a few etch pits. This shows that two different mechanisms were responsible. The oscillation of the carbon during the force measurements appeared responsible for the latter etching; electrical phenomena being responsible for the former etching. The etch pits, however, were probably due to the same cause; i.e. discharges between the electrodes. The etching of the carbon in a vacuum environment was related to the absorbed gases and vapours within the carbon as the initial results show. The glass specimen was not etched possibly due to its not having these absorbed gases. With the undesorbed carbon the etching was accompanied by the current decreasing during the experimental run. Also the current of a subsequent run with the same specimen but with a different contact spot was initially equal to or less than that at the end of the previous run. This was undoubtedly due to the desorption of the whole carbon specimen. The rate of decrease in current was higher than any previous measurements had shown, (e.g. the decrease due to the vacuum alone or during force measurements). This could have been due to the higher currents heating the specimen more. Using eq. (1.1.3) and taking the contact 'sphere' to be of radius c, typically about 180 μm and the current flow to be typically 10 μA the temperature rise was calculated to be about 20^{o}C assuming 550 volts to be applied to the contact. The absorbed water could also be desorbed by electroosmosis as is discussed later.

The dimensions of the annuli, table 9.1, are all similar. The central unetched region probably corresponds to the region of mechanical contact and if the region of etching corresponds to the region of current flow across the gap then E_o can be calculated from eq. (5.1.1). The average value is $8 \times 10^{8} Vm^{-1}$, (see table 9.1), which is in reasonable agreement with previous force measurements, which indicates that the region of etching does indeed correspond to that of current emission. The mechanism of etching is thus some type of interaction between the current in the gap with the desorbed gas.

The etching process seems to differ with the polarity of the applied voltage as the form of the annulus, its depth and the current traces differ with the polarity. This could be due to electroosmosis which is polarity dependent, moving the water in the carbon when a voltage is applied. This is discussed later with

regard to subsequent experiments.

It is almost impossible to establish the mechanism of etching from these results, as can be appreciated from considering the case of water vapour, which is probably the principal absorbant in the carbon, as it is desorbed into the gap. It can form negative ions, (Massey), in collision with low energy incident electrons,(about a few eV, (Reed)), and positive ions. It can also dissociate possibly into oxygen and hydrogen ions. The process is complex and depends on the energy of the incident electron and the cross-section for the particular collision process (von Engel). The interaction between the ions and the carbon electrode is also complex, and many possible processes can occur. As the etching only becomes significant at 400 volts and above, any ions created in the gap would have large kinetic energies and sputtering could possibly occur. A rough calculation of the sputter yield gives a value of about 10^{-3} sputtered atoms per incident ion showing that the process is possible, a yield of above 5 being an unrealistic value. However, the explanation of sputtering must also apply to the etching when the carbon is the anode which seems improbable unless high energy negative ions are formed in the gap.

Whatever the processes occurring in the gap they are capable of creating micro-discharges, evidenced by the platinum found in the etch pits of one specimen. These micro-discharges were probably responsible for the noisy current produced when the carbon was at a positive potential, as the current when it was at a negative potential was less noisy and fewer discrete etch pits are seen on the annulus formed. The noise largely disappeared after 30 minutes to an hour indicating that high currents flow when etching occurs.

9. 3 MEASUREMENTS UNDER ATMOSPHERIC CONDITIONS

The previous results showed that the etching in vacuum was due to water vapour being desorbed from the carbon. Under atmospheric conditions, however, there is more gas in the gap which alters the current and also causes more severe etching, (see Chapters 7 and 3).

9.3.1 EXPERIMENTAL METHOD

The ball-on-flat apparatus with the 5cm diameter ball was used as before but the vacuum chamber containing it was left at atmospheric pressure. Lower voltages than those applied in the vacuum runs were initially used to avoid any catastrophic breakdown which is more likely at this pressure than at 10^{-5} torr. The ball and carbon specimen were cleaned in the usual manner before they were inserted into the apparatus. The same specimen of carbon was used for all the experimental runs, as it was not desorbed excessively during each run. The position of the carbon on the lever was altered so that contact with the ball was made at a different spot, and any new etch marks could be seen clearly.

9.3.2 RESULTS

When the carbon was at a negative potential with respect to the ball there was no significant etching on either the ball or the carbon at voltages of up to 200 volts. Over the half hour of the application of a voltage the current decreased little as table 9.5 shows for two measurements made at 150 volts.

When the carbon was at a positive potential, however, the current decreased rapidly, by approximately 20%, table 9.5, over the duration of the current flow. The duration was half an hour as significant etching occurred in that period. Fig.9.9 shows the etch annuli formed when voltages between 50 volts and 250 volts were applied across the ball and flat. The etch annulus formed at 250 volts is similar in appearance to those formed in vacuo at 550 volts, but the others are completely different. They have what appear to be tracking marks around the outside of the annulus and the annulus is not so much a depression as a surface mark. This was determined from profilometer traces which showed negligible depression on the annulus above that produced by the roughness of the surface.

No corresponding etch marks were found on the steel ball when it was examined on the optical microscope.

9.3.3 DISCUSSION

The etch annuli described above are different from those formed in vacuo. This is probably because the mechanisms of etching are different. In the atmosphere desorption of water from the bulk of the carbon is highly unlikely with no vacuum environment and voltages as low as 25 volts which would cause negligible contact heating. The mechanism must be related to the atmospheric environment in the interfacial gap.

Compared to surfaces in vacuo the contacts in atmospheric conditions have water vapour and other gases adsorbed from the environment. Also the carbon has absorbed water vapour in its pores near the surface, unlike the situation when it is in vacuo with the surface and near-surface water vapour desorbed. Also small gaps such as that near the contact between the ball and flat often condense water vapour from the atmosphere. Kelvin's equation, (defined in fig.9.10), for the condensation of water vapour at 25°C in a capillary of radius r is ;

$$\ln\left(\frac{P}{P_o}\right) = -\frac{4.6 \times 10^{-8}}{r} \qquad (9.3.1)$$

where P_o is the saturated vapour pressure and P is the vapour pressure. This shows that significant condensation does not occur for radii greater than 100 Å. This would correspond to a gap width of about 200 Å between the ball and flat.

Thus water can form in the gap around the contact between the ball and flat. When a voltage is applied, with the carbon at a positive potential, electrolysis probably occurs near the contact as water is drawn, by electroosmosis, (see 9.4.3), towards the negative electrode, i.e. the ball. The motion of surface water is probably responsible for the tracking marks around the etch annuli, fig.9.9. Thus the etching appears to be an electrolytic process which marks the carbon surface rather than plucking it, as happens when etching occurs in vacuo.

When the applied voltage is reversed, however, electroosmosis would move water away from the contact, preventing any electrolytic etching. This would account for there being no etch annuli formed when the carbon is at a negative potential.

Comparison of the 200Å gap width inwhich water vapour was estimated to condense with the larger gap widths over the region of etching, table 9.7, would indicate that condensed water vapour alone would not be responsible for providing enough water for the etching. Adsorbed and absorbed water would also have to

contribute. These results agree with Stuckes' findings that the positive electrode was always etched, but that when stainless steel was used as the positive electrode no etching was found.

As in the etching in vacuo the etching here occurs over the region of current flow across the gap, as calculations of E_o from annular dimensions yield values of about 5×10^8 Vm^{-1}, table 9.7, in agreement with the values from force measurements. The values vary between the experimental runs, however, probably due to the variation in the condensation occurring in the gap.

9.4 INVESTIGATION WITH THE FIZEAU INTERFEROMETER

In Chapter 3 preliminary investigations showed that the carbon was etched when a voltage was applied between it and the tin oxide coated glass. This is re-examined here to compare with the ball-on-flat results and also to get some insight into the etching which could occur between the members of a working device using nominally flat contacts.

9.4.1 EXPERIMENTAL METHOD

The Fizeau interferometer described in Chapter 3 was used for this investigation, and the usual cleaning proceedure was followed before inserting the carbon specimen and the glass.

In order that etching at different voltages could be compared the same specimen was required for all the experimental runs so that the interfacial geometry remained constant. Initial experiments showed that applying voltages between 100 volts and 500 volts to the carbon and glass for five minutes did not excessively damage the carbon,. but showed detectable traces of etching. Thus initially a voltage of 100 volts was applied for 5 minutes, during which the current was monitored on the meter (fig. 3.4) and the interference pattern photographed to determine the interfacial geometry. The specimen was then examined for etching on an optical microscope, and photomicrographs taken to compare with photomicrographs taken before the application of the voltage. Profilometer traces were also taken before and after the experimental run and the average C. L. A. value of 10 readings was calculated but they were not

very sensitive to the small amount of etching which occurred to varying degrees over the specimen.

The proceedure was then repeated with the applied voltage increased by 100 volts. This was done up to 500 volts. Then the specimen was carefully polished for about an hour with 1 μm Linde powder suspended in water to remove the etch marks which were quite deep and the proceedure of applying increasing voltages was repeated with the polarity of the voltage reversed.

9.4.2 RESULTS

Initial experimental runs with a previously unused specimen of carbon were terminated when the current rapidly increased upon the application of 500 volts, with the carbon at a negative potential, until the carbon broke down electrically and discharges could be seen tracking across the interfacial gap. Fig. 9.11 shows the damage caused to the specimen. This demonstrates that for large area contacts the attendant large currents can have catastrophic effects.

With the second specimen used no electrical breakdown occurred although the current still increased but to a lesser extent upon the application of high voltages.

Fig. 9.13 shows the etching and fig. 9.12 shows the interference fringes for various voltages when the carbon specimen was at a negative potential. The etching became most noticeable after the 300 volt run when the specimen appeared dull to the naked eye and etch pits could be seen with the microscope at the edge of it. The etching was very pronounced after the 500 volt run. The C.L.A. values measured after each run are shown in table 9.8. The glass was not etched during these runs.

Fig. 9.14 shows the etching and fig. 9.12 shows the interference fringes when the carbon specimen was at a positive potential. The etching was greater than that which occurred with the opposite polarity of voltage. After the 100 volt run what appeared to be a multi-coloured film could be seen with the naked eye on the carbon. The tin oxide coated glass also had a corresponding brownish

coloured film on it, fig.9.15. To assess how the glass was affected by the etching a new piece was used for each run. The film became more pronounced with increasing voltage as did the etching of the carbon surface. Distinct etch pits were formed on the edge of the specimen as was the case with the reverse polarity of voltage.

The interference fringe patterns at 500 volts, fig.9.12 are very interesting as they show the central region to become darker as the duration of the current flow increased. When the glass was moved slightly the dark central region shifted more slowly than the fringes, suggesting that it was caused by liquid being present in the interfacial gap around the contact. This occurred to lesser extents at lower voltages. No such dark central region was generated when the carbon was at a negative potential, as fig.9.12 shows .

Throughout the experimental runs when the carbon was at a negative potential a 'tinkling' noise was emitted after the voltage had been applied for up to a minute. This was due to the oscillation of the contacting members as the fringe pattern was discerned to vibrate at the same time and was rather unstable. Table 9.8 gives the C.L.A. values measured after each experimental run.

9.4.3 DISCUSSION

At voltages up to 200 volts for either polarity the etching roughened the surface less than the force 'flattened' the asperities reducing the roughness, table 9.8. At 300 volts and above the etching was more severe especially when the carbon was at a positive potential. The current at these voltages also steadily increased during the experimental run due to Joule heating.

Although the etching had different forms for the different polarities of the applied voltage, both showed etch pits at the edge of the specimen, forming a dull annular region. These etch pits were deeper than the other etch marks as was found when the specimen had to be polished for the second set of experiments. They were probably caused by discharges occurring due to electrical breakdown

of the gas in the gap. Paschen's law shows that for breakdown to occur with an applied voltage of 500 volts the gap must be between 3 μm and 30 μm wide. At 330 volts the gap must be about 7 μm wide. This explanation corresponds to the observation that the pits were formed around the edge of the carbon specimen where the gap was largest, about 6 μm, and that the pitted region enlarged as the voltage increased. Generation of gas from the electrodes would increase the pressure in the interfacial gap so that breakdown could occur at gap widths slightly less than the values quoted.

The etching at regions where the interfacial gap width was less than that required for breakdown , however, varied with the polarity of the voltage. When the carbon was at a negative potential, liquid appeared in the gap to an extent dependent on the voltage. The generation of this liquid was probably due to electroosmosis.

Electroosmosis is the motion of a liquid in an electric field relative to a fixed solid, (Lorenz). Usually the solid is a porous system, such as a glass capillary. In the majority of cases the liquid moves to the cathode as is the case for water which is present in the carbon. The motion is caused by the interaction of the electric field and the diffuse double layer, (Debye), between the solid and the liquid. (For a detailed analysis see Hartman). The equations describing electroosmosis only apply to simple systems, but in the case of the carbon it is far from simple. The water vapour absorbed in the carbon could be simply condensed in the pores of the material, physiorbed or chemisorbed on the internal or external surfaces and if there is any cellulose or other impurities present, dissolving them and forming ions as happens in the case of paper, (Constandinou). The complex nature of absorbed water is discussed in more detail in relation to its dielectric properties by Hasted.

Electroosmosis is most likely responsible for the phenomena occurring when the carbon is the anode. The absorbed water migrates towards the cathode forming the liquid in the gap. The pressure of this liquid emanating from the carbon lifts the glass contact slightly and the Johnsen-Rahbek force

tends to restore it to the original position, hence the glass oscillates. The hydrostatic pressure of water produced by electroosmosis in a tube of radius r is:

$$P = \frac{2 \xi V_o D}{\pi r^2} \qquad (9.4.1)$$

where ξ is the zeta potential, V_o the voltage, and D the dielectric constant of liquid. For water at 25^oc, assuming ξ is 100mV eq (9.4.1) becomes

$$P = 5.6 \times 10^{-5} \frac{V_o}{r^2} \qquad (9.4.2)$$

Estimating the field near the contact to be of the order of 10^6 Vm^{-1} and with r at a value of 1 μm then P equals $\sim 6 \times 10^6$ Nm^{-2}. The above equation refers to a capillary, but the carbon is far from that. The water in it is much more tightly bound than that in a capillary tube and the pores are not straight tubes so that the pressure given by the equation is only a rough estimate. However, it indicates that the pressure is high as was indeed found to be the case when a specimen was fractured upon the application of a high voltage, as was noted in Chapter 2. It would also be of an order of magnitude sufficient to push the glass away from the contact slightly, producing the observed oscillation.

Once the aqueous solution was in the gap electrolysis could occur as was found to be the case in the previous section. This would explain the film-like deposit on the carbon's surface and also the thin film on the glass.

The etching phenomenon occurring when the carbon was at a negative potential is more difficult to explain. Electroosmosis would still occur, only driving the water away from the contact as the polarity is reversed from that of the previous instance. Near the contact surface, however, the water would tend to desorb from the carbon, setting up an opposing force to the electroosmotic force. This would set up high stresses within the carbon and could possibly damage it. Once the water had desorbed into the gap ionic etching and to an extent electrolysis could occur, again etching the carbon surface.

The above discussion about electroosmosis also applies to the results from the ball-on-flat experiments in vacuum, except that when the carbon was at a positive polarity the aqueous solution would not exist as a liquid in the gap but would be pumped away by the vacuum system as a vapour. This vapour would, however, increase the gas pressure in the gap increasing the possibility of discharges occurring. Indeed, more etch pits due to discharges are seen around the carbon positive etch annuli than around the carbon negative annuli as would be expected if electroosmosis were occurring, and the current trace when the carbon was at a positive potential was probably noisy due to these discharges occurring. The shape of the current trace for the reverse polarity and the faint brown film sometimes observed on the ball could have resulted from the stress in the carbon, discussed in connection with the Fizeau results, breaking pieces of carbon from the surface which were then deposited on the ball to form the film which would slightly increase the resistance to current flow and could cause the observed step-functions in the trace.

The experiments done under vacuum conditions like those with the Fizeau interferometer showed the etching to be more severe when the carbon was at a positive potential. Again electroosmosis could be responsible, adding to the damage of the carbon surface caused by the etching process already occurring in the gap.

Electroosmosis could also contribute to the polarity effect on the force measurements, (see Chapter 7), by reducing the field in the gap during the measurement by desorbing more vapour into the gap around the contact when the carbon was at a positive potential. Also the ionisation of the vapour would increase the current enhancing the Joule heating thus reducing the force.

9. 5 CONCLUSION

When the parameters of the interfacial gap between two contacts generating the Johnsen-Rahbek effect do not fulfill the condition for electrical breakdown in the gap, as predicted by Paschen's law, the etching is not so severe but it still exists, enhanced by water in the gap either condensed from the

atmosphere or desorbed from the carbon or both. The etching is most severe at interfacial voltages above 300 volts and when the carbon is at a positive potential. Although the etching in the gap, which seems to be caused by electrolysis or ion bombardment, is little understood and requires more investigation, electroosmosis seems responsible for the etching being more severe when the carbon is at a positive potential.

Previous results, (Chapter 3), have shown that etching can greatly roughen the contacting surfaces and considerably reduce the force generated. The work described in this chapter shows that the etching can be reduced by maintaining the contacts in a vacuum of about 10^{-5} torr and keeping the applied voltage below 400 volts, with the carbon at a negative potential. Higher voltages can cause electrical breakdown of the carbon and should be avoided.

TABLE 9.1

DIMENSIONS OF ETCH ANNULI FORMED ON CARBON IN VACUO WITH 550 VOLTS APPLIED BETWEEN THE BALL AND FLAT FOR ABOUT 3 HOURS.

CARBON SPECIMEN	POLARITY OF POTENTIAL OF CARBON (POS/NEG)	INNER DIAMETER OF ANNULUS (μm)	OUTER DIAMETER OF ANNULUS (μm)	* CALCULATED VALUE OF E_o (10^8 Vm^{-1})
C4	POS	265 ± 5	370 ± 25	8.4 ± 2.7
C4	NEG	270 ± 10	400 ± 20	6.4 ± 1.6
C8	POS	270 ± 5	360 ± 10	9.9 ± 1.7
C8	NEG	260 ± 20	360 ± 20	9.0 ± 3.6
C10	POS	290 ± 5	385 ± 5	8.7 ± 0.9
C10	NEG	290 ± 5	390 ± 10	8.2×1.3
AVERAGE VALUE				8.4

*

THIS ASSUMES THAT THE INNER DIAMETER CORRESPONDS TO 2 d AND THE OUTER DIAMETER TO 2c. USING THESE VALUES IN EQ. (5.1.1) E_o CAN BE CALCULATED.

TABLE 9.2

DEPTHS OF ETCH ANNULI FORMED ON CARBON IN VACUO. MEASURED FROM PROFILOMETER TRACES.

SPECIMEN OF CARBON	POLARITY OF POTENTIAL OF CARBON (POS/NEG)	DEPTH OF ETCH ANNULUS (μm)
C4	POS	0.15 ± 0.05
C4	NEG	0.09 ± 0.01
C10	POS	0.12 ± 0.01
C10	NEG	0.06 ± 0.01
C11	NEG	0.07

TABLE 9.3

TYPICAL DECREASES IN CURRENTDURING THE FORMATION OF ETCH ANNULI, CALCULATED FROM STATIC IV PLOTS TAKEN BEFORE AND AFTER THE ANNULI WERE FORMED. THE ANNULI WERE FORMED ON IN VACUO.

CARBON SPECIMEN	POLARITY OF POTENTIAL OF CARBON (POS/NEG)	CHANGE IN CURRENT AT 200 VOLTS (% OF INITIAL CURRENT BEFORE ANNULUS FORMED)
C4	POS	-29
C4	NEG	-19
C8	POS	-16
C8	NEG	-17
C10	POS	-17
C10	NEG	-37

TABLE 9.4

THE DECREASES IN CURRENT DUE TO SUCCESSIVE EXPERIMENTAL RUNS WITH THE SAME SPECIMEN OF CARBON.

EXPERIMENTAL RUN	INITIAL CURRENT AT 550 V (μA)	FINAL CURRENT AT 550 V (μA)
1	13.8	11.0
2	10.5	8.0
3	7.9	6.45
4	6.5	5.8

TABLE 9.5

A DEMONSTRATION THAT THE CURRENT VARIED ONLY SLIGHTLY BETWEEN A BALL AND CARBON FLAT IN THE ATMOSPHERE WHEN THE CARBON WAS AT A NEGATIVE POTENTIAL WITH RESPECT TO THE BALL.

TIME (MIN.)	CURRENT AT 150 VOLTS (μA)
0	0.97
30	0.95

TABLE 9.6

TYPICAL MEASUREMENTS OF THE CURRENT BETWEEN A BALL AND CARBON FLAT IN THE ATMOSPHERE, SHOWING THE CURRENT TO HAVE RAPIDLY DECREASED. THE CARBON WAS AT A POSITIVE POTENTIAL WITH RESPECT TO THE BALL.

VOLTAGE APPLIED BETWEEN BALL AND FLAT (VOLT)	INITIAL CURRENT (μA)	FINAL CURRENT, AFTER THE VOLTAGE HAD BEEN APPLIED FOR $\frac{1}{2}$ HOUR (μA)
50	0.36	0.28
100	1.13	0.92
150	2.08	1.64
175	2.12	1.61
250	2.5	2.09

TABLE 9.7

THE DIMENSIONS OF ETCH ANNULI FORMED UNDER ATMOSPHERIC CONDITIONS.

VOLTAGE APPLIED BETWEEN BALL AND FLAT (VOLT)	INNER DIAMETER OF ANNULUS (μm)	OUTER DIAMETER OF ANNULUS (μm)	CALCULATED* VALUE OF E_o (10^8 Vm^{-1})	GAP WIDTH BETWEEN OUTER DIAM. AND BALL (Å)
25	60 ± 15	80 ± 10	9.1 ± 11.0	138
50	50 ± 10	125 ± 10	4.23 ± 1.3	590
75	80 ± 5	165 ± 5	3.7 ± 0.4	1020
100	100 ± 5	180 ± 10	4.5 ± 0.9	1100
125	110 ± 10	210 ± 10	4.07 ± 0.8	1575
150	120 ± 10	240 ± 10	3.5 ± 0.6	2120
175	135 ± 5	235 ± 10	4.8 ± 0.1	1820
250	175 ± 10	300 ± 20	4.3 ± 1.1	2900
AVERAGE VALUE			4.8	

* THIS ASSUMES THAT THE INNER DIAMETER CORRESPONDS TO 2**c**. USING THESE VALUES IN EQ. (5.1.1) E_o CAN BE CALCULATED

TABLE 9.8

SURFACE ROUGHNESSES OF THE CARBON AFTER 5 MINUTES IN THE FIZEAU INTERFEROMETER AT VARIOUS VOLTAGES.

VOLTAGE APPLIED (VOLT)	ROUGHNESS OF CARBON AFTER 5 MINUTES AT STATED VOLTAGE.	
	CARBON AT A POSITIVE POTENTIAL (μM C.L.A.)	CARBON AT A NEGATIVE POTENTIAL (μM C.L.A.)
	0.066	0.055
100	0.061	0.053
200	0.061	0.052
300	0.069	0.058
400	0.068	0.050
500	0.11	0.067

PASCHEN'S CURVE

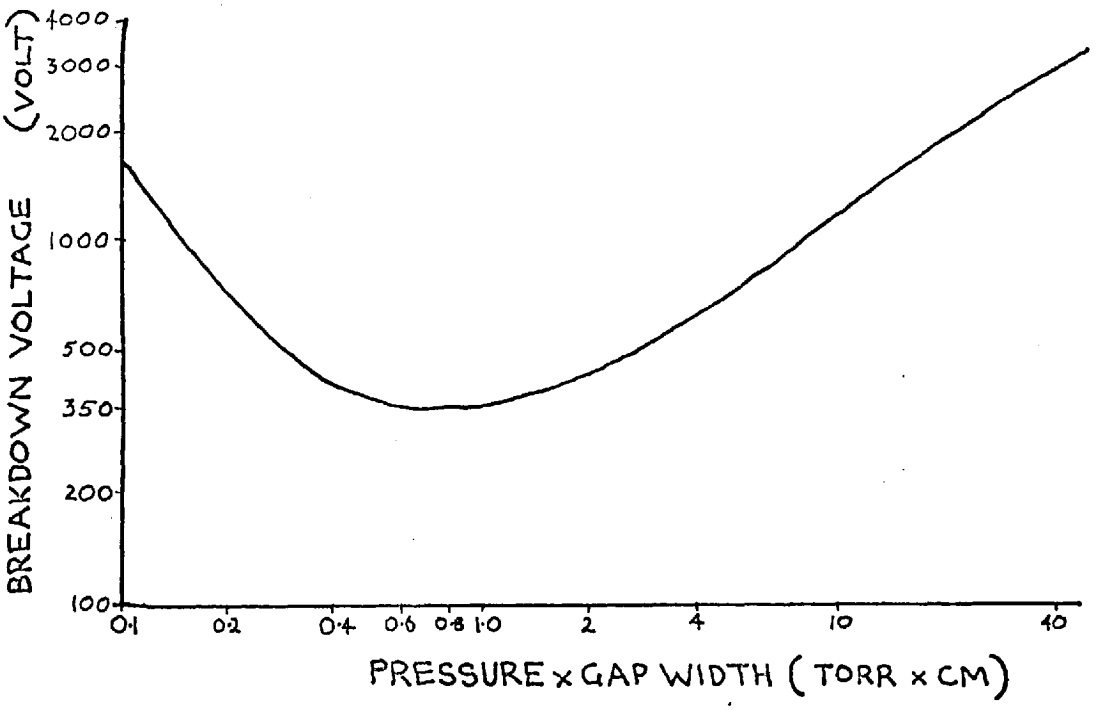

FIG.9.1

THE FAILURE OF PASCHEN'S LAW

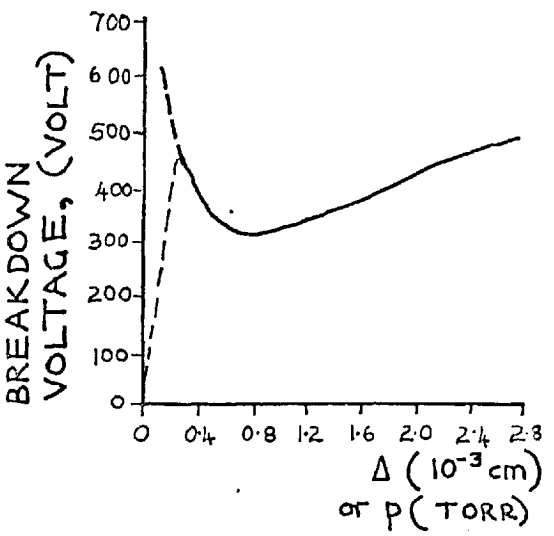

BREAKDOWN VOLTAGE PLOTTED AGAINST DISTANCE AT A CONSTANT PRESSURE OF 1 TORR (– – –) AND AGAINST PRESSURE AT A CONSTANT DISTANCE OF 1 cm (— — —), TO SHOW THE FAILURE OF PASCHEN'S LAW AT SHORT DISTANCES. IN THE SOLID PORTION (——) THE TWO CURVES COINCIDE AND PASCHEN'S LAW IS VALID. (AFTER BOYLE AND KISLIUK)

FIG.9.2

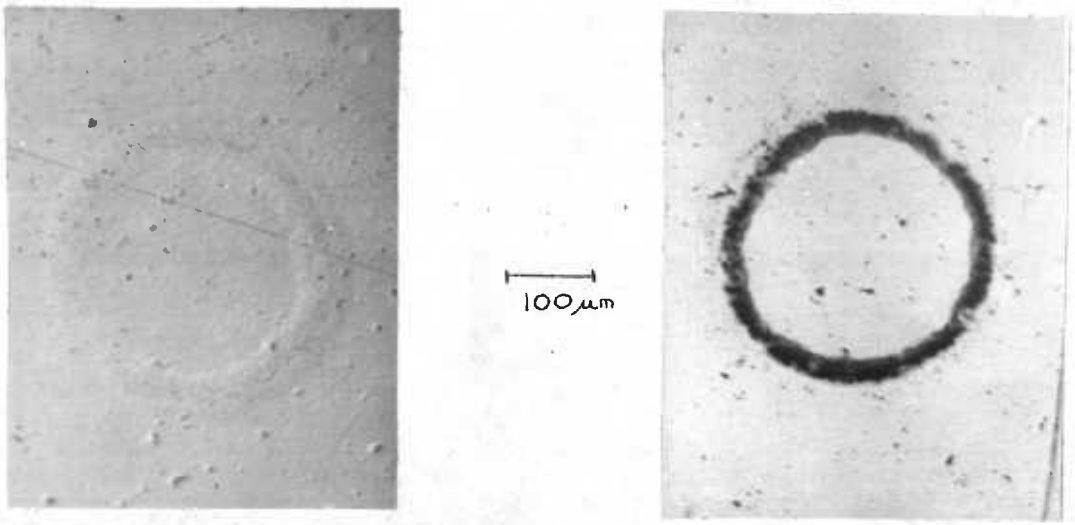

AT A NEGATIVE POTENTIAL

AT A POSITIVE POTENTIAL

MICROGRAPHS OF ETCH ANNULI FORMED ON CARBON IN VACUO. TAKEN IN PHASE CONTRAST.

FIG.9.4

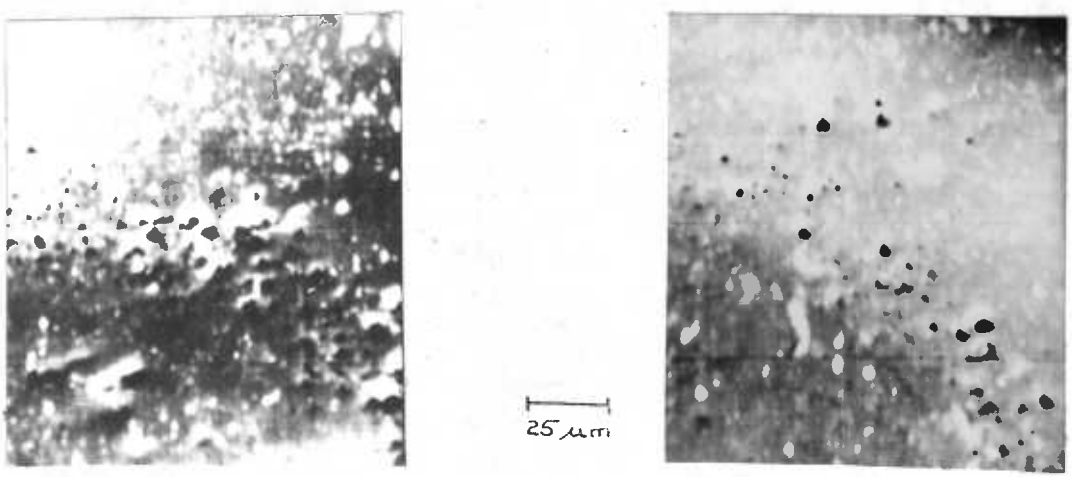

ELECTRON MICROGRAPHS OF ETCH PITS ON CARBON FORMED IN VACUO

FIG.9.6

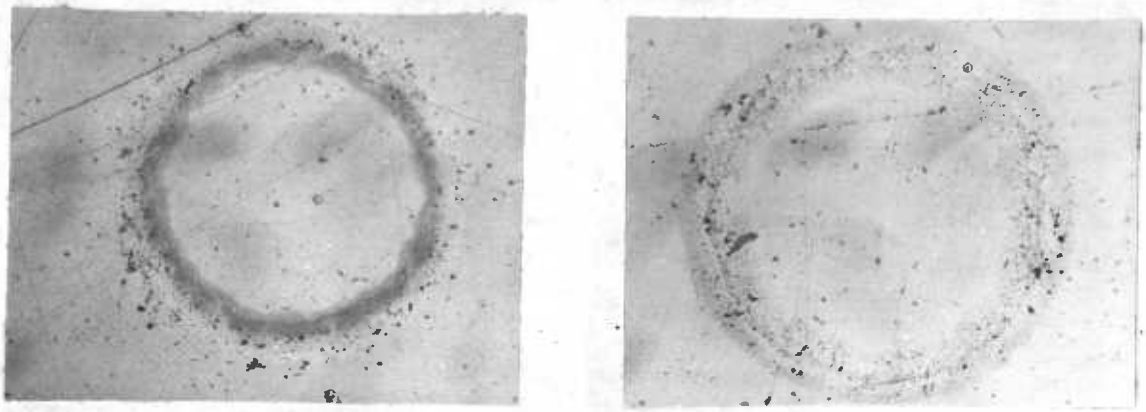

AT A POSITIVE POTENTIAL

AT A NEGATIVE POTENTIAL

TYPICAL CARBON ETCH ANNULI AND THEIR PROFILES

FIG.9.5

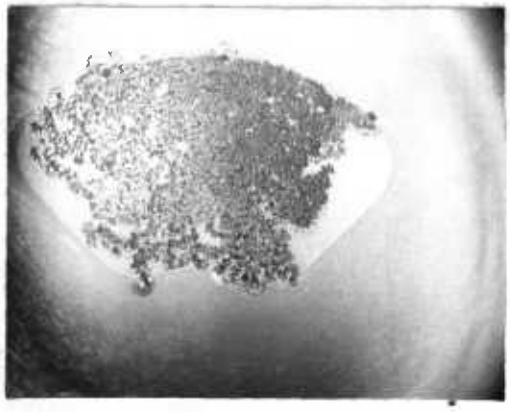

X2 MAGNIFICATION

CARBON SPECIMEN AFTER ELECTRICAL BREAKDOWN

FIG.9.11

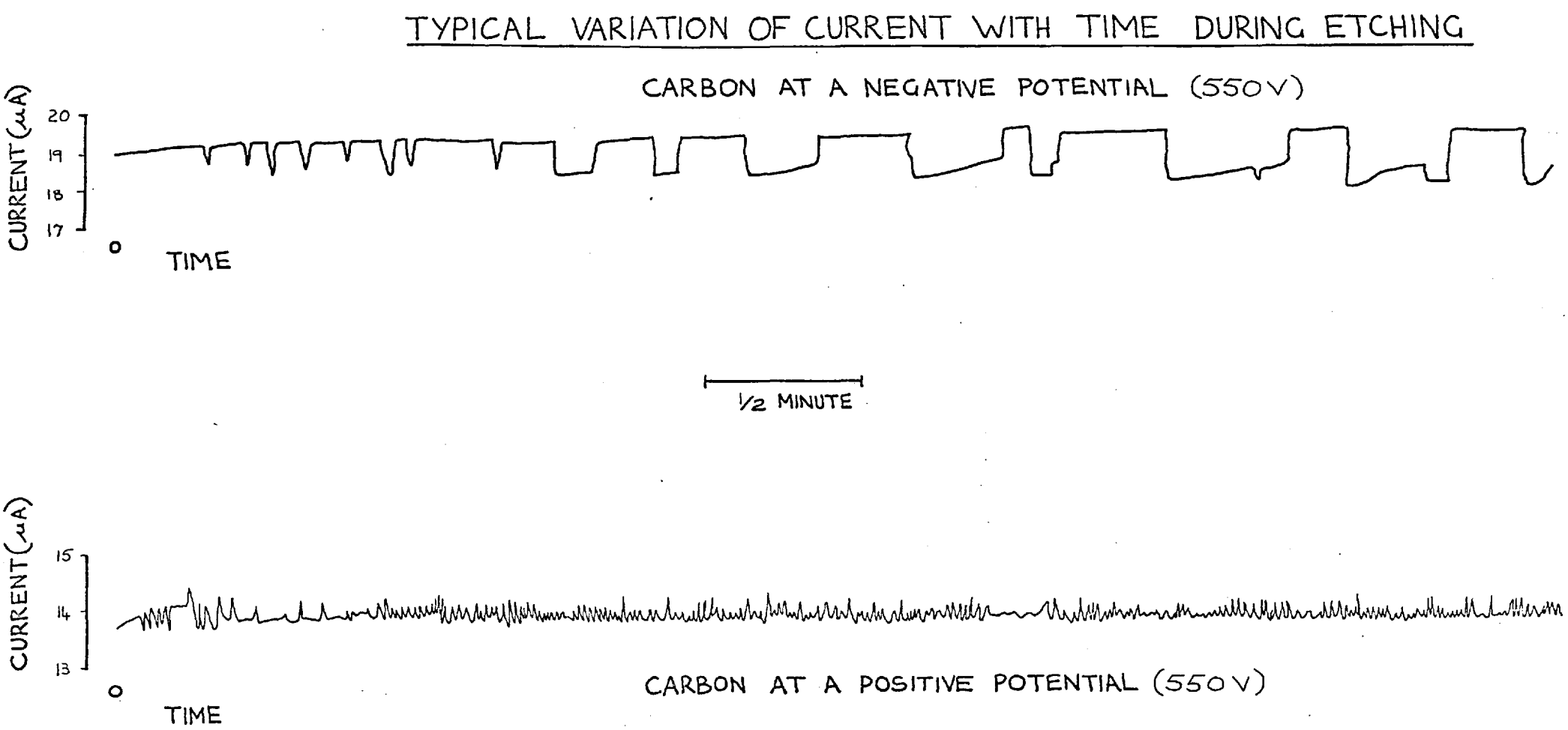
TYPICAL VARIATION OF CURRENT WITH TIME DURING ETCHING
CARBON AT A NEGATIVE POTENTIAL (550V)
CURRENT (μA)
20
19
18
17
0
TIME
1/2 MINUTE
CURRENT (μA)
15
14
13
0
TIME
CARBON AT A POSITIVE POTENTIAL (550V)

FIG.9.7

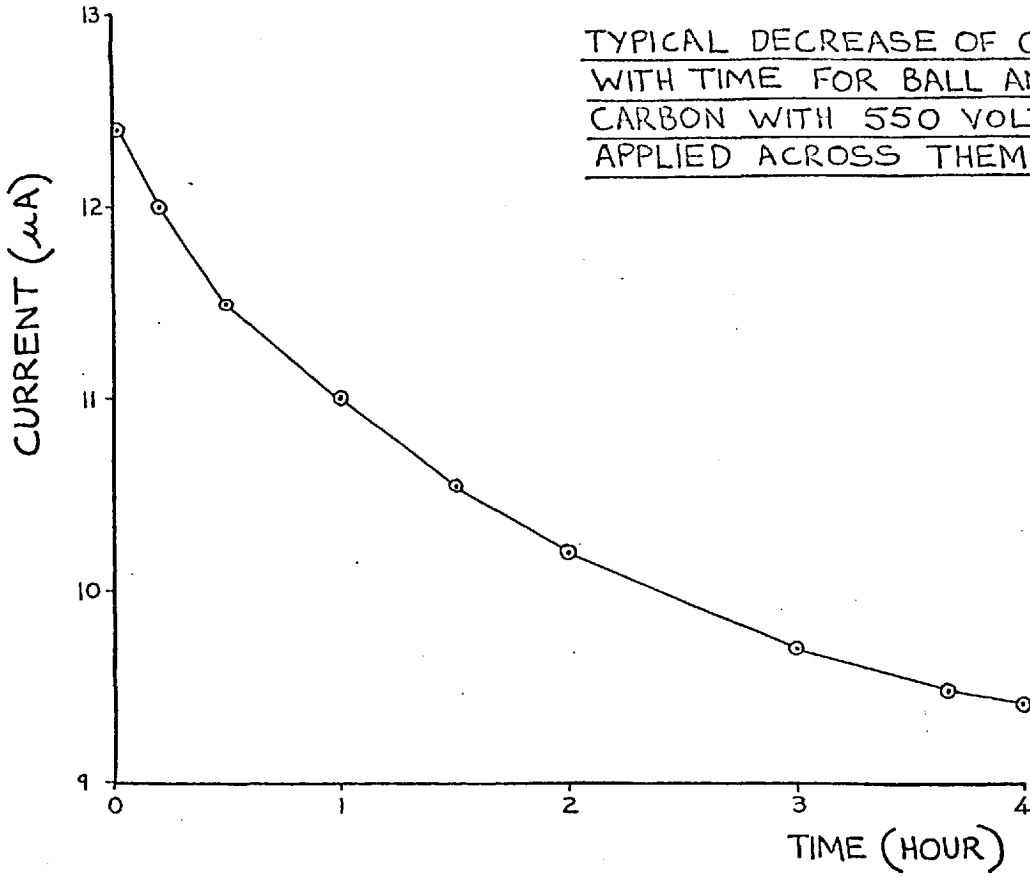

TYPICAL DECREASE OF CURRENT WITH TIME FOR BALL AND CARBON WITH 550 VOLTS APPLIED ACROSS THEM

FIG.9.8

KELVIN'S EQUATION FOR CONDENSATION IN A CAPILLARY: $LN\left(\frac{P}{P_0}\right) = -\frac{2M\gamma}{R\theta\rho' r}\cos\beta$ WHERE ρ' IS THE DENSITY OF THE LIQUID, M THE MOLECULAR WEIGHT OF THE VAPOUR, R THE GAS CONSTANT AND θ THE TEMPERATURE, °K. (SEE TEXT FOR DEFINITION OF P AND P_0).

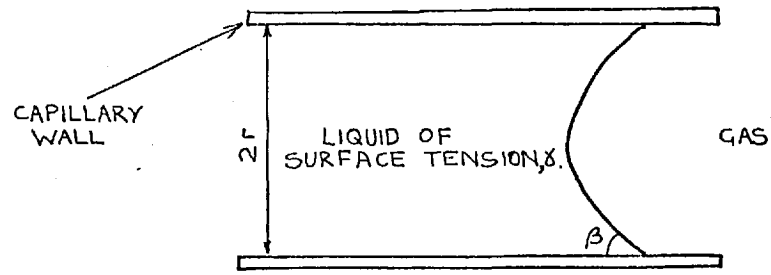

LIQUID IN A CAPILLARY TUBE

FIG.9.10

FIG.9.15

MICROGRAPHS OF FILMS LEFT ON THE CARBON AND THE GLASS AFTER THEY HAD BEEN USED IN THE FIZEAU INTERFEROMETER WITH 500 VOLTS APPLIED

(C.F. CORRESPONDING FRINGE PATTERNS OF FIG. 9·12)

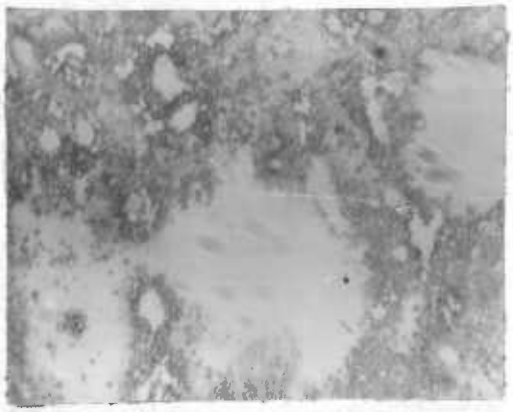

X140 MAGNIFICATION OF TIN OXIDE COATED GLASS. IT HAD BEEN AT A NEGATIVE POTENTIAL.

X2 MAGNIFICATION. AFTER BEING AT A POSITIVE POTENTIAL.

X2 MAGNIFICATION. AFTER BEING AT A NEGATIVE POTENTIAL

CARBON SPECIMENS

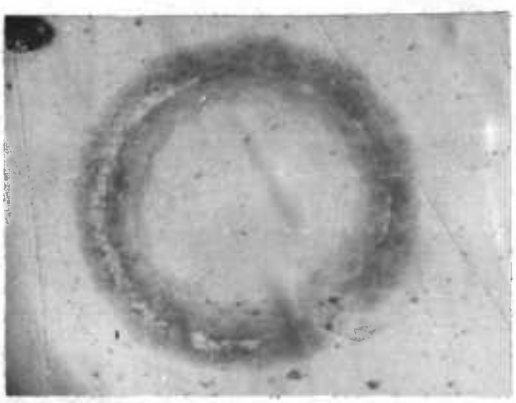

250 VOLTS

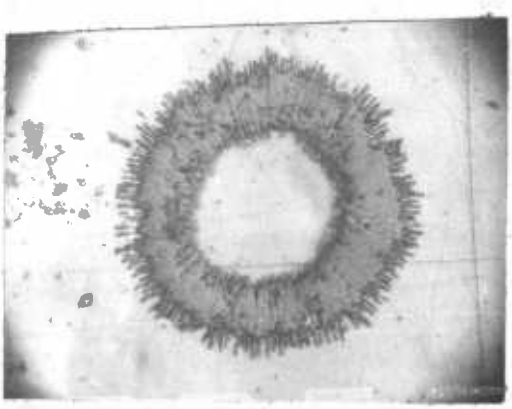

150 VOLTS

FIG.9.9

MICROGRAPHS OF ETCH ANNULI FORMED ON THE CARBON WHEN IT WAS AT A POSITIVE POTENTIAL IN THE ATMOSPHERE

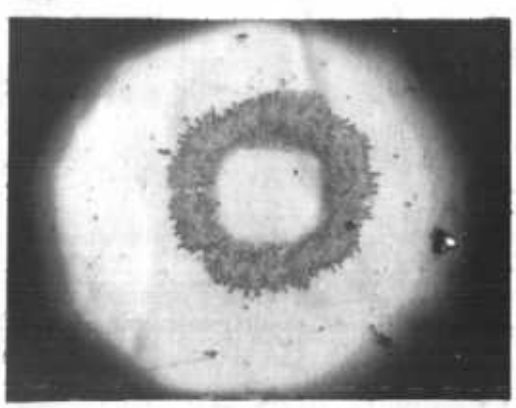

75 VOLTS

100 μm

AFTER ½ MINUTE

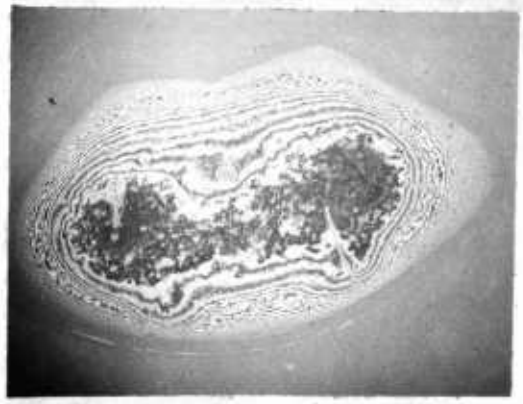

AFTER 2 MINUTES

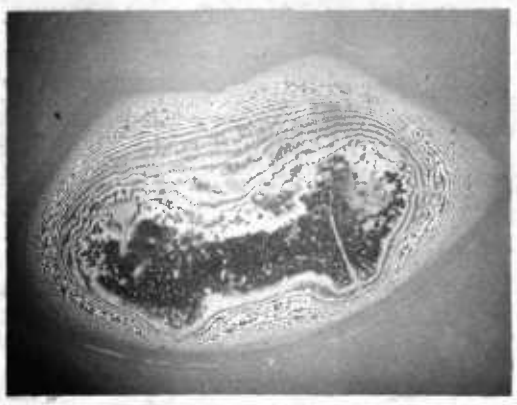

AFTER 5 MINUTES

CONSECUTIVE MICROGRAPHS WITH THE CARBON AT A POSITIVE POTENTIAL OF 500 VOLTS SHOWING THE FORMATION OF LIQUID IN THE GAP.

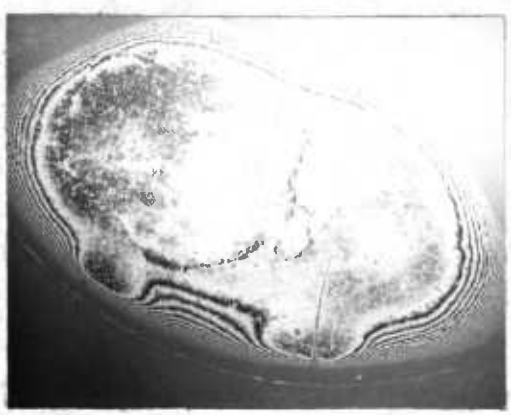

AFTER 5 MINUTES

MICROGRAPH WITH THE CARBON AT A NEGATIVE POTENTIAL OF 500 VOLTS. FOR COMPARISON WITH ABOVE MICROGRAPHS.

MICROGRAPHS OF FRINGE PATTERNS DURING ETCHING EXPERIMENT

FIG.9.12

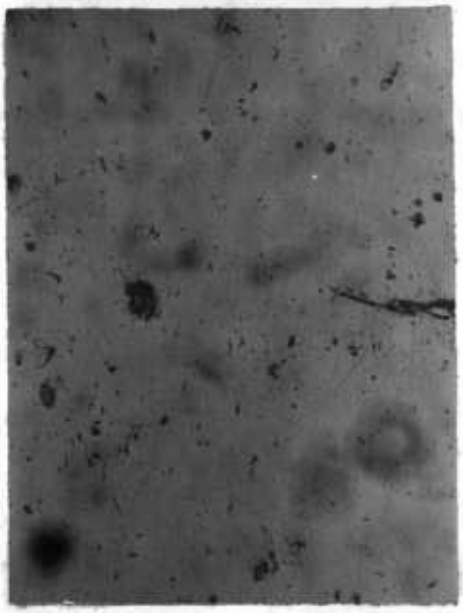

0 VOLTS

100 VOLTS

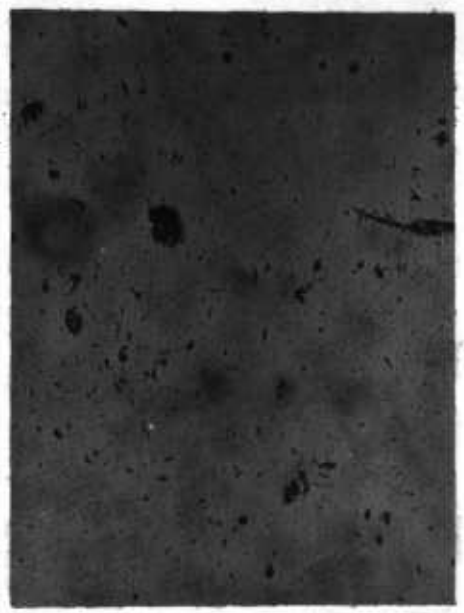

200 VOLTS

300 VOLTS

400 VOLTS

500 VOLTS

x200 MAG. OF CARBON AFTER 5 MINUTES AT NEGATIVE POTENTIAL STATED

FIG.9.13

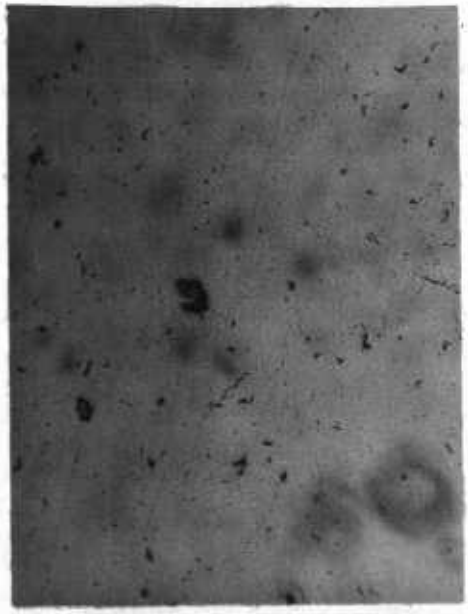

0 VOLTS

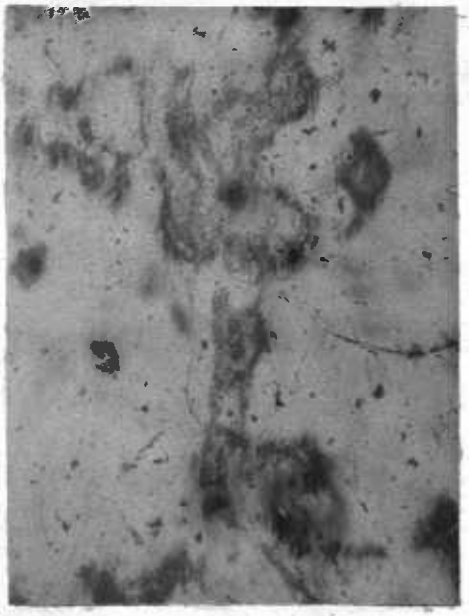

100 VOLTS

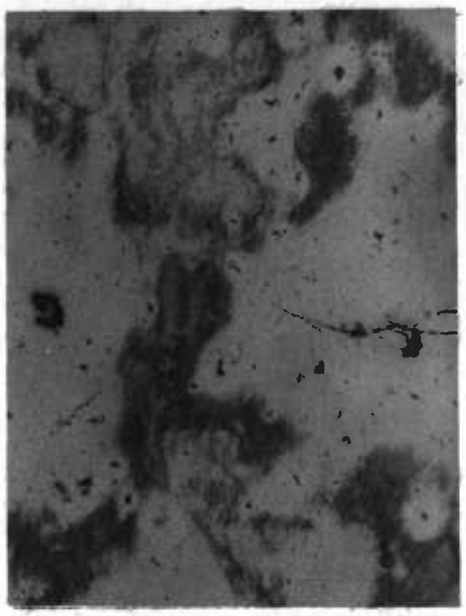

200 VOLTS

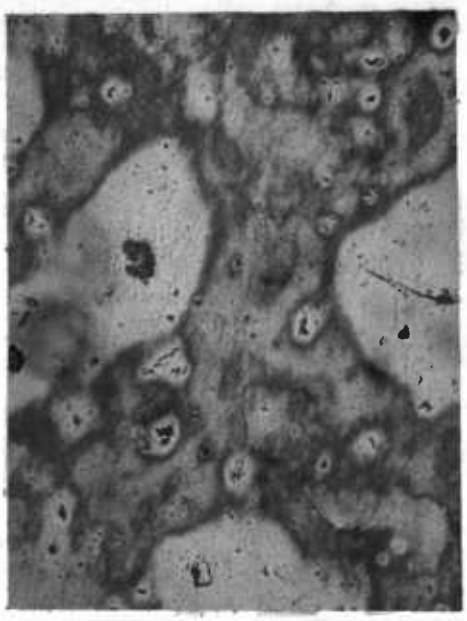

300 VOLTS

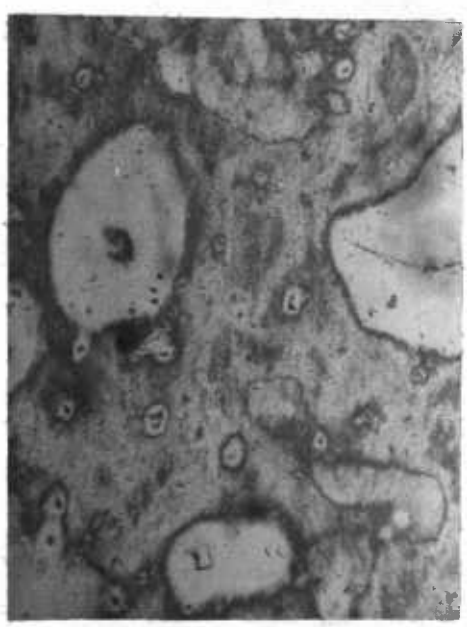

400 VOLTS

500 VOLTS

×200 MAG. OF CARBON AFTER 5 MINUTES AT POSITIVE POTENTIAL STATE

FIG.9.14

CHAPTER X

SUMMARY AND CONCLUSION

The motivation for this work has been the desire to understand better the Johnsen-Rahbek effect in order to be able to produce a reliable working device. Little mention has been made of devices so far as the work has been concerned with investigating the situation of a simple contact in almost ideal conditions. Such a situation is not, however, divorced from that of a practical device and the results can be applied to the practical case.

In this chapter the present work is summarized and the practical implications that it has for a clutch or a similar device are examined. Suggestions are then made for the design of a reliable device. Finally proposals for further work are outlined.

10. 1 SUMMARY OF PREVIOUS WORK

The main points of the present work are listed below.

1. The basic requirement of a material to produce the effect was formulated in terms of ρ k, a suitable material having a large value of this product. A material which satisfies this condition is a high resistivity semiconductor. This means that ρ is very temperature dependent and it was found that this made the force very temperature dependent. A rise in the temperature of the contact spot of a piece of carbon from $20^{\circ}C$ to $80^{\circ}C$ was found to produce a decrease in the force of about 40%.

2. Although the effect is due to simple electrostatic attraction between the contacts previous workers' attempts to accurately measure the force produced different results and different force/voltage relationships, and showed the effect to be far from simple. The complicated nature of the effect was demonstrated by the unreliability of devices which were built.

3. Initial attempts to measure the force in the present work were hampered by the variation of interdependent parameters varying with the applied voltage (e.g. the deformation of the contacts, the interfacial voltage

and current, surface roughness and the resistivity of the carbon).

4. The ball-on-flat method reduced the variation of these parameters by simplifying the contact. It enabled quantitative rather than qualitative analysis of the effect. The force was measured by separating the surfaces rather than shearing them as calculations showed the force to be reduced when there was a large mechanical contact.

5. The measurements made with this method showed the force/voltage relationship to be linear which is not the simple inverse square relationship of electrostatics and is also different from most previous work. Electric fields of up to 8×10^8 Vm^{-1} were calculated to exist near the contact, (c.f. Atkinson's estimate of about 2×10^8 Vm^{-1}), which produced current flow across the interfacial gap.

6. This current emission process is not a Fowler-Nordheim type of field emission, however, as the field was found to be independent of the work function of the pure cathode material. This was probably due to the surface being covered with adsorbed gases and the field and current being more dependent on this film and possibly gases desorbed into the interfacial gap than the work function of the pure cathode material.

7. The force between the ball and flat was found to be very dependent on the roughnesses of the contacting surfaces. Measurements showed that an increase in the surface roughness of the carbon from 0.02 μm C.L.A. to 0.4 μm C.L.A. produced a decrease in the force of about 90%.

8. Most of the investigation of the effect was made with semi-pyrolised cellulose carbon which was found to contain 2% by weight of absorbed water. This water affected the electrical resistivity of the carbon, ρ, increasing it by a factor of 10 when the water was desorbed. An increase in ρ of 200% was found to lower the saturation electric field, E_o, by almost 30%.

9. The desorption of the absorbed water into the interfacial gap was found to be responsible for the severe etching in vacuo at high voltages. Under atmospheric conditions etching also occurred which was enhanced by the presence of atmospheric gas and condensed water vapour in the gap. The etching was found to be most severe when the carbon was at a positive potential due to electroosmosis moving absorbed water towards the negative electrode and hence into the gap. An important factor in the force generated was the etching which occurred as it roughened the contact surfaces, reducing the force.

10. 2 FACTORS AFFECTING A WORKING DEVICE

From the above summary can be drawn important factors concerning the operation of a device using carbon as the semiconductor and possible causes of a device's unreliability can be predicted.

1 SURFACE ROUGHNESS AND FLATNESS

The roughnesses of the contacting surfaces greatly affect the force generated. The wear of the surfaces of a working device would alter the roughnesses of the surfaces and alter the performance of the device. This was the cause of eventual failure of early devices; the wear becoming excessive and roughening the surfaces considerably. This was overcome to a large extent by Dudding and Losty who used semi-pyrolised cellulose carbon in their devices. It appeared that the surfaces initially became polished due to their wearing and then they maintained an equilibrium roughness due to the etching counteracting the polishing. However, for this to happen the condition of the carbon, (as regards absorbed gases), must be kept constant and the environment also kept constant (see Appendix 3) which is not easy to accomplish. Also the carbon coats the counter surface of the device with a thin film of carbon and this increases the roughness of the metal surface reducing the performance initially.

The wear process also alters the flatness of the contacts, especially in a 'carbon' device. This is the same problem as encountered in the polishing of a specimen of carbon, (see Chapter 2), when trying to keep it reasonably flat.

For a spherical surface a change in the curvature of it produces a directly proportional change in the force.

Thus it is clear that a major problem in producing a reliable device is to produce one which maintains a constant interfacial gap geometry.

2 THE TEMPERATURE OF A DEVICE

When a device is slipped, frictional heating occurs which raises the mean temperature of the contacts up to about $80^{o}C$ and that of the individual contacting asperities to a much higher temperature. This would greatly reduce the Johnsen-Rahbek force obtainable and also the frictional force would decrease. At this raised temperature the carbon in a device would desorb water vapour causing :

a) etching in the gap;

b) the electrical resistivity, ρ , to increase;

c) the friction and wear of the carbon to increase, depending on the amount of desorption (see Appendix 3). This would in turn increase the frictional drag and hence further increase the frictional heating, and possibly roughen the surfaces.

All these factors tend to decrease the torque of a device, and the effect of them on the performance of a device can be illustrated by data obtained from operating under atmospheric conditions a 5 cm diameter band clutch, (see fig.10.1), at 350 r.p.m. with 200 volts applied between the band and rotor. (The torque and current were monitored by means of the system shown in fig. 10.1). When the voltage was initially applied the torque drastically increased, fig.10.2, as did the current, due to frictional heating. As thermal equilibrium was reached the torque and current decreased. The decrease in torque was probably due to 'running-in', the surfaces becoming initially smoothed and easier slipping occurring at the elevated temperature. The decrease in current could have been due to desorption of water from the carbon. It should be noticed from fig.10.2 that although the current and torque became almost constant after a few minutes, they slowly decreased with time which can be considered as an indication that the condition of the device was slowly changing.

3 APPLIED VOLTAGE AND SPEED OF ROTATION

These relate to the heating of a device and follow on from (2). An increase in the applied voltages means:

(a) a greaterforce and therefore greater frictional heating;

(b) greater joule heating;

(c) greater desorption of the carbon due to electroosmosis;

(d) an increased rate of etching.

If the carbon were kept at negative potential and only up to 300 volts were applied then (c) and (d) would be reduced and (a) and (b) would be kept to practical limits.

An increase in the speed of rotation would simply increase the frictional heating with the attendant change in performance described earlier. At high speeds, of the order of 1000 r.p.m.*, aerodynamical effects greatly reduce efficiency and only speeds of up to 500 r.p.m.* were found to be practical, (Dudding[P]).

4 ENVIRONMENT

The experimental work done with the ball-on-flat apparatus was performed in vacuo to reduce the possibility of etching. Devices, however, have usually been operated under atmospheric conditions and consequently etching has occurred. As far as a device made with carbon is concerned a satisfactory environment is difficult to determine due to two competing factors:

(a) carbon has a moderately low coefficient of friction and wears well so long as it has absorbed moisture in it, (see Appendix 3);

(b) etching occurs under atmospheric conditions due to absorbed moisture and the gas in the interfacial gap.

These two factors could possibly both be satisfied if a gas other than water vapour could be absorbed into the carbon which retained the good wear properties of the carbon yet did not produce etching when it was desorbed. The device could then operate in a dry and possibly evacuated environment. It is significant

* for rotor 5cm. dia.

that Stuckes found that the etching in her device was reduced when it was operated in a desiccator.

The environment should also be such as not to cause contamination to the device. This is of more concern to the metal, e.g. mild steel, which would rust and tarnish on exposure to a moist atmosphere. Tarnish layers have high resistivities and rusting roughens a surface so that the overall effect would be to reduce the Johnsen-Rahbek force.

Changes in the environment would alter the performance of a clutch and could be responsible for a device being unreliable unless care is taken.

5 MECHANICAL STRENGTH

Semi-pyrolised cellulose carbon is not a very rigid material and deforms to a large extent when a force is generated, (see Chapter 3). This deformation alters the force generated and it would thus produce a complicated if not unpredictable performance. The deformation can be reduced by giving the semiconductor a rigid backing. Dudding and Losty used aluminium backing plates for this purpose in their disc clutches.

The carbon has a hardness of about $10^9 Nm^{-2}$ and a Young's modulus of about $7 \times 10^9 Nm^{-2}$. This means that although plastic deformation is unlikely when the Johnsen-Rahbek effect is generated, the elastic deformation is large. This deformation reduces the force, (see Chapter 5). The problem can only be overcome by using a material with a higher Young's modulus.

6 FRICTION

Most devices utilizing the Johnsen-Rahbek effect use it to increase the frictional force between the contacts. However, the Johnsen-Rahbek force is normal to the contacting surfaces and its effect on the frictional force depends on the coefficient of friction, μ, according to the equation :

$$F = \mu N \qquad (10.2.1)$$

Where N is the normal force, (the Johnsen-Rahbek force plus a small force required to keep the contacts in intimate contact when no voltage is applied),

and F the frictional force. So the performance of most devices depends on the Johnsen-Rahbek force generated and also on μ. The previous five factors mainly relate to the possible variation in the former, so the performance of a device is further complicated by the fact that almost as many factors can cause a variation in μ. They are :

(a) the roughnesses of the contacting surfaces;

(b) the temperature of the device, especially that of the contacting surfaces;

(c) the amount of water absorbed in the carbon.

These factors are dependent on the speed of rotation of the device, the applied voltage and the environment in which the device is situated.

The variation in μ, (which is nominally 0.3), due to these factors could reasonably be expected to be from 0.4 to 0.2. This would require the voltage to be varied from between -25% and +50% to maintain the initial performance. This shows that the variation in the coefficient of friction is crucial to the performance of a device.

The interdependence of the above six factors makes the performance of a device very complex. The possibility of any one of these factors changing and thereby producing possible changes in the other factors would tend to render the device unreliable.

10.3 GUIDELINES FOR A BETTER DEVICE

From the above discussion of actual and possible pitfalls of a carbon device guidelines can be set for producing a better device. The guidelines are divided into three sections; the first two concerned with material requirements and the third with design considerations.

10.3.1 PROPERTIES OF AN IDEAL SEMICONDUCTOR FOR A DEVICE

(1). A semiconductor of high electrical resistivity, ρ, is required to generate the Johnsen-Rahbek effect as it has a high value of ρk. An ideal

semiconductor would have both a high value of ρ and of k. A high value of ρ would mean small currents would flow reducing the Joule heating, and a high value of k would mean any heat within the semiconductor would quickly be conducted away. The value of ρ cannot be too high, however, otherwise the electrical time constant would increase and the on/off switching time of the device would become very long, see Appendix 4.

The resistivity should also be independent of any absorbed gases in the material, but preferably the material should not be absorbant. Most materials used up to now, however, have been absorbant.

(2) The semiconductor should have a good wear characteristic and a moderately low coefficient of friction, μ. These properties are related to an extent, but they will be discussed separately.

The former requirement can be obtained with a self-lubricating material. Most of these materials rely on their structure and on the generation or presence of adsorbed and absorbed gas for their good wear characteristics, see Appendix 3. However, an ideal material for the present purposes is one which if it does desorb gas does not alter its electrical resistivity in the process. Moreover, the desorbed gas must not assist the etching process.

The requirement of a material of moderately low coefficient of friction is not dogmatic as each device and the performance required from it merits consideration of the most appropriate coefficient. However, two factors must be considered. They are :

(a) the higher μ is the greater the frictional force produced from a given Johnsen-Rahbek force;

(b) the higher μ is the larger the frictional heating of the device is. Also the wear rate tends to be large with high values of μ.

(3) The semiconductor should be mechanically hard and rigid so that the contact does not deform to a large extent, decreasing the force produced. A hard semiconductor would also resist mechanical damage which could roughen

its surface and thus reduce the force.

(4) The semiconductor should also resist etching. This would enable the device to be used in atmospheric conditions or in any other environment.

10.3.2 PROPERTIES OF AN IDEAL METAL FOR A DEVICE

(1) It should be a metal which does not tarnish or rust easily, so that the device can be operated under atmospheric, moist conditions without any special precautions being necessary.

(2) The metal need not have a high work function, (as also applies to the semiconductor), as the force developed is not dependent on it.

(3) It should be a metal which is not easily etched, such as stainless steel, (see Chapter 9). The reason for this is that it would enable the device to operate under atmospheric conditions, or in any similar environment.

10.3.3 THE DESIGN AND CONSTRUCTION OF A DEVICE

The device must be constructed with the aim of keeping the geometry of the interfacial gap as constant as possible and the gap width as small as possible, so that it gives a reproducible and large force. This is easily achieved with a band clutch, but intimate contact between the contacts of a disc clutch requires the 'semiconductor plate' to be made of spring loaded segments, as in Dudding and Losty's device.

Also in the design of a device the size of the semiconductor is important for five reasons :

(1) if it is too thin it easily deforms, (mounting on a base plate is required if it is a mechanically weak material);

(2) also if it is too thin, (e.g. less than 1 μm), there is the possibility of it breaking down electrically due to the high electric field across it ;

(3) if it is too thick it does not conduct heat away from the contact quickly ;

(4) if the contact area is large in relation to the semiconductor surface area, then the density of electrical power dissipated in the semiconductor becomes high and it is heated ;

(5) if the ratio of its thickness to its surface area is high then its bulk resistance, is high, (see eq. (3.2.1)), and a significant proportion of the applied voltage could be dropped across the bulk as opposed to interfacal gap.

The environment of the device is also important in relation to the etching of the contacting surfaces. This must be considered with regard to the materials used and their tendency to etching.

The speed of operation of the device must be carefully considered so that frictional heating and possibly aerodynamic effects are not excessive. Also too high a voltage must not be used so that Joule heating is not great.

It must be remembered that the device needs to be 'run-in' for a few minutes after starting to acheive a stable temperature and to reach an equilibrium interfacial surface topography. A running-in time is also required when a large voltage is suddenly applied to the device although the time is shorter than the initial running-in period. So a device is best used for operations where it is kept 'warmed-up' .

10.4 POSSIBLY SUITABLE MATERIALS FOR A DEVICE

The present investigation has been made with specimens of carbon and conducting glass. The former was used as it was the most suitable device material used to date, and the latter was used for comparative measurements although it would be unsuitable for use in a device due to its poor wear and friction properties.

The carbon is a suitable device material because it is self-lubricating and produces little wear when run against mild steel. It also has a moderately low coefficient of friction. (The mechanism of the friction and wear of self-lubricating materials is discussed in Appendix 3).

Other self-lubricating materials are materials with a lamella structure such as molybdenum disulphide, boron nitride and heavy metal sulphides, tellurides and selenides, (Magie; McTaggart and Moore). Few of them, however, have a suitable value of electrical resistivity. Molybdenum disulphide has rather a low resistivity for our purposes of 10 Ωm. However, boron nitride has a resistivity of about 10^4 Ωm, hafnium disulphide, 10^5 Ωm; thorium diselenide 10^3 Ωm. Although the latter three are uncommon materials, it could be possible to form them into a mixture with a resin or another material, as is done with nylon, (Materials and Methods), and P.T.F.E. Nylon and P.T.F.E. themselves might be useful device materials but they are very bad heat conductors, have low melting points and are not very rigid in themselves.

However, solid lubricants are in the development stage at present and undoubtedly new and cheaper materials will become available. Surface coatings of materials produced by sputtering and plasma spraying offer hope of new composite materials for devices.

10.5 FUTURE WORK

The present work has left a lot of questions unanswered such as what the exact mechanism of the etching is, and the nature of the current flow in the gap , and also the electrical behaviour of the carbon and glass are not fully understood. Further research could be profitable in these areas.

Little work was done on actual devices in this project and a thorough investigation of them, (an examination of the Johnsen-Rahbek under dynamic, practical conditions), would produce valuable information. Also an investigation into new clutch materials is needed.

However, as can be deduced from sections 10.2 and 10.3 the production of a reliable disc or band clutch is fraught with complex problems. Perhaps the effect could be better employed in a different device such as a small electrostatic speaker, as shown in fig.10.3. This, however, would have to compete with the already successful electrostatic speaker employing an electret. The effect

could find use in clamping one body to another, such as a piece of material to be clamped in a certain position for machining. At present this is sometimes done by electrostatic attraction through a thin dielectric which means that voltages of a few kilovolts are required. Perhaps, also, the effect could be employed in making glass to metal seals, the glass becoming semiconducting when its temperature is raised.

Electrostatics is an undeveloped field as far as man's employment of it is concerned and only a few successful devices utilize it, (Moore). It is hoped that the present work has furthered its cause slightly, and will perhaps encourage future work along the lines discussed above.

BAND CLUTCH AND EXPERIMENTAL SET UP

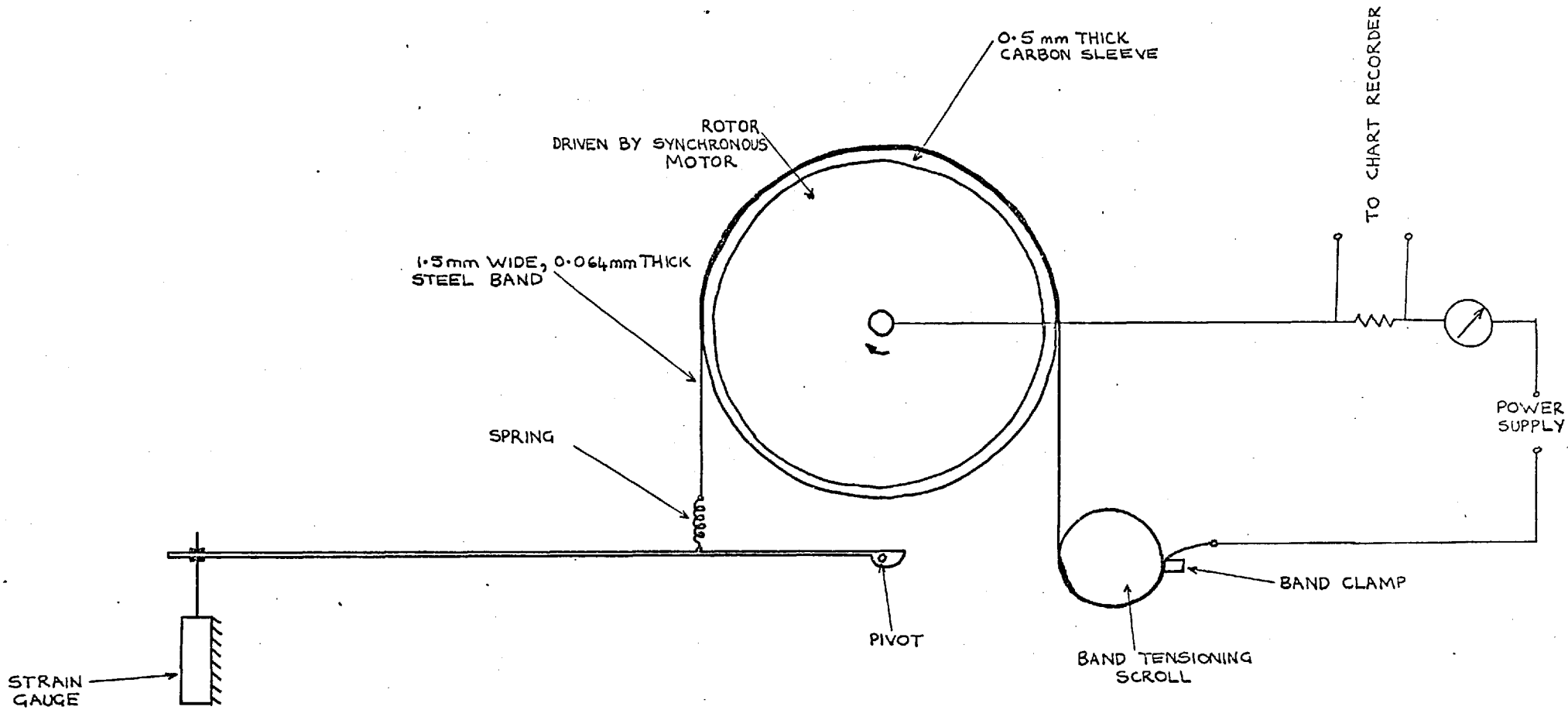

FIG.10.1

THE TORQUE AND CURRENT FLOW OF A BAND CLUTCH WHEN 200 VOLTS WAS APPLIED TO IT

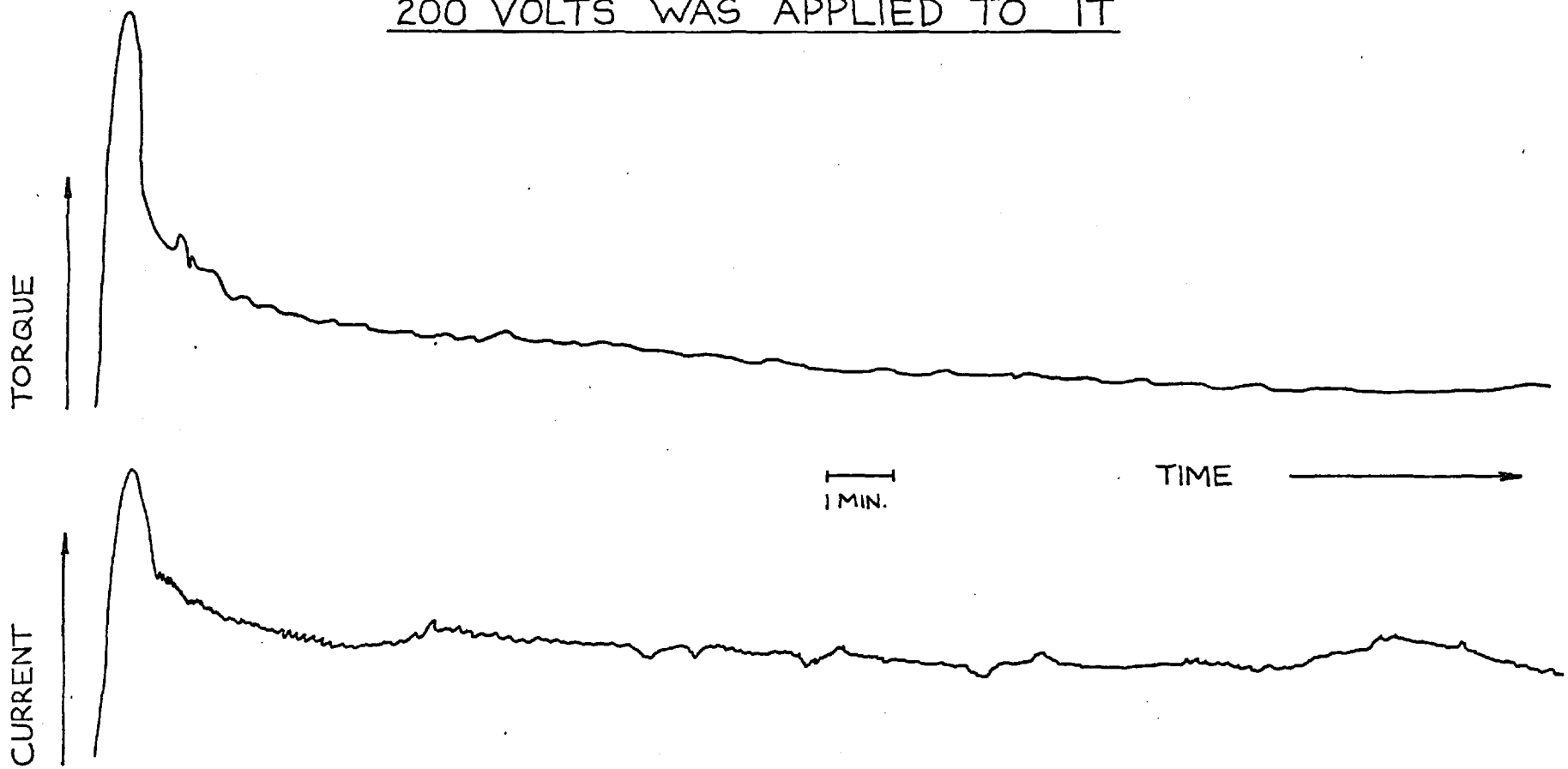

FIG.10.2

THE PRINCIPLE OF AN ELECTROSTATIC SPEAKER UTILIZING THE JOHNSEN-RAHBEK EFFECT

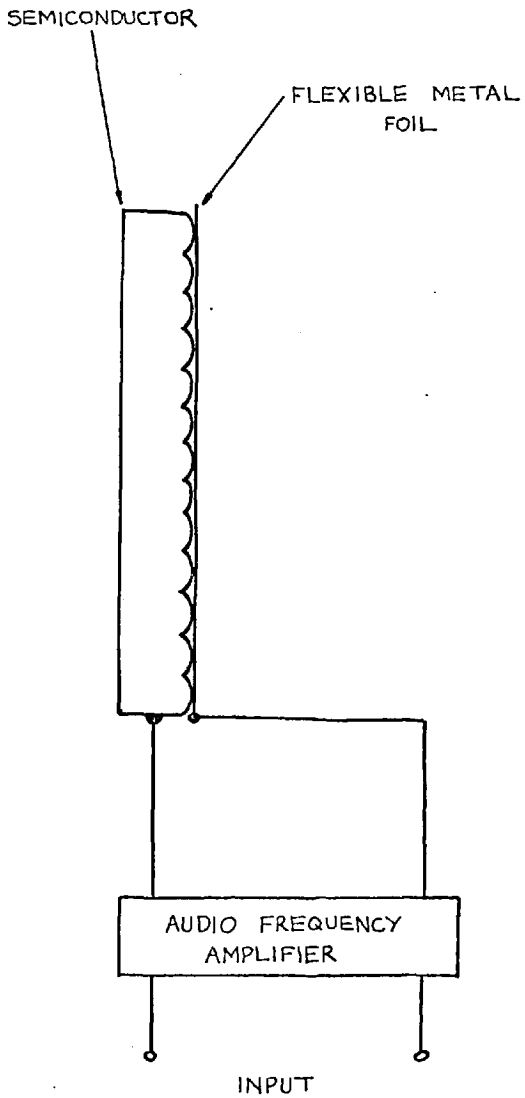

FIG.10.3

APPENDIX 1

CIRCUIT MODEL

In the calculation of the force between a ball and flat, (Chapter 4), a small annular section of the interfacial gap, radius r and width δr , (fig.A1.1), was considered and the total force calculated by integrating over all such sections. The assumption that a constant saturation electric field, E_o, existed in the gap close to the mechanical contact region over which current flowed was made to simplify the integral of the force and to derive an analytical solution.

In this appendix the contact behaviour is investigated by considering this elementary section and its electrical behaviour without this assumption to examine the parameters which determine E_o. Certain other assumptions, however, have to be made in this model as the situation is complex.

Let the equipotential surfaces be concentric hemispheres around the contact as shown in fig. A1.1 Consider the current flow through the hemisphere of radius $r + \delta r$. The current carriers can travel by path 1 to the mechanical contact through a resistance of:

$$\frac{\rho}{2\pi \left(\frac{1}{d} - \frac{1}{r} \right)^{-1}} \qquad \text{(A1.1)}$$

by path 2, across the gap of width, Δ , or by a path between the two. The equivalent circuit for the first two paths is shown in fig. A1.2 This ignores the intermediate paths which can be taken into account by adding more components, but for simplicity this circuit will be considered. It is similar to Stuckes' equivalent circuit for the effect, but in the present case R_B and R_C are both part of the constriction resistance. R_B is not the bulk resistance of the specimen as in Stuckes' model,as the specimens used in the present work have bulk resistances which are negligible compared to the constriction resistance.

The equations for the circuit shown in fig. A1.2 are :

$$I_T = I_1 + I_2 \qquad \text{(A1.2)}$$

$$I_1 = 2\pi r\, \delta r\, A \exp\left(-\frac{B}{E} \right) \qquad \text{(A1.3)}$$

$$V_o = I_T R_B + I_2 R_C \qquad \text{(A1.4)}$$

$$E = \frac{I_2 R_C}{\Delta} \qquad \text{(A1.5)}$$

Eq. (A1.3) is an approximate form of the Fowler-Nordheim equation, where A varies slowly with E, the field in the gap and has a value in the region of 10^{10} to 10^{13} A m^{-2} and B which is initially taken as a constant has a value of about 10^{10} to 10^{11} Vm^{-1} (Sillars). To obtain experimentally realistic values of I_T, V and E, A was taken as 10^{12} A m^{-2} and B as 1.2×10^{10} V m^{-1}. Values of ρ of 10^5 Ω m, d of 50 μm, and of δr of 1 μm were used. The equations can be solved for I_1, I_2 and E by iteration for various values of V and r. This is a crude model and is simply used to quantitively assess the variation in the effect with the circuit parameters.

A1.1 THE SATURATION ELECTRIC FIELD

For a variety of values of r, the field in the gap, E, is found to be constant to less than 10%, table A1.1, over a range of 500 volts. Thus the assumption that the field over the current emitting region is constant at E_o is reasonably valid.

The value of r is taken as 60 μm and δr as 1 μm representative annular section in the following calculations.

A1.2 THE VARIATION OF RESISTIVITY

In Chapter 1 it was shown that materials with high values of ρ k were

potentially good for use in devices because they maintained low contact temperatures. With the simple circuit model the effect on E_o and the current of different values of ρ can be assessed. Fig. A1.3 shows E_o to vary slowly with ρ whilst I_1 and I_2 vary almost linearly with it, fig A1.4. This means that a resistivity of $10^2\ \Omega$m although increasing E_o by about a factor of 2 would increase the current I by a factor of 10^4 from those values obtained with ρ of $10^6\ \Omega$m. This increase would greatly increase the contact temperature.

A1.3 THE VARIATION OF WORK FUNCTION

Initially B was regarded as a constant. If, however, the work function of the cathode, ϕ, changes then B changes as

$$B \propto \phi^{3/2} \qquad \text{(A1.6)}$$

If for example ϕ increases from 4eV to 5eV then B goes from 1.2×10^{10} to 1.7×10^{10} Vm^{-1}. The resultant increase in E_o is shown in table A1.2, which also shows that the total current, I_T, does not alter significantly.

A1.4 THE EFFECT OF CONTAMINATION

The previous results show that I_T is not greatly affected by the work function of the cathode. This is because the current is dominated by the resistance of the circuit, in this case R_B. Consideration of gaps further from the contact shows that R_B decreases and hence the limitation of the current becomes less, but as the gap has widened the current has decreased. If gas is introduced into this gap and ionisation takes place then the gap becomes more conducting tending to short-circuit the contact and smaller gaps, reducing the force. This gas could be generated by surface contamination of the electrodes or absorbed gas from the carbon if it is the semiconductor used.

A1.5 THE EFFECT OF HEATING THE CONTACT

If the contact is heated, (but not the bulk of the semiconductor), then R_c decreases and so to a lesser extent does R_B. Considering R_c only to change, table A1.3 shows how E_o decreases and I increases for circuit values determined from r = 60 m, $\delta r = 1\ \mu$m and d = 50 μm.

TABLE A1.1

THE VARIATION IN THE SATURATION ELECTRIC FIELD, E_o, FOR VARIOUS DISTANCES FROM THE CONTACT CENTRE, r , (DEFINED IN FIG. A.1.1)

APPLIED VOLTAGE, V_o (VOLTS)	SATURATION ELECTRIC FIELD, E_o, (10^8 Vm^{-1})		
	r = 51 μm	r = 60 μm	r = 100 μm
100	5.47	5.38	5.16
200	5.77	5.7	5.40
300	5.92	5.90	5.74
400	6.02	6.00	5.89
500	6.10	6.09	6.00

TABLE A1. 2

THE VARIATION IN THE SATURATION ELECTRIC FIELD AND CURRENT WITH THE WORK FUNCTION OF THE CATHODE

APPLIED VOLTAGE (VOLT)	SATURATION ELECTRIC FIELD E_o $(10^8\ Vm^{-1})$		I_1 $(10^{-7}A)$		I_2 $(10^{-7}A)$		I_T $(10^{-7}A)$	
	WORK FUNCTION 5. 0 eV	WORK FUNCTION 4. 0 eV	5. 0 eV	4. 0 eV	5. 0 eV	4. 0eV	5. 0eV	4. 0eV
100	7.2	5.4	0.20	0.76	1.9	1.4	2.1	2.2
200	8.0	5.7	2.4	3.1	2.1	1.5	4.5	4.6
300	8.3	5.9	4.7	5.5	2.2	1.5	6.9	7.0
400	8.5	6.0	7.1	7.9	2.2	1.6	9.3	9.5
500	8.6	6.1	9.5	10.3	2.2	1.6	11.7	11.9

TABLE A1.3

THE VARIATION IN THE SATURATION ELECTRIC FIELD AND CURRENT AS R_C HEATS UP AND R_B REMAINS CONSTANT AT A TEMPERATURE OF $20^{o}C$

APPLIED VOLTAGE (VOLT)	SATURATION ELECTRIC FIELD E_o ($10^{8} Vm^{-1}$)			TOTAL CURRENT I_T (10^{-7} A)		
	TEMPERATURE OF R_c			TEMPERATURE OF R_c		
	20^{o} C	29^{o}C	38^{o}C	20^{o}	29^{o}C	38^{o}C
100	5.4	5.1	5.1	2.2	2.2	2.3
200	5.7	5.7	5.6	4.5	4.6	4.6
300	5.9	5.9	5.8	7.0	7.0	7.1
400	6.0	5.9	5.9	9.4	9.4	9.5
500	6.1	6.1	6.0	11.8	11.9	11.8

HYPOTHETICAL CURRENT FLOW BETWEEN THE BALL AND FLAT

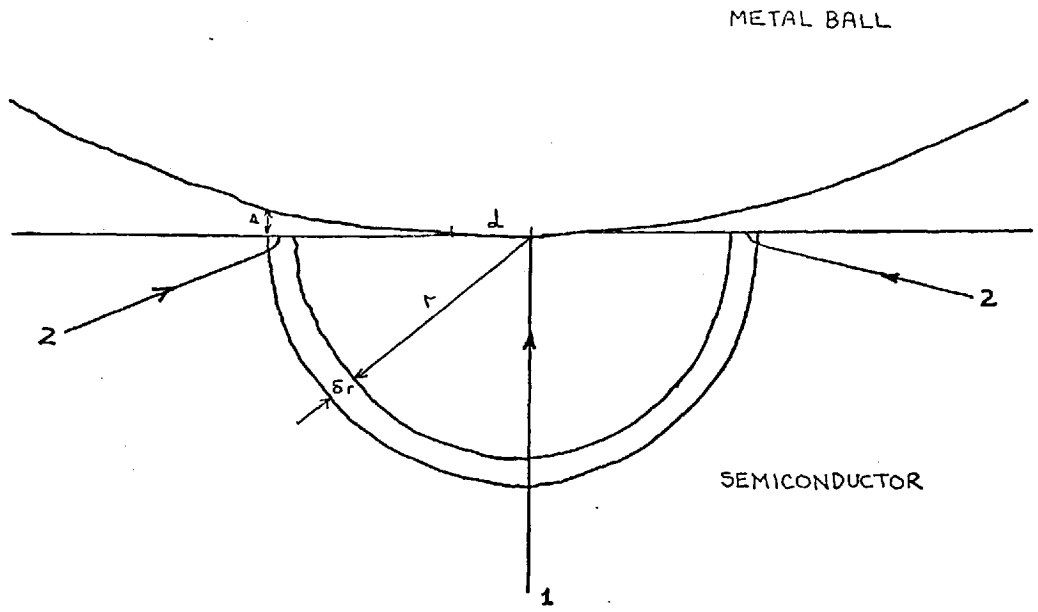

FIG.A.1.1

THE EQUIVALENT CIRCUIT FOR THE ABOVE CURRENT FLOW

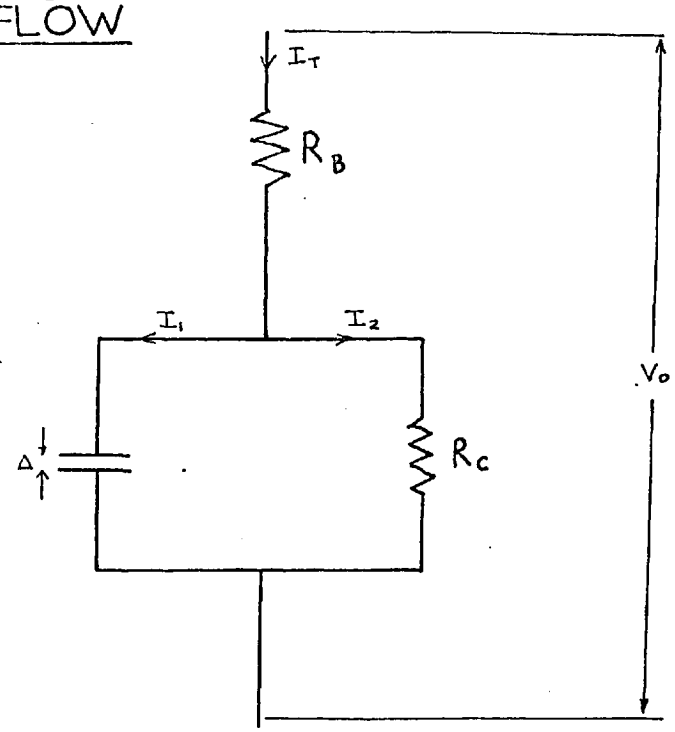

FIG.A.1.2

THE VARIATION OF E_o WITH ρ AS DERIVED FROM THE EQUIVALENT CIRCUIT WITH 200 VOLTS APPLIED

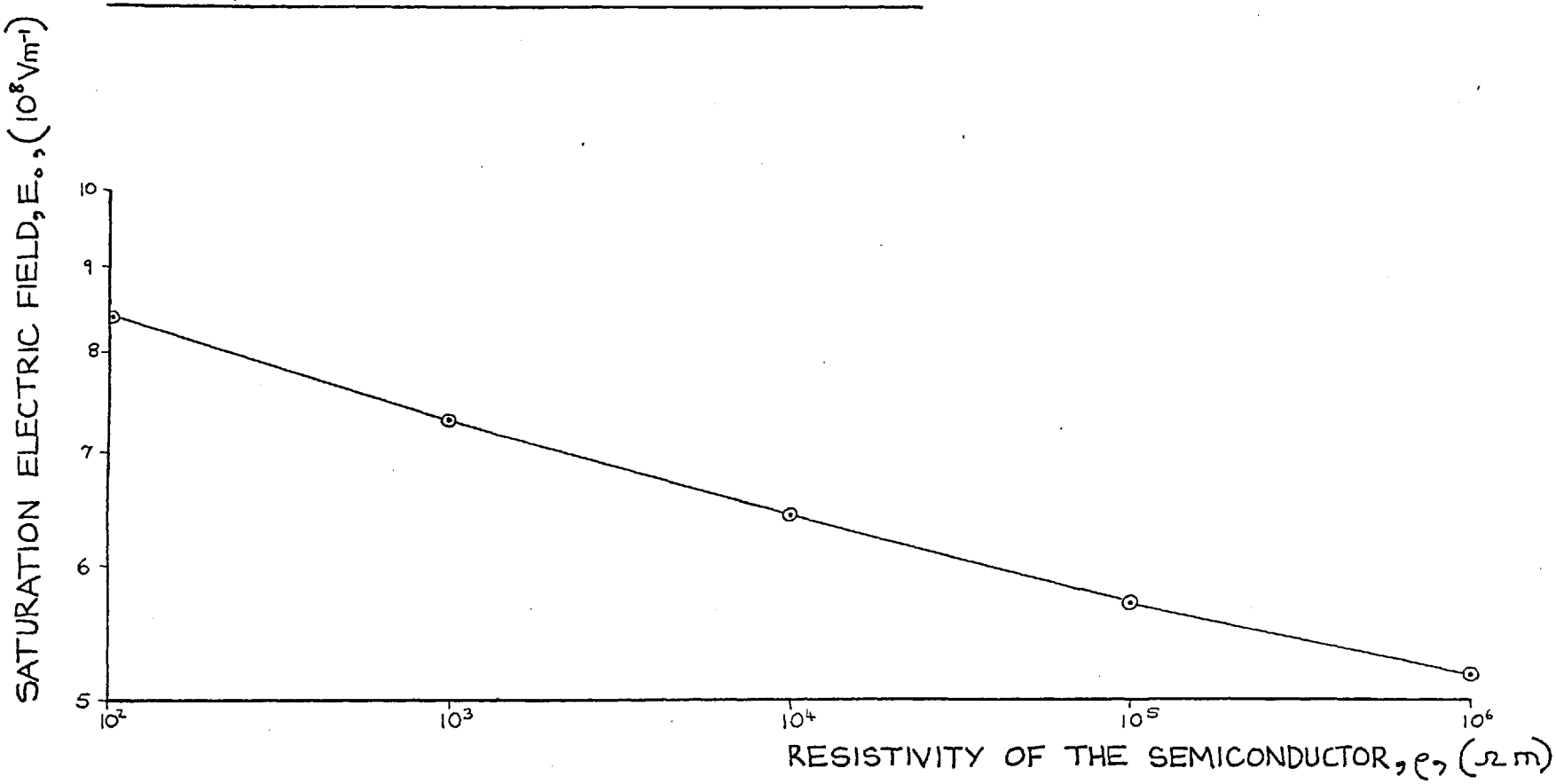

FIG.A.1.3

THE VARIATION OF CURRENT THROUGH THE EQUIVALENT CIRCUIT WITH ρ WITH 200 VOLTS APPLIED

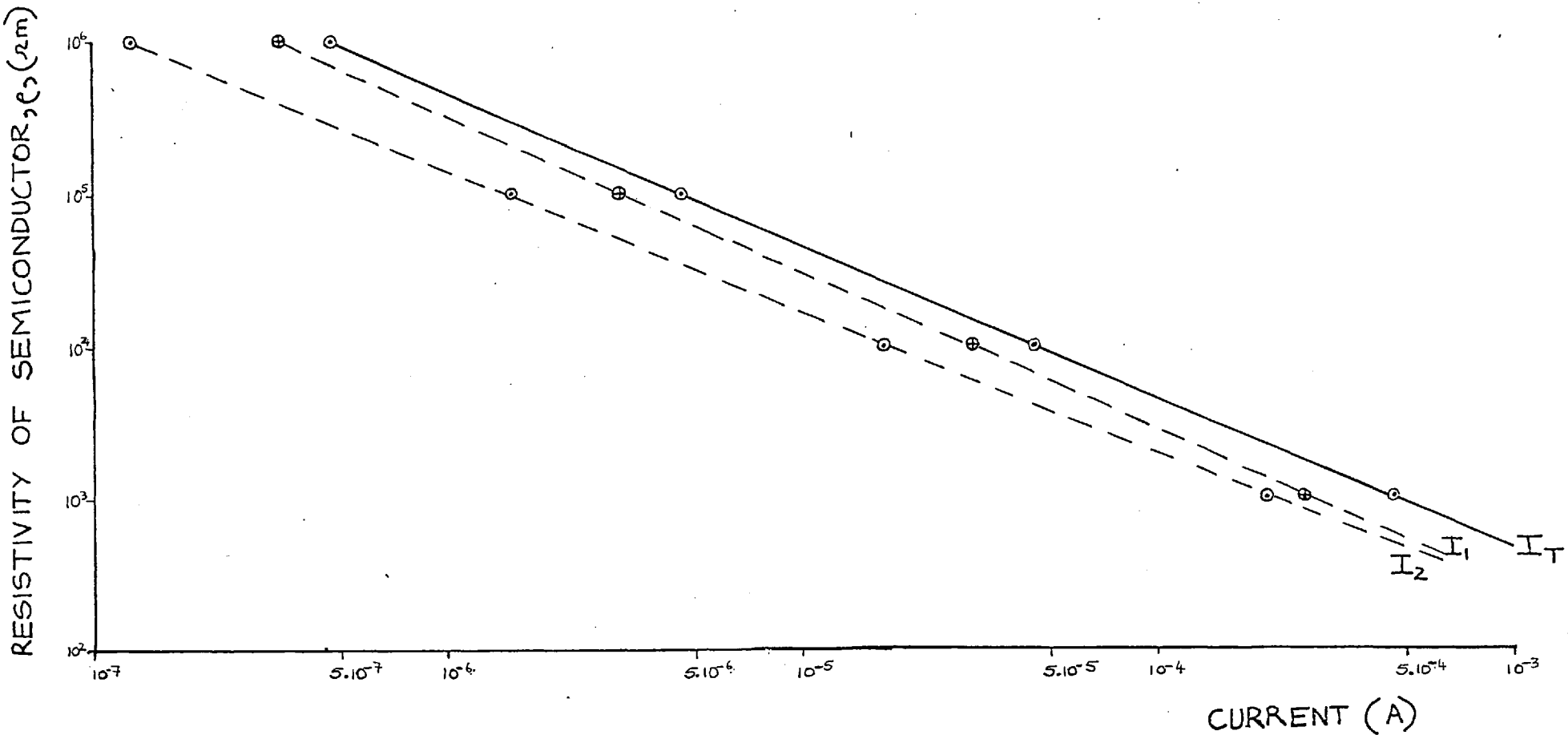

FIG.A.14

APPENDIX 2

SURFACE ROUGHNESS

The most common instrument for measuring surface roughness is the stylus profilometer which produces a magnified trace of the surface from an electric signal generated by a fine stylus moving across the surface. This signal can be integrated to give a centre line average, C. L. A., which is a measure of the surface roughness, (B. S. 1134: 1950). With reference to fig. A2.1, the centre line is positioned at $x = 0$ if

$$\int_0^L f(l)\, dl = 0 \qquad \text{(A2.1)}$$

For this case the C. L. A. is defined as

$$\text{C. L. A.} = \frac{\int_0^L f(l)\, dl}{L} \qquad \text{(A2.2)}$$

If the surface heights form a normal or Gaussian distribution then it is described by the density function, given by ;

$$f(x) = \frac{1}{\sqrt{2\pi}\,\sigma} \exp\left[-\frac{1}{2\sigma^2}(x-\mu)^2\right] \qquad \text{(A2.3)}$$

where $f(x).\Delta x$ is the probability of a value of x being between x and $x + \Delta x$ where Δx is small, μ the mean and σ the standard deviation, (Fraser). The probability of a value of x being less than or equal to x is given by the distribution function;

$$F(x) = \frac{1}{\sqrt{2\pi}\,\sigma}\int_{-\infty}^{x} \exp\left[-\frac{(x-\mu)^2}{2\sigma^2}\right] dx \qquad \text{(A2.4)}$$

By numerical analysis the C. L. A. value is found to equal 1.2σ .

Eq. (A2.3) and eq. (A2.4) can be simplified by putting

$$z = \frac{x-\mu}{\sigma} \qquad \text{(A2.5)}$$

and the equations standardized by making $\sigma = 1$ and $\mu = 0$. The standardized equations are used in this thesis.

To estimate the 'shape' of the roughness of a surface a bearing area curve can be constructed by drawing equally spaced lines across the profile trace parallel to the centre line, see fig. A. 2. 2. The fraction of the line inside the surface can be found and a graph of this versus the height of the line above some arbitrary datum line is a bearing area curve. This curve, rotated about the height axis through an angle of 2π is the average asperity of the surface. For a Gaussian distribution of surface heights the bearing area curve would be the distribution function.

THE CENTRE-LINE-AVERAGE HEIGHT OF SURFACE ROUGHNESS

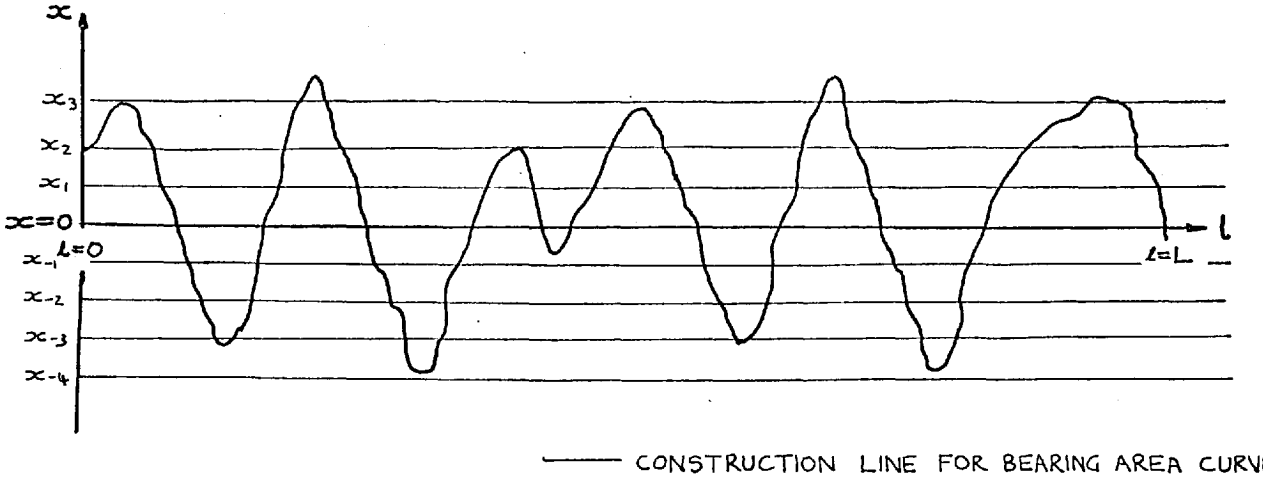

FIG.A.2.1

BEARING AREA CURVE OF ABOVE PROFILE

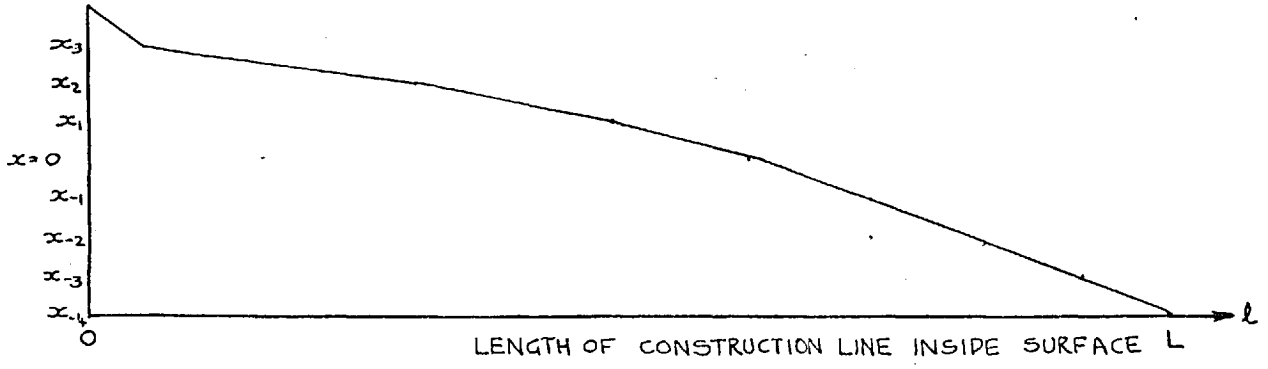

FIG.A.2.2

APPENDIX 3

THE FRICTIONAL BEHAVIOUR OF GRAPHITE

Semi-pyrolised cellulose carbon has been the most successful semi-conductor used in devices so far. This is because it is self-lubricating and wears well. The good wear property depends on the carbon having absorbed water vapour and an environment which does not desorb the vapour. The reason for this is not known as little research has been done on this material, but it is a common feature of other carbons, especially the graphites. For this reason it is worth describing the frictional behaviour of graphite.

Graphite, like most self-lubricating materials, has a lamellar structure. Its carbon atoms are arranged in a series of parallel planes or sheets, (see fig. A3.1), which are 3.35 Å apart whilst the carbon atoms in the individual planes are in a regular hexagonal array, the distance between each atom and its neighbour being 1.42 Å, (Bragg). Covalent bonds exist between the atoms in each layer which are able to withstand high pressures normal to their surface, but the forces between the layers are van der Waal and hence comparatively weak. Bragg attributed the lubricity of graphite to this anisotropic structure with its interplanar weakness producing easy slip between the planes. This is too simple a picture as lattice imperfections, (Cottrell), play an important part in the mechanism, (Tsuzuku). Consider a piece of graphite rubbing against another material. On both rubbing surfaces a thin graphite film is formed, (Jenkins; Midgley and Teer; Quinn), which consists of graphite platelets of single crystals with their basal plane oriented at an inclination of 5^{o} to the direction of sliding. Thus the sliding is essentially between basal planes of graphite. Good friction and wear characteristics only occur when these films are formed. When the graphite is baked in a vacuum environment it wears excessively and has a high coefficient of friction, about 0.5. However, when it is placed in an environment containing water vapour, or another condensable vapour, its wear rate decreases and its coefficient of friction drops to about 0.15, (Savage, Rowe). This is attributed to the vapour satisfying the edge bonds,(the broken covalent bonds), of the platelets, stopping them reaggregating into wear débris and disrupting the oriented films

and also allowing easy shear between the layers.

This is a simple explanation of the friction and wear of graphite showing the importance of the environment in which the material is used. This also applies to an extent to semi-pyrolised cellulose carbon, but like most carbons its behaviour is complex and unlikely to be identical to that of graphite.

THE CRYSTALLINE STRUCTURE OF GRAPHITE

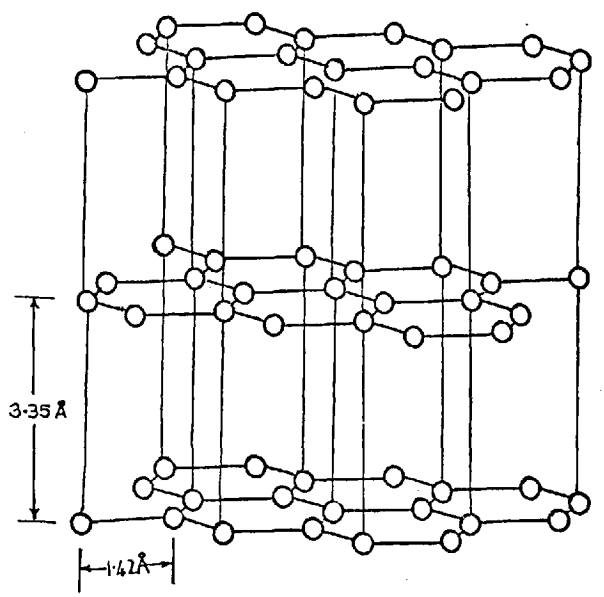

FIG.A.3.1

APPENDIX 4

THE SWITCH ON/OFF TIME

For a linear, isotropic, homogeneous material the general form of Ohm's law is :

$$\underline{J} = \frac{1}{\rho} \underline{E} \qquad \text{(A4.1)}$$

where $\underline{J}$ is the vector current density, ρ the volume resistivity of the material and $\underline{E}$ the vector electric field. From this can be derived :

$$\nabla \cdot \underline{J} = \frac{1}{\rho} \nabla \cdot \underline{E}$$

where $\nabla . \underline{A}$ is the divergence of a vector $\underline{A}$. Using one of Maxwell's equations, (see Feynman);

$$\nabla . \underline{D} = \sigma' \qquad \text{(A4.3)}$$

where $\underline{D}$ is the vector displacement, Cm^{-3}. $\underline{D}$ is related to $\underline{E}$ by :

$$\underline{D} = K_e \epsilon_o \underline{E} \qquad \text{(A4.4)}$$

where K_e is the relative permittivity. From this equation one can derive :

$$\nabla . \underline{E} = \frac{1}{K_e \epsilon_o} \nabla . \underline{D} = \frac{\sigma'}{K_e \epsilon_o} \qquad \text{(A4.4)}$$

Combining this with eq. (A4.2):

$$\nabla . \underline{J} = \frac{\sigma'}{K_e \epsilon_o \rho} \qquad \text{(A4.5)}$$

Charge must be conserved, i.e.

$$\nabla . \underline{J} = - \frac{\partial \sigma'}{\partial t} \qquad \text{(A4.6)}$$

where t is time, seconds, thus :

$$\frac{\partial \sigma'}{\partial t} = - \nabla \cdot \underline{J} \qquad \text{(A4.7)}$$

$$\therefore \quad \frac{\partial \sigma'}{\partial t} = - \frac{\sigma'}{K_e \epsilon_o \rho} \qquad \text{(A4.8)}$$

Solving this yields :

$$\sigma' = \sigma_o' \exp\left(-\frac{t}{K_e \epsilon_o \rho}\right) \qquad \text{(A4.9)}$$

where σ_o' is a constant charge density.

$K_e \epsilon_o \rho$ is termed the relaxation time of the material and it is a measure of the time for electrical charge to diffuse through it. For a metal this time is about 10^{-19} seconds and for a good insulator a few days.

This means that if a semiconductor with a high value of value of ρ and K_e were used to generate the Johnsen-Rahbek effect the switch on/off time would be large due to the long relaxation time of the semiconductor. Thus an insulator would be of little use in a device. So materials suitable for use in a device must have a high value of ρ k, but a low value of ρ K_e.

REFERENCES

ABBOT, E.J. and FIRESTONE, F.A., 1933, Mech. Eng., 55, 569.

ADLER, D, 1971, Amorphous Semiconductors, Butterworths, London.

ALPERT, D., LEE, D., LYMAN, E.M., and TOMASCHKE, H.E., 1966, J. Appl. Phys. 38, 2, 880-881.

ANTINORI, A., 1925, Z. Phys., 34, 705-14.

ATKINSON, R., 1969, Brit. J. Appl. Phys. (J. Phys. D.) Ser. 2, 2, 325-32.

BALAKRISHNAN, C., 1950, Brit. J. Appl. Phys., 1, 211-3.

BARFORD, N.C., 1967, Experimental Measurements: Precision, Error and Truth. Addison-Wesley, London.

BARTENEV, G.M., 1970, The Structure and Mechanical Properties of Inorganic Glasses, Wolters Noordhoff, Groninger.

BERGMAN, L., 1923, Zeitschrift fur Techrische Physik, 4, 11.

BOWDEN, F.P., and TABOR, D., The Friction and Lubrication of Solids, Part 1, 1954; Part 2, 1964; Clarendon Press, Oxford.

BOYLE, W.S., and KISLIUK, P., 1955, Phys. Rev., 97, 2, 255-259.

BRAGG, W.L., 1928, Introduction to Crystal Analysis, G. Bell and Son, Ltd., London.

BRAITHWAITE, E.R., 1964, Solid lubricants and Surfaces, Pergamon Press London.

CARSLAW, H.S., and JAEGER, J.C., 1959, Conduction of Heat in Solids, Clarendon Press, Oxford.

CHAPMAN, B.N., 1974, J. Vac. Sci. Tech., 11, 106-113.

COLLINS, F.M., 1970, J. Non- Cryst. Sol. 2, 496-503.

CONSTANDINOU, T.E., 1965, Proc. I, E.E., 112, 9, 1783-1793.

COTTRELL, A.H., 1967, An Introduction To Metallurgy, Arnold, London.

DAVIDSON, H.W., and LOSTY, H.H.W., (2), 1960, Proc. Fourth Conf. on Carbon, Pergamon Press, London, 585.

DAVIDSON, H.W., and LOSTY, H.H.W., (1), 1963, G.E.C. Jnl., 30, 22-30.

DAVIES, D.K., 1973, J. Vac. Sci. Technol., 10, 1, 115-121.

DEBYE, P., and HUCKEL, E., 1923, Phys. 2., 24, 305.

DUDDING, R.W., and LOSTY, H.H.W., 1966, G.E.C. Jnl., 33, 2-8.

DUDDING, R.W., 1968, Electrical Review,, 1st March and 8th. March.

DUDDING, R.W., (P), 1974, Private Communication.

Von ENGEL, A., 1955, Ionised Gases, Clarendon Press, Oxford.

FEYNMAN, R.P., LEIGHTON, R.B., and SANDS, M., 1964, The Feynman Lectures on Physics, Vol. 2, Addison-Wesley, Massach.

FITCH, C.J., 1957, I.B.M. J. Res.Dev., 1, 49-56.

FOWLER, R.H., and NORDHEIM, L., 1928, Proc.Roy.Soc., A, 119, 193.

FOXHALL, G.F., and LEWIS, A.J., 1964, Bell Syst. Techn. J., 43, 1609.

FRASER, D.A.S., 1967, Statistics an Introduction, Wiley, New York.

FRITZSCHE, H., 1973, Electronic and Structural Properties of Amorphous Semiconductors. Edited by P.G. Le Comber and J. Mort, Academic Press, London.

FURY, M.J., 1964, Trans.Amer. Soc. Lub. Eng., 7, 133-146.

GERMER, L.H. and HAWORTH, F.E., (1), 1948, Phys.Rev., 73, 1121.

GERMER, L.H. and HAWORTH, F.E., (2), 1949, J.Appl. Phys.20, 1085.

GERMER, L.H. and HAWORTH, F.E., (3), 1951, J.Appl.Phys. 22, 955.

GERMER, L.H. and SMITH, J.L., (4), 1952, J.Appl. Phys.23, 553.

GOMER, R., 1961, Field Emission and Field Ionisation, Harvard Univ.Press, Camb. Massach.

GRAF von HARRACH, H., and CHAPMAN, B.N., 1972, Thin Solid Films, 13, 157.

GREENWOOD, J.A., and TRIPP, J.H., 1971, Proc. Inst.Mech.Eng., 1970-71 Vol 185 48/71.

GREENWOOD, J.A., and WILLIAMSON, J.B.P., 1966, Proc.Roy.Soc., A, 295, 300-318.

GUNDRY, P.M., and TOMPKINS, F.C., 1968, Advances in Catalysis, Academic Press, London.

HALLING, J., and EL-REFAIE, M., 1974, Inst.Mech.Eng. Tribology.

HARRACH, GRAF, V., see GRAF von HARRACH.

HARTMAN, R.J., 1947, Colloid Chemistry, Houghton Mifflin, New York.

HASTED, J.B., 1973, Aqueous Dielectrics, Chapman and Hall, London.

HAWLEY, R., 1960, Vacuum, 10, 310-318.

HEIGHWAY, R.J., and TAYLOR, D.S., 1966, Wear, 9, 310-319.

HERTZ, H., 1882, J. reine angew. Math., 92, 156-71.

HOLM, R., 1967, Electric Contacts, Theory and Application, Springer-Verlag, New York.

JANAKIRAMA-RAO, Bh. V., 1965, J. Amer. Ceram. Soc., 48, 311.

JENKINS, R.O., and TRODDEN, W.G., 1965, Electron and Ion Emission from Solids. Routledge and Kegan Paul, London.

JENKINS, R.O., 1934, Phil. Mag., 12, 457.

JOHNSEN, A, and RAHBEK, K., 1923, Jnl. I.E.E., 61, 713-725.

LEVESON, R.C., 1969, Internal Report of the Electrical Eng. Dept. Imperial College.

LEWIS, T.J., 1955, J. Appl. Phys., 26, 12, 1405-1410.

LINDSLEY, G.S., OWEN, A.E., and HAYAJEE, F.M., 1970, J. Non-Crystalline Solids, 4, 208.

LITTLE, R.P., and SMITH, S.T., 1965, Trans. I.E.E.E. on Electron Devices, Ed-12, 77.

LLEWELLYN-JONES, F., 1962, Electrical Review, 27 July, 125-130.

LLEWELLYN-JONES, F., and MORGAN, C.G., 1953, Proc.Roy.Soc. A. 218, 88.

LLEWELLYN-JONES, F., and OWEN, W.D., 1964, Proc.Phys.Soc 83, 283-291.

LLEWELLYN-JONES, F., and de la PERRELLE, E.T., 1953, Proc.Roy.Soc. A, 216, 267.

LORENZ, P.B., 1964, The Encyclopedia of Electrochemistry, Ed. C.A. Hampel Chapman and Hall, London.

MAGIE, P.M., 1966, J. Amer.Soc.Lub.Eng., July, 262-269.

MAISSEL, L.I., 1966, Physics of Thin Films, Vol.3, Academic Press, London.

MANSFIELD, W.K., 1957, Brit. J. Appl. Phys., 8, 73.

MARGULIS, N., 1947, J. Phys. U.S.S.R., 11, 67.

MASSEY, H.S.W., 1950, Negative Ions, Cambridge University Press.

MATERIALS and METHODS, 1957, Reinhold.

McTAGGERT, F.K., and MOORE, A., 1958, Austral. J. Chem. 11,4, 481-484.

MIDGLEY, J.W., and TEER, D.G., 1963, Trans. A.S.M.E. Dec. 488.

MOORE, A.D., 1972, Nature, March, 47-58.

MOTT, N., 1974, Inst. Phys. Bulletin, October, 25, 448-451.

MULLER, E.W., 1956, Phys. Rev., 102, 3, pt. 2, 618.

PASCHEN, F., 1889, Ann. Phys. Chem., 37, 69,

QUINN, T.F.J., 1964, Brit. J. Appl. Phys., 15, 513.

REED, R.I., 1962, Ion Production by Electron Impact, Academic Press London.

ROTTGARDT, K., 1922, Jahrbuch der Drahtlooer Telegraphie und Telephone, 19-20. 299.

ROWE, G.W., 1960, Wear 3, No.4, 274.

SAVAGE, R.H., 1948, J. Appl. Phys. 19, 1.

SHARMAN, H.B., 1968, Conf. Properties and Metrology of Surfaces, Proc. Inst. Mech. Eng. 1967-68, 182 (Pt. 3k), 21.

SILLARS, R.W., 1955, Proc. Phys. Soc., B, 68, 881-893.

SMID, A.P., 1968, J. Appl. Phys., 39, 3140.

STILL, J.E., and CLULEY, H.J., 1965, Proc. S.A.C. Conference, 405-15.

STILL, J.E., and CLULEY, H.J., 1972, The Analyst, 97, 1150, January.

STRATTON, R., 1955, Proc. Phys. Soc. B, 68, 746-757.

STUCKES, A.D., 1956, Proc. I. E.E., B103, 125-31.

TARASOVA, L, V., 1966, Soviet Physics-Doklady, 11, 3, 258-261.

TOWNSEND, J.S., 1915, Electricity in Gases, Clarendon Press, Oxford.

TOWNSEND, J.S., 1947, Electrons in Gases, Hutchinson, London.

TSUZUKU, T., 1957, Proc. 1957 Conf. on Carbon, 434. Pergamon Press, London.

WASZIK, J, 1924, Zeitschrift fur Physik, 5, 29.

WILLIAMSON, J.B.P., 1968, Conf. Properties and Metrology of Surfaces, Proc. Inst. Mech. Eng. 1967-68, 182, (Pt. 3K).